TECHNISCHE UNIVERSITÄT MÜNCHEN

Ingenieurfakultät Bau Geo Umwelt

Lehrstuhl für Siedlungswasserwirtschaft

Enhanced Removal of Trace Organic Chemicals from Wastewater Treatment Plant Effluents Using UV-Based Advanced Oxidation Processes

David B. Miklos

Vollständiger Abdruck der von der Ingenieurfakultät Bau Geo Umwelt der Technischen Universität München zur Erlangung des akademischen Grades eines

Doktor - Ingenieurs

-Dr.-Ing.-

genehmigten Dissertation.

Vorsitzende: apl. Prof. Dr. Brigitte Helmreich

Prüfer der Dissertation: 1. Prof. Dr. Jörg E. Drewes
                                2. Prof. Dr. Karl G. Linden
                                3. Prof. Dr. Torsten C. Schmidt

Abstract

In recent years, trace organic chemicals (TOrC) such as pharmaceuticals, consumer products, and industrial chemicals have been detected in the aquatic environment. As municipal wastewater treatment plants (WWTPs) have been identified as a major source of TOrCs, advanced treatment of wastewater effluent is becoming increasingly important for system operators. A promising technique to attenuate TOrCs from effluent streams are advanced oxidation processes (AOP) which are based on the *in-situ* formation of radicals in the water. Especially, if UV-disinfection systems are already implemented at full-scale, these existing infrastructures could be modified to UV-based AOPs to remove TOrCs from wastewater effluents by addition of radical promoters. UV-AOPs are established in drinking water and industrial applications but to the best of our knowledge, full-scale AOP systems for municipal wastewater effluent oxidation have not been implemented so far. Therefore, the core objective of this study was to investigate the TOrC removal potential by the combination of UV-light with radical promoters in municipal wastewater effluents.

For the general evaluation of AOPs, established processes as well as recent progress in emerging technologies were reviewed. In addition to a discussion of major radical generation mechanisms and formation of by-products, data on energy efficiency were collected in an extensive analysis of studies reported in the peer-reviewed literature enabling a critical comparison of various AOPs based on electrical energy per order (E_{EO}) values. Despite strong variations within reviewed E_{EO} values, results revealed substantial differences between three groups of AOPs: (1) median E_{EO} values of <1 kWh/m³, (2) median energy consumption in the range of 1-100 kWh/m³, and (3) median values of >100 kWh/m³. Specific evaluation of the UV/H_2O_2 process revealed strong effects of operational conditions on reported E_{EO} values. Besides water type and quality, a major influence was observed for process capacity and, in case of UV-based processes, of the lamp type. Based on these findings, recommendations regarding the use of the E_{EO} concept, including the upscaling of laboratory results, were derived.

Experimental results applying UV/H_2O_2 as an AOP at lab- and pilot-scale showed no significant difference on TOrC oxidation performance. During continuous pilot-scale operation at constant fluence of 800 mJ/cm² and a H_2O_2 dosage of 10 mg/L, the removal efficiency of various TOrCs was investigated. Additionally, based on removal kinetics of photo-resistant TOrCs, continuous pilot-scale operation revealed high variations of OH radical exposure primarily due to nitrite concentration fluctuations in the feed water. Furthermore, a correlation between OH radical exposure and scavenging capacity could be determined and verified by mechanistic modeling using fluence, H_2O_2 dosage, and bulk water quality parameters (i.e., DOC, NO_3^-, NO_2^- and HCO_3^-) as model input data. This correlation revealed the possibility of OH radical exposure prediction by water matrix parameters and proved its applicability during pilot-scale operations.

In addition, peroxodisulfate (PDS) was investigated as an alternative radical promoter to H_2O_2. The effect of water matrix was examined on $^{\cdot}OH$ and $SO_4^{\cdot-}$ scavenging. UV/PDS showed higher selectivity towards TOrC removal than UV/H_2O_2 in wastewater effluent. Compounds with electron-rich moieties, such as diclofenac, venlafaxine and metoprolol were eliminated faster in UV/PDS whereas UV/H_2O_2 was more efficient in

degrading compounds with lower reactivity to $SO_4^{\cdot-}$ which could not be reproduced at pilot-scale UV/PDS most likely due to higher effluent organic matter and nitrite concentrations.

Direct comparison of three UV-AOPs in municipal wastewater revealed general oxidation performance of a wide range of TOrCs following the order of UV/$H_2O_2 \approx$UV/PDS<UV/Chlorine, while UV/PDS and UV/Chlorine exhibited higher compound selectivity than UV/H_2O_2. Evaluating potential optical surrogates to predict TOrC removal in UV-AOPs, nine parameters were selected representing chromophore and fluorophore features of DOM. UV absorption (UVA), total fluorescence (TF) and the selected fluorescence peak P_IV revealed the highest linear correlation coefficients and were therefore selected as surrogates representing underlying mechanistic reactions of each UV-AOP.

Evaluating the applicability of existing UV-disinfection plants for enhanced removal of TOrCs, two specific target definitions were set and investigated during an on-site sampling campaign at the WWTP Munich II and by kinetic modeling to identify modification and retrofitting possibilities: (i) Compliance regarding proposed diclofenac thresholds (50 and 100 ng/L) in the river Isar by UV-photolysis of wastewater effluent and (ii) 50% removal of the radical indicator primidone by UV/H_2O_2 AOP. Investigations revealed UV-fluences and peroxide doses needed to comply with the defined targets. Adapting process parameters and retrofitting the existing UV-infrastructure is sufficient to comply with target (i). However, implementation of full-scale UV/H_2O_2 is needed to meet target definition (ii). This option would require major capital investments and infrastructure changes at Munich II and was therefore not considered as modification of an existing UV-disinfection system.

In conclusion, this dissertation suggests the general applicability of UV-AOPs for advanced oxidation of TOrCs in municipal wastewater effluent. Since oxidation performance of UV-AOP efficiency generally relies on the predominant radical scavenger concentrations, water matrix-coupled process control might be a reasonable solution to overcome this limitation. Finally, oxidation by-product formation potential and overall toxicity assessment should be studied further to allow a final assessment of UV/PDS and UV/Chlorine application in municipal wastewater regarding minimizing potential adverse effects on ecological health.

Zusammenfassung

In den letzten Jahren wurde vermehrt der Eintrag organischer Spurenstoffe wie Pharmazeutika, Haushalts- und Industriechemikalien in die aquatische Umwelt nachgewiesen. Da kommunale Kläranlagen als Hauptemittenten identifiziert wurden, wird eine weitergehende Abwasserbehandlung für Anlagenbetreiber immer wichtiger. Eine vielversprechende Technik zur Minderung von Spurenstoffeinträgen aus Abwasserströmen sind weitergehende Oxidationsverfahren (engl.: advanced oxidation processes, AOP), die auf der *in-situ*-Bildung von Radikalen im Wasser basieren. Insbesondere, wenn UV-Desinfektionsanlagen bereits im Vollstrom etabliert sind, könnten diese bestehenden Infrastrukturen auf UV-basierte AOPs umgestellt werden, um Spurenstoffe aus Abwasser durch Zugabe von Radikalpromotoren zu entfernen. UV-AOPs haben sich im Trinkwasser- und Industriebereich etabliert, sind aber nach dem aktuellen Wissenstand noch nicht im Großmaßstab für die Oxidation kommunaler Abwässer implementiert. Das allgemeine Ziel dieser Studie war daher die Untersuchung der potenziellen Spurenstoffentfernung in kommunalen Abwässern durch die Kombination von UV-Licht mit Radikalpromotoren.

Für die allgemeine Einordnung von AOPs wurden Literaturstudien über etablierte Prozesse sowie aktuelle Entwicklungen bei neueren Technologien, die einem peer-review Prozess unterliegen, in einer umfangreichen Analyse gesammelt und ausgewertet. Neben einer Darstellung der wichtigsten Radikalbildungsmechanismen und der Bildung von Nebenprodukten wurden Daten zur Energieeffizienz gesammelt, die einen kritischen Vergleich verschiedener AOPs auf der Grundlage der spezifischen elektrischen Energie pro 90-prozentiger Entfernung einer Zielsubstanz (E_{EO}) ermöglichen. Trotz starker Schwankungen innerhalb der überprüften E_{EO}-Werte zeigten die Ergebnisse erhebliche Unterschiede zwischen drei Gruppen: (1) AOPs mit Median E_{EO}-Werte von <1 kWh/m³, (2) AOPs mit einem Energieverbrauch im Median von 1-100 kWh/m³ und (3) AOPs mit Median E_{EO}-Werte von >100 kWh/m³. Die detaillierte Auswertung des UV/H_2O_2-Verfahrens zeigte starke Auswirkungen der Betriebsbedingungen auf E_{EO}-Werte. Neben der Wasserqualität wurde ein signifikanter Einfluss der Ausbaugröße und bei UV-basierten Prozessen durch den Lampentyp beobachtet. Basierend auf diesen Erkenntnissen wurden Empfehlungen zur Anwendung des E_{EO}-Konzepts, einschließlich dem Upscaling von Labordaten, abgeleitet.

Experimentelle Ergebnisse mit UV/H_2O_2 als AOP im Labor- und Pilotmaßstab zeigten keinen signifikanten Unterschied hinsichtlich ihrer Oxidationsleistung. Die Entfernung verschiedener Spurenstoffe wurde im kontinuierlichen Pilotbetrieb bei konstanter UV-Fluenz von 800 mJ/cm² und einer H_2O_2-Dosierung von 10 mg/L untersucht. Basierend auf der Entfernungskinetik photoresistenter Spurenstoffe, zeigte der kontinuierliche Pilotanlagenbetrieb hohe Schwankungen der OH Radikalexposition, die hauptsächlich auf Nitritkonzentrationsschwankungen im Speisewasser zurückzuführen waren. Darüber hinaus konnte durch kinetische Modellierung eine Korrelation zwischen OH Radikalexposition und Scavengerkapazität unter Verwendung der Parameter UV-Fluenz, H_2O_2-Dosierung und Standardwasserqualitätsparametern (z.B. DOC, NO_3^-, NO_2^- und HCO_3^-) als Modelleingangsdaten bestimmt und verifiziert werden. Diese Korrelation ergab die Möglichkeit der Vorhersage der OH

Radikalexposition durch Wasser-Matrix-Parameter und bewies ihre Eignung für den Pilotbetrieb.

Zusätzlich wurde Peroxodisulfat (PDS) als alternativer Radikalpromotor zu H_2O_2 untersucht. Dabei wurde der Einfluss der Wassermatrix auf das Scavenging von $\cdot OH$ und $SO_4^{\cdot-}$ untersucht. Zusätzlich wurden Versuche im Pilotmaßstab durchgeführt, um die Machbarkeit einer UV/PDS-Behandlung unter realen Speisewasserbedingungen zu untersuchen. Im Kläranlagenablauf zeigte UV/PDS eine höhere Selektivität als UV/H_2O_2 gegenüber der Spurenstoffentfernung. Verbindungen mit elektronenreichen Gruppen wie Diclofenac, Venlafaxin und Metoprolol wurden in UV/PDS schneller eliminiert, während UV/H_2O_2 bei Verbindungen mit geringerer Reaktivität zu $SO_4^{\cdot-}$ eine höhere Effizienz zeigte. Die fluenzbasierten Reaktionskonstanten k_{obs-UV/H_2O_2} der Spurenstoffe zeigten während des UV/H_2O_2-Verfahrens aufgrund der konstanten Scavengerwirkung der Abwassermatrix eine lineare Abhängigkeit zu der anfänglichen H_2O_2-Dosis. Im Gegensatz wurde mit steigender PDS-Dosis ein exponentieller Anstieg von $k_{obs-UV/PDS}$ für die meisten Verbindungen während des UV/PDS Verfahrens beobachtet. Dies weist auf den abnehmenden Scavengereffekt der Wassermatrix durch $SO_4^{\cdot-}$ bei niedriger PDS-Dosis hin (durch anfänglichen Abbau elektronenreicher Gruppen der gelösten organischen Substanz). Darüber hinaus war das UV/PDS-Verfahren im Pilotmaßstab mit Experimenten im Labormaßstab vergleichbar, jedoch waren die Gesamt-entfernungsraten aufgrund der höheren Konzentration gelöster organischen Substanz und Nitrit geringer.

Der direkte Vergleich von drei UV-AOPs in kommunalem Abwasser für die Oxidation eines breiten Spektrums von Spurenstoffen ergab hinsichtlich der Oxidationsleistung die Reihenfolge UV/$H_2O_2 \approx$UV/PDS<UV/Chlor, wobei UV/PDS und UV/Chlor eine höhere Selektivität mit den Spurenstoffen aufwiesen als UV/H_2O_2. Bei der Bewertung potenzieller optischer Surrogate zur Vorhersage der Spurenstoffentfernung in UV-AOPs wurden neun Parameter ausgewählt, die chromophore und fluorophore Merkmale von gelöstem organischen Kohlenstoff darstellen. Die UV-Absorption (UVA), die Gesamtfluoreszenz (TF) und der ausgewählte Fluoreszenzpeak P_IV zeigten die höchsten linearen Korrelationskoeffizienten und wurden daher als Surrogate bestimmt, die die zugrunde liegenden mechanistischen Reaktionen der einzelnen UV-AOPs darstellen.

Zur Beurteilung der Eignung bestehender UV-Desinfektionsanlagen für die weitergehende Entfernung von Spurenstoffen wurden zwei spezifische Zieldefinitionen festgelegt und durch eine Probenahmekampagne vor Ort in der Kläranlage München II sowie durch kinetische Modellierung zur Identifizierung von Modifikations- und Nachrüstoptionen untersucht: (i) Einhaltung der vorgeschlagenen Schwellenwerte für Diclofenac (50 und 100 ng/L) in der Isar durch UV-Photolyse von Kläranlagenablauf und (ii) eine 50 prozentige Entfernung des Radikalindikators Primidon durch UV/H_2O_2. Die Untersuchungen ergaben minimale UV-Fluenzen und H_2O_2-Dosen, die notwendig sind, um die definierten Ziele zu erreichen. Die Modifikation der Prozessparameter und die Nachrüstung der bestehenden UV-Infrastruktur sind ausreichend, um das Ziel (i) zu erreichen. Jedoch ist der Einsatz von UV/H_2O_2 im Vollstrom erforderlich, um die Zieldefinition (ii) zu erfüllen. Da diese Option signifikante Investitionen und

anlagentechnische Baumaßnahmen in der Kläranlage München II erfordert, wird sie nicht als Modifikation eines bestehenden UV-Desinfektionssystems betrachtet.

Insgesamt konnte diese Arbeit die Eignung von UV/AOPs zur Entfernung von Spurenstoffen aus kommunalen Abwässern darlegen. Da die Oxidationsleistung der UV-AOPs-Effizienz signifikant von dem Einfluss schwankender Wassermatrix-parameter abhängt, ist eine dynamische, wassermatrixgekoppelte Betriebssteuerung eine sinnvolle Kompensationslösung. Abschließend sollten das Bildungspotenzial von Nebenprodukten und die Gesamttoxizität weiter untersucht werden, um eine finale ökotoxikologische Bewertung der beiden UV-AOPs, UV/PDS und UV/Chlor, in kommunalem Abwasser zu ermöglichen.

Acknowledgements

Contents

List of Figures

List of Tables

Abbreviations

$\cdot$Cl	Chlorine radical
$\cdot$Cl$_2^-$	Dichlorine radical anion
$\cdot$OH	Hydroxyl-radical
^{3}DOM*	Triplet excited states of dissolved organic matter
AA-EQS	Annual average environmental quality standard for inland surface waters
AOC	Assimilable organic carbon
AOP	Advanced oxidation processes
AOX	Adsorbable organic halides
ATL	Atenolol
BAC	Biological activated carbon
BDD	Boron-doped diamond
BOD	Biological oxygen demand
BZT	Benzotriazole
cAOP	Catalytic advanced oxidation processes
CBD	Collimated beam device
CBZ	Carbamazepine
CFSF	Coagulation-flocculation-sedimentation-filtration
COD	Chemical oxygen demand
DOC	Dissolved organic carbon
DOM	Dissolved organic matter
eAOP	Electrochemical advanced oxidation processes
EEM	Excitation emission matrix
E_{EO}	Electrical energy per order of magnitude
EfOM	Effluent organic matter
EINECS	European Inventory of Existing Chemical Substances
EQS	Environmental quality standards
FI	Fluorescence index
GAC	Granular activated carbon
HAA	Haloacetic acids
HAN	Haloacetonitriles
IOP	Iopromide
IUPAC	International Union of Pure and Applied Chemistry
LED	Light emitting diodes
LfU	Landesamt für Umwelt
LOQ	Limit of quantification
LP	Low-pressure
MP	Medium pressure
NDMA	N-Nitrosodimethylamine
NF	Nanofiltration

NTU	Nephelometric turbidity unit
OBP	Oxidation by-product
pAOP	Physical advanced oxidation processes
PARAFAC	Parallel factor analysis
*p*CBA	*para*-chlorobenzoic acid
PDS	Peroxodisulfate
PMD	Primidone
PMS	Peroxymonosulfate
PNEC	Predicted no effect concentrations
PP	Pilot plant
RCS	Reactive chlorine species
REACH	Registration, Evaluation, Authorization and Restriction of Chemicals
ROS	Reactive oxygen species
SCADA	Supervisory control and data acquisition
SI	Supplemental information
SMART	Sequential managed aquifer recharge technology
$SO_4^{\cdot-}$	sulfate radical
STD	Standard deviation
TAN	Tree Augmented Naïve Bayes
TCEP	Tris (2-chloroethyl) phosphate
TF	Total fluorescence
THM	Trihalomethanes
TOrCs	Trace organic chemicals
TOX	Total organic halides
TPs	Transformation products
UBA	Umweltbundesamt
US	Ultrasound
UVA	UV-absorbance
UVT	UV-transmittance at 254 nm
VLF	Venlafaxine
WWP	Wastewater percentage
WWTP	Wastewater treatment plant
ΔUVA_{272}	Differential absorbance of UVA at 272 nm

1. General Introduction

1.1 Problem Definition

The occurrence of trace organic chemicals (TOrCs) in the aquatic environment has been investigated in water research for more than thirty years (Richardson and Bowron, 1985; Petrie et al., 2015; Noguera-Oviedo and Aga, 2016). TOrCs comprise pharmaceuticals, endocrine disrupting compounds, consumer products, and industrial chemicals, such as flame-retardants or corrosion inhibitors. By 2018, more than 100,000 chemicals have been registered in the European Union (EU) (EINECS, European Inventory of Existing Chemical Substances) and in 2018 almost 21,000 chemicals were regulated by the REACH legislation (Registration, Evaluation, Authorization and Restriction of Chemicals, 1907/2006/EC) which only applies for chemicals that are produced or imported in volumes above one ton per year. Additionally, REACH excludes food additives, cosmetics, medical products, biocides and pesticides (van Arnam, 2008) which are regulated by other legislations (e.g., pesticides in regulation 1107/2009/EC). Consequently, estimates of total chemicals in regular use vary between 30,000 and 90,000 (Holt, 2000; Schwarzenbach et al., 2006). An unknown share of these compounds accompanied by their environmental transformation products can potentially be released into the aquatic environment polluting natural waters (Loos et al., 2009). Especially persistent and mobile organic chemicals are of major concern because they are neither attenuated by biodegradation, nor by sorption processes due to their high polarity and thus excellent water solubility (Reemtsma et al., 2016). Several studies have reported the ubiquitous occurrence of TOrCs in water sources (Loos et al., 2009; Gabet-Giraud et al., 2014; Sengupta et al., 2014; Montes-Grajales et al., 2017; Peng et al., 2017) resulting in adverse effects to the aquatic environment (Schäfer et al., 2011; Brodin et al., 2013; Muschket et al., 2018). While TOrCs generally demonstrate low acute toxicity (Brausch et al., 2012), several substances at low concentrations have been shown to cause significant adverse effects on test organisms after long-term exposure (Brun et al., 2006; Galus et al., 2013). In contrast to single toxicity studies (Murray et al., 2010), toxicity of TOrC mixtures are largely unknown and may pose a serious threat to aquatic ecosystems (Cleuvers, 2004; Cizmas et al., 2015; Petrie et al., 2015). In addition, environmental parameters, e.g. temperature, have shown to affect the chronic toxicity of single substances (Martins et al., 2013). Long-term effects of chemicals and especially chemical mixtures on aquatic life and human health are therefore largely unforeseeable (Schwarzenbach et al., 2006). In contrast to ecotoxicity, direct toxic effects on human health seem unlikely (Schriks et al., 2010).

Major sources of TOrCs include industrial, municipal and hospital wastewater effluents, agriculture run-offs and landfill leachate (Mompelat et al., 2009). However, municipal wastewater treatment plants (WWTP) have been identified as a major source of TOrC emissions into the aquatic environment (Reemtsma et al., 2006; Dong et al., 2015a). Because WWTPs are most frequently based on activated sludge systems aiming for a biological removal of nutrients and bulk organic parameters, only insufficient TOrC attenuation is achieved during conventional biological wastewater treatment (Luo et al., 2014).

Due to the potential risk of TOrCs on the aquatic environment, monitoring and regulating of TOrCs are crucial following the precautionary principle (Petrie et al., 2015). Several regulatory steps have already been adopted by the European Union, however, legal discharge limits for TOrCs do currently not exist. The discharge of chemicals into the environment was already addressed in 1976 (76/464/EEC) presenting a framework for the elimination or reduction of pollution by particularly dangerous substances. In the year 2000, the European Union implemented a strategy against chemical pollution of surface waters as presented in Article 16 of the Water Framework Directive (2000/60/EC). In 2001, a first list of 33 priority substances was defined that represent a significant risk to or via the aquatic environment of European Waters (2455/2001/EC). This list contained 11 substances rated as priority hazardous substances which were subject to cessation or gradual decrease of discharges and emissions within a period of 20 years. Seven years later, the Directive 2008/105/EC ratified environmental quality standards (EQS) for the 33 priority substances and certain other pollutants. The Directive 2013/39/EU updated existing EQS and extended the list of priority substances to a total number of 45 compounds. To support the prioritization process, the European Commission implemented a watch-list of ten substances of possible concern for Union-wide monitoring (2015/495/EU). The watch-list comprises compounds that *"(…) may pose a significant risk (…) to the aquatic environment, but for which monitoring data are insufficient to come to a conclusion on the actual risk posed"* (2015/495/EU). The ten selected compounds on the watch-list included diclofenac, estrogens, several antibiotics and pesticides. In a recent update of the watch-list (2018/840/EU), amongst other changes, diclofenac was removed since meanwhile a risk-based assessment is possible without further monitoring. This decision, however, does not change the relevance of diclofenac in the aquatic environment.

The non-steroidal anti-inflammatory drug diclofenac is of high relevance, since it is considered harmful to several aquatic species at environmental concentrations of ≤1 µg/L and is frequently detected in wastewater effluents, surface waters, groundwater, and marine water at relevant concentrations (Letzel et al., 2009; Vieno and Sillanpää, 2014; Barbosa et al., 2016; Lonappan et al., 2016; Bonnefille et al., 2018). For these reasons, an annual average EQS for inland surface waters (AA-EQS) of 100 ng/L was discussed in the European Community document (COM(2011)876) while the German Federal Environment Agency (Umweltbundesamt, UBA) proposed an AA-EQS of 50 ng/L (UBA, 2014). The Bavarian Environment Agency (Landesamt für Umwelt, LfU) then commissioned a georeference-model at regional scale for the entire Bavarian river network to identify exceedances of proposed EQS for selected TOrCs in certain river sections. In this model, the WWTP Munich II (Gut Marienhof) was revealed as a major emitter of TOrCs into the river Isar. Furthermore, diclofenac was identified as the most relevant TOrC in the river with slight exceedances above 100 ng/L after the discharge of Munich II (Klasmeier et al., 2011).

To cope with TOrC emissions into the aquatic environment, additional and more advanced wastewater treatment steps are needed. Established water treatment processes are investigated as end-of-pipe solutions for advanced wastewater treatment (Luo et al., 2014). Sustainable and low-cost biological treatment steps such as sequential biofiltration (Müller et al., 2017) and sequential managed aquifer recharge technology

(SMART) (Regnery et al., 2016) result in effective attenuation of biodegradable compounds but achieve only poor removal on chemicals not amendable to biodegradation. Adsorption and filtration processes with (powdered or granular) activated carbon are relatively cheap and easy to handle treatment steps that achieve sufficient reduction of TOrCs but only have poor effect on substances with higher polarity (Altmann et al., 2014). More advanced processes, such as nanofiltration and reverse-osmosis can efficiently reject TOrCs but have substantially higher energy requirements and result in brine concentrates that have to be treated further (Taheran et al., 2016; Garcia-Ivars et al., 2017). Ozone-based treatment processes are very effective in contaminant oxidation. However, in bromide containing waters ozonation bears the risk of bromate formation, which is a regulated carcinogen in drinking water (von Gunten, 2003a).

Besides the aforementioned technologies, advanced oxidation processes (AOPs) have shown great potential of effectively degrading TOrCs. AOPs are generally defined as processes or process combinations that intentionally form *in-situ* highly reactive radicals (Comninellis et al., 2008). The type of radicals that is mainly formed during AOPs is hydroxyl radical ($\cdot$OH) exhibiting a high redox potential of 1.9-2.85 V (Wardman, 1989). Additionally, sulfate radical ($SO_4^{\cdot-}$) with a similar redox potential of 2.5-3.1 V (Neta et al., 1988) as $\cdot$OH and chlorine radical ($\cdot$Cl, 2.4 V) as well as dichlorine radical anion ($\cdot Cl_2^-$, 2.0 V) with slightly lower redox potentials can be generated (Grebel et al., 2010). While the redox potential is a general measure for the tendency of a chemical to be reduced, other factors, i.e., the selectivity towards electron-rich moieties, are more relevant for assessing the potential of an oxidant (Lutze et al., 2015b). $\cdot$OH are known to react unselectively, whereas $SO_4^{\cdot-}$ and $\cdot$Cl are rather selective oxidants. Depending on the oxidation process and treated water matrix, the abundance of radicals and consequently process performance are highly variable.

Today, the activation of radical promoters (i.e., H_2O_2 or $HOCl/OCl^-$) by low-pressure UV irradiation are established in drinking water applications for odor and taste removal (Scheurer et al., 2010; Wang, 2015) as an effective treatment barrier in water reuse (Drewes and Khan, 2011) and in industrial water applications (Gül and Özcan-Yıldırım, 2009; Cardoso et al., 2016; Wu et al., 2016b). These UV-AOPs proved effective in degrading a wide range of contaminants in drinking (Toor and Mohseni, 2007; Guo et al., 2017) and surface waters (Kruithof et al., 2002; Sarathy et al., 2012). However, only few studies exist on effectiveness of UV-AOPs in municipal wastewater effluents (Rosario-Ortiz et al., 2010; Mahdi-Ahmed and Chiron, 2014; Gerrity et al., 2016; Hofman-Caris et al., 2017). Recognition of UV-AOPs for treatment of secondary effluents is mostly limited due to estimation of operational and capital costs. The latter can be reduced if UV infrastructures are already available on-site. Currently, a total number of 12,600 UV systems are installed at WWTPs worldwide (Ulliman et al., 2018b). In Bavaria, UV systems are installed at WWTPs located along the river Isar to reduce microbial and viral contamination of secondary effluents and ensure bathing water quality along the river (Huber and Popp, 2005). These existing infrastructures could be modified to also remove TOrCs from WWTPs, which might significantly reduce the treatment implementation costs compared to greenfield AOP projects. However, residual organic carbon, suspended solids and nutrients, such as inorganic ions potentially limit the

application of UV-based AOPs. Especially in wastewater, where UV transmittance (UVT) at λ=254 nm hardly exceeds 70% and significant competition of radicals towards other water constituents, so called radical scavenging occurs, a mechanistic understanding of reactions between radicals and radical scavengers is essential. Major water constituents that scavenge radicals are carbonate, bicarbonate, chloride, nitrite, and dissolved organic carbon (DOC) (Keen et al., 2012; Wols and Hofman-Caris, 2012; Keen et al., 2014; Li et al., 2017). Reactivity of these scavengers towards $\cdot OH$, $SO_4{}^{\cdot-}$, and $\cdot Cl$ vary widely. Based on the specific reactivity, water quality and target contaminants directly affect the oxidation efficiency. TOrC removal prediction and process control approaches are therefore key for efficient and economic process management.

Today, UV disinfection systems are usually equipped with integrated radiometer sensors to monitor UV irradiance inside the reactor. Some systems automatically adjust electrical power if irradiance changes due to fluctuating UVT or, in a longer time frame, lamp aging to maintain fluence targets. In UV-AOPs, however, a more comprehensive approach is required due to the complexity of radical scavenging. Two essential concepts are examined in the literature addressing this challenge, i.e., kinetic and surrogate models. For this purpose, established kinetic models (Pereira et al., 2007b; Gerrity et al., 2012; Wols et al., 2013; Gerrity et al., 2016) are applied, verified and further developed in this study. A comprehensive and detailed model for UV/H_2O_2, which captures radical formation by H_2O_2 activation, direct photolysis and radical based removal of target compounds and scavenging of OH radicals by bulk water parameters was implemented and complemented (Bolton and Stefan, 2002; Wols et al., 2013). This model has mostly been used for process description and removal prediction. Applying this kinetic model into an operation control system, UV-AOPs could be controlled as a function of water matrix parameters. Surrogate approaches apply bulk water parameters such as UVA or fluorescence to track performance measures of treatment processes (Dickenson et al., 2009; Chys et al., 2018). To control oxidation performance during AOP operation, e.g., reduction of UV absorbance (ΔUVA) can be measured by applying online sensors directly before and after the UV reactor. ΔUVA is an easy to handle surrogate and bypasses continuous analysis of target TOrCs which usually is associated with high instrumental and financial efforts. Correlations between ΔUVA and the removal of TOrCs have been investigated for (powdered) activated carbon (Anumol et al., 2015; Altmann et al., 2016), ozonation (Dickenson et al., 2009; Altmann et al., 2014; Stapf et al., 2016; Chys et al., 2017), and UV/H_2O_2 (Yu et al., 2015). By detailed evaluation of fluorescent DOC by 3D-fluorescence analysis, excitation emission matrix (EEM) information can be particularized into relevant underlying characteristics with different reactivities to radical species and probably specific correlations to different TOrC groups.

The need of mitigating TOrCs from municipal wastewater effluents and the potential of modifying existing UV disinfection infrastructures for advanced TOrC removal has led to the core objective of this study: "Investigation of TOrC removal potential by the combination of UV light with radical promoters in municipal wastewater effluents."

1.2 State-of-The-Art

1.2.1 UV light technologies for water treatment

Ultraviolet light is characterized by the wavelength range of 10-400 nm including UV-A (315-400 nm), UV-B (280-315 nm), UV-C (100-280 nm), and vacuum UV (VUV, 10-200 nm) (ISO 21348).

$$E = h\nu = h\frac{c}{\lambda} \qquad\qquad (1)$$

Following Planck's Law of Radiation (Equation 1), where E is the energy of one photon [eV], ν is the frequency [s^{-1}], c is the speed of light in a vacuum (3.0 $\cdot 10^8$ m/s), λ is the wavelength [m], and *h* is the Planck constant (6.626 $\cdot 10^{34}$ Js), UV-C has a higher energy than UV-A and UV-B. The most common UV-C sources are mercury vapor lamps that are available as low- and medium-pressure systems emitting mono- and polychromatic light. The monochromatic emission pattern of low-pressure (LP) UV lamps is usually described as a single narrow peak in the UV-C wavelength range at 253.7 nm. However, LP mercury vapor lamps also emit a second monochromatic peak at 185 nm which is usually absorbed in the optical glass applied in germicidal lamps. If a specific quartz glass is used that transmits wavelengths <240 nm, LP-lamps are referred to as VUV lamps (Masschelein, 2002). Polychromatic emission spectra of medium-pressure (MP) UV lamps emit a wide range of wavelengths across 200-300 nm (EPA, 2003). For disinfection applications, however, in Germany, MP emission wavelengths are limited to >240 nm to reduce the generation of photolysis by-products (DVGW, 2006).

UV light emitting diodes (LED) which emit light with a specific polychromatic wavelength distribution have been investigated and summarized for water treatment purposes (Song et al., 2016; Chen et al., 2017). Compared to conventional medium- and low-pressure lamps, the principal advantages of LEDs are the elimination of mercury, unique peak emission wavelengths, compact size and consequently flexible application design as well as a short start-up phase. The electrical to UV conversion efficiency of the aforementioned technologies is usually at about 30-40% for LP and 10-20% for MP systems (EPA, 2003). Currently, LEDs emit UV radiation at efficiencies of <15% with lower values towards lower wavelengths (Chen et al., 2017). However, with technological developments an increase of efficiency is expected, which could already be observed in the last years raising from <1% in 2002 (Zhang et al., 2002) to 14.3% in 2015 (Hirayama et al., 2014). However, overrated predictions from Ibrahim (2012) who estimated a 75% wall plug efficiency in 2020, are not yet realistic today.

Generally, electrical power that is not converted to (UV) light is primarily lost as heat. Hence, thermal management is an important design parameter for LED chips but also has to be considered for MP-UV systems that operate at temperatures of 600-900°C (EPA, 2003). In this study, investigations focus on LP-UV technologies. But general observations are transferable to alternative UV systems if the polychromatic emission spectrum is considered.

Major process parameters for UV systems are *irradiance* (*I*, [mW/cm²]) and *fluence (F', [mJ/cm²]).* Following the definition of Bolton and Linden (2003) *ir*radiance

is the total radiant power incident onto a cross-sectional area dA, divided by dA (measured by a radiometer), where the term is further differentiated based on the direction of light: if UV light is received from all directions the term *fluence-rate* is used, while for the use of UV light radiating from one direction (e.g. in a collimated beam system) the term irradiance is used (Bolton and Linden, 2003). *Fluence* can be calculated as a product of *irradiance* and *exposure time* [s]. In this study, fluence is also referred to as UV dose.

1.2.2 *UV light applications for water treatment*

LP-UV technologies are widely applied for water treatment. Major applications of UV light include drinking water and tertiary wastewater disinfection (Hassen et al., 2000; Masschelein, 2002; Zhuang et al., 2015; Gibson et al., 2017) as well as industrial applications such as ballast water (Moreno-Andrés et al., 2016; Olsen et al., 2016) or process water disinfection (Chang and Lin, 2014; Rubio et al., 2015). UV technologies are also applied in the food industry (Cristóvão et al., 2015; Ignat et al., 2015; Bustillo-Lecompte et al., 2016) and aquaculture (Klausen and Grønborg, 2010; Gullian et al., 2012) for maintaining water hygiene. Besides disinfection, UV light can be combined with radical promoters to intentionally generate highly reactive radicals. As a result, generated radicals can be used to effectively oxidize organic compounds. These UV-AOPs are applied in multiple barrier approaches to remove undesired color, taste and odor or TOrCs. The full-scale application of UV/H_2O_2 in direct and indirect potable reuse was reviewed by Gerrity et al. (2013). A first full-scale application of UV/Chlorine for indirect potable reuse recently started operation at the Los Angeles Terminal Island Water Reclamation Plant (Xylem, 2015).

UV-AOPs are not established for advanced municipal wastewater treatment mainly because of low UVT and high scavenging capacity of secondary or tertiary treated wastewater effluents. Some studies investigated UV-AOP applicability to wastewater effluents by applying pretreatment e.g. by ion exchange (Hofman-Caris et al., 2017), or coagulation (Qian et al., 2018) as well as direct treatment of secondary effluents (Rosario-Ortiz et al., 2010; De La Cruz et al., 2013; Keen and Linden, 2013a). In some industrial applications, UV-AOPs are applied to lower chemical oxygen demand (COD) or decolorize dye-bath effluents (Alaton et al., 2002; Gül and Özcan-Yıldırım, 2009; Cardoso et al., 2016).

1.2.3 *Chemistry of UV light in water*

The interaction of UV radiation with matter has to be distinguished between physical (refraction, reflection and scattering), photophysical (absorption, luminescence), and photochemical processes (photooxidation reactions) (Oppenländer, 2003). Following the recommendations of Verhoeven (1996), the latter can be grouped into (i) photo-induced oxidation *(direct photolysis)*, (ii) photooxygenation (photon absorption by photosensitizers to produce reactive oxygen species, referred to as *indirect photolysis*), and (iii) photo-initiated oxidation (photochemically assisted production of radicals). A short explanation of the three groups is provided below:

(i) If an atom or molecule (M) absorbs photons with the energy of UV-C light, it is transferred into an excited electronic state (M*) (Equation 2). Direct photolysis of water constituents is mainly based on photo-induced oxidation by reactions between photolytically excited molecules and oxygen (Equation 3) or photoionization (Equation 4).

Activation:	$M + h\nu \rightarrow$	M^*	(2)
Subsequent oxidation:	$M^* + O_2 \rightarrow$	Products	(3)
Ionization:	$M^* \rightarrow$	$M^{\cdot +} + e^-$	(4)

(ii) With regard to water quality parameters, photooxygenation is only relevant for dissolved organic matter (DOM) and nitrate photolysis, which react as photosensitizers to produce reactive oxygen species (Lester et al., 2013). A general mechanistic understanding of photooxygenation is presented elsewhere (Oppenländer, 2003).

(iii) Photo-initiated oxidation describes the activation of radical promoters (e.g., H_2O_2) by photolysis and subsequent radical reactions (Oppenländer, 2003).

Direct and indirect photolysis (i and ii) are summarized in this study since the effect of the latter is not easy to differentiate from direct photolysis and in an AOP, steady-state concentrations of reactive species from indirect photolysis are 2-3 orders of magnitude lower than steady-state radical concentrations generated by photo-initiated oxidation (Lester et al., 2013; Ulliman et al., 2018b).

If UV light is emitted in water, the penetration depth is dependent on photon absorption at a given wavelength which can be described as $A = \log(I_0/I_1)$. I_0 and I_1 are the irradiances incident on the cell and transmitted through a path length (*l*), respectively. Absorbance (*A*) divided by the path length results in the absorption coefficient (*a [cm^{-1}]*). The percent UVT of light through a given path length (usually 10 mm) is explained by Beer-Lambert Law: $UVT = 100 \cdot 10^{-a\,l}$ [%] (Braslavsky, 2007). Municipal wastewater effluents usually transmit light at $\lambda = 254$ nm with a UVT of 60-70% depending on treatment technologies applied (Masschelein, 2002). In contrast, drinking water transmits UV light at 254 nm with >90% (EPA, 2003).

Photochemical reaction kinetics are described by the photochemical rate constants quantum yield and molar absorption coefficient. The molar absorption coefficient (*ε*) is the absorption coefficient (*a*) divided by amount-of-substance concentration of the absorbing material in the sample solution (*ε = a/c) (Braslavsky, 2007)*. Quantum yield (*ϕ*) is defined as the number of events (chemical reactions) which occur per photons absorbed by the system [mol/Einstein] or [/] (Oppenländer, 2003). Compounds speciation in water influences the molar absorption coefficient. E.g., Lian et al. (2015) investigated the kinetics of sulfonamide photolysis and revealed an increase of *ε* with higher pH which is explained by the liberation of lone-pair electrons of the sulfinol-groups (R-S(=O)2-NH-R) through deprotonation resulting in a hypochromic effect. *ε*

and ϕ should therefore be determined at neutral pH or reported with pH values that were applied during experimental procedure.

While ε and ϕ are well described in literature for the single absorption of λ=254 nm, only a few studies investigated their wavelength dependency (Pereira et al., 2007b; Pereira et al., 2007a). Based on the UV radiation source applied, the molar absorption coefficient at other wavelengths significantly differs from values measured at 254 nm.

1.2.3.1 Direct and indirect photolysis

Direct photolysis of TOrCs by UVC radiation is driven by the wavelength dependent molar absorption coefficient and quantum yield of the target compound. For low TOrC concentrations, pseudo first-order kinetics with linear correlation of the logarithmic relative concentration ($\ln c/c_0$) to the fluence (F') can be assumed (Equation 5) (Bolton and Stefan, 2002):

$$ln\left(\frac{c}{c_0}\right) = -k_{UV}F' = -\ln(10)\frac{\Phi\varepsilon}{U_{254}} F' \qquad (5)$$

For the use of monochromatic LP-UV lamps, the photolytic reaction rate constant k_{UV} can be calculated from the quantum yield, the molar absorption coefficient, and the energy of a mole of photons at λ=254 nm U_{254} [J/Einstein]. A comprehensive list of photochemical rate constants (ε and ϕ) for TOrCs is provided in the Supplemental Information (Section 9.7).

Besides the photolysis of TOrCs, application of LP-UV radiation to wastewater effluent involves additional photochemical reactions between photons and water constituents.

- Following the mechanisms of DOM photolysis proposed by Sharpless and Blough (2014), absorption of light by chromophoric DOM results in triplet excited state DOM ($^3DOM^*$) and subsequent generation of reactive intermediates, i.e., singlet oxygen ($^1O_2$), superoxide (O_2^-), H_2O_2, ·OH and DOM· (Canonica et al., 2006; Sharpless, 2012). The reactivity of DOM to photolysis is influenced by pH, dissolved oxygen, and the chromophoric characteristics of DOM (Du et al., 2014; Sharpless and Blough, 2014).
- The complexity of nitrate and nitrite photolysis in the 200–300 nm region was reviewed and summarized by Mack and Bolton (1999). The major reactive photolysis products are NO·, NO_2·, and ·OH (Mack and Bolton, 1999; Sharpless and Linden, 2001). In addition, Keen et al. (2012) investigated the generation of ·OH by NO_3^- photolysis in wastewater effluent by MP-UV. For LP systems, however, this effect is negligible.

1.2.3.2 Photo-initiated oxidation

Radical generation by photolytic excitement of radical promoters (oxidants) is based on (i) absorption of a photon and subsequent formation of an electronically excited

molecule, and (ii) homolytic cleavage of a chemical bond and formation of primary radicals ($^\cdot$OH, $SO_4^{\cdot-}$, and $Cl^\cdot$) that are available for TOrC oxidation. Radical promoter activation reactions for H_2O_2, peroxodisulfate and chlorine (HOCl/OCl$^-$) and respective photochemical rate constants are presented in Table 1 for λ=254 nm. The deprotonation of HOCl is in equilibrium with pK_a=7.6 at 20°C. A more detailed description of radical generation mechanisms in UV-AOPs is given in Section 3.2.2.

Table 1: Radical promoter activation reactions and respective photochemical rate constants for λ=254 nm

Reaction equations	Quantum yield [mol/E]	Molar absorption coefficient [M/cm]	References
$H_2O_2 + h\nu \rightarrow 2\ HO^\cdot$	0.5	18.6	Ike et al., 2018
$S_2O_8^{2-} + h\nu \rightarrow 2\ SO_4^{\cdot-}$	0.7	21.1	Ike et al., 2018
$HOCl + h\nu \rightarrow HO^\cdot + Cl^\cdot$	1.0	59.0	Feng et al., 2007
$OCl^- + h\nu \rightarrow O^{\cdot-} + Cl^\cdot$	0.9	66.0	Feng et al., 2007

1.2.4 Chemistry of radicals in water

Radical reactions are defined based on the net number of radicals that are formed. If the net formation of radicals is positive, chemical reactions are referred to as radical initiation. If a reaction does not change the number of free radicals (e.g. in radical substitution reactions), it is referred to as radical propagation which is a radical chain reaction. If the net formation of radicals is negative, e.g., by radical-radical recombination, it is defined as radical termination (Crittenden et al., 1999).

Radical initiation has been described above as a result of direct and indirect photolysis or photo-initiated oxidation reactions. General reactions of radicals involve hydrogen abstraction, electrophilic addition, and electron transfer reactions. In pure water, reactions between $^\cdot$OH and water constituents already result in a high variety of reactive oxygen species (ROS) (e.g., superoxide radicals ($O_2^{\cdot-}$), superoxide (O_2^-), hydroperoxyl radicals ($HO_2^\cdot$), $^1O_2$, and H_2O_2) (Burns et al., 2012). With the addition of other primary radicals ($SO_4^{\cdot-}$, and $Cl^\cdot$) and inorganic ions CO_3^-/HCO_3^-, $H_2PO_4^-$/ HPO_4^{2-} or Cl^-, the system is extended by $CO_3^{\cdot-}$ and $PO_4^{\cdot-}$ as well as reactive chlorine species (RCS; ClOH$^{\cdot-}$, OCl$^\cdot$, OCl$^-$, Cl$^\cdot$, Cl$_2^{\cdot-}$) (Fang et al., 2014; Lian et al., 2017). Additionally, complex reactions of primary radicals, ROS and RCS with DOM lead to organic oxyl (R-O$^\cdot$) or peroxyl (R-O$_2^\cdot$) radicals and the liberation of $HO_2^\cdot$ (Burns et al., 2012).

Especially if applied in wastewater, radical distribution and transformation in UV/AOPs associated to TOrC removal is highly complex. Thus, in modeling approaches, the complexity is usually simplified by considering only the most potent oxidants which are selected based on the level of detail in each study (see Section 1.2.5). Since AOPs are implemented for the removal of specific targets, primary radicals compete with water constituents. The unintended reaction of radicals with water matrix is usually described as radical scavenging (Zwiener and Frimmel, 2000). The scavenging rate of a specific water matrix can be described as the overall scavenging capacity $\sum(k_{i,radical}[S_i])$ [s^{-1}] which

is the product of a scavenger concentration $[S_i]$ multiplied by its second-order rate constant $k_{i,radical}$ with $\cdot$OH, $SO_4^{\cdot-}$, or $Cl\cdot$ summarized over all scavengers considered (Kwon et al., 2014).

Compared to drinking water, wastewater effluents carry higher loads of UV absorbing species (i.e., aromatic and conjugated double bonds of DOM (Yu et al., 2015)), which consequently lower UVT conditions and reduce the photolysis rate of UV susceptible TOrCs and radical promoters. The latter results in the reduction of radical generation. In addition, besides higher DOM concentrations, wastewater effluents may contain significant amounts of inorganic scavengers, e.g., Cl^-, HCO_3^-/CO_3^{2-} and NO_2^-. An overview of second-order rate constants for major radical scavengers in wastewater with $\cdot$OH, $SO_4^{\cdot-}$, and $Cl\cdot$ is given in Table 2. The reactivity of DOM and Cl^- to the selected radicals is within the same order of magnitude, while the rate constants of NO_2^-, HCO_3^-, CO_3^{2-} vary over two orders of magnitude between the three radical types. Based on the specific reactivity of the scavengers shown, water quality not only affects the oxidation efficiency of UV-AOPs, it also might already indicate which UV-based AOP is the most effective for a given matrix.

Table 2: Second-order rate constants for reactions between $\cdot$OH, $SO_4^{\cdot-}$, and $\cdot$Cl with major radical scavengers.

Radical scavenger	$k_{\cdot OH}$ [M^{-1} s^{-1}]	reference	$k_{SO_4^{\cdot-}}$ [M^{-1} s^{-1}]	reference	$k_{\cdot Cl}$ [M^{-1} s^{-1}]	reference
DOM	1.7 - 7.9 $\cdot 10^8$	See Section 4.3.3	1.13 $\cdot 10^8$	Yang et al., 2016b	1.6 $\cdot 10^8$	Fang et al., 2014
NO_2^-	1.0 $\cdot 10^{10}$	Coddington et al., 1999	8.8 $\cdot 10^8$	Neta et al., 1988	n/a	-
HCO_3^-	8.5 $\cdot 10^6$	Buxton et al., 1988	9.1 $\cdot 10^6$	Dogliotti and Hayon, 1967	2.2 $\cdot 10^8$	Mertens and von Sonntag, 1995
CO_3^{2-}	3.9 $\cdot 10^8$	Buxton et al., 1988	2.5 $\cdot 10^6$	Padmaja et al., 1993	5.0 $\cdot 10^8$	Mertens and von Sonntag, 1995
Cl^-	4.3 $\cdot 10^9$	Jayson et al., 1973	3.8 $\cdot 10^8$	Das, 2001	8.5 $\cdot 10^9$	Yu and Barker, 2003

Radical scavenging does not directly terminate the radical cycle by radical recombination, but rather results in the formation of other radicals with significantly lower reactivity which is defined in this study as de facto-termination. As an example, the scavenging of primary radicals with bicarbonate via electron transfer results in $CO_3^{\cdot-}$ with reactivities towards TOrCs of 10^6-10^7 M^{-1}s^{-1} which is 1-2 orders of magnitude lower than the reactivity of primary radicals with target contaminants (Wols et al., 2014; Li et al., 2017). Termination of radical chain reactions in water is mostly based on radical-radical recombination and disproportionation reactions (Hoigné, 1998).

1.2.5   Removal of TOrCs in UV-AOPs

Most important pathways to degradation of target constituents in UV-AOP systems are direct photolysis and radical reactions. Consequently, UV-AOPs can be described by TOrC specific kinetic parameters quantum yield, molar absorption and radical-based second-order rate constants of TOrCs and scavengers. Since in UV/H_2O_2 the major oxidant is ·OH, for simplicity reasons only reactions of ·OH with target compounds and relevant scavengers (e.g., DOC, NO_2^- and HCO_3^-) have to be considered in a mechanistic model (Wols and Hofman-Caris, 2012). Extending Equation 5 by the the pseudo first-order rate constant with OH radicals $k_{radical}$, TOrC removal can be estimated in UV/H_2O_2 as depicted in Equation 6.

$$ln\left(\frac{c}{c_0}\right) = -(k_{UV} + k_{radical})F' \qquad (6)$$

This equation can be derived according to Wols et al., (2013) and Bolton and Stefan (2002) as shown in Equation 7, considering only oxidation by direct photolysis and ·OH neglecting the influence of ROS. $k_{radical}$ is a function of the photolysis of H_2O_2 (where the index 'H' represents hydrogen peroxide) and the peroxide concentration, the compound specific second-order rate constant k_{OH} for the reaction of TOrCs with ·OH and the overall scavenging capacity $\sum(k_{i,OH}·[S_i])$ [s^{-1}]. This model is applied in Chapter 4.

$$k = k_{UV} + k_{radical} = \ln(10)\frac{\Phi\varepsilon}{U_{254}} + 2\ln(10)\frac{\Phi_H\varepsilon_H}{U_{254}}\frac{k·_{OH}[H_2O_2]}{\Sigma(k_i[S_i]) + k_H[H_2O_2]} \quad (7)$$

In literature, a variety of models have already been developed and compared to experimental data showing significant differences regarding the level of detail. For UV/H_2O_2, some models include only reactions of ·OH with scavengers (Sharpless and Linden, 2003; Pereira et al., 2007b; Wols and Hofman-Caris, 2012; Yao et al., 2013; Gerrity et al., 2016; Lee et al., 2016) and neglect intermediate ROS and their respective reactions with scavengers or TOrCs like the model presented in Equation 7. A couple of research articles presented more complex models of UV/H_2O_2 that include ·OH, ROS and $CO_3^{·-}$ usually resulting in >20 chemical equations (Glaze et al., 1995; Crittenden et al., 1999; Wols et al., 2014; Wols et al., 2015). Both levels of complexity result in acceptable correlations between predicted and experimental values.

Models for UV/PDS are more complex, since $SO_4^{·-}$ are not the only major oxidant in the system. The reaction of $SO_4^{·-}$ with Cl$^-$, for example, results in ·OH and Cl· turning UV/PDS into a Cl· and ·OH dominated process (Lutze et al., 2015b). Therefore, more reactions have to be considered for modeling UV/PDS (Yang et al., 2014; Yuan et al., 2014; Zhang et al., 2016; Lian et al., 2017; Ye et al., 2017). As an example, Yang et al. (2014) investigated the degradation of TOrCs in synthetic human urine and fed their model with 140 chemical equations including reactions with ·OH, $SO_4^{·-}$, Cl·, ROS, RCS, and reactive nitrogen species.

In the UV/Chlorine system, direct chlorination of target compounds and pH dependency of HOCl/OCl$^-$ which additionally affects the radical generation, both increase the level of complexity. For radical based oxidation, kinetic models usually

include reactions with ·OH, Cl·, ROS and RCS (Fang et al., 2014; Guo et al., 2017; Li et al., 2017).

1.2.6   *Process control and monitoring approaches*

Process control of UV-AOPs in flow-through reactors can be applied by adjustments of flowrate or UV intensity. The radical promoter is dosed ahead of the reactor based on pre-set target concentrations and homogenized with a static mixer. Usually, UV systems are operated at a specific fluence based on chemical oxidation targets. During operation UV intensity is adapted by an automatic control system if changes in UVT or flow occur. Especially if applied in wastewater, UV-AOPs are additionally influenced by water matrix components which can substantially vary over time and consequently lower oxidation performance of TOrCs. Therefore, system operation at a static fluence (and oxidant dose) might result in insufficient TOrC degradation. Quantitative measurement of TOrCs at concentration levels ranging from ppt to ppm is of high instrumental and financial effort and not feasible on-line. Hence, alternative options have to be developed to supply real-time performance of UV-AOPs. In scientific literature kinetic models and optical surrogates are investigated for TOrC removal prediction (Yu et al., 2015; Gerrity et al., 2016). These methods could be applied to operate UV-AOPs based on dynamic operational targets (e.g., real-time scavenger variability or change of surrogate signal).

1.2.6.1   *Process control applying mechanistic models*

Based on the level of detail, kinetic modeling of TOrC attenuation in UV-AOPs include a variety of input parameters like process parameters fluence and radical promoter dose, scavenger concentrations, and kinetic parameters (see Section 1.2.5). If these parameters are available on-line at the reactor influent, mechanistic models can be applied in the process control system (e.g., by a PID-controller) to provide a dynamic control of UV-AOPs and a real-time prediction of TOrC removal. Best to our knowledge, such integrated control systems do not yet exist at full-scale applications.

1.2.6.2   *Process control applying surrogates*

Surrogates are defined as quantifiable parameters within bulk water that can be applied as performance measures of treatment processes relating to the removal of specific contaminants (Dickenson et al., 2009). The optical parameters (UV) absorbance and fluorescence are easy to measure and provide valuable information about the chromophore and fluorophore characteristics of DOM. The absorption of UV light by organic molecules in water is mainly based on changes of energy states in double bonds (C=O, C=C, C=N) and aromatic rings. If electronically excited states of aromatic molecules return to ground state by emission of a photon, observed light is referred to as fluorescence (Lakowicz, 2010). Following the suggestion of Chen et al. (2003) and Coble (1996), 3D-fluorescence excitation emission matrices can be classified into five key fluorescent peaks representing aromatic proteins, tryptophan-, fulvic acid-, soluble microbial by-product-, and humic acid-like molecules which represent common constituents of surface water and wastewater. Hence, these optical parameters are

already discussed as monitoring and surrogate parameters as presented elsewhere (Henderson et al., 2009; Korshin et al., 2018).

In advanced water treatment processes, UVT or UVA have been investigated as surrogates to prove correlations with TOrCs during (powdered) activated carbon (Anumol et al., 2015; Altmann et al., 2016), ozonation (Dickenson et al., 2009; Wert et al., 2009; Altmann et al., 2014; Stapf et al., 2016; Park et al., 2017), and UV/H_2O_2 (Rosario-Ortiz et al., 2010; Yu et al., 2015).

Fluorescence has been investigated as a surrogate for TOrCs attenuation by direct photolysis applying simulated sunlight (Yan et al., 2017), conventional wastewater treatment (Sgroi et al., 2017), activated carbon (Anumol et al., 2015), UV/H_2O_2 (Yu et al., 2015) and Ozonation (Gerrity et al., 2012; Li et al., 2016; Park et al., 2017). Additionally, Korshin et al. (2018) recently reviewed the current state of investigation on optical surrogates for TOrC removal based on absorbance and fluorescence. Fluorescence was also suggested as a monitoring tool for recycled water systems (Henderson et al., 2009). The interesting aspect of expanding absorbance-based surrogates by fluorescence is a potentially higher informative value since different groups of chromophore and fluorophore DOM fractions might differently react with radicals generated by UV-AOPs. Correlations between surrogates and TOrCs might therefore substantially vary for different surrogates investigated. Based on advancements in LED development, specific wavelength emissions that were previously found in lab-scale studies can be applied in optical sensors measuring absorbance and/or fluorescence on-site (Li et al., 2016) and in real-time.
Besides optical surrogates, Keen and Linden (2013b) suggested the use of the artificial sweetener sucralose as a probe compound to track TOrC oxidation performance in UV-AOPs mainly based on its resistance to photolysis and its slow reaction with $\cdot$OH (1.56 $\cdot 10^9$ $M^{-1}s^{-1}$, Keen and Linden, 2013b).

1.2.7 AOP post-treatment

Post-treatment of oxidation processes might be reasonable or obligatory depending on further use of the oxidized water. During UV/H_2O_2 advanced oxidation, DOM can be broken down into smaller molecules affecting biostability by increasing assimilable organic carbon (AOC) (Sarathy and Mohseni, 2007; Bazri et al., 2012). Especially if oxidative water treatment processes are operated in potable water reuse systems, already low levels of AOC (<0.1 mg/L) might promote regrowth of heterotrophic bacteria in distribution systems (Escobar et al., 2001). Since radical promoters are always added in access, residual oxidants need to be removed. Quenching of residual H_2O_2, peroxodisulfate, and HOCl/OCl^- in lab-scale experiments is usually performed using the chemicals sodium thiosulfate, sodium sulfite (which leads to an increase of salinity of the water) or methanol, as well as the enzyme catalase (Liu et al., 2003; Li et al., 2017). In full-scale systems, it is usually achieved by biological activated carbon (BAC) where the oxidants are enzymatically degraded in the biofilm (Sarathy et al., 2012) or by granular activated carbon (GAC) (Bourgin et al., 2017).

Organic and inorganic oxidation by-products can be removed by GAC (Gonce and Voudrias, 1994) or BAC (Toor and Mohseni, 2007; Tang and Xie, 2016). Some studies comprise all effects of post-treatment and reveal that treatment of AOP effluents by GAC

is capable of removing residual oxidant concentrations, AOC, transformation products as well as some residual TOrCs (Bourgin et al., 2017; Bourgin et al., 2018).

1.2.8   *Assessment of AOPs*

In UV-AOP applications radical oxidation performance is usually evaluated based on resulting target compound oxidation or radical exposure calculations. These values, however, are highly dependent on energy and/or chemical input. Besides UV-based AOPs, a huge amount of proposed technologies and process combinations are available for radical generation in advanced water treatment processes in which radical generation mechanisms are fundamentally different.

Critical assessment of AOPs should consider the intricacy of influencing factors i.e., operational costs (energy consumption, chemical input), sustainability (resource use, carbon footprint), and general feasibility (physical footprint and toxicological factors resulting from oxidation by-product and transformation product formation) to enable comparison of their efficiency with other AOPs and alternative treatment processes. An overview of influencing factors with regard to AOP assessment is given in Figure 1.
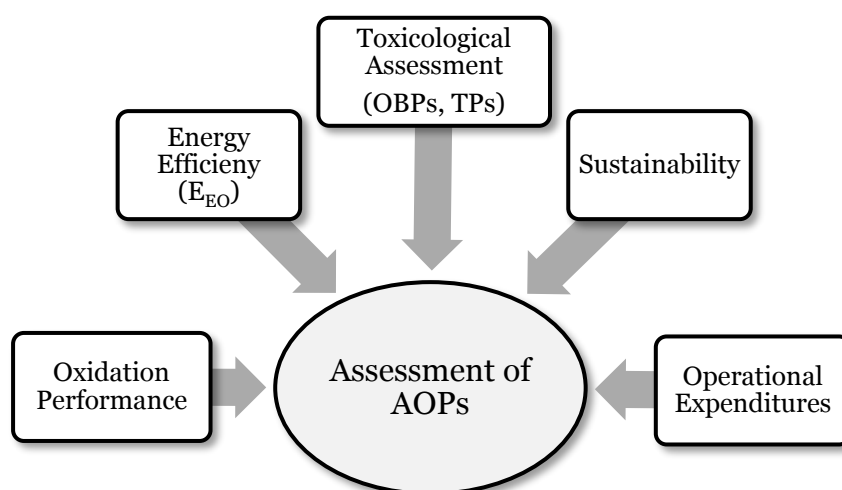
Figure 1: Relevant factors that are important assessing an AOP

The comparison of AOPs by their oxidation performance towards single compounds is straight forward. It is biased, however, since some radicals react more selectively than others and direct oxidation paths (e.g., photolysis or ozonation) might significantly contribute to compound degradation. AOPs are defined as processes that generate radicals *in-situ*. Quantification of radicals formed is therefore an appropriate figure of merit to assess the oxidation performance of an AOP. Radical exposure calculations can easily be conducted for processes that are dominated by one major radical type (Rosenfeldt et al., 2006). This approach is discussed in Chapters 3 & 4.

The decision whether a specific AOP is suitable for full-scale application or not, strongly depends on the type of implementation with various degrees of efficiency subject to the specific water matrix, process configuration and targeted TOrCs resulting in highly varying energy needs and consequently operational expenditures. Process specific

energy consumption data is considered as the E_{EO} figure of merit (i.e., electrical energy per order of magnitude (E_{EO}) removal in 1 m³ of water volume), which enables a direct energy related comparison of various AOPs (Bolton et al., 2001). E_{EO} values have been reported in literature for numerous AOPs for different applications and are critically reviewed and compared in Chapter 3.

Toxicological assessment of AOPs is based on analyzing the change of toxicity in water by oxidation. Since the main aim for AOPs in wastewater is the reduction of TOrCs and potential toxicity for aquatic organisms and human health, transformation and by-product formation shouldn't increase toxicity in water (measured based on specific biological endpoints (Jia et al., 2015)).

The formation of transformation products (TPs) and change of toxicity during UV/H_2O_2 and photocatalysis was recently reviewed by Wang et al. (2018). Hübner et al. (2015a) reviewed the persistence of ozone-induced transformation products and evaluated the biodegradability of transformation products in the environment. These two studies indicate the complexity of toxicity assessment for some selected TPs in a limited number of oxidation processes. Hence, actual impact of TPs on the aquatic environment by advanced oxidation of wastewater effluents are usually evaluated as mixed toxicity in bioassays with several potential biological endpoints (Jia et al., 2015).

Oxidation by-product (OBP) formation in AOPs is discussed in Section 3.3 focusing on radical reactions and direct oxidation i.e., photolysis and ozonation. In terms of toxicity, the formation of OBPs might significantly increase mutagenicity after wastewater oxidation while, simultaneously, genotoxicity is effectively reduced (Magdeburg et al., 2014). Therefore, discussions about toxicity assessment have to be evaluated carefully, since overall toxicity might not be significantly affected by the increase of a single biological endpoint (Jia et al., 2015).

Sustainability aspects of water treatment processes can be investigated in life cycle assessment approaches comparing the respective environmental impact of energy and chemical inputs as well as waste streams (Holloway et al., 2016; Rodríguez et al., 2016). To assess operational expenditures, process specific energy efficiency and chemical consumption data with site specific costs of electrical energy and chemicals need to be combined. If post-treatment is considered, it has to be included in the calculations.

Due to the complexity of influencing factors on AOP assessment, investigations in this study are limited to oxidation performance and energy efficiency.

2. Research Significance and Hypotheses

Since municipal WWTP have been identified as a major source of TOrC emissions into the aquatic environment, established water treatment processes are investigated as end-of-pipe solutions for advanced wastewater treatment. A promising technique to attenuate TOrCs from effluent streams are AOPs which are based on the *in-situ* formation of radicals in the water. Especially, if UV disinfection systems are already implemented at full-scale, these existing infrastructures could be modified to UV-based AOPs to remove TOrCs from wastewater effluents by addition of radical promoters. UV-AOPs are established in drinking water and industrial applications but according to current knowledge, full-scale AOP systems for municipal wastewater effluent oxidation have not been implemented so far. In wastewater, generated radicals (e.g., $\cdot OH$, $SO_4^{\cdot-}$, $Cl^{\cdot}$) react with a higher variety of water matrix constituents than in drinking water applications. Therefore, radical distribution and transformation in UV-AOPs associated to TOrC removal is highly complex. Based on the specific reactivity of the scavengers with different radicals, water quality not only affects the oxidation efficiency of UV-AOPs, it also might already indicate which UV-based AOP is the most effective for a given matrix. For this reason, this dissertation focused on the applicability of AOPs for TOrC removal in wastewater and specifically on the evaluation of TOrC removal potential by the combination of UV light with different radical promoters in municipal wastewater effluents. Five detailed objectives were derived to investigate the general objective of this dissertation:

Research objectives:

1. Energy efficiency comparison of emerging and established AOPs to assess their applicability for advanced wastewater treatment.

2. a) Evaluation of UV/H_2O_2 applicability to degrade TOrCs in municipal wastewater effluent and investigation of process resilience towards water quality changes at pilot-scale.

    b) Development of a kinetic model to predict TOrC removal during advanced wastewater oxidation by UV/H_2O_2.

3. Evaluation of peroxodisulfate as an alternative radical promoter for advanced oxidation of wastewater effluent by UV-based AOPs at lab- and pilot-scale.

4. Direct lab-scale comparison of H_2O_2, peroxodisulfate and chlorine as alternative radical promoters and development of a surrogate model for TOrC removal prediction and process control.

5. Investigation of modification and retrofitting potential of the full-scale UV disinfection system at the WWTP Munich II for advanced TOrC removal.

The following research hypotheses will be tested in this dissertation to complete the objectives.

Research hypothesis № 1:

The full-scale UV disinfection plant at WWTP Munich II can be modified to an advanced oxidation process while achieving a radical chemical indicator removal of 50% by injecting H_2O_2 and enhancing UV dose.

Testing of this hypothesis is threefold and will be addressed with the following sub-hypotheses:

1.1 The UV/H_2O_2 process is applicable for advanced oxidation of wastewater effluent achieving a substantial removal of TOrCs.

1.2 The UV disinfection system at the WWTP Munich II can be modified to achieve a significant attenuation of photo-susceptible TOrCs by enhanced photolysis.

1.3 The UV disinfection system at the WWTP Munich II can be retrofitted to achieve a radical indicator removal of 50% by applying H_2O_2 as a radical promoter.

Research hypothesis № 2:

The removal of TOrCs during UV/H_2O_2 in treated wastewater can be predicted by mathematical models considering the water parameters DOC, NO_2^- and alkalinity, process parameters and specific kinetic data of target compounds.

Research hypothesis № 3:

Applying the radical promoters peroxodisulfate and chlorine as substitutes for H_2O_2, a comparable oxidation performance of UV-AOPs can be achieved in municipal wastewater effluents.

Research hypothesis № 4:

The removal of photo-susceptible and photo-resistant TOrCs during UV/AOPs correlate with intensity changes of specific chromophore or fluorophore DOC components.

Testing of this hypothesis is twofold and will be addressed with the following sub-hypotheses:

4.1 Chromophore or fluorophore DOC components of municipal wastewater effluent can be attenuated by UV photolysis and correlated to photolytic degradation of photo-susceptible TOrCs.

4.2 Chromophore or fluorophore DOC components of municipal wastewater effluent can be attenuated by UV-based advanced oxidation and correlated to radical-based degradation of photo-resistant TOrCs.

2.1 Dissertation Structure

This thesis is structured as a cumulative collection of different peer-reviewed publications. A total number of six research papers are the outcome of this dissertation including major and minor contributions as stated in Section 9.1.1. This chapter outlines the content of each publication and presents the structure of the dissertation.

Paper I is presented in *Chapter 3* and provides a literature review of established processes as well as recent progress in emerging technologies for AOPs. In addition to a discussion of major radical generation mechanisms and formation of by-products, data on energy efficiency were collected in an extensive analysis of studies reported in the peer-reviewed literature enabling a critical comparison of various established and emerging AOPs based on electrical energy per order (E_{EO}) values.

In *Chapters 4-6*, **Papers II-IV** represent research articles on UV-based advanced oxidation of TOrCs in municipal wastewater effluents. In **Paper II**, the removal of 15 TOrCs from municipal wastewater effluent is investigated by advanced oxidation using UV/H_2O_2 at lab- and pilot-scale addressing hypotheses № 1.1 and № 2. Major objectives of this study include the validation of piloting results, development of a mechanistic model to predict OH radical exposure by water matrix parameters (i.e., DOC, NO_2^- and HCO_3^-) and evaluation of water quality impact on continuous operation. **Paper III** comparatively addresses the oxidation performance of 12 TOrCs during UV/H_2O_2 and UV/PDS investigating hypothesis № 3 for peroxodisulfate. The effect of water matrix was investigated in this study on OH and sulfate radical scavenging. Additionally, pilot-scale experiments were carried out at a municipal WWTP to explore the feasibility of UV/PDS treatment under real feed water conditions. **Paper IV** comparatively investigates the oxidation performance of UV/H_2O_2, UV/PDS and UV/Chlorine for the removal of 17 TOrCs from municipal wastewater effluent testing hypothesis № 3. Additionally, optical surrogates, including absorbance and fluorescence parameters, are evaluated to predict TOrC removal performance addressing hypothesis № 4.

Chapter 7 investigates potential modifications of the full-scale UV disinfection process at the WWTP Munich II for TOrC removal testing hypotheses № 1.2 and № 1.3. Occurrence of TOrCs and current TOrC removal performance during UV disinfection are evaluated by a sampling campaign. Moreover, modeling of TOrC removal by photolysis and UV/H_2O_2 complement the investigations and depict potential TOrC removal performances.

This dissertation additionally yielded two peer-reviewed publications (**Papers V-VI)** with significant co-author contributions, however, they are not presented as stand-alone chapters in this thesis but are shortly summarized and discussed in the overall discussion of this dissertation (Chapter 8). In **Paper V**, four different pre-treatment processes for secondary treatment wastewater effluents were studied as options for improving water quality conditions just prior to UV treatment, with and without added H_2O_2. In **Paper VI**, data driven machine-learning algorithms were investigated to predict AOP feed water quality by real data for estimating oxidation performances of AOPs. In Figure 2 the

structure of this dissertation is depicted, including the investigated processes, related objectives and hypotheses, as well as resulting publications.
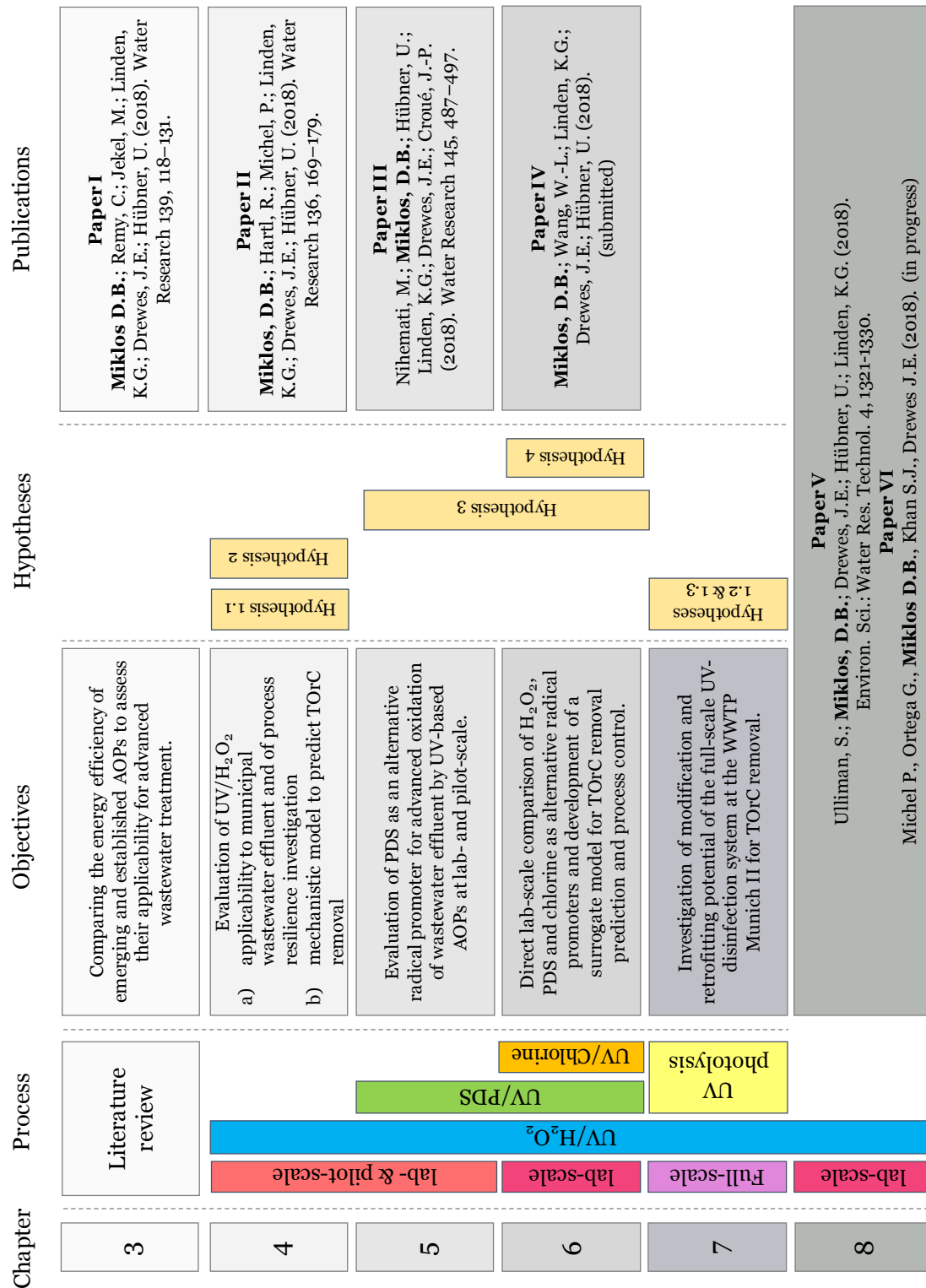
Figure 2: Overview of dissertation structure

3. Evaluation of Advanced Oxidation Processes for Water and Wastewater Treatment – A Critical Review

Abstract

This study provides an overview of established processes as well as recent progress in emerging technologies for advanced oxidation processes. In addition to a discussion of major reaction mechanisms and formation of by-products, data on energy efficiency were collected in an extensive analysis of studies reported in the peer-reviewed literature enabling a critical comparison of various established and emerging AOPs based on electrical energy per order (E_{EO}) values. Despite strong variations within reviewed E_{EO} values, significant differences could be observed between three groups of AOPs: (1) O_3 (often considered as AOP-like process), O_3/H_2O_2, O_3/UV, UV/H_2O_2, UV/persulfate, UV/Chlorine, and electron beam represent median E_{EO} values of <1 kWh/m³, while median energy consumption by (2) photo-Fenton, plasma, and electrolytic AOPs were significantly higher (E_{EO} values in the range of 1-100 kWh/m³). (3) UV-based photocatalysis, ultrasound, and microwave-based AOPs are characterized by median values of >100 kWh/m³ and were therefore considered as not (yet) energy efficient AOPs. Specific evaluation of 147 data points for the UV/H_2O_2 process revealed strong effects of operational conditions on reported E_{EO} values. Besides water type and quality, a major influence was observed for process capacity (lab- vs. pilot- vs. full-scale applications) and, in case of UV-based processes, of the lamp type. However, due to the contribution of other factors, correlation of E_{EO} values with specific water quality parameters such as UV absorbance and dissolved organic carbon were not substantial. Also, correlations between E_{EO} and compound reactivity with OH radicals were not significant (photolytically active compounds were not considered). Based on these findings, recommendations regarding the use of the E_{EO} concept, including the upscaling of laboratory results, were derived.

3.1 Introduction

In recent years, trace organic chemicals (TOrC) such as pharmaceuticals, consumer products, and industrial chemicals have been detected in the aquatic environment (Huerta-Fontela et al., 2010). Besides urban and agricultural run-offs, wastewater treatment plant effluents are considered to be the most significant TOrC emitters (Lim, 2008; Gros et al., 2010; Luo et al., 2014). TOrCs remain in wastewater treatment plant effluents being discharged into surface waters, since conventional physical and biological

wastewater treatment can only partially remove these substances (Lim, 2008; Zhang et al., 2008; Luo et al., 2014).

The application of advanced oxidation processes provides a viable and effective attenuation option due to the oxidation of a wide range of TOrCs (Comninellis et al., 2008; Klavarioti et al., 2009; Yang et al., 2014; Giannakis et al., 2015; Stefan, 2018). According to the definition of Bolton et al. (1996) and Bolton et al. (2001), AOPs are based on the *in-situ* generation of strong oxidants for the oxidation of organic compounds. This includes processes based on OH radicals ($\cdot$OH), which constitute the majority of available AOPs, but also processes based on other oxidizing species favoring sulfate or chlorine radicals. There are several different process technologies which have been investigated for use as AOPs. Several AOPs, especially those involving ozonation and UV irradiation are already well established and operated at full-scale in drinking water treatment and water reuse facilities. However, new studies of numerous emerging AOPs for water treatment (i.e., electrochemical AOP, plasma, electron beam, ultrasound or microwave based AOPs) are constantly being reported by various researchers (Stefan, 2018). The huge amount of different studies and an increasing number of proposed technologies and process combinations pose an enormous challenge for a critical assessment of AOPs concerning their operational costs (i.e., energy consumption, chemical input), sustainability (i.e., resource use, carbon footprint), and general feasibility (e.g., physical footprint and oxidation by-product formation) to enable comparison of their efficiency with other AOPs and alternative treatment processes.

To address this issue, Bolton and coworkers developed figures of merit for the comparison of advanced oxidation processes (Bolton et al., 2001). These are based on electrical energy consumption which often represents a major fraction of the AOP operating costs. For low contaminant concentrations (typically < 100 mg/L), the kinetics of destruction of organic contaminants by AOPs can often be described phenomenologically by simple pseudo first-order rate expressions. Thus, the oxidant or energy dosage scales with the volume and treatment goals (i.e. orders of magnitude of reduction per unit volume). Consequently, the figure of merit for electrical-driven AOPs is defined as E_{EO} (*electrical energy per order*):

> *"Electrical energy per order is the electrical energy in kWh required to degrade a contaminant C by one order of magnitude in 1 m³ of contaminated water"* (Bolton et al., 1996).

This figure of merit has been accepted by the International Union of Pure and Applied Chemistry (IUPAC) in 2001 (Bolton et al., 2001) and numerous E_{EO} values have been reported since then in literature for various oxidation processes and applications. Giving a direct link to the electrical efficiency of the AOP, this approach allows not only for a simple comparison of different AOP technologies, but also provides the requisite data for scale-up and economic as well as sustainability analyses for comparison with conventional treatment technologies (e.g., activated carbon adsorption, air stripping).

In aqueous systems, oxidation of a specific compound C follows a second-order reaction, where the relative residual concentration is a function of compound specific rate constant k_{OH} and the $\cdot OH$ exposure. Accordingly, $\cdot OH$ exposure can be determined from experimental data (Equation 8).

$$\int (^{\bullet}OH)dt = \frac{\ln\left(\frac{C}{C_0}\right)}{-k_{^{\bullet}OH,S}} \qquad (8)$$

The $\cdot OH$ exposure is controlled by the radical formation efficiency of the respective process as well as competing reactions with other constituents in the water called radical scavenging. Major radical scavengers are carbonate, bicarbonate, nitrite, and organic matter indicating a strong dependency of compound removal and thus E_{EO} values on the water matrix. Besides radical scavenging, the water matrix might also directly affect the *in-situ* generation of radicals in several processes, e.g. by reducing UVT or reactions with ozone in ozone-based AOPs. For these reasons, the application of E_{EO} values for a comparison of experimental results from different water matrices is not recommended and comparative studies to evaluate efficiency of different AOPs in a defined water matrix are needed (Bolton et al., 2001). To date, only few studies directly comparing different AOPs are available (Bolton et al., 1998; Müller et al., 2001; Alaton et al., 2002; Katsoyiannis et al., 2011; Ureña de Vivanco et al., 2013; Lutterbeck et al., 2015; Fast et al., 2017) and they are mostly limited to a few established processes. To the best of our knowledge, such a comprehensive comparison across different AOPs has not yet been conducted.

This article provides a critical review of different established and emerging AOPs based on data compiled during an extensive literature study. An initial comparative assessment is conducted based on E_{EO}-values reported in the peer-reviewed literature for different AOPs. Influencing aspects, such as reaction rate constants of target substances, water matrix, process capacity or system parameters are considered and critically evaluated. As a result, recommendations for the use of the E_{EO}-concept in future studies are presented. In addition, this article also provides an assessment on by-product formation in different AOPs based on reaction mechanisms of different oxidants.

3.2 Background Regarding Advanced Oxidation Processes for Contaminant Removal in Water

Technologies for AOPs involve widely different methods of activation as well as oxidant generation and can potentially utilize a number of different mechanisms for organic destruction. An overview of different established and emerging AOPs is given in Figure 3, categorized into ozone-based, UV-based, electrochemical (eAOP), catalytic (cAOP), and physical (pAOP) AOPs. However, it is noteworthy that this classification scheme should not be viewed as strict since several processes involve different technologies and thus could be assigned to various categories. The different processes summarized in Figure 3 represent processes of very different degrees of implementation from well-established AOPs to processes only tested at laboratory scale yet.
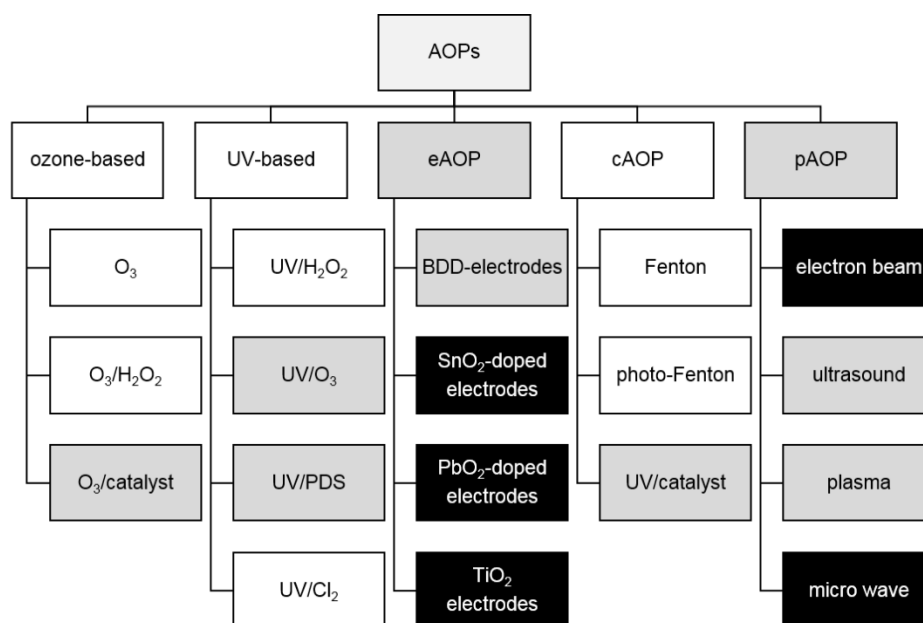
Figure 3: Broad overview and classification of different AOPs. Individual processes are marked as established at full-scale (green), investigated at lab- and pilot-scale (orange), and tested at lab-scale (red).

All AOPs comprise of two steps, the *in-situ* formation of reactive oxidative species and the reaction of oxidants with target contaminants. Mechanisms of radical formation depend on process specific parameters and can be affected by system design and water quality. Besides radical scavenging also other parameters (e.g., radical mass transfer in

surface based AOPs, hydrodynamics) play an important role for efficiency of contaminant destruction. In the following sections, the current status of implementation is reviewed, major mechanisms and principles of radical generation are illustrated, and constraints of different AOPs are briefly discussed. More comprehensive overview on system design, reaction principles and kinetics can be found in various book publications on AOPs (Parsons, 2004; Collins and Bolton, 2016; Stefan, 2018). Mechanisms for the formation of oxidation by-products (OBPs) in different AOPs are discussed separately in Section 3.3.

3.2.1   Ozone based AOPs

Ozone has long been used as an oxidant and disinfectant in water treatment. As an oxidant, ozone is very selective and attacks primarily electron-rich functional groups like double bonds, amines, and activated aromatic rings (e.g. phenol). Since its reactions in real aqueous solutions often involve the formation of ·OH, ozonation itself is often considered an AOP or AOP-like process. ·OH can be formed from the reaction of ozone with hydroxide ions (Merényi et al., 2010a, 2010b). The initiation of this reaction, however, is quite slow with a second-order rate constant of 70 $M^{-1}s^{-1}$.

In addition, radicals are formed as a side product from the reaction of ozone with organic matter (mainly phenol and amine functional groups) (Buffle and von Gunten, 2006). Especially during ozonation of secondary effluents these reactions are the major contributors to radical formation. Methods to actively initiate formation of radicals include the ozonation at elevated pH and the combinations O_3/H_2O_2 (also called peroxone-process), O_3/UV, and $O_3/catalysts$. The combination of ozonation and UV irradiation will be discussed as a UV-based AOP in Section 3.2.2.

3.2.1.1   Ozonation at elevated pH

Ozonation at elevated pH is considered as an AOP if ·OH generation is intentionally favored (Elovitz and von Gunten, 1999; Buffle et al., 2006). The pH of treated water influences direct ozonation efficiency since dissociated target organic compounds might have significantly different k_{O_3} values (Calderara et al., 2002). Furthermore, the abundance of hydroxide ions directly influences the ·OH generation and therefore indirect ozonation. Especially if the water to be treated has a pH > 8, ozonation applied as an AOP might be a promising process, if the precipitation of calcium carbonate is not of concern.

3.2.1.2   Peroxone-process (O_3/H_2O_2)

In the peroxone process, ozone reacts with the peroxide anion (HO_2^-) to form ·OH precursors, which are subsequently reacting to ·OH. For a detailed mechanistic description of the peroxone process see Merényi et al. (2010a). Residual H_2O_2 might have to be destroyed before discharging the treated water to the receiving aqueous environment. The optimum molar ratio for the peroxone process is $H_2O_2/O_3=0.5$ mol/mol (Katsoyiannis et al., 2011; Pisarenko et al., 2012). Typical ozone doses in the peroxone process are 1–20 mg/L. Peroxide can also be formed from reactions of ozone with the water matrix but its contribution to overall ·OH formation during wastewater

ozonation is not significant (Nöthe et al., 2009). O_3/H_2O_2 is a well-established process in drinking water treatment and water reuse applications (e.g. Windhoek, Namibia). However, recent studies have shown that benefits for its application in wastewater are limited due to high competition reactions and already efficient radical formation with ozone alone (Hübner et al., 2015). However, it might still be a valuable treatment option to minimize bromate formation during ozonation as discussed in Section 3.3.

3.2.1.3 O_3/catalysts

Catalytic ozonation is distinguished between homogeneous and heterogeneous catalytic ozonation, depending on the water solubility of the catalyst. Homogeneous catalytic ozonation can be described as a three-step catalytic cycle as approached by Pines and Reckhow (2002) using Co(II) as a catalyst and oxalic acid: (1) formation of Co(II)-oxalate complex, (2) oxidation by ozone to Co(III)-oxalate complex, and (3) decomposition of Co(III)-oxalate complex forming an oxalate radical and Co(II). Heterogeneous catalytic ozonation mechanisms are mediated by metal oxides (e.g., TiO_2, Al_2O_3, MnO_2) and result in more complex reaction paths based on multiple-phase transport mechanisms and respective reactions as described in detail by Beltrán (2004).

Both homogeneous and heterogeneous catalytic ozonation have shown their potential for water treatment at laboratory scale mainly based on lower ozone demand compared to ozonation alone (Bai et al., 2016; Wu et al., 2016a; Wu et al., 2016b; Xing et al., 2016). However, full-scale application is limited due to catalyst recovery and a lack of understanding of the catalytic ozonation mechanisms (Nawrocki and Kasprzyk-Hordern, 2010). Some studies report the use of activated carbon as a catalyst in catalytic ozonation (Kaptijn, 1997). However, ·OH production in this process is based on the reaction of ozone with pyrrol groups present on the activated carbon surface indicating that it acts rather as a radical promoter than a catalyst, which needs to be continuously renewed to maintain efficient radical generation (Sánchez-Polo et al., 2005).

3.2.2   UV-based AOPs

UV-based AOPs comprise processes based on UV irradiation (mostly UV-C) and the combination of UV light with different radical promoters. UV fluences applied for advanced oxidation are usually >200 mJ/cm² and therefore exceed UV dose requirements for 4-log inactivation of most pathogens including UV resistant organisms (e.g. adenovirus) (EPA, 2006). UV irradiation sources usually consist of either low- (LP) or medium-pressure (MP) mercury lamps with mono- or polychromatic emission spectra, respectively. Recently, UV light emitting diode (LED) light sources with specific wavelength distributions have been investigated and summarized for disinfection purposes (Song et al., 2016). The principal advantages of LEDs compared to conventional medium and low-pressure lamps are the elimination of mercury, unique peak emission wavelengths, compact size and therefore flexible application design as well as a short start-up phase. However, despite the prediction of future UV-LED wall plug efficiencies of about 75% in 2020 (Autin et al., 2013), current diodes emit UV radiation at efficiencies of <10% (Chen et al., 2017). This results in E_{EO} values for LED systems that are not yet

competitive with conventional UV systems (Wang et al., 2017a) and are therefore not considered in this study.

The most frequently applied UV-based AOP is the combination with H_2O_2. Other radical promoters such as persulfate (to form sulfate radicals) and chlorine (hydroxyl radicals and radical chlorine species) are also being investigated. Besides established oxidants, Keen et al. (2012) investigated the applicability of nitrate in combination with MP-lamps as an alternative UV-based AOP. However, to the best of our knowledge, no E_{EO} values are available for this process.

3.2.2.1   *UV/H_2O_2*

The combination of UV irradiation and H_2O_2 leads to the photolytic cleavage of H_2O_2 into two ·OH. However, the molar absorption coefficient of H_2O_2 is relatively low with $\varepsilon=18.6$ $M^{-1}cm^{-1}$ at $\lambda=254$ nm resulting in a H_2O_2 turnover of <10%. If LP UV lamps are used, high concentrations of H_2O_2 are required to generate sufficient ·OH ($[H_2O_2]$ = 5-20 mg/L) leading to the necessity of removing residual H_2O_2 in a subsequent step. Applied H_2O_2-doses are mainly set based on economic aspects. However, at higher concentrations also scavenging of ·OH with H_2O_2 ($k_{OH,H2O2}$= 2.7 10^7 $M^{-1}s^{-1}$) might affect the radical yield (Buxton et al., 1988).

UV/H_2O_2 for TOrC removal has been examined widely throughout peer-reviewed journal articles at lab-scale (Wols and Hofman-Caris, 2012; Wols et al., 2013; Keen et al., 2016) for water qualities ranging from ultrapure water to landfill leachate (Ghazi et al., 2014; Xiao et al., 2016). First full-scale applications are already established for potable water reuse (Audenaert et al., 2011) and surface water treatment applications (Kruithof et al., 2007). UV/H_2O_2 is not established for advanced wastewater treatment mainly because of low UVT and high scavenging capacity of secondary or tertiary treated wastewater effluents but is used in some potable reuse treatment trains employing integrated membrane systems (ultrafiltration/reverse osmosis) (Drewes and Khan, 2015) based on its negligible OBP formation potential as discussed in Section 3.3.

3.2.2.2   *UV/O_3*

In the UV/O_3 process, UV irradiation ($\lambda<300$ nm) results in a cleavage of dissolved ozone, followed by a fast reaction of atomic oxygen with water to form a thermally excited H_2O_2. Subsequently, the excited peroxide decomposes into two ·OH (von Sonntag, 2008). Ozone has a molar extinction coefficient of $\varepsilon=3300$ $M^{-1}s^{-1}$ at $\lambda=254$ nm, which is significantly higher than that of H_2O_2 at this particular wavelength. However, due to cage recombinations only a small proportion of generated H_2O_2 decomposes to ·OH resulting in a free ·OH quantum yield of only 0.1 (Reisz et al., 2003). Furthermore, both UV lamps and ozone generator need large amounts of electrical energy, resulting in relatively high energy demands for the combination of UV and ozone. Direct oxidation by the combination of ozonation and photolysis covers a wide range of TOrC reactivity and leads to the main advantage of this process. However, low energy efficiency of radical generation might explain that to the best of our knowledge, no published data on full-scale UV/O_3 application are available.

3.2.2.3 UV/SO$_4$·-

An interesting alternative to ·OH-based AOPs is UV/SO$_4$·- which generates primarily sulfate radicals (SO$_4$·-) for the oxidation of organic contaminants in water (Lutze, 2013; Ao and Liu, 2016; Wacławek et al., 2017; Ike et al., 2018). Sulfate radicals have a strong oxidizing power and are more selective oxidants than ·OH (Lutze et al., 2015b).

Peroxydisulfate (PDS, S$_2$O$_8^{2-}$) is homolytically cleaved by UV-C activation. The quantum yield of S$_2$O$_8^{2-}$ is larger than H$_2$O$_2$ (1.4 compared to 1.0) and molar absorption for S$_2$O$_8^{2-}$ is slightly higher as well (22 M^{-1}cm^{-1} and 18.6 M^{-1}cm^{-1}, respectively) resulting in a higher generation of radicals using PDS as oxidizing agent (Legrini et al., 1993; Lutze, 2013; Xiao et al., 2016). Peroxymonosulfate (PMS, HSO$_5^-$) is activated by UV radiation into a SO$_4$·- and a ·OH with a quantum yield of 0.52 at pH 7 (Guan et al., 2011). Several studies have investigated the mechanisms and application of UV/PMS (Antoniou et al., 2010; Khan et al., 2014; Mahdi-Ahmed and Chiron, 2014). However, based on its lower quantum yield, high commercial pricing and low availability of E$_{EO}$ values it is not considered in this study (Wacławek et al., 2017).

Recent research has shown the advantages of UV/SO$_4$·- compared to UV/H$_2$O$_2$ in lab-scale experiments (Khan et al., 2014; Zhang et al., 2015a; Xiao et al., 2016). However, based on more selective reactivity of sulfate radicals, results reveal a higher sensitivity to water matrix changes and DOM composition compared to UV/H$_2$O$_2$ (Ahn et al., 2017). Depending on the respective target compound and water matrix, SO$_4$·- based AOPs can be a considerable alternative to ·OH-based processes. However, UV/PDS yields in higher formation potential of OBPs in comparison to UV/H$_2$O$_2$ (see Section 3.3).

3.2.2.4 UV/Cl$_2$

UV/Cl$_2$ is another promising AOP, where UV-activated chlorine forms radical species, i.e. Cl· and ·Cl$_2^-$ and ·OH which then oxidize target compounds (Watts and Linden, 2007). Cl· is a more selective oxidant than ·OH, since it reacts favorably with electron-rich contaminants (Fang et al., 2014). The two oxidants mainly used are hypochlorite and chlorine dioxide (Jin et al., 2011; Sichel et al., 2011; Fang et al., 2014; Wang et al., 2016). However, regarding hypochlorite, pH dependency of HOCl/OCl$^-$ speciation needs to be considered since it influences the molar absorption coefficient significantly. UV/Cl$_2$ is especially favorable for waters with lower pH values such as reverse osmosis permeate (Watts et al., 2007). Research has mainly been conducted on lab-scale systems degrading organic indicator compounds (Jin et al., 2011; Sichel et al., 2011; Fang et al., 2014; Wang et al., 2016). A first full-scale application for indirect potable reuse recently started operation at the Los Angeles Terminal Island Water Reclamation Plant (Xylem, 2015) . However, Cl· based reactions involve the formation of oxidative chlorine species (e.g., ClO·, OCl$^-$), which might be oxidized by ·OH to chlorate, perchlorate and halogenated OBPs (see Section 3.3 for more details).

3.2.3 Electrochemical AOPs

Electrochemical AOPs for water treatment applications were recently reviewed in detail by Chaplin (2014). The major electrode types commonly used in this process are doped SnO$_2$ (Zhuo et al., 2011), PbO$_2$ (Bonfatti, 1999; Fernandes et al., 2014), RuO$_2$ (Quan et al.,

2013), boron-doped diamond (BDD) (Chaplin et al., 2013), and sub-stoichiometric and doped-TiO_2 (Kesselman et al., 1997; Bejan et al., 2009). However, BDD-electrodes are the most applied eAOP method due to their relatively low production costs compared to other electrodes and high stability of the diamond layer under anodic polarization (Chaplin, 2014).

The electrochemical oxidative treatment of contaminated water with BDD electrodes can generate ·OH directly via O_2 evolution from water oxidation (Tröster et al., 2004). As diamond is a non-conductor it is doped with boron to use it as an electrode material that is deposited onto a carrier material such as niobium, tantalum or silicon by chemical vapor deposition (Haenni et al., 1998). The radicals are generated without the addition of further chemicals. Therefore, BDD-electrode treatment attracts interest as an eco-friendly and efficient method for the removal of various pollutants. However, since ·OH generation occurs directly on the electrode surface and reactivity range of ·OH is limited to about 1 µm (Kapałka et al., 2009), diffusive transport through the boundary layer at the electrode surface is the limiting factor of high oxidation efficiencies. For eAOP processes, hydrodynamic parameters therefore have to be considered, as energy used to pump water, might account for the greatest share of energy consumption in this process. This applies especially if low current densities are used to achieve higher ·OH formation efficiency prolonging overall treatment duration and pumping energy requirements.

Apart from the oxidation of TOrCs in water treatment, BDD-electrodes are investigated for disinfection purposes as well as for the removal of COD (Rajab et al., 2013; Rajab et al., 2015). Besides the generation of ·OH, secondary oxidants, which enhance elimination reactions and disinfection in the bulk solution, can be produced (Rajab et al., 2015). A limiting factor for the applicability of BDD is unintentional formation of halogenated OBPs as discussed in Section 3.3 (von Gunten, 2003b; Bergmann and Rollin, 2007; Bergmann et al., 2011). Nevertheless, several full-scale eAOP systems for COD removal are already applied (Woisetschläger et al., 2015).

3.2.4   Catalytic AOPs

3.2.4.1   Fenton process

The combination of ferrous iron (Fe(II)) and H_2O_2 at acidic conditions results in ·OH formation (Fenton reaction). Iron acts as a catalyst with maximum catalytic activity at pH=3, particularly due to the precipitation of ferric oxyhydroxide at higher pH value (Wadley and Waite, 2004). Excess addition of H_2O_2 leads to the reduction of Fe(III) to Fe(II) (Safarzadeh-Amiri et al., 1996). By substitution of iron oxides by other transition metals, enhanced TOrC removal performance can be achieved (Jiang et al., 2010; Rahim Pouran et al., 2014; Piscitelli et al., 2015). To prevent iron precipitation, the Fenton process is restricted to acidic conditions. Therefore, alternative iron-free Fenton-like processes have recently been investigated as summarized by Bokare and Choi (2014). Main advantages of the Fenton process are operation at low-costs (Sánchez Pérez et al., 2013) and possibility of easy magnetic separation of residual iron. The Fenton process is therefore established in several industrial full-scale applications (e.g. Bae et al. (2015)).

3.2.4.2 Photocatalytic AOPs

The use of photo-active catalysts for oxidation processes in water treatment has been investigated intensively over the last decades (Blake, 2001; Dong et al., 2015b; Vallejo et al., 2015). Although there are numerous catalysts with photocatalytic properties (i.e., TiO_2, WO_3 or ZnO), research has mainly concentrated on two types of reactions based on the solubility of the catalyst:

homogeneous photo-Fenton processes:

$$Fe(OH)^{2+} + hv \rightarrow Fe^{2+} + {}^{\bullet}OH \qquad (\,9\,)$$
$$Fe(OH)^{2+} + hv \rightarrow Fe^{2+} + {}^{\bullet}OH \qquad (\,10\,)$$
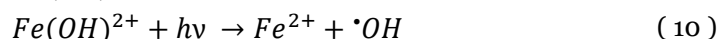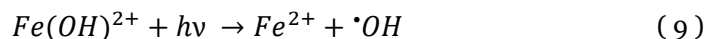
heterogeneous photocatalysis based on semiconductors (TiO_2) (Simonsen et al., 2010):

$$TiO_2 + hv \rightarrow (e^- + h^+) \qquad (\,11\,)$$
$$h^+ + OH^-_{ad} \rightarrow {}^{\bullet}OH_{ad} \qquad (\,12\,)$$
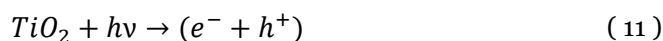
UV and visible light (λ=180–400 nm) accelerate the Fenton process by photoreduction of Fe(III), however, the quantum yield for this reaction is relatively low (Wadley and Waite, 2004). Hence, it is directly coupled with the Fenton process. Photo-Fenton processes with an organic ligand (e.g. ferrioxalate) have a higher quantum yield and thus a higher efficiency due to the high UV absorption of Fe(III)-polycarboxylates. Additionally, the ferrioxalate complex can absorb radiation up to a wavelength of λ<550 nm, making it suitable for solar-driven AOPs (Hislop and Bolton, 1999). A recent review of photo-Fenton applications for wastewater treatment is given by Rahim Pouran et al. (2015).

In TiO_2-based photocatalysis, a semiconductor material is irradiated by UV light (λ < 400 nm). It is usually investigated as suspended colloidal particles or immobilized on different substrates. If photons with sufficient energy hit the photocatalyst surface, an electron is excited to the conduction band, leaving a positively charged hole (h^+) in the valence band (eq. 3). These species can cause oxidative or reductive transformations of water constituents, either directly on the semiconductor surface or via radical reactions (eq. 4). A sufficient amount of dissolved oxygen is necessary for the latter reactions. The combination of oxidation and reduction mechanisms is specific for photocatalysis, whereas other AOPs are based only on ·OH reactions. Unfortunately, the quantum yield of TiO_2 photocatalysis for oxidation and reduction of contaminants is usually very low (ϕ=0.04) due to the fast recombination of electron-hole pairs (Sun and Bolton, 1996). Addition of an electron donor (e.g. citric acid) may lead to the "filling" of positive holes and increased reduction rates from the negative electrons in the conduction band (Vohra and Davis, 2000; Oliveira et al., 2015).

Advantages of TiO_2 photocatalysis for TOrC removal include low costs of the catalyst itself and easy commercial availability in various crystalline forms and particle characteristics. Furthermore, the catalyst is non-toxic and photochemically stable. The limitation of heterogeneous photo-catalysis application at full-scale is mainly based on

two factors: (1) separation of colloidal catalyst from the water suspension after treatment and (2) mass transfer limitations to the surface of the immobilized catalyst on a substrate (Qu et al., 2013). Despite strong research efforts in the field of photocatalysis, the process is rarely applied in industrial or municipal water treatment facilities because of the low quantum yield for ·OH radical production.

3.2.5   *Physical AOPs*

3.2.5.1   *Electrohydraulic discharge (Plasma)*

Liquid-phase electrical discharge reactors have been investigated as AOPs in water treatment (Locke et al., 2006; Hijosa-Valsero et al., 2014). Strong electric fields applied within the water (electrohydraulic discharge) or between water and gas phase (nonthermal plasma) initiate both chemical and physical processes. Beside the direct oxidation of contaminants in the water, various oxidizing radicals or active species, UV radiation, and shock waves are formed during the discharge, which can promote oxidation (Jiang et al., 2014).

3.2.5.2   *Ultrasound*

Sonication of water by ultrasound (US) (20 – 500 kHz) leads to the formation and collapse of micro-bubbles from acoustical wave-induced compression and rarefaction. These bubbles implode violently after reaching a critical resonance size and generate transient high temperatures (>5000 K), high pressures (>1000 bar) and highly reactive radicals. Destruction of water contaminants occurs by thermal decomposition and various radical reactions (Mason and Pétrier, 2004). Cavitation via ultrasound exhibits low interference from water matrix and less heat transfer compared to UV irradiation. A comprehensive review of sonochemical methods is provided by Pang et al. (2011). Sonochemical processes have proven to oxidize various aquatic contaminants in lab-scale experiments (Mahamuni and Adewuyi, 2010). However, the application of ultrasound is highly energy intensive and results in a very low electrical efficiency of this AOP in comparison to other technologies (Goel et al., 2004; Mahamuni and Adewuyi, 2010). Therefore, the coupling of ultrasound with UV irradiation (sonophotolysis), oxidants (O_3, H_2O_2), or catalysts (TiO_2) (sonocatalysis) or both (sonophotocatalysis) receives increased attention. These hybrid processes can yield additional advantages. However, major improvement of energy efficiency is often achieved due to the higher efficiency of the coupled additional processes (e.g. UV/H_2O_2 in $US/UV/H_2O_2$) (Mahamuni and Adewuyi, 2010).

3.2.5.3   *Microwave*

The application of highly energetic radiation in the microwave range (300 MHz – 300 GHz) has been investigated for the oxidation of water contaminants. Microwaves have been used in combination with oxidants (H_2O_2) or catalysts (TiO_2, GAC) to assist in the destruction of organic pollutants (Han et al., 2004; Zhihui et al., 2005; Bo et al., 2006). Microwaves can enhance reaction rates and induce selective heating of the contaminants through internal molecule vibration. Additionally, microwaves can generate UV radiation via an electrodeless discharge lamp for combined MW/UV reactors.

Unfortunately, most of the applied microwave energy is converted into heat. Beside the low electrical efficiency (E_{EO} not readily available in literature), cooling devices have to be employed to prevent treated water from overheating.

3.2.5.4 *Electron beam*

The utilisation of ionizing radiation from an electron beam source (0.01–10 MeV) for water treatment has been tested since the 1980s. The accelerated electrons penetrate the water surface and result in the formation of electronically excited species in the water, including various ionic species and free radicals. The maximum penetration depth of the accelerated electrons is directly proportional to the energy of the incident electrons (e.g. 7 mm, reported by Nickelsen (1994)). Therefore, water is irradiated in a thin film or as a sprayed aerosol. This process exhibits a high oxidizing power and little interference by the water matrix and the electrical efficiency is within the feasibility range (E_{EO} < 3 kWh/m³*order for most contaminants (Bolton et al., 1998). Due to the high capital costs for an electron accelerator (usually > 1 million US-$), the related risk potential from X-rays and hence the necessary security measures, further development of the electron beam process does not seem profitable.

3.3 Oxidation By-Products

Oxidation by-product generation during the application of AOPs is a critical factor for process viability. The abundance of nitrogen, halogens and DOM during disinfection of AOPs might lead to formation of organic halogenated by-products such as total organic halides (TOX), trihalomethanes (THM), haloacetic acids (HAA), haloacetonitriles (HAN), and inorganic by-products (e.g., chlorate, perchlorate and bromate). All AOPs are based on radical oxidation paths. However, OBP formation is diverse depending on radical type (e.g., OH, sulfate or chlorine radical), radical exposure, abundance of other influencing water constituents (e.g. radical scavengers), and direct reactions of applied oxidants such as for instance ozone or chlorine. Occurrence and health risks of by-products in drinking water as well as an overview of regulations and guidelines for specific disinfection by-products is comprehensively reviewed (Richardson et al., 2007; Stalter et al., 2016). While assessing the health risks from OBPs is challenging, there is a general desire to minimize their formation. Thus, in the following sections OBP formation is discussed considering main reaction mechanisms divided into reactions with inorganic and organic compounds to identify opportunities to minimize their formation

3.3.1 *Reactions with inorganic compounds*

The oxyhalides (chlorite, chlorate, perchlorate and bromate) are potential inorganic by-products of oxidation processes. Bromate (BrO_3^-) which is regulated in drinking water worldwide, can generally be formed in a pure ·OH reaction if Br^- is abundant in the feed water (von Gunten and Oliveras, 1998). However, this reaction is suppressed by DOM (Lutze et al., 2014) and in processes with excess H_2O_2 (UV/H_2O_2, Fenton reaction), where the oxidation of the intermediate HOBr to BrO_3^- is hindered by the fast reductive reaction with H_2O_2 to Br^- (k = 7.6 ·10^8 $M^{-1}s^{-1}$) (von Gunten, 2003b). Therefore, BrO_3^- formation is

negligible in most ·OH dominated systems. Chlorate and perchlorate formation during OH radical processes only occurs under certain conditions. The initial reaction of OH radicals with Cl^- is slow with a rate constant in the order of 10^3 $M^{-1}s^{-1}$ at pH 7 and formation of Cl radicals can therefore be neglected at neutral conditions (von Gunten, 2003b). If oxidative chlorine species are abundant (e.g., $ClO^·$, OCl^-), however, sequential oxidation by OH radicals to chlorate and perchlorate is possible. In $SO_4^{·-}$-based processes, BrO_3^- formation may be formed in a direct reaction of Br^- with $SO_4^{·-}$ ($k_{SO_4^{·-}}=3.5·10^9$ $M^{-1}s^{-1}$ (Redpath and Willson, 1975)) in the absence of DOM (Lutze et al., 2014). In addition, BrO_3^- formation may occur from $SO_4^{·-}$ reaction with Cl^- to form ·OH and $Cl^·$ turning $SO_4^{·-}$-based process into a $Cl^·$ and ·OH dominated process.

In some cases, ·OH are directly formed on active surfaces (e.g. the anode surface in eAOPs or the catalyst surface in heterogeneous cAOPs) and can only react within the diffusion limited zone of about <1 µm (Kapałka et al., 2009). These conditions might induce high radical densities at the surface allowing kinetically unfavored oxidation of Cl^-, Br^- and intermediate species forming bromate, chlorate and perchlorate (e.g. Bergmann and Rollin, 2007). A detailed literature review on OBP formation in eAOPs has recently been compiled by Chaplin (2014).

In ozone based AOPs at elevated bromide concentrations (> 100 µg/L), direct reaction of ozone can lead to 5 – 50% conversion of bromide to bromate, depending on ozone exposure. The fast decomposition of ozone in AOPs limits this reaction (von Gunten, 2003a), but significant bromate formation was still observed at elevated ozone dosages in the O_3/H_2O_2 process (Hübner et al., 2015b). Since chloride is not oxidized by ozone, chlorate formation is only relevant for ozonation, if pre-oxidation by reactive chlorine species is applied (von Gunten, 2003b). As discussed above, formation of chlorate, perchlorate and bromate is not critical in UV based AOPs, but other inorganic by-products can be formed. If DOM-containing water samples (10 mgC/L) are exposed to vacuum UV or LP-UV irradiation, H_2O_2 formation can reach up to 1.5 and 0.3 mg/L, respectively (Buchanan et al., 2006). Furthermore, photolysis of nitrate may form nitrite during UV irradiation. While the molar absorption coefficient of nitrate at $\lambda=254$ nm is low ($\varepsilon=4$ $M^{-1}cm^{-1}$), it increases dramatically below 240 nm (Sharpless and Linden, 2001) revealing higher nitrite formation potentials for MP and VUV systems.

3.3.2   *Reactions with organic compounds*

Reactions of ·OH with DOM generally involve hydrogen abstraction, electrophilic addition and radical combination. Despite their electrophilic character, these reactions are quite diverse and formation of significant OBP concentrations was not observed in ·OH dominated oxidation processes for general water applications. UV/H_2O_2, for example, was described as an AOP without significant OBP formation and no or minor increase of genotoxic activity if applied to surface water (Linden et al., 2005). Some studies, however, describe significant organic OBP formation during UV/H_2O_2 at high pH and Cl^- concentrations (>1 g/L) evaluated as adsorbable organic halides (AOX) (Baycan et al., 2007). Despite the slow reactivity of ·OH with Cl^-, at high concentrations of Cl^- formation of chlorine radicals ($Cl^·$, $Cl_2^·$) and active chlorine species (e.g., Cl_2, OCl^-, HOCl) is sufficient. These species can subsequently react with organic compounds by addition and substitution reactions resulting in halogenated OBPs (Oppenländer, 2003).

Main formation paths of halogenated organic OBPs (e.g., THM, HAN and HAA) are based on reactions between oxoacids/hypohalites (HOX/OX$^-$) and DOM, where the addition of halogens to DOM increases following the order Cl < I < Br (von Gunten, 2003b). Consequently, UV/Chlorine process may involve formation of AOX. In contrast, under mass transfer limited conditions organic OBPs are continuously generated (Bagastyo et al., 2012).

In ozone based AOPs, the main pathway for generation of halogenated organic compounds is still the reaction of HOX/OX$^-$ with DOM as described above. Formation of bromo-organic compounds (<10 µg/L depending on bromide concentration) during raw surface water ozonation has been confirmed by Huang et al. (2005). Since the oxidation of HOI and OI$^-$ by ozone is fast (pH<8), reaction of HOI with DOM can be neglected for ozonation processes (von Gunten, 2003b). Formation of OCl$^-$ is not relevant for ozonation based on the low reactivity of ozone with chloride, as described in Section 3.3.1 resulting in a low relevance of chlorinated organic OBPs. Of higher concern is the formation of N-Nitrosodimethylamine (NDMA), a highly carcinogenic substance mainly formed by chlorination of nitrogen- and organic carbon-containing waters. Some studies reported its occurrence after ozonation (Andrzejewski et al., 2008). Detailed reaction pathways for NDMA formation during ozonation are proposed by Yang et al. (2009). However, NDMA is not a major by-product of ozonation (von Gunten, 2003b; Andrzejewski et al., 2008). During UV/Chlorine NDMA formation could be inhibited in a pilot-scale system by quenching excess chlorine with thiosulfate (Sichel et al., 2011).
In UV-based processes, NDMA is effectively removed by UV photolysis (Stefan and Bolton, 2002; Mitch et al., 2003; Sharpless and Linden, 2003). Other AOPs are less efficient removing NDMA due to moderate and low second-order rate constants with ·OH (k_{OH}=3.8x10^8 M^{-1}s^{-1} (Wols and Hofman-Caris, 2012) and ozone (k_{O3}=0.052 M^{-1}s^{-1} (Lee et al., 2007)). A common strategy to control NDMA concentrations in water is the removal of precursors, such as dimethylamine, which can easily be oxidized by ozonation or AOP (Lee et al., 2007). However, also subsequent biological steps are effective to mitigate NDMA (Drewes et al., 2006).

Recently, researchers have shown the potential of mutagenic organic by-product formation during application of medium-pressure UV irradiation to water containing nitrate (Hofman-Caris et al., 2015; Kolkman et al., 2015). The photolysis products of nitrate (mainly peroxynitrite) react with DOM by hydroxylation, nitration and nitrosation reactions forming organic OBPs (Martijn et al., 2014). While potential reaction mechanisms have been proposed (Reckhow et al., 2010; Shah et al., 2011), a comprehensive understanding has not yet been completed. However, nitrated aromatic compounds are expected to be the most toxic OBPs formed in this process (Martijn et al., 2014).

3.4 Comparison of Advanced Oxidation Processes

E_{EO} values derived for a specific AOP are depending on the molecular structure, the physico-chemical characteristics, such as specific reaction rate constants, and the concentration range of the respective contaminant (only if >1 mg/L). Furthermore, water matrix, process capacity and energy independent process parameters (e.g., oxidant or

catalyst dose) can have a significant influence on the efficiency of the process. In general, E_{EO} values should only be determined for an AOP which is optimized with respect to oxidant demand, reactor geometry, and other process-specific parameters. All these interdependencies should be kept in mind while comparing different AOP technologies via E_{EO}. Hence, the boundary conditions in which E_{EO} values were determined are very important for the overall comparison of AOPs via E_{EO}.

It should be noted that additional energy demand for chemicals or catalysts is not reflected within this figure of merit. The demand for auxiliary oxidants (e.g. H_2O_2), however, can be reflected within the E_{EO} concept by regarding H_2O_2 as "stored electric energy" (Rosenfeldt et al., 2006). For example, Müller et al. (2001) calculated an equivalent of 10 kWh for 1 kg of H_2O_2 (100%) based on the commercial prices in Germany. However, the majority of published E_{EO} values are limited to the electricity which is directly used in the process, e.g. for ozone generation or UV lamp operation.

Several peer-reviewed journal articles deal with the direct comparison of different AOPs in a defined experimental setup with controlled conditions, i.e. in terms of water quality to be treated, target contaminant and other process conditions, with the aim to reveal the most efficient AOP technology. However, many of these studies are lacking important information, neglecting relevant parameters or testing removal of substances with specific reactivity to oxidants other than ·OH, e.g. ozone-reactive or photolytically degradable compounds. Furthermore, comparison is only conducted in few water matrices and generalization of those results and their transfer to application with other water types, contaminants etc. should therefore be made with careful consideration of the respective conditions.

For this reason, we critically reviewed and compared reported E_{EO} values from different AOPs. Results are discussed and put in context to studies showing direct comparison, if available. In addition, we analyzed major influencing factors on E_{EO} determination based on literature data for the UV/H_2O_2 process.

3.4.1   *Comparative screening of E_{EO} values for different AOPs*

E_{EO} values for numerous AOPs from literature data are illustrated in Figure 4 as box plots sorted according to their respective median values. A summary of all data including specific information on water type, system size and measured compounds is given at Mendeley Data (http://dx.doi.org/10.17632/n7h8kb4dfh.2). Only data meeting the following criteria were included in the figure:

- Incorporated data is published in a peer-reviewed process
- Manufacturer data and data from non-peer reviewed sources are included if detailed information about the experimental setup is given
- If kinetic data is available, compounds, which are susceptible to direct oxidation by e.g. ozone or UV photolysis will not be regarded. Threshold values for rate constants in O_3- and UV-based processes are set at $k_{O_3} < 10$ $M^{-1}s^{-1}$ and $k_{UV} < 10^{-5}$ m^2/J

Data evaluation was conducted in three steps: screening of E_{EO} values, single outlier detection and removal and descriptive statistics. Outlier detection was performed by the Dixon test assuming log-normal distribution for all data sets using an online tool available at http://contchart.com/outliers.aspx. Significance testing was performed using the two-sample t-test provided by another online tool (http://www.evanmiller.org/ab-testing/t-test.html) assuming log-normal distribution for all data-sets.

Reported E_{EO} values for individual AOPs often vary by several orders of magnitude. In case of ozonation, the strong variability might be explained by the dependence of radical formation from water matrix since it is only initiated by hydroxide ions at elevated pH or from ozone reactions with organic matter. Little variability of other processes might either indicate lower sensitivity to water quality and system design or limited experimental differences in literature data, e.g. oxidation with microwaves was only tested in ultrapure water.

Despite cases of high variability, significant differences between AOPs can be observed from the literature study. Based on median values, AOPs are classified in three groups: processes with median E_{EO} values <1 kWh/m³ (O_3, O_3/H_2O_2, O_3/UV, UV/H_2O_2, UV/persulfate, UV/Chlorine and electron beam) represent a realistic range for full-scale application (group 1). Photo-Fenton, plasma and eAOP with median E_{EO} values of 2.6, 3.3, and 38.1 kWh/m³ (1-100 kWh/m³), respectively, are likely too energy intensive for most practical applications (group 2). However, they might still provide attractive solutions for specific challenges and full-scale applicability of these processes should be further investigated. E_{EO} values for group 2 processes are significantly higher than values of group 1 ($p=0.045$). Processes with $E_{ÉO}$ values >100 kWh/m³, i.e. UV-based photocatalysis, ultrasound and microwave-based AOPs representing high median values of 335, 2,616 and 543 kWh/m³, respectively, are considered as not (yet) energy efficient AOPs. Significance of difference between group 2 and 3 is calculated as $p=0.002$.

There are only few quality studies directly comparing processes from these different groups. A direct comparison of UV/H_2O_2 and BDD treatment for aniline removal from synthetic wastewater solutions confirmed lower E_{EO} values for UV/H_2O_2 by about 30% (Benito et al., 2017). However, extensive concentrations of H_2O_2 were applied in this study (1-5 g/L) that might have influenced calculated E_{EO} values of UV/H_2O_2 by re-scavenging of $\cdot OH$ by H_2O_2.

Observed differences between AOPs in the first group are statistically not significant ($p>0.2$ in between all AOPs) and most likely depend on experimental conditions. This is confirmed by several studies comparing O_3/H_2O_2 and UV/H_2O_2. Sutherland and coworkers published a comprehensive evaluation of MTBE oxidation from five contaminated groundwaters with highly variable water quality characteristics (Sutherland et al., 2004). Depending on water type and adjusted pH, either O_3/H_2O_2 or UV/H_2O_2 achieved lower E_{EO} values. In contrast, Lester et al. (2011) reported lowest $E_{ÉO}$ values for O_3/H_2O_2 followed by O_3, $UV/H_2O_2/O_3$, UV/O_3 and UV for pharmaceutical degradation in phosphate buffer. Also, Müller et al. (2001) showed advantages of the O_3/H_2O_2 combination in comparison to UV/H_2O_2 and UV/O_3. A recent study compared the efficiency of UV/PDS and UV/H_2O_2 during iodoacids degradation, considering most relevant influencing factors (e.g. photo-susceptibility and process capacity) (Xiao et al.,

2016). Special emphasis was directed to water matrix and oxidant dose effect. Results revealed higher energy efficiencies for the sulfate radical based AOP by a factor of >3. However, comparison of these processes using single compounds or specific compound groups needs to be evaluated carefully since sulfate radicals react more selectively than ·OH.
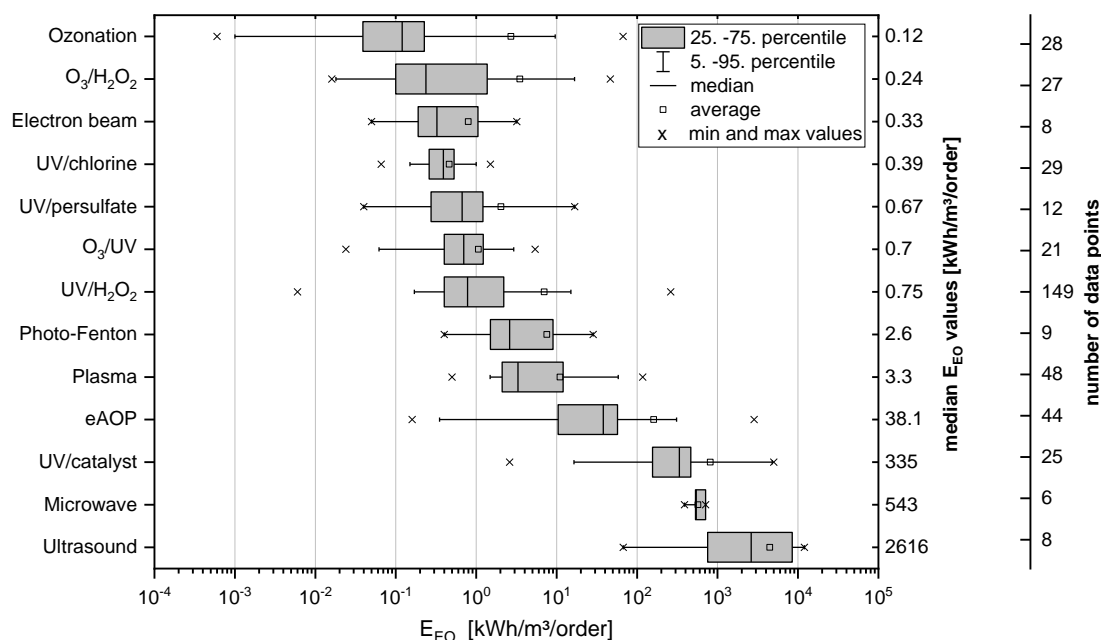
Figure 4: Overview of published E_{EO}-values of different AOPs sorted according to median values. For O_3- and UV-based AOP data, only substances resistant to direct ozonation/photolysis are shown (references are shown in Table S1). Median values and number of data points are reported on the second and third y-axis, respectively.

3.4.2 *Principal influences on E_{EO}-values shown at the UV/H₂O₂ process*

Most boxplots for individual AOPs in Figure 4 reveal high variances, being mainly based on data variability considered in this review. Water quality, process capacity and the selection of target chemicals are key parameters, which may lead to large deviations of E_{EO} values within one process. Effects of these factors is exemplarily illustrated in the following section using the dataset of UV/H₂O₂, which is one of the most intensively investigated AOPs and therefore supplies high data density of E_{EO} values (n=149, excluding single outliers and data of photo-susceptible compounds). However, transferability of influencing factors is not ensured for other AOPs since most influences are process specific.

3.4.2.1 *Influence of process capacity*

E_{EO} values from UV/H₂O₂ studies conducted at laboratory, pilot and full scale are illustrated in Figure 5. Median E_{EO} values decrease with process capacity from 2.2 kWh/m³ at lab-scale to 0.68 and 0.5 kWh/m³ for pilot- and full-scale applications, respectively. A significant difference could be observed ($p<0.05$) between lab- and pilot-scale data. The median values indicate that up-scaling enhances energy efficiency, which

confirms the findings from Bolton and Stefan (2002). Results furthermore emphasize that comparison of lab-scale energy consumption not necessarily represents operation at full-scale. If possible, energy demand should rather be estimated based on full-scale system design with relevant operational parameters (i.e., oxidant dosage, UV fluence) determined in standardized lab- or pilot-scale experiments.
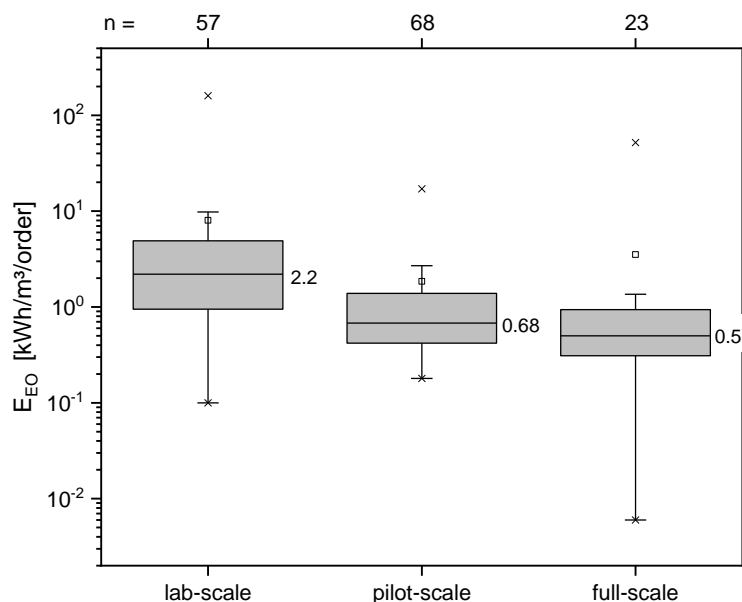
Figure 5: Overview of published E_{EO}-values of the UV/H_2O_2 process, classified into lab-, pilot- and full-scale data. n refers to the number of data points behind the boxplots. Median values are reported next to the 50th percentile line.

3.4.2.2 Influence of compound reactivity

Energy efficiency of AOPs is also dependent on compound reactivity. Therefore, gathered E_{EO} values from reviewed UV/H_2O_2 publications were correlated to second-order rate constants (k_{OH}) of photo-resistant target chemicals. Results indicated a slightly negative correlation ($R^2=0.21$), confirming, that substances with higher k_{OH} values are more efficiently oxidized with a lower energy effort (Figure S1). However, due to the low correlation coefficient the influence of other parameters (e.g. process capacity) is assumed to be higher.

3.4.2.3 Influence of water quality

Water quality mainly affects the UV/H_2O_2 process by UVT and radical scavengers. Therefore, E_{EO} values were investigated based on water characteristics reported from the respective article. Since numerous water types were included in all data gathered, ranging from ultrapure lab water to industrial wastewater effluents, E_{EO} values were classified into main water application groups: pure water, drinking water, groundwater and wastewater applications. Pure water applications include lab-scale experiments with deionized and ultrapure water but also pilot-scale applications with reverse osmosis permeate (i.e. in water reuse). Drinking water applications summarize UV/H_2O_2 processes with surface water after pre-treatment with various process combinations.

Groundwater applications include AOPs at contaminated sites as well as drinking water applications from groundwater. Wastewater consists of secondary and tertiary effluent from municipal wastewater treatment plants and industrial applications. Resulting E_{EO} values of pure water, drinking water, groundwater, and wastewater applications are presented in Figure 6 as box plots. Median E_{EO} values of each application were determined as 2.7, 0.63, 2.7 and 2.2 kWh/m³, respectively. However, no significant difference could be observed between different groups ($p > 0.05$). The concentration of radical scavengers and UVA are the most influential parameters for radical yield and radical oxidation efficiency. Consequently, waters with higher scavenger concentrations (and different scavenger composition) and higher UVA should result in higher E_{EO} values. Surprisingly, ultrapure water applications reveal the highest median E_{EO} value in this comparison. A possible explanation for this finding might be the predominant use of pure water in lab-scale experiments which biases the illustration as already discussed in Section 3.4.2.1. Data comparison from drinking and wastewater applications reveal higher energy needs with increasing scavenger content. Especially, DOC and consequently UVA are expected to be higher in this order. In contrast to drinking water, the median E_{EO} value from groundwater applications is similar to wastewater oxidation. Groundwater may contain strongly variable inorganic concentrations, e.g. alkalinity (HCO_3^-/CO_3^{2-}), but also reduced species like manganese and iron, which might significantly scavenge OH radicals.

Overall, the operational classification of AOPs presented in Figure 5 did not suggest any significant effects of water matrix on E_{EO} values, probably because the selected categories like pure water, drinking water, groundwater and wastewater are not specific enough and can include a wide range of different applications and water qualities. Therefore, a direct correlation of water quality parameters with reported E_{EO} values was also investigated. Considered as most relevant parameters, DOC, UV transmittance and turbidity (reported as NTU) data were provided for 124, 131 and 31 of the reviewed 147 data sets, respectively. A direct relationship within the reviewed data set between E_{EO} values and DOC concentrations, UV transmittance or NTU, however, could not be revealed (Figure S2 and Figure S3).
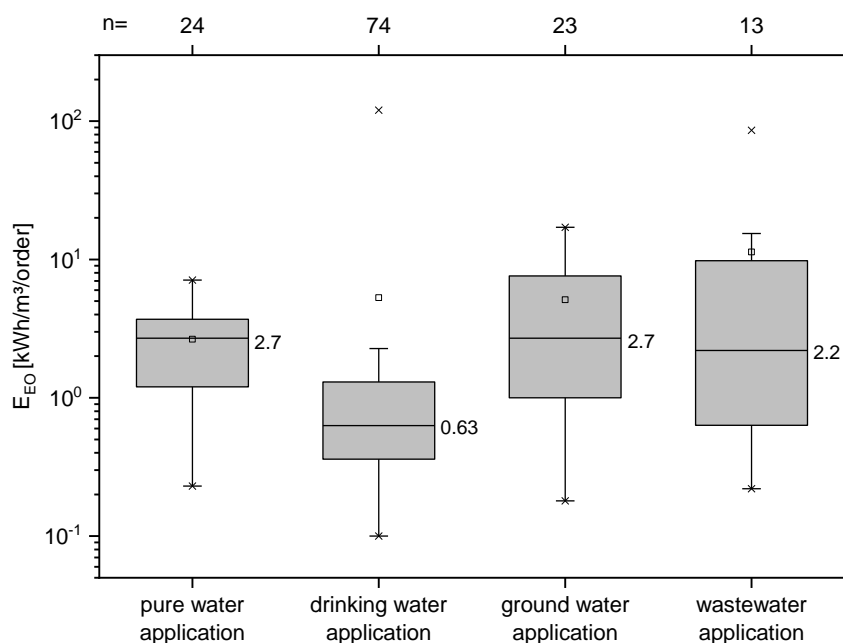
Figure 6: Reviewed E_{EO} values of the UV/H_2O_2 process: Effect of different water matrix applications; n refers to the number of data points behind the boxplots. Median values are reported next to the 50th percentile line.

3.4.2.4 Influence of lamp type

The influence of different lamp types on E_{EO} values is illustrated in Figure 7. MP UV lamps result in significantly higher E_{EO} values compared to LP lamps ($p<0.001$). The respective median values can be determined as 1.0 and 0.4 kWh/m³. This is not surprising, since the molar absorption coefficient of H_2O_2 increases at wavelengths <260 nm and LP lamps depict higher (<35% at 254 nm) energy efficiencies than MP lamps (<10 % at 254 nm). Inevitably, LP lamps yield in a higher H_2O_2 activation and consequently in lower E_{EO} values. This was also confirmed by Rosenfeldt et al. (2005), who directly compared LP and MP UV lamps for the oxidation of 2-methyl-isoborneol (2-MIB) and geosmin. Raw blend surface water and filtered clearwell water were used in lab-scale reactors. E_{EO} values revealed that LP lamps can be more energy efficient than MP lamps for ·OH generation.
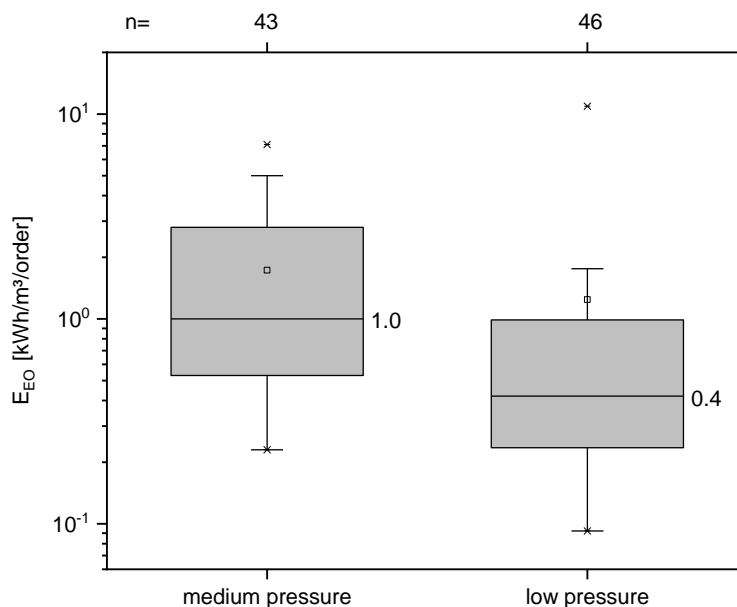
Figure 7: Overview of published E_{EO}-values of the UV/H_2O_2 process, classified into data based on medium- and low-pressure lamps. Headline shows the number of data points behind the boxplots. Median values are reported next to the 50th percentile line.

3.5 Conclusions

This study provides a critical review of different established and emerging AOPs including a mechanistic discussion of process-specific by-product formation. To facilitate a comparison of energy efficiency, data were collected for various AOPs in an extensive analysis of peer-reviewed journal articles and critically compared based on reported E_{EO} values. Despite high variability of results from individual processes, significant differences between AOPs efficiency were observed. Based on reported E_{EO} values, processes were classified into (1) AOPs with median E_{EO} values of <1 kWh/m³ (O_3, O_3/H_2O_2, O_3/UV, UV/H_2O_2, UV/persulfate, UV/Chlorine, electron beam), (2) processes with median E_{EO} values in the range of 1-100 kWh/m³ (Photo-Fenton, plasma, and electrolytic AOPs) and (3) UV-based photocatalysis, ultrasound, and microwave-based AOPs (median E_{EO} values of >100 kWh/m³), which are considered as not (yet) energy efficient AOPs. A more detailed evaluation of data for the UV/H_2O_2 process showed highest impact of UV-lamp type, water matrix, and process capacity (lab-scale vs. pilot- and full-scale) on resulting E_{EO} values. No significant correlation could be observed between E_{EO} values and compound reactivity with OH radicals. In addition, reviewed literature indicates that by-product formation from hydroxyl radicals is not critical unless formed at high density on surface areas (e.g. in electrolytic AOPs). However, AOPs involving other oxidants such as ozone, sulfate radicals or chlorine radicals need to be evaluated in more detail since site- and process-specific by-products might be formed.

This study confirmed the main limitation to use the E_{EO} concept for a general comparison of different AOPs due to the variability of the above-mentioned influencing factors. However, if all factors are considered within a direct comparison, the E_{EO} concept provides a powerful figure of merit to directly compare and evaluate AOPs based on energy efficiency.

4. UV/H₂O₂ Process Stability and Pilot-Scale Validation for Trace Organic Chemical Removal from Wastewater Treatment Plant Effluents

Abstract

This study investigated the removal of 15 trace organic chemicals (TOrCs) occurring at ambient concentrations from municipal wastewater treatment plant effluent by advanced oxidation using UV/H₂O₂ at pilot-scale. Pseudo first-order rate constants (k_{obs}) for photolytic as well as combined oxidative and photolytic degradation observed at pilot-scale were validated with results from a bench-scale collimated beam device. No significant difference was determined between pilot- and lab-scale performance. During continuous pilot-scale operation at constant UV fluence of 800 mJ/cm² and H₂O₂ dosage of 10 mg/L, the removal of various TOrCs was investigated. The average observed removal for photo-susceptible ($k_{UV}>10^{-3}$ cm²/mJ; diclofenac, iopromide and sulfamethoxazole), moderately photo-susceptible ($10^{-4}<k_{UV}<10^{-3}$ cm²/mJ; climbazole, tramadol, sotalol, citalopram, benzotriazole, venlafaxine and metoprolol), and most photo-resistant ($k_{UV}<10^{-4}$ cm²/mJ; primidone, carbamazepine and gabapentin) compounds was 90%, 49% and 37% including outliers, respectively. The poorly reactive compound TCEP was not significantly eliminated during pilot-scale experiments. Additionally, based on removal kinetics of photo-resistant TOrCs, continuous pilot-scale operation revealed high variations of OH radical exposure determined from removal kinetics of photo-resistant TOrCs, primarily due to nitrite concentration fluctuations in the feed water. Furthermore, a correlation between OH radical exposure and scavenging capacity could be determined and verified by mechanistic modeling using UV fluence, H₂O₂ dosage, and standard water quality parameters (i.e., DOC, NO_3^-, NO_2^- and HCO_3^-) as model input data. This correlation revealed the possibility of OH radical exposure prediction by water matrix parameters and proved its applicability for pilot-scale operations.

4.1 Introduction

In recent years, trace organic chemicals (TOrC) such as pharmaceutical residues, personal care products, emerging pesticides, and industrial chemicals have been detected and extensively investigated in the aquatic environment and in all parts of the water cycle (Lim, 2008; Blum et al., 2017; Hofman-Caris et al., 2017; Yang et al., 2017b).

Besides urban and agricultural run-off, wastewater treatment plant (WWTP) effluents are considered to be the most significant TOrC emitters to the aqueous environment (Gros et al., 2010; Luo et al., 2014; Dong et al., 2015a). Although concentrations hardly exceed µg/L concentrations, persistent substances remain in WWTP effluents being discharged in surface waters, since conventional physical and biological wastewater treatment can only partially remove these substances (Lim, 2008; Zhang et al., 2008; Luo et al., 2014). For the removal of these compounds from WWTP effluents, advanced oxidation might be a promising treatment approach. Advanced oxidation processes are generally defined as processes that intentionally form highly reactive radicals in-situ (Comninellis et al., 2008; Yang et al., 2014). Specifically, OH radicals produced are known for their rapid and non-selective oxidation of organic water contaminants with second-order reaction rate constants in the range of 10^8 - 10^{10} $M^{-1}s^{-1}$. In current practice, utilization of AOPs is mostly limited to highly treated wastewater effluents including reverse osmosis treatment and advanced drinking water treatment with high UVT.

Among UV-based AOPs, UV/H₂O₂, where H₂O₂ is directly activated by UV light to form two OH radicals, is a commonly applied AOP in water reuse and advanced drinking water treatment for contaminant as well as taste and odor removal. TOrC removal during low pressure UV/H₂O₂ is achieved by two major reaction pathways, direct photolysis by UV-C irradiation at 254 nm and oxidation by hydroxyl radicals formed in-situ. Since generated OH radicals react unselectively with all water constituents, transformation of target compounds in wastewater is competing with oxidation of other organic and inorganic compounds. The occurrence of so-called radical scavengers, which terminate radical chain reactions, can significantly reduce oxidation efficiency in AOPs (Keen et al., 2012). Furthermore, changes in UVT directly affect the activation of H₂O₂. Therefore, UV/H₂O₂ effectiveness is highly susceptible to water matrix changes. The influence of scavenging on UV/H₂O₂ has been investigated thoroughly (Liao et al., 2001; Rosenfeldt and Linden, 2004) and a good overview of scavengers and their reactivity with OH radicals is given by Wols and Hofman-Caris (2012). Kinetic models can be adopted to estimate the influence of radical scavengers on the degradation performance and represent a useful tool to predict TOrC degradation by UV/H₂O₂ in different water matrices as proposed by Bolton and Stefan (2002) and Wols et al. (2013).

UV/H₂O₂ is a thoroughly examined AOP (Pereira et al., 2007b) for all kinds of water applications, with most studies performed at laboratory scale (Yuan et al., 2011a). Only a limited number of studies, however, have been carried out specifically on wastewater effluent at the laboratory (Rosario-Ortiz et al., 2010; Keen and Linden, 2013a; Yu et al., 2015) or pilot-scale (Audenaert et al., 2011; Köhler et al., 2012; De La Cruz et al., 2013; Lester et al., 2014; Merel et al., 2015; Cedat et al., 2016). Some pilot-scale studies on UV/H₂O₂ investigated its viability for TOrC removal (Sarathy et al., 2012; Wang et al., 2015; Cedat et al., 2016; Chu et al., 2016; Gerrity et al., 2016; Miralles-Cuevas et al., 2016). However, to the best of our knowledge, verifying pilot-scale studies using data from standardized lab-scale systems combined with mechanistic modeling efforts are lacking in the peer-reviewed literature. Furthermore, little is known about UV/H₂O₂ applicability for municipal wastewater effluents with respect to OH radical scavenging across changing water qualities (Gerrity et al., 2016; Lee et al., 2016).

In this study, we characterize the applicability of UV/H_2O_2 for advanced municipal wastewater treatment using lab- and pilot-scale set-ups in this chapter. Piloting results are directly compared to results conducted using a lab-scale collimated beam device (CBD) to verify the up-scaling effort. A total of 15 TOrCs occurring at ambient concentrations and representing a range of different photolytic and OH radical reactivities were measured. To assess the viability of UV/H_2O_2 for continuous treatment of tertiary effluents, a comprehensive investigation of OH radical scavenging caused by different water quality parameters, such as dissolved organic carbon, nitrite, nitrate and alkalinity, was performed during continuous operation of a pilot-scale UV/H_2O_2 system. Finally, the experimental results were compared to mechanistic modelling estimations.

This publication tested the hypotheses that UV/H_2O_2 is applicable for advanced oxidation of wastewater effluent achieving a substantial removal of TOrCs (Hypothesis № 1.1) and the removal of TOrCs during UV/H_2O_2 can be predicted by mathematical models considering the water parameters DOC, NO_2^- and alkalinity, process parameters and specific kinetic data of target compounds (Hypothesis № 2).

4.2 Experimental Approach

4.2.1 UV-AOP pilot-scale experiments

4.2.1.1 Description of the pilot-scale setup

The shipping container-based UV/AOP pilot-scale plant was designed by Wedeco (Xylem, Germany) and installed on site at the WWTP Gut Marienhof (Munich, Germany) with a capacity of 11-35 m³ per hour. In 2015, the WWTP with a capacity of one million population equivalents treated approximately 55.7 million m³ of wastewater. The treatment plant consists of a mechanical treatment stage including screens, aerated sand-/fat traps and preliminary sedimentation, followed by a two-stage activated sludge process for biological carbon and nutrient removal. The activated sludge process is a two-stage biological process with an intermediate clarification stage. The first stage has a solids retention time of 2-3 days and the second stage of 6-8 days. The water is then filtered using tertiary granular media filters with a resulting UVT at 254 nm of 65-75%. Relevant water quality parameters of the granular media filter effluent are reported in Table 3. During summer months, methanol is added to a third of all 24 granular media filter cells as an external carbon source for denitrification. Furthermore, the filter effluent is disinfected by a LP-UV system at a targeted fluence of 50 mJ/cm² from May-September to maintain microbial bathing water quality in the river Isar.

The pilot-scale system consisted of two LP-UV reactors (Wedeco LBX 90e and LBX 10, Xylem, Germany), operated to deliver high (100-4,000 mJ/cm²) and low (40-400 mJ/cm²) levels of fluence, respectively (see specifications in Table 3). The pilot system was fed with tertiary effluent delivered by an external process water pump station. The inflow was divided into two streams and controlled by diaphragm valves (MV310, ASV Stübbe, Germany). Flow rates were measured by magnetic inductive flow sensors (Proline Promag 50, E+H Messtechnik, Germany).

Table 3: Technical specifications of the UV/AOP pilot-plant

LP-UV reactors	LBX 90e	LBX 10
LP-UV lamp performance	4 x 315 W	3 x 80 W
Max. flowrate [m³/h]	35	11
Applicable fluence [mJ/cm²]	100-4,000	40-400
Reactor volume [L]	45	13

UV intensity was measured by two internal radiometers and corrected by manufacturer specific correction factors based on UVT (Figure S5, SI). UVT was measured by an online flow through sensor (Wedeco TMO IV, Xylem, Germany). Both reactors were equipped with mechanical cleaning wipers to minimize the influence of deposits resulting in reduced intensity over time. H_2O_2 was injected by a magnetic dosing pump (gamma/x, ProMinent, Germany) with a maximum flow rate of 6.8 L/h. Homogeneous distribution of the oxidant was maintained by a static mixer (series 400, Statiflo, Germany). H_2O_2 influent and effluent concentrations were measured with a potentiostatic online sensor using bypass pipes (NEON Des, Kuntze Instruments, Germany). Influent and effluent samples were taken right before and after each reactor. After UV oxidation, both reactor streams were combined before the water was discharged.

4.2.1.2 Determination of removal kinetics in pilot experiments

Short-term experiments were conducted during dry weather conditions. Flow rates of the pilot system for respective exposure times were calculated and adjusted based on desired fluences, current UV intensities, and UVT. A fluence range of 40-160 mJ/cm² was maintained in the smaller reactor LBX 10 and a range of 200-2,000 mJ/cm² in reactor LBX 90e. H_2O_2 dosing at 10 mg/L was adjusted based on respective flow rates. Before sampling, the system was constantly operated with a minimum of ten reactor volumes to establish steady-state conditions in the pilot-scale system. While effluent samples were taken for each setting, influent samples were taken hourly. The samples were filled in amber glass bottles and stored at 4°C pending analyses. During sampling, UVT and H_2O_2 concentration was analyzed on site. Online measurement of H_2O_2 was validated for each sample by manual analysis directly after sampling as described in Section 4.2.3.2. In addition, nitrate and nitrite concentrations as well as alkalinity were directly analyzed on site. DOC and TOrCs analyses were conducted within 24 hours after sampling.

4.2.1.3 Continuous operation of the pilot-scale system

To assess a continuous operation of UV/H₂O₂ processes at the WWTP as a function of naturally fluctuating feed water conditions, two independent experiments were conducted over a period of five days each. The first experiment was scheduled during a dry weather period in the summer from 08/29 - 09/02/2016 (dry weather). The second experiment was conducted during a wet weather period from 09/26 - 09/30/2016 and was dominated by several heavy rain events (rain-event). Each day, influent and effluent samples were taken at 6 and 9 a.m. and 12, 3, 6 and 8 p.m. For both campaigns, a fluence of 800 mJ/cm² and a H_2O_2 dose of 10 mg/l were targeted. Sampling procedure and

analyses were conducted analogously to the determination of removal kinetics experiment.

4.2.2 Determination of removal kinetics in laboratory-scale experiments

Lab experiments were conducted using a collimated beam device containing three 15 W low-pressure Hg UV lamps (UV Technik Meyer, Germany) which were installed in an aluminum housing with mounted cooling ribs. For active heat dispersion two air coolers were installed to keep the lamps at optimal irradiation temperature of 35-40°C. A black 20 cm PVC-tube with a diameter of 10 cm was attached to the aluminium housing serving as a quasi-collimator. To increase radiation through the collimator tube, an anodized aluminum UV-C reflector (UV Technik Meyer) was attached to the inside of the housing lid bent at both sides at an angle of 45°. Below the collimator, a xy-cross slide table with a magnetic stirrer placed on top included the mounting for the petri dishes. Resulting UV-C irradiation intensity at the sample position was determined as 1-1.4 mW/cm² on average across the petri dish by a certified UV-C surface radiometer (sglux, Germany). To verify measurement accuracy of UV intensity, a radiometer factor of 0.997 (actinometer/radiometer) was determined by uridine actinometry as described in Scheurer et al. (2014).

Experimental procedure followed the standardized method for fluence determination (Bolton and Linden, 2003). Fluences of 40-2,000 mJ/cm² were applied to 30 mL of sample in a 100 mm glass petri dish. H_2O_2 was added directly before UV exposure from a stock solution (1 g/L H_2O_2). TOrCs were present at ambient levels and not spiked into the wastewater. Dark experiments were conducted in the same experimental set-up in triplicates applying dosages of 5, 10, 15 and 20 mg/L H_2O_2 to investigate direct TOrC attenuation by H_2O_2. After 30 minutes, residual H_2O_2 was quenched in dark experiment samples with Na_2SO_3 (2:1 molar ratio). All samples were stored in amber glass bottles at 4°C and analyzed for DOC and TOrCs within 24 hours. For verification of the pilot-scale results, a composite sample of the wastewater effluent was taken at the inlet to the AOP reactors hourly during pilot-scale operation which was subsequently used for lab-scale experiments the following day.

4.2.3 Analytical Methods

4.2.3.1 Trace organic chemical analysis

For TOrC quantification, all samples were filtered through 0.22 µm PVDF syringe filters (Berrytec, Germany). Samples were measured using high performance liquid chromatography (Knauer PLATINBLUE UHPLC) coupled with tandem mass spectrometry (LC-MS/MS) (SCIEX QTRAP 6500) with direct injection. Isotope dilution was used to account for matrix suppression and instrument variability. More detailed description of the analytical method can be found elsewhere (Müller et al., 2017). TOrCs as well as isotope labelled analytical standards for TOrCs analysis were purchased of analytical grade. All solvents used for liquid chromatography were HPLC-grade. Analyzed TOrCs are summarized in Table 4 along with previously reported kinetic data for the reaction with UV light (quantum yield and molar absorption) and OH radicals and their measured concentrations in wastewater during lab- and pilot-scale experiments.

Table 4: Average TOrC concentrations and summary of compound specific reaction rate constants for direct UV photolysis and OH radical oxidation

Compound	Limit of quantification (LOQ) [ng/L]	Average TOrC concentration [ng/L]			OH radical oxidation	Direct UV photolysis			References
		Lab-scale experiment	Pilot-scale experiment		k_{OH} [10^9 M^{-1} s^{-1}]	ϕ [10^{-2} mol/E]	ε [m²/mol]	k_{UV} [10^{-5} m²/J]	
			Short-term (n=5)	Continuous (n=58-60)					
Diclofenac	5	2,610	2,540 ± 80	2,160 ± 790	8.2	23	680	76.5	Wols et al. (2014)
Iopromide	50	6,700	5,880 ± 830	3,860 ± 2,330	3.3[a]	3.9	2,100	40	Canonica et al. (2008)
Sulfamethoxazole	10	280	260 ± 10	300 ± 60	6.3	8.4	1,300	53.4	Wols et al. (2014)
Benzotriazole	50	10,520	9,750 ± 210	6,950 ± 2,030	8.0[b]	1.6	614	4.8	Bahnmüller et al. (2015)
Phenytoin	5	<LOQ	<LOQ	11 ± 3	6.28	27.9	126	17.2	Yuan et al. (2009)
Tramadol	5	570	550 ± 10	340 ± 50	6.3	n/a	n/a	n/a	Zimmermann et al. (2012)
Climbazole	5	210	200 ± 5	140 ± 20	n/a	17.7	0.616	5.17	Liu et al. (2016b)
Sotalol	5	70	70 ± 5	60 ± 11	7.9[a]	39	37	7.05	Wols et al. (2014)
Citalopram	5	210	200 ± 5	170 ± 30	n/a	0.026	400	0.05	Kwon and Armbrust (2005)
Venlafaxine	2.5	490	440 ± 10	360 ± 60	8.8	9.7	38	1.8	Wols et al. (2014)
Metoprolol	2.5	530	500 ± 5	370 ± 70	8.1	6.6	33	1.06	Wols et al. (2014)
Primidone	25	140	140	120 ± 20	6.7	8.2	22	0.882	Real et al. (2009)
Carbamazepine	5	520	490 ± 10	530 ± 210	8.2[c]	0.06	607	0.178	Pereira et al. (2007b)
Gabapentin	2.5	4,010	3,960 ± 60	3,670 ± 780	9.1	n/a	n/a	-	Lee et al. (2014)
TCEP	50	<LOQ	<LOQ	120 ± 30	0.56	n/a	n./a	-	Watts and Linden (2009)

[a] Huber et al. (2003); [b] Vel Leitner and Roshani (2010); [c] Wols and Hofman-Caris (2012)

4.2.3.2 Bulk water parameters

H_2O_2 concentration in wastewater samples was determined according to DIN 38 409 H15 using titanium (IV) oxysulfate colorimetry (DIN 38 409, 1987). Hydrogen peroxide solution (H_2O_2; 50%; technical grade) was obtained from Bernd Kraft GmbH, Germany. Titanium (IV) oxysulfate solution (2%) for H_2O_2-measurements in wastewater was purchased from Sigma-Aldrich. Bulk water parameters were measured using Hach cuvette tests: nitrate (LCK 340, HACH, Germany), nitrite (LCK 341/342, HACH, Germany), acid capacity $K_{a\,4.3}$ (LCK 362, HACH, Germany). UVT_{254}, as well as all cuvette tests were analyzed using a DR6000 UV/Vis spectrophotometer (HACH, Germany). DOC was analyzed after filtration through cellulose nitrate membrane filters with a pore size of 0.45 μm (Sartorius AG, Germany) on a varioTOC cube (elementar, Germany).

4.2.4 Modeling

Prediction of lab- and pilot-scale experiments was performed by modeling. Assuming only direct photolysis and OH radical based TOrC removal, pseudo first-order kinetics with linear correlation of the logarithmic relative concentration (ln c/c_0) to the fluence (F') can be assumed for low TOrC concentrations:

$$ln\left(\frac{c}{c_0}\right) = -kF' = -(k_{UV} + k_{radical})F' \tag{13}$$

In this equation, k represents the apparent degradation rate constant for a specific compound, which equals the sum of the photolytic rate constant k_{UV} and the pseudo first-order oxidation rate constant with OH radicals, $k_{radical}$. It can be derived according to Wols et al., (2013) and Bolton and Stefan (2002) as shown in equation 14. For the use of monochromatic LP lamps, the photolytic reaction rate constant k_{UV} can be calculated from the quantum yield ϕ [mol/Einstein], the molar absorption coefficient ε [L/mol/cm], and the energy of a mole of photons at 254 nm U_{254} [J/Einstein]. The oxidative degradation rate constant $k_{radical}$ is a function of the photolysis of H_2O_2 (where the index 'H' represents hydrogen peroxide), the peroxide concentration, the compound specific second-order rate constant k_{OH} for the reaction with OH radicals and the overall scavenging capacity $\sum(k_{i,OH}\cdot[S_i])$ [s^{-1}] which is described as the product of a scavenger concentration multiplied by its second-order rate constant with ·OH (Kwon et al., 2014). In this study, scavenging capacity was calculated by using rate constants summarized in Table 5. The rate constant for DOC was selected to optimize model results for oxidation of photo-resistant compounds carbamazepine and primidone in lab- and pilot-scale comparison experiments. This value was then used to calculate scavenging capacity during long-term operation. Concentrations of scavengers were converted into molar concentration units.

$$k = k_{UV} + k_{radical} = \ln(10)\frac{\Phi\varepsilon}{U_{254}} + 2\ln(10)\frac{\Phi_H\varepsilon_H}{U_{254}}\frac{k_{\cdot OH}[H_2O_2]}{\Sigma(k_i[S_i]) + k_H[H_2O_2]} \tag{14}$$

For OH radical based reactions, a steady state OH radical concentration is assumed. Compound specific values for ϕ, ε, k_{UV} and k_{OH} are given in Table 4.

4.3 Results and Discussion

4.3.1 *Lab-scale determination of UV photolysis and OH radical enhanced removal*

Lab-scale CBD experiments with effluent from the WWTP were conducted to quantify oxidant specific removal of TOrCs and to evaluate UV/H$_2$O$_2$ viability as an advanced treatment process for tertiary treated effluents. H$_2$O$_2$ experiments without UV irradiation revealed degradation of <10% for the 15 TOrCs investigated in all experiments without significant influence of H$_2$O$_2$ concentration on compound removal.

The observed pseudo first-order degradation rate constants of TOrCs (k$_{obs}$) from lab-scale UV photolysis and UV/H$_2$O$_2$ experiments are compared in Figure 8. Kinetic data for TCEP and phenytoin are not shown since their ambient concentrations in the tertiary effluent were below the limit of quantification in this experiment. For each compound, the natural logarithm of the relative residual concentration c/c$_0$ from 11 experiments at different UV fluences is plotted as a function of UV fluence. Regression curves were determined and the respective slopes (representing k$_{obs}$) were obtained. Exact values of k$_{obs}$ and R^2 are reported in Table S2 (SI). The TOrCs presented in Figure 8 are sorted according to their observed photolytic reactivity and classified based on published k$_{UV}$ values into photo-susceptible (>1·10^{-3} cm^2/mJ), moderately photo-susceptible (1·10^{-4} − 1·10^{-3} cm^2/mJ), and photo-resistant (<1·10^{-4} cm^2/mJ) compounds. Observed photolytic degradation rate constants for photo-susceptible compounds like diclofenac, iopromide and sulfamethoxazole were high with values of 67, 25 and 14 ·10^{-4} cm^2/mJ, respectively, achieving up to 99% removal at fluence of 600 mJ/cm^2. Climbazole, tramadol, sotalol, citalopram, benzotriazole, venlafaxine and metoprolol exhibited observed photolytic degradation rate constants in the range of 1-4.8 ·10^{-4} cm^2/mJ resulting in moderate removal at 600 mJ/cm^2, while primidone, carbamazepine and gabapentin with rate constants of <1 ·10^{-4} cm^2/mJ were considered photo-resistant. In the following sections, these photo-resistant compounds are also used to determine OH radical exposures for the UV/H$_2$O$_2$ process.

In comparison to k$_{UV}$ values reported in the literature (Table 4), all experimental k$_{obs}$ values were slightly lower. For tramadol, no reported k$_{UV}$ could be found. However, based on lab-scale experiments the photolytic reactivity could be determined as 3.62 ·10^{-4} cm^2/mJ.
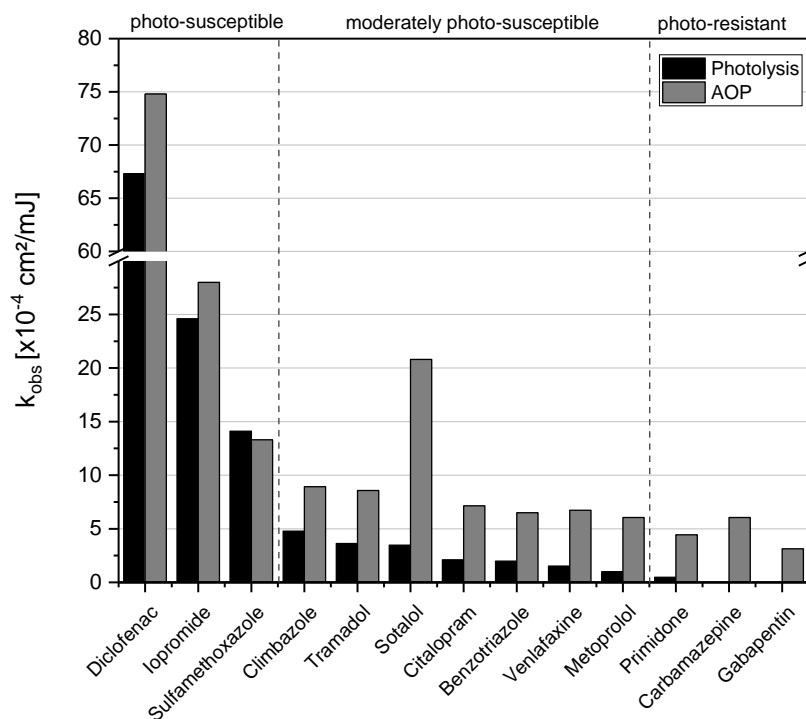
Figure 8: Observed pseudo first-order rate constants of indicator TOrCs during lab-scale UV photolysis and UV-AOP with UV doses of 40–2,000 mJ/cm^2 and 10 mg/L H_2O_2 (n=11, each); correlation coefficients are given in Table S2; TCEP and phenytoin were excluded due to influent concentrations <LOQ.

Due to the unique scavenging of a given water matrix, observed rate constants for AOP are very site specific. In our study, the addition of 10 mg/L H_2O_2 led to an increase of k_{obs} values for all substances except sulfamethoxazole, where no significant difference could be observed between photolytic and OH radical enhanced k_{obs} values. The addition of H_2O_2 resulted in little benefit for photo-susceptible compounds. Only minor enhancement of 1.6-14% could be observed. Apparent rate constants for moderately photo-susceptible compounds were enhanced by factors varying between 1.87 (climbazole) and 6.1 (metoprolol). Even though the radical enhanced k_{obs} value for sotalol is likely an outlier (Figure 8), its enhancement factor of 5.9 is within the range for moderately photo-susceptible compounds. For photo-resistant compounds, enhancement by H_2O_2 addition can only be quantified for primidone (enhancement factor of 9.5) since photolysis of carbamazepine and gabapentin did not result in significant removal. In UV/H_2O_2, the k_{obs} value of carbamazepine exceeds the k_{obs} of gabapentin by a factor of 1.9 even though respective k_{OH} values are similar (Table 4). Based on the dataset no reasonable explanation could be derived from this phenomenon. k_{obs} values determined in this study confirm values reported in other studies (Rosario-Ortiz et al., 2010; Wols et al., 2013; Gerrity et al., 2016; Lee et al., 2016).

4.3.2 *Verification of result at pilot scale*

The observed kinetic rate constants at pilot scale ($k_{obs,pp}$) were compared with those determined during lab-scale experiments ($k_{obs,cbd}$) to evaluate consistency in the measured rate constants between the two scales of treatment. To enable comparison of

pilot- and lab-scale oxidation with minimum influence of water matrix fluctuations, lab experiments were conducted with tertiary effluent collected as a composite sample on the day of pilot-scale experiments. Average water quality parameters of lab- and pilot-scale experiments are reported in Table 5.

Table 5: Operational and chemical parameters of water samples used in lab- and pilot- scale studies. Single measurements of a batch sample from lab-scale and average values with standard deviation (n=10) from pilot-scale experiments.

	H_2O_2 [mg/L]	UVT [%]	NO_2^--N [mg/L]	NO_3^--N [mg/L]	DOC [mg/L]	HCO_3^- [mg/L]
Lab-scale	n/a	66.4	0.21	17	8.2	330
Pilot-scale	9.90 ± 0.4	70.0 ± 2.2	0.20 ± 0.1	15.0 ± 4	8.2 ± 0.2	310 ± 12
k_{OH} [$M^{-1} s^{-1}$]	$2.7 \cdot 10^7$ [e]		$1 \cdot 10^{10}$ [a]	$5 \cdot 10^6$ [b]	$3.0 \cdot 10^8$ [c]	$8.5 \cdot 10^6$ [d]

[a] Coddington et al. (1999); [b] Keen et al. (2012); [c] estimated in this study; [d] Buxton et al. (1988); [e] Liao and Gurol (1995)

The ratios of observed reaction rate constants in pilot- and lab-scale experiments ($k_{obs,pp}/k_{obs,cbd}$) are illustrated in Figure 9 for UV photolysis and UV/H₂O₂. The median k_{obs} ratio for all data points in this evaluation is 1.06. Statistical tests did not show any systematic difference of lab- and pilot-scale k_{obs} values (*p*=0.24) indicating that determination of fluence was accurate in both systems and reactor geometry did not show a general impact on treatment efficiency. However, the k_{obs} ratio for photo-resistant compounds showed significantly better agreement between the two scales than for (moderately) photo-susceptible compounds.

A general reason for performance deviations between lab- and pilot-scale might be the fluctuating water matrix during continuous operation. However, water matrix parameters between lab- and pilot-scale tests were very similar indicating that the total amount of scavenging did not vary at the two different scales. Even though the wastewater samples used in the lab-scale investigations were collected hourly during the pilot-scale experiment, instant back wash of granular media filter cells could cause a temporary increase of UVT or change in scavengers, which would not be reflected in the composite sample and therefore is neglected in lab-scale UV/H₂O₂ average TOrC attenuation evaluation. However, this only applies to single samples and not to k_{obs} values that comprise the combined 11 samples collected throughout the pilot-scale experimental procedure. Furthermore, matrix effects would induce systematic errors rather than deviation of single substances.

Another possible explanation for the observed deviation of TOrCs with lower or no photo-susceptibility might be the lower significance of k_{obs} values for photolysis. The plotted natural logarithm of c/c₀ did in some cases not exceed correlation coefficients of $R^2 > 0.9$ (see Table S2), which therefore lowered the confidence of these specific k_{obs} values. In addition, analytical inaccuracies might have occurred as compound removal was measured without spiking of TOrCs. Influent concentrations of some compounds, e.g. sotalol and primidone, were close to the limit of quantification introducing larger uncertainties regarding removal efficiency (Table 4).

The compounds benzotriazole and sotalol showed largest differences in kinetic constants from pilot- and lab-scale operations. Benzotriazole was better removed at pilot-scale by a factor of 1.8 (UV/H_2O_2) and 3.7 (photolysis), while sotalol was removed to a higher extent during pilot-scale experiments due to photolysis (4.8) and to a lower extent due to UV/H_2O_2 (0.3). To the best of our knowledge such discrepancy has not been reported and discussed previously. Further research is needed to understand removal of these compounds.
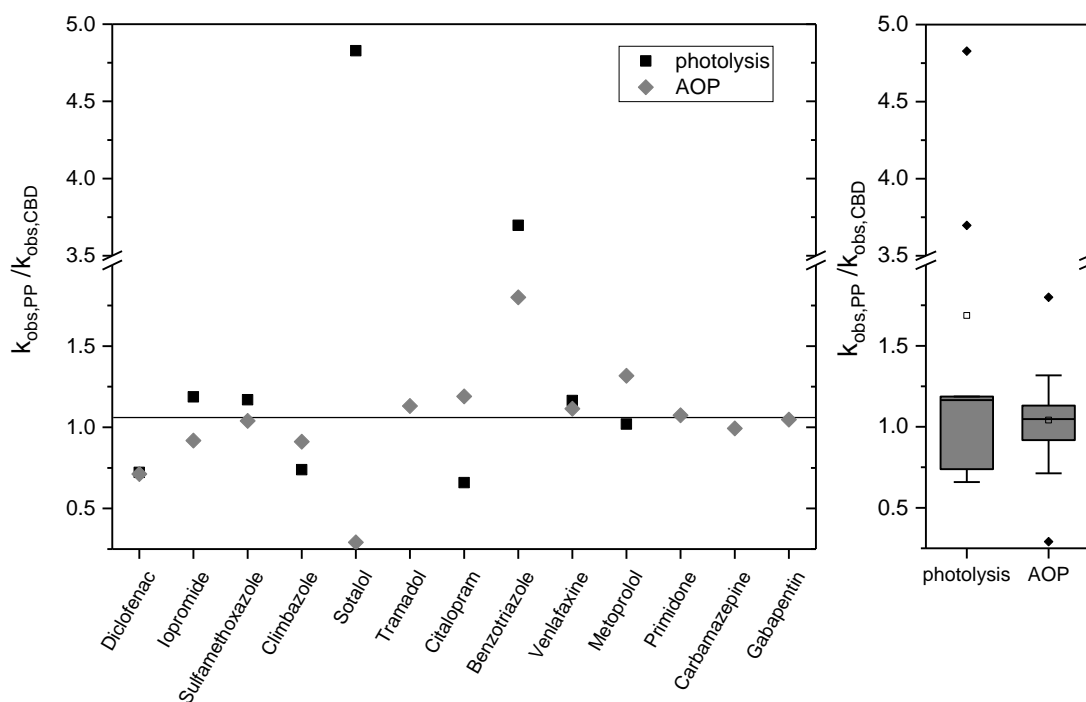
Figure 9: Ratio of pilot- (PP) and lab-scale (CBD) observed reaction rate constants applying UV photolysis (black) and UV-AOP (grey) with 10 mg/L H_2O_2. Respective k_{obs} values and R^2 are reported in Table S2 (SI). Solid line represents the median of all k_{obs} ratios. Boxplots cover a descriptive analysis of all data points shown on the left ($n_{photolysis}$=9 and n_{AOP}=13).

4.3.3 Modeling of lab- and pilot-scale UV/H_2O_2

Sample specific data, including water quality parameters as well as process parameters UV fluence and H_2O_2-dose from lab- and pilot-scale experiments were used as inputs for the model validation exercise. In this study, OH radical scavenging by hydrogen peroxide, nitrite, nitrate, DOC and bicarbonate was incorporated into the model following the approach described by Wols et al. (2013). Specific second-order rate constants used for the reaction of different scavengers with OH radicals as well as their average concentration in lab- and pilot-scale experiments are summarized in Table 5. Depending on the water matrix, DOC can contribute up to 95% of total scavenging capacity (Keen et al., 2014). Its reactivity with OH radicals is reported as 1.7-7.9 $\cdot 10^8$ $M_c^{-1}s^{-1}$ (Westerhoff et al., 2007; Rosario-Ortiz et al., 2008; Katsoyiannis et al., 2011; McKay et al., 2011; Nagarnaik and Boulanger, 2011; Lee et al., 2013). In this study, the rate constant was adjusted to a value of 3.0 $\cdot 10^8$ $M_c^{-1}s^{-1}$, which showed the best modeled fit for photo-

resistant TOrCs from lab- and pilot-scale rate constant determination experiments (Figure 10).

Nitrite is described as a scavenger with a second-order reaction rate constant with OH radicals of $1 \cdot 10^{10}$ M^{-1}s^{-1} (Buxton et al., 1988). Since its reactivity with OH radicals is 1-2 orders of magnitude higher than the reactivity of most TOrCs (10^8-10^9 M^{-1}s^{-1}) (Huber et al., 2003; Wols and Hofman-Caris, 2012), low nitrite concentrations of <1 mg/L can significantly impact the performance of an AOP. In biological wastewater treatment, nitrite can result from insufficient nitrification and denitrification and should therefore always be considered as a possible scavenger when oxidative treatment is applied downstream of biological nutrient removal processes. Nitrate was also included as a relevant scavenger due to highly variable concentration even though its reactivity with OH radicals is relatively low (Table 5).

Predicted pseudo-first order removal rate constants are compared with results from lab- and pilot-scale experiments in Figure 10. Modeling depicts an overestimation for both UV photolysis and UV/H$_2$O$_2$ in pilot- and lab-scale experiments with a median k_{obs} ratio of 0.87 for all data points, 0.78 for photolysis and 0.91 for AOP. Observed overestimation in both processes can be attributed to photolytic degradation of TOrCs, since the model for radical scavenger capacity was adjusted to experimental data. A slight overestimation of photo-resistant compounds applying a similar model was also observed by Gerrity et al. (2016).

Photolytic k_{obs} values determined in this study are slightly lower compared to k_{UV} values reported in the literature (Table 4), which might explain the general modeled overestimation over most TOrCs. Since a systematic error in photolytic rate constants from literature is unlikely, inaccuracies in fluence determination are suspected to cause the observed overestimation. This would also apply to H$_2$O$_2$ photolysis and consequently OH radical generation. However, it has to be noted that the estimation of $k_{DOC,°OH}$ to model experimental data also compensated for overestimation of H$_2$O$_2$ photolysis during radical generation.

Modeling results for benzotriazole exhibit highest variances (k_{obs} ratio of 0.4-1.5) which is based on the different scale comparison (Figure 10): 2-4 times higher attenuation was achieved at pilot-scale compared to the CBD leading to a substantial over- or underestimation of experimental k_{obs} values. Other possible reasons for deviations between modeled and experimental data are simplified assumptions that were set within this study:

- The model only considers direct photolysis and OH radical based oxidation. In wastewater, however, a variety of complex (radical) side reactions occur: indirect photolysis resulting in additional OH radicals (Dong and Rosario-Ortiz, 2012) and radical chain reactions involving carbonate (Liao et al., 2001; Wu and Linden, 2010), chlorine (Liao et al., 2001), sulfate, and phosphate radicals as well as reactive oxygen species (e.g., perhydroxyl and superoxide radicals). However, this would result in an underestimation of TOrC removal.

- ▪ Consideration of only four scavengers neglects the influence of various other inorganic scavengers and consequently reduces the estimated scavenging capacity.
- ▪ In general, all reaction rate constants were taken from literature. Reported values might differ from real reactivities for each TOrC.
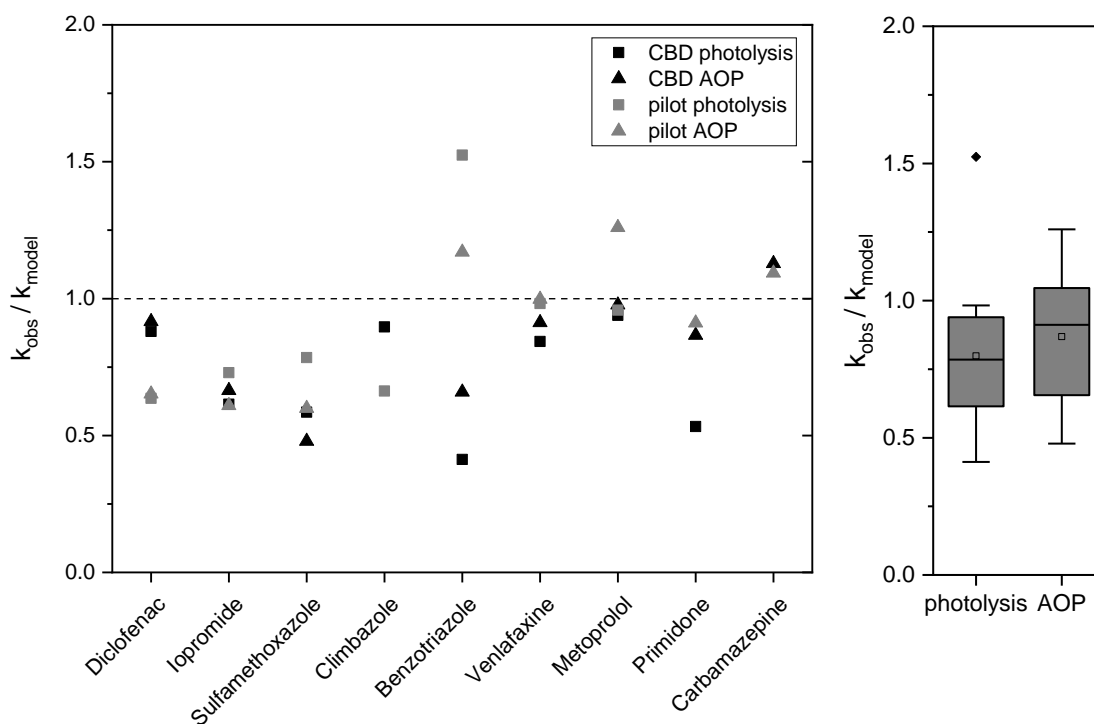
Figure 10: Ratio of observed and modeled reaction rate constants in pilot- (grey) and lab-scale experiments (black) applying UV photolysis (squares) and UV-AOP (triangles) with 10 mg/L H_2O_2. Respective k_{obs} values and R^2 can be found in Table S2 (SI). Dashed line depicts the ideal modeled fit, Boxplots cover a descriptive analysis of all data points shown on the left ($n_{photolysis}$=15, n_{AOP}=16).

4.3.4 Continuous pilot-scale operation of UV/H_2O_2

The evaluation of water matrix influence on UV/H_2O_2 oxidation performance was investigated in two continuous pilot-scale experiments for a period of five days each. Application of 800 mJ/cm² and 10 mg/L H_2O_2 was targeted in both experiments. However, final UV fluence and H_2O_2-dose were slightly higher during dry weather compared to rain-event experiments (Table 6).

For evaluation, chemical parameters of the water matrix and respective TOrC removal were investigated and assessed by descriptive statistics. Influent concentrations of relevant water quality parameters are summarized in Table 6. Boundary conditions for these experimental periods were chosen to reflect the highest variances during biological wastewater treatment. The dry weather experiment was scheduled during the summer holiday season resulting in constantly low nutrient loads and efficient removal

53

of scavenger concentrations during the activated sludge process as well as during granular media filtration (based on annual average water quality data of WWTP Gut Marienhof). During the rain-event, higher nitrogen loads were insufficiently removed during post denitrification and resulted in nitrite peaks of up to 2 mg-N/L. UVT at 254 nm could be measured at 74.3% during dry weather experiment and slightly lower values during the rain-event week (71.4%). While NO_3^--N, bicarbonate, and DOC concentrations were similar in both experiments, large fluctuations were observed for average NO_2^--N concentrations of 0.13 mg-N/L during dry weather and 1.1 mg-N/L during the rain-event experiment.

Table 6: Bulk water and process parameters during continuous operation of pilot-scale UV/H₂O₂ experiments and OH radical rate constants of the scavengers considered.

	UV dose [mJ/cm²]	H_2O_2 [mg/L]	UVT [%]	NO_2^--N [mg/L]	NO_3^--N [mg/L]	DOC [mg/L]	HCO_3^- [mg/L]
dry weather	822 ± 18	10.2 ± 1	74.3 ± 1.2	0.13 ± 0.1	9.6 ± 0.8	6.7 ± 1.5	280 ± 44
rain-event	794 ± 24	9.7 ± 0.5	71.4 ± 1.5	1.1 ± 0.5	8.8 ± 1.2	6.9 ± 0.4	350 ± 40

4.3.4.1   Water matrix influences on TOrC removal efficiency

TOrC removal results are illustrated in Figure 11. During continuous pilot-scale operation at constant UV fluence and H₂O₂ dosage, the removal of photo-susceptible moderately photo-susceptible and most photo-resistant compounds including outliers varied in a range of 44-99.6%, 1-90% and 1-81%, respectively. The respective removal is in agreement with the illustrated reaction rate constant groupings depicted in Figure 8. TOrC removal during the rain-event indicated significantly lower oxidation performance compared to the dry weather experiment for all substances except diclofenac, which was removed by more than 2 orders of magnitude in both sampling periods since it is highly reactive to direct photolysis. Differences in oxidation performance during the two continuous experiments can be explained based on slightly different process parameters and water quality parameters summarized in Table 6. Also, higher variances in nitrite concentrations could have influenced the scattering of removal data, resulting in a wider range of 25th and 75th percentiles during the rain-event illustrated by a wider spread in the boxplots. A detailed chronological sequence of oxidation performance illustrated by four representative substances iopromide, sulfamethoxazole, primidone and TCEP is shown in Figure S4 (SI).

Contribution of individual scavengers to overall scavenging capacity during continuous operation of the UV/H₂O₂ pilot-scale experiments is illustrated in Figure 12. Scavenging by nitrate is not considered in the figure, since its scavenging capacity is three orders of magnitude lower than the illustrated ones. Calculated scavenger capacities agree well with the range of values reported in the literature (Lee et al., 2013). Results confirm that continuous operation during dry weather condition revealed a consistent scavenging potential, while experiments during the rain-event exhibited highly variable scavenging capacities. However, scavenging capacities by DOC and bicarbonate remained mostly stable and at a comparable level in both weeks. In September, the

overall scavenging capacity was dominated by nitrite peaks in the tertiary effluent. These data confirm the importance to monitor and manage nitrite concentration, if oxidative processes for advanced treatment are considered.
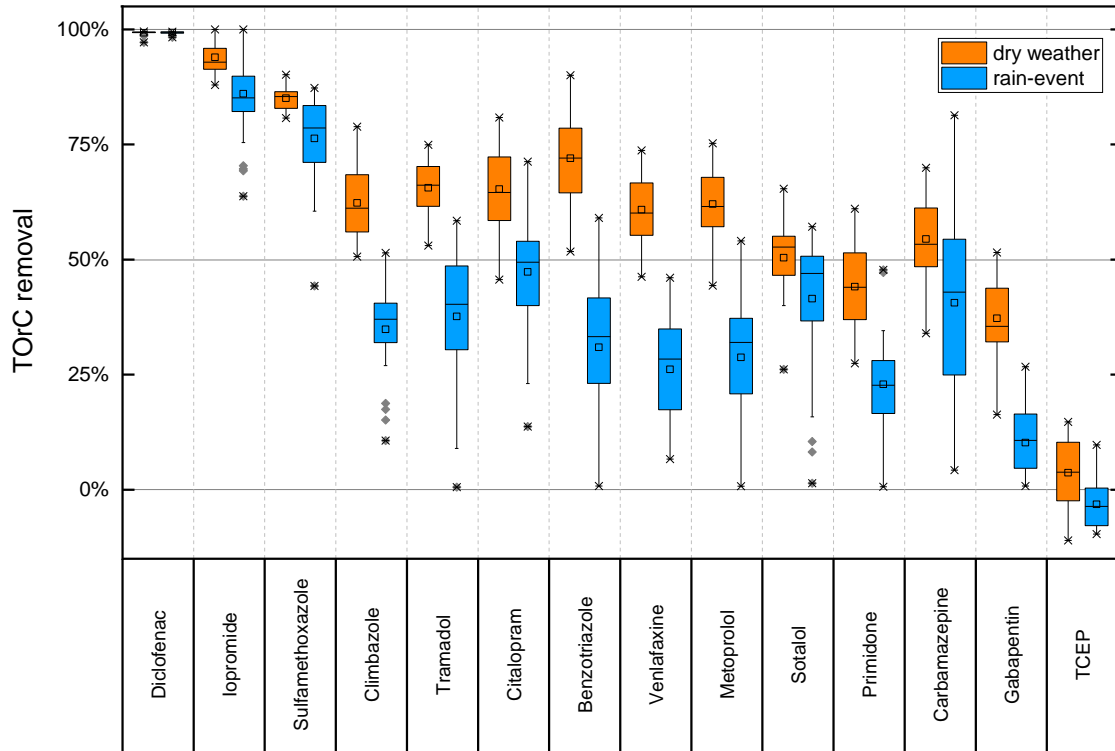
Figure 11: Oxidative removal of TOrCs from WWTP effluent during continuous operation of pilot-scale UV/H_2O_2 at 800 mJ/cm² and 10 mg/L H_2O_2 during dry weather (n=28-29) and rain-event- (n=13-29) operation. Diclofenac effluent concentrations <LOQ were considered as LOQ/2=12.5 ng/L.
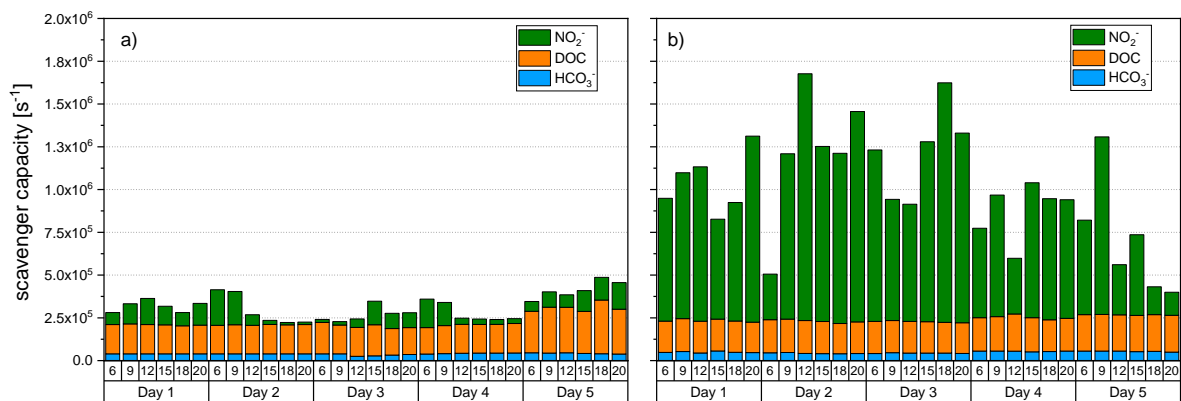
Figure 12: Scavenging capacity during one week of continuous operation of pilot-scale UV/H_2O_2 at 800 mJ/cm² and 10 mg/L H_2O_2 during dry weather (a) and rain-event (b). Scavenging capacity calculated based on kinetic data and respective concentrations from Table 6.

4.3.4.2   Influence of scavenging capacity on OH radical exposure

To determine the impact of scavenging capacity on OH radical based oxidation performance, the OH radical exposure was used as a figure of merit to assess OH radical abundance over time. Compound specific reaction rate constants of photo-resistant radical indicators were used to calculate the OH radical exposure (Rosenfeldt et al., 2006):

$$\int (OH)dt \; [M \; s] \; = \frac{ln\left[\frac{c}{c_0}\right]}{-k_{OH,i} \; [M^{-1}s^{-1}]} \qquad\qquad (\,15\,)$$

Based on the data obtained from continuous experiments, OH radical exposure was calculated from relative residual concentrations (c/c_0) of primidone and carbamazepine. Gabapentin was not included in the calculations since photolytic rate constants were not available for this compound. Average exposures from both experiments are shown in Figure 13 as a function of the radical scavenging capacity (data from Figure 12). The dashed line represents calculated exposures applying the model for constant fluence of 800 mJ/cm² and H₂O₂ dosage of 10 mg/L. During the dry weather experiment, OH radical exposure values ranged from $4.8 \cdot 10^{-11}$ M·s to $1.3 \cdot 10^{-10}$ M·s, whereas higher variation of scavenging capacity during the rain-event experiment resulted in a wider range of OH radical exposure from $2.9 \cdot 10^{-12}$ to $1.4 \cdot 10^{-10}$ M·s. Relatively large extent of scattering during the rain-event experiment might be explained by unstable nitrite concentrations in reactor influent samples. It is assumed that sampling did not exactly represent the true water quality in effluent samples. With increasing scavenging capacities, the OH radical exposure decreased following a quasi-hyperbolic correlation. The findings could be corroborated using the calculated OH radical exposure based on modeling. Performing an ordinary least squares regression analysis between modeled and observed data points, the median of all residuals is determined as 23% and 121% for dry weather and rain-event experiments, respectively.

Three major conclusions can be drawn from these results:

- At the municipal WWTP Gut Marienhof a high impact of OH radical scavenging on radical formation and oxidative compound removal was identified which triggers the need for monitoring and control of effluent water quality.
- The modeled and experimental correlation between scavenging capacity and OH radical exposure indicates the possibility of OH radical exposure prediction by water matrix parameters and proves its applicability at pilot- or full-scale, which confirms results by Gerrity et al. (2016). Online sensors for water quality parameters (i.e., NO₂⁻-N, DOC and HCO₃⁻) are commercially available and could be considered for future AOP-process control.
- TOrC removal from tertiary effluents by UV/H₂O₂ is highly dependent on nitrite concentrations. Therefore, oxidation performance of UV/H₂O₂ can be improved by nitrite control in WWTP effluents.
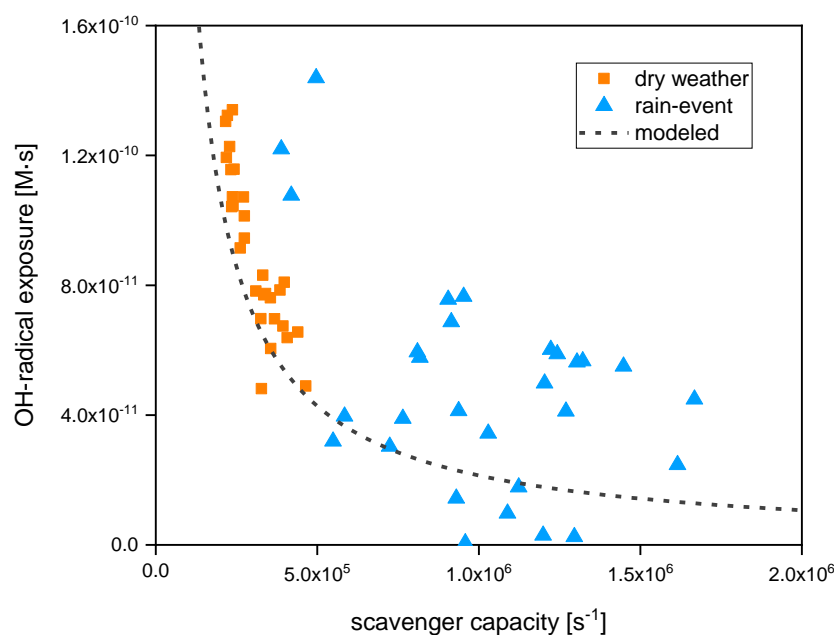
Figure 13: OH radical exposure (calculated using averaged carbamazepine and primidone c/c_0-values) as a function of scavenging capacity (determined by bulk water parameters, H_2O_2 and second order rate constants); the dashed line represents the exposure calculated at 800 mJ/cm² and 10 mg/L using equation 19 (SI).

4.4 Conclusion

This study demonstrates through pilot-scale investigations that UV/H_2O_2 is applicable to remove TOrCs from municipal wastewater effluents. UV/H_2O_2 pilot-plant performance was verified by a bench-scale collimated beam device for removal of 15 TOrCs occurring at ambient concentrations and representing a range of photolytic- and OH radical reactivity in wastewater effluent. The impact of water matrices on OH radical exposure was evaluated during continuous pilot-scale operation using the removal kinetics of photo-resistant ambient TOrCs. Furthermore, successful application of a model was confirmed using UV fluence, H_2O_2 dosage and standard water quality parameters (i.e., DOC, NO_2^- and HCO_3^-) as input parameter.

Key findings of this study are:

- High variations of OH radical exposure during pilot-scale UV/H_2O_2 operation primarily due to fluctuations of nitrite concentration which suggests the need for online water quality monitoring and control of tertiary effluent nutrient removal if UV/H_2O_2 is implemented.
- A correlation between OH radical exposure and scavenging capacity could be determined and verified by modeling. This correlation reveals the possibility of OH radical exposure prediction by water matrix parameters and proves its applicability at pilot- or full-scale operations.

The tested hypotheses that (i) UV/H$_2$O$_2$ is applicable for advanced oxidation of wastewater effluent achieving a substantial removal of TOrCs (Hypothesis № 1.1) and (ii) the removal of TOrCs during UV/H$_2$O$_2$ can be predicted by mathematical models considering the water parameters DOC, NO$_2^-$ and alkalinity, process parameters and specific kinetic data of target compounds (Hypothesis № 2) can be accepted.

4.5 Acknowledgements

5. Removal of Trace Organic Contaminants in Wastewater Effluent by UV/H₂O₂ and UV/PDS

Abstract

In this study, we comparatively investigated the degradation of 12 trace organic chemicals (TOrCs) during UV/H₂O₂ and UV/peroxydisulfate (PDS) processes. Second-order rate constants for the reactions of iopromide, phenytoin, caffeine, benzotriazole and primidone with sulfate radical ($SO_4^{\cdot-}$) were determined for the first time. Experiments were conducted in buffered pure water and wastewater effluent with spiked TOrCs. UV/PDS degraded all TOrCs more efficiently than UV/H₂O₂ in buffered pure water due to the higher yield of $SO_4^{\cdot-}$ than that of hydroxyl radical ($^{\cdot}OH$) at the same initial molar dose of PDS and H₂O₂, respectively. UV/PDS showed higher selectivity toward TOrCs removal than UV/H₂O₂ in wastewater effluent. Compounds with electron-rich moieties, such as diclofenac, venlafaxine and metoprolol, were eliminated faster in UV/PDS whereas UV/H₂O₂ was more efficient in degrading compounds with lower reactivity to $SO_4^{\cdot-}$. The fluence-based rate constants (k_{obs-UV/H_2O_2}) of TOrCs in wastewater effluent linearly increased as a function of initial H₂O₂ dose during UV/H₂O₂, possibly due to the constant scavenging impact of the wastewater matrix on $^{\cdot}OH$. However, exponential increase of $k_{obs-UV/PDS}$ with increasing PDS dose was observed for most compounds during UV/PDS, suggesting the decreasing scavenging effect of the water matrix (electron-rich site of effluent organic matter (EfOM)) after initial depletion of $SO_4^{\cdot-}$ at low PDS dose. Fulvic and humic-like fluorophores appeared to be more persistent during UV/H₂O₂ compared to aromatic protein and soluble microbial product-like fluorophores. In contrast, UV/PDS efficiently degraded all identified fluorophores and showed less selectivity toward the fluorescent EfOM components. Removal pattern of TOrCs during pilot-scale UV/PDS was consistent with lab-scale experiments, however, overall removal rates were lower due to the presence of higher concentration of EfOM and nitrite.

5.1 Introduction

Trace organic chemicals (TOrCs) including pharmaceutical residues, personal care products and industrial chemicals are present in surface water, groundwater, wastewater effluents, reclaimed water and even in drinking water (Coday et al., 2014). Regardless of their relatively low occurrence (i.e., few ng/L to several µg/L), TOrCs in aquatic resources have been a growing concern due to their potential adverse effects on human health and

ecosystem, such as endocrine disruption, spread of antibiotic resistance, and bioaccumulation (Dodd, 2012; Belhaj et al., 2015). Insufficiently treated effluent from municipal wastewater treatment plant (WWTP) is considered as one of the main sources of TOrCs to the aquatic environment. Many TOrCs are persistent during conventional biological and chemical treatment processes in WWTP. The removal efficiency of TOrCs always depends on their physicochemical and biological properties, as well as the removal principles of individual treatment processes (Grandclément et al., 2017).

Advanced oxidation processes involving the generation of powerful oxidant species, such as hydroxyl radicals ($\cdot$OH), chlorine radicals (Cl$\cdot$) and sulfate radicals ($SO_4\cdot^-$), have gained increasing interests as an alternative way to remove refractory and/or non-biodegradable pollutants (Huber et al., 2003; Wols et al., 2013; Lian et al., 2017).

Removal of TOrCs by hydroxyl radical-based AOPs has been extensively studied (Miklos et al., 2018b). Hydroxyl radical is a strong oxidant (1.8–2.7 V, depending on solution pH) with low selectivity (Neta et al., 1988). Previous studies confirmed the high potential of UV/H_2O_2 to remove TOrCs from WWTP effluents (Wols et al., 2015; Miklos et al., 2018a). However, some TOrCs are resistant to $\cdot$OH, such as tris-(2-chloroethyl)-phosphate (TCEP) and tris-(2-chloroisopropyl)-phosphate (Gerrity et al., 2011). Although UV/H_2O_2 process effectively limits the formation of toxic by-products (i.e., NDMA, bromate) as compared to ozonation or O_3/H_2O_2, and reduces the formation of disinfection by-products (e.g., haloacetamides) as a pre-oxidation (Chu et al., 2014), the process needs high energy input due to the low UV molar absorbance of H_2O_2 (e.g., 18.6 $M^{-1}cm^{-1}$) to generate sufficient $\cdot$OH, especially in complex water matrix (Lee et al., 2016). High reactivity of $\cdot$OH with water matrix components (e.g., organic matter, carbonate, nitrite) results in a low steady-state $\cdot$OH concentration that is available to degrade target contaminants (Rosario-Ortiz et al., 2010; Lee et al., 2013).

Sulfate radical (2.5–3.1 V) has a comparable or even higher redox potential than $\cdot$OH (Neta et al., 1988). Unlike $\cdot$OH, $SO_4\cdot^-$ reacts mainly through electron transfer, less by addition or H-atom abstraction (Neta et al., 1988), which makes $SO_4\cdot^-$ more selective to compounds with electron-rich moieties (Li et al., 2017). Recent statistical analysis indicated that TOrCs with electron-donating groups (e.g., $-NH_2$, $-OH$) have higher second-order rate constants with $SO_4\cdot^-$ than compounds with electron-withdrawing groups (e.g., $-COOH$) (Ye et al., 2017). $SO_4\cdot^-$ can be generated from the activation of peroxydisulfate (PDS) or peroxymonosulfate by transition metal ions, heating, UV irradiation, and quinones (Ike et al., 2018).

Limited studies are available on the removal of TOrCs during sulfate radical-based AOPs. Previous work has reported the efficient degradation of cyanotoxin cylindrospermopsin (He et al., 2014), chlorotriazine pesticides (Lutze et al., 2015a), and sulfonamide antibiotics (Zhang et al., 2016) by $SO_4\cdot^-$. Contaminants that show low reactivity to $\cdot$OH can be degraded by $SO_4\cdot^-$, such as perfluorocarboxylic acids (Hori et al., 2005). Recent studies comparing UV/H_2O_2 and UV/PDS treatment of pharmaceuticals present in reverse osmosis brines (Yang et al., 2016b) and wastewater effluent (Lian et al., 2017) confirmed that $SO_4\cdot^-$ reacted more selectively than $\cdot$OH. UV/PDS was reported to effectively control the formation of nitrogenous disinfection by-products in organic nitrogen-rich waters (Chu et al., 2015). Similar to $\cdot$OH, $SO_4\cdot^-$ is also scavenged by organic

matter and inorganic ions in the water matrix, which further reduces the degradation efficiency of TOrCs (Zhang et al., 2013; Lutze et al., 2015b).

The aim of this study was to investigate the removal efficiency of TOrCs by UV/PDS in comparison to UV/H_2O_2. $SO_4^{\cdot-}$ and $\cdot$OH were generated by UV irradiation (low pressure UV lamp) of PDS and H_2O_2, respectively. Experiments were conducted in pure water (5 mM phosphate buffer) and municipal WWTP effluent with spiked TOrCs to study the influence of the water matrix on treatment efficiency. Additionally, pilot-scale experiments were carried out at a municipal WWTP to explore the feasibility of UV/PDS treatment under real feed water conditions.

This study tested the hypothesis that applying the radical promoters peroxodisulfate as a substitute for H_2O_2, a comparable oxidation performance of UV-AOPs can be achieved in municipal wastewater effluents (Hypothesis № 3 for peroxodisulfate).

5.2 Material and Methods

5.2.1 Chemicals

All TOrCs and isotope labeled analytical standards for TOrCs analysis were of analytical grade. Details on TOrCs were provided in Supplementary Information (Table S3). All solvents used for Liquid Chromatography were in HPLC-grade. A mixture of all TOrCs was prepared in Milli-Q water with a concentration of 0.5 mg/L for each compound. Hydrogen peroxide 30% (Thermo Fisher Scientific) and sodium persulfate (≥98%, Sigma-Aldrich) were used to prepare the stock solutions of H_2O_2 and PDS, respectively.

5.2.2 Wastewater treatment plant effluent

The WWTP Gut Marienhof (Munich, Germany) treats wastewater from the city of Munich. The treatment plant consists of a mechanical treatment stage including screens, aerated sand/fat traps and preliminary sedimentation, followed by a two-stage activated sludge process for biological carbon and nutrient removal (solids retention time of 2-3 and 6–8 days, respectively). The water is then filtered using tertiary granular media filters with a resulting UVT at 254 nm of 65–75% prior to UV disinfection. In this study, samples were collected directly after granular media filtration. Hach cuvette tests were applied to measure bulk water parameters. DOC was analyzed on a vario TOC cube (Elementar, Germany) after filtration through cellulose nitrate membrane filters (0.45 µm, Sartorius AG, Germany). The concentrations of relevant parameters in WWTP effluent are summarized in Table 7.

Table 7. Water quality parameters of WWTP effluent[a] and the scavenging capacity of each component[b] for $\cdot OH$ and $SO_4^{\cdot-}$

	Lab-scale experiments			Pilot-scale experiments	
	Concentration	Scavenging capacity (s⁻¹)		Concentration	Scavenging capacity (s⁻¹) UV/PDS
		UV/H₂O₂	UV/PDS		
DOC (mg-C/L)	6.8	$2.23\cdot10^5$	$6.35\cdot10^4$	10.7	$1.01\cdot10^5$
Bicarbonate (mg/L)	307	$4.33\cdot10^4$	$1.41\cdot10^4$	319	$1.47\cdot10^4$
Nitrite (mg-N/L)	0.028	$2\cdot10^4$	$1.76\cdot10^3$	0.15	$9.28\cdot10^3$
Nitrate (mg-N/L)	10.6	<75	22.7	13.5	29.0
Chloride[c] (mg/L)	110±13	NA	$9.30\pm1.10\cdot10^5$	110±13	$9.30\pm1.10\cdot10^5$
UV₂₅₄ (m⁻¹)	14.5			16.7	
pH	7.4			7.5	

[a] WWTP effluent samples used for lab and pilot-scale experiments were from different days (i.e., 17/10/16 and 03/11/16, respectively); [b] Calculated by multiplying the molar concentration of each component with its second-order reaction rate constants with radicals. Reaction rate constants and references are provided in Table S4; [c] Annual average concentration; NA: not applicable

5.2.3   *Trace organic chemicals analysis*

All samples were filtered through 0.22 μm PVDF syringe filters (Berrytec, Germany) before TOrCs quantification. Samples were measured using a high-performance liquid chromatography (Knauer PLATINBLUE UHPLC) coupled with a tandem mass spectrometry (LC-MS/MS) (SCIEX QTRAP 6500) by direct injection. Isotope dilution was used to account for matrix suppression and instrument response. A detailed description of the analytical method was reported elsewhere (Müller et al., 2017). The concentrations of TOrCs in wastewater effluent during lab- and pilot-scale experiments are presented in Table 8.

Table 8. Fluence-based rate constants [a], second-order rate constants and initial concentrations of TOrCs

Compounds	Fluence-based rate constant (k_{obs-UV}) (10^{-4} cm² mJ^{-1})	Second-order rate constants (10^9 M^{-1} s^{-1})		Initial concentration (ng/L)	
		$k_{\bullet OH}$	$k_{SO_4^{\bullet-}}$	Lab-scale[b]	Pilot-scale[c]
Group I: k_{obs-UV} > 1·10^{-3} cm² mJ^{-1}					
Diclofenac	68.3 (R²=0.99)	8.38±1.2[d]	9.2±0.6[e]	3,601	2,979±60
Iopromide	26.5 (R²=0.99)	3.3±0.6[e]	0.36±0.07 (in this study)	2,867	6,268±469
Sulfamethoxazole	19.7 (R²=0.99)	5.82±2[d]	12.5±1.9[e]	1,564	348±30
Group II: 1·10^{-4} < k_{obs-UV} < 1·10^{-3} cm² mJ^{-1}					
Phenytoin	7.74 (R²=0.97)	6.28[g]	0.62±0.02 (in this study)	1,082	13±2
Benzotriazole	2.21 (R²=0.86)	8.34±0.4[h]	0.87±0.03 (in this study)	9,552	9,490±391
Group III: k_{obs-UV} < 1·10^{-4} cm² mJ^{-1}					
Venlafaxine	0.54 (R²=0.65)	8.8±1.5[i]	3.53±0.05[j] 4.99±0.05 (in this study)	1,245	630±31
Metoprolol	0.30 (R²=0.60)	7.84±0.8[d]	5.11±0.12[j] 3.89±0.01 (in this study)	1,453	551±7
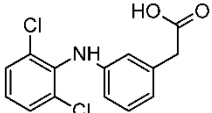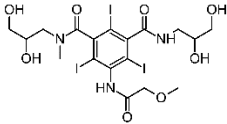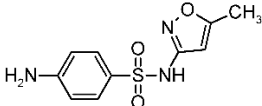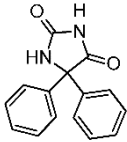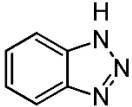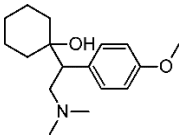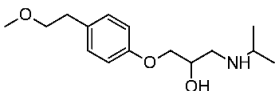
Compounds	Fluence-based rate constant (k_{obs-UV}) (10^{-4} cm² mJ⁻¹)	Second-order rate constants (10^9 M⁻¹ s⁻¹)		Initial concentration (ng/L)	
		$k_{\cdot OH}$	$k_{SO_4^{\cdot-}}$	Lab-scale[b]	Pilot-scale[c]
Carbamazepine	< 1	8.02±1.9[d]	1.92±0.01[k] 1.50±0.21 (in this study)	1,737	650±40
Caffeine	< 1	6.4±0.71[d]	2.39±0.18 (in this study)	965	71±32
Primidone	< 1	6.7±0.2[j]	0.53±0.03 (in this study)	1,048	124±4
Gabapentin	< 1	9.1[m]	< 1[n]	3,013	4,404±93
Tris(2-chloroethyl) phosphate (TCEP)	< 1	0.56[o]	< 1[n]	1,312	125±6
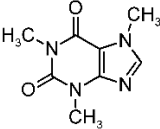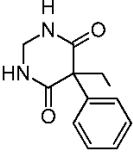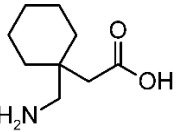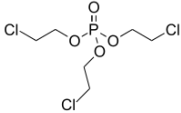
[a] Obtained during direct UV photolysis of TOrCs in wastewater effluent (115–1,380 mJ/cm²). The exact k_{obs-UV} was not calculated for group III (except venlafaxine and metoprolol) due to their low removal (see Section 5.3.1); [b] Sum of background and spiked concentrations; [c] Average concentration from triplicated samplings within 6 hours; [d] Wols and Hofman-Caris (2012); [e] Mahdi Ahmed et al. (2012); [f] Huber et al. (2003); [g] Yuan et al. (2009); [h] Bahnmüller et al. (2015); [i] Wols et al. (2013); [j] Lian et al. (2017); [k] Matta et al. (2011); [l] Real et al. (2009); [m] Lee et al. (2014); [n] Estimated in this study (see Text S3 in Section 9.4); [o] Watts and Linden (2009).

5.2.4 Fluorescence excitation-emission matrix analysis

EEMs were recorded using an Aqualog Fluorescence Spectrometer (Horiba Scientific, Germany). Four fluorescence peaks were selected from different regions on fluorescence spectra previously defined by Chen et al. (2003). The fluorescence intensities of selected peaks were used as representative indices of EfOM in wastewater to study the effect of

radical exposure on EfOM during UV/H$_2$O$_2$ and UV/PDS (Sgroi et al., 2017). More information on EEM analysis is provided in the Supplementary Information (Text S1 in Section 9.4).

5.2.5   Lab-scale experiments

Bench-scale experiments were conducted using a LP-UV collimated beam device following the standard operation procedure suggested by Bolton and Linden (2003). The collimated beam device contained three 15 W low-pressure Hg UV lamps (UV Technik Meyer, Germany). To precisely determine the petri factor, a xy-cross slide table with a magnetic stirrer was placed below the collimator, on top of which was the mounting for the petri dishes. Average UV-C intensity across the petri dish was determined as 1– 1.4 mW/cm^2 by a certified UV-C radiometer (UV-surface-D, sglux, Germany).

Fluences were applied to 30 mL of solution in a 100 mm glass petri dish. Experiments were conducted in solutions prepared with 5 mM of phosphate buffer (pH 7) (57.5–920 mJ/cm²) and wastewater effluent (115–1380 mJ/cm²) spiked with 1 μg/L of each TOrC. Due to the natural buffering capacity of wastewater effluent (i.e., bicarbonate=307 mg/L, Table 7), its pH remained stable at pH 7.4 throughout UV-AOP experiments. H$_2$O$_2$ and PDS were added directly from stock solutions before UV exposure. 0.15 mM of oxidant was applied for buffered pure water experiments. The oxidant doses used for wastewater effluent experiments were 0.15, 0.30, 0.45, and 0.60 mM. Dark experiments to investigate the effect of H$_2$O$_2$ and PDS on TOrCs attenuation were conducted in duplicates for 30 minutes and 24 hours with oxidant dose of 0.15, 0.3, 0.45 and 0.6 mM. Residual oxidants were quenched with excess sodium thiosulfate at the end of each experiment. All samples were stored in amber glass bottles at 4°C and analyzed for TOrCs within 24 hours.

The second-order rate constants for the reaction of TOrCs with SO$_4$$^{\cdot-}$ were determined by competition kinetics based on the methods published before (Lutze et al., 2015a; Lian et al., 2017). *para*-chlorobenzoic acid (*p*CBA) was used as a probe compound, k (SO$_4$$^{\cdot-}$ + *p*CBA) = 3.6 $\cdot10^8$ M^{-1}s^{-1} (Neta et al., 1977). Experiments were conducted in phosphate buffer (2.5 mM) at pH=7 with 20 μM of *p*CBA and target compound. SO$_4$$^{\cdot-}$ was generated by UV photolysis of PDS (1 mM). 10 mM of *tert*-Butanol was added as $\cdot$OH scavenger. Nitrobenzene (1 μM) was monitored to confirm that $\cdot$OH was scavenged efficiently by 10 mM of tert-Butanol. The concentrations of *p*CBA and TOrCs were analysed on a HPLC (Agilent 1100) equipped with an Agilent XDB-C18 column (5 μm, 4.6 $\cdot150$ mm). Details on competition kinetic experiments are provided in Text S2 in Section 9.4.

5.2.6   Pilot-scale experiments

Pilot-scale UV/PDS investigations were conducted using a container-based AOP system designed by WEDECO (Xylem, Germany) consisting of two LP-UV reactors (WEDECO LBX 90e and LBX 10, Xylem, Germany) operated to deliver the required fluence range. The pilot system was fed with wastewater effluent delivered by an external process water pump station at WWTP Gut Marienhof (Munich, Germany) directly after tertiary

granular media filtration. Specific details about the pilot system are described elsewhere (Miklos et al., 2018a).

For pilot-scale experiments, fluences were set by adjusting flow rates to current UV intensities, and UVT in each reactor. Fluence of 200, 400 and 800 mJ/cm² were maintained in reactor LBX 10, while 1,200 mJ/cm² was maintained in reactor LBX 90e. Oxidant dosing was targeted at concentrations of 0.3 and 0.6 mM and was adjusted based on the flow rate. The concentration of PDS was determined iodometrically (Liang et al., 2008). Before sampling, the system was constantly operated with a minimum of ten reactor volumes to establish steady-state conditions. Samples from reactor influent and effluent were filled in amber glass bottles and stored at 4°C until analysis. UVT as well as nitrate, nitrite, acid capacity and oxidant concentration were analyzed on site. TOrCs and DOC analysis were conducted

5.3 Results and Discussion

5.3.1 Characteristics of selected TOrCs: photolytic reactivity and rate constants with ·OH and $SO_4{}^{·-}$

Twelve TOrCs spanning a range of photolytic reactivity were selected based on their frequent detection in wastewater effluent and diverse physicochemical characteristics (Gerrity et al., 2011; Luo et al., 2014). Degradation of selected TOrCs by direct photolysis was investigated in WWTP effluent (115–1,380 mJ/cm²). The relative removal of TOrCs is illustrated in Figure S6 (SI) and their fluence-based rate constants (k_{obs-UV}) are presented in Table 8. The percent removal of diclofenac, iopromide and sulfamethoxazole were >90% at 1,380 mJ/cm², followed by phenytoin (68%) and benzotriazole (30%). About 9% of venlafaxine and 5% of metoprolol were eliminated at 1,380 mJ/cm². The removal of other TOrCs was negligible within the applied fluence.

The selected TOrCs were classified into 3 groups in accordance with literature (Miklos et al., 2018a). Group I includes photo-sensitive compounds (i.e., diclofenac, iopromide, and sulfamethoxazole) with k_{obs-UV} >1·10⁻³ cm²/mJ. Group II are moderately photo-sensitive compounds (i.e., phenytoin and benzotriazole) (1·10⁻⁴ < k_{obs-UV} <1·10⁻³ cm²/mJ). All other selected TOrCs belong to group III and are considered as photo-resistant compounds (k_{obs-UV} <1·10⁻⁴ cm²/mJ).

The second-order rate constants of selected TOrCs with ·OH and $SO_4{}^{·-}$ are shown in Table 8. The $k_{·OH}$ values of TOrCs were obtained from literature. Unlike the well-studied hydroxyl radical-based oxidation processes, $k_{SO_4{}^{·-}}$ values of most TOrCs are not known. To the best of our knowledge, the $k_{SO_4{}^{·-}}$ of iopromide, phenytoin, caffeine, benzotriazole and primidone were determined for the first time in this study. The $k_{SO_4{}^{·-}}$ of venlafaxine, metoprolol and carbamazepine are in good agreement with literature values (Matta et al., 2011; Lian et al., 2017). The selected TOrCs have complex structures with multiple functional groups. Hydroxyl radicals react with almost all organic moieties with nearly diffusion-controlled rates (Buxton et al., 1988). As shown in Table 2, ·OH reacts relatively slowly with TCEP (Watts and Linden, 2009) while all other TOrCs have $k_{·OH}$ values greater than 1·10⁹ M⁻¹s⁻¹. In contrast, $SO_4{}^{·-}$ is a selective oxidant and preferentially reacts with electron-rich groups (Neta et al., 1988). Compounds with

activated aromatic ring and amine moieties, such as diclofenac (aromatic amine), sulfamethoxazole (aromatic amine), venlafaxine (methoxybenzene and tertiary amine), metoprolol (methoxybenzene and secondary amine) are highly reactive with $SO_4^{\bullet-}$ among the selected TOrCs (i.e., $k_{SO_4^{\bullet-}}$ >3.89 ·10^9 M^{-1}s^{-1}). Carbamazepine (olefin) and caffeine (imidazole) exhibit slightly lower reactivity toward $SO_4^{\bullet-}$ (i.e., $k_{SO_4^{\bullet-}}$=1.5−2.39·10^9 M^{-1}s^{-1}). Iopromide contains benzene ring substituted by multiple halogens and electron-withdrawing amide group. Phenytoin and primidone are composed of weakly-activated benzene ring as well as electron-withdrawing amide group. Benzotriazole has a protonated triazole ring at pH 7 (pK_a=8.2). Consequently, these compounds might have limited electron transfer to $SO_4^{\bullet-}$ and their $k_{SO_4^{\bullet-}}$ values are <1 ·10^9 M^{-1}s^{-1}. However, phenytoin, benzotriazole and primidone are still highly reactive towards ·OH, with $k_{\bullet OH}$ values of one order of magnitude higher than their $k_{SO_4^{\bullet-}}$ values, possibly due to the rapid benzene ring addition mechanism (Vel Leitner and Roshani, 2010; Lee et al., 2014). The $k_{SO_4^{\bullet-}}$ of gabapentin and TCEP were not determined by competition kinetics but estimated to be below 1 ·10^9 M^{-1}s^{-1} based on their removal in pure water during UV/PDS (Text S3 in Section 9.4).

5.3.2 *Degradation of TOrCs in pure water during UV/H₂O₂ and UV/PDS*

Preliminary experiments indicated that the oxidation of selected TOrCs by H_2O_2 and PDS in the dark was negligible (Figure S7, SI). Figure 14 presents the percent removal of TOrCs during UV/H_2O_2 and UV/PDS in buffered pure water (57.5 mJ/cm^2, 0.15 mM oxidants). Radical oxidation significantly improved the degradation efficiency of TOrCs compared to direct photolysis. About 40−70% removal of TOrCs (except TCEP) was found during UV/H_2O_2, while the concentration of all TOrCs (except TCEP) reached the limit of quantification (LOQ) during UV/PDS within the same applied fluence and molar oxidant dose. For this reason, expected differences in TOrCs removal based on second-order rate constants with $SO_4^{\bullet-}$ could not be illustrated in UV/PDS experiments. The photolysis rate of PDS is higher than that of H_2O_2 due to its higher quantum efficiency (i.e., 0.7 mol/E for PDS and 0.5 mol/E for H_2O_2) and higher molar extinction coefficient (i.e., 21.1 M^{-1} cm^{-1} for PDS and 18.6 M^{-1} cm^{-1} for H_2O_2) at 254 nm (Ike et al., 2018). Moreover, the main radical scavengers in buffered pure water included the phosphate buffer ions (i.e., mainly HPO_4^{2-} and $H_2PO_4^-$ at pH 7, pK_{a2}=7.2), primary oxidants (H_2O_2 or PDS) and TOrCs. The scavenging capacity of each component was calculated by multiplying its molar concentration with its second-order rate constants with radicals. As shown in Table S5 (SI), the overall scavenging capacity of the buffered pure water matrix on $SO_4^{\bullet-}$ (3.4·10^3 s^{-1}) was lower compared to that on ·OH (4.8 ·10^3 s^{-1}). The product phosphate radicals (e.g., $HPO_4^{\bullet-}$) are known to be less reactive than ·OH and $SO_4^{\bullet-}$ (Neta et al., 1988), thus their contribution to TOrCs removal should be insignificant and can be ignored. Therefore, the more efficient removal of TOrCs during UV/PDS in buffered pure water was attributed to two factors: the higher photolysis rate of PDS at 254 nm and the lower scavenging effect of the water matrix on $SO_4^{\bullet-}$, which led to the higher steady-state concentration of $SO_4^{\bullet-}$ than ·OH (Xiao et al., 2016; Pari et al., 2017).

TCEP was degraded much slower than other compounds due to its low second-order rate constants with radicals (Table 8). In buffered pure water experiments, only about 10% of TCEP was removed by UV/H_2O_2 at 57.5 mJ/cm^2 and the removal was increased to 43% at 920 mJ/cm^2 (Figure S8, SI). However, the degradation of TCEP was faster in UV/PDS and reached LOQ at 920 mJ/cm^2, which was attributed to the high $SO_4^{\cdot-}$ exposure in pure water during UV/PDS.
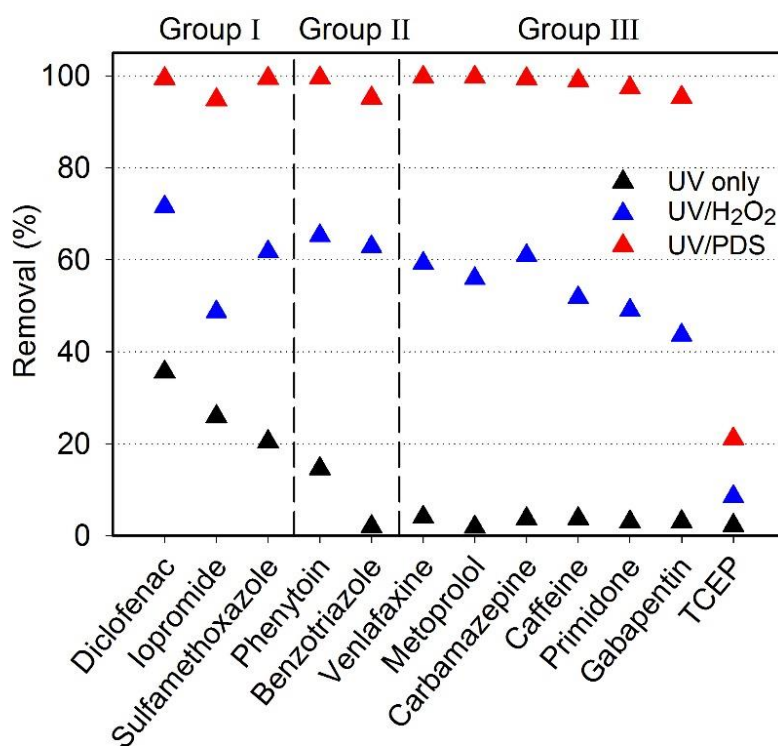
Figure 14. Percent removal of TOrCs in pure water (Fluence=57.5 mJ/cm^2, Oxidants = 0.15 mM, 5 mM phosphate buffer, pH 7)

5.3.3 *Degradation of TOrCs in wastewater effluent during UV/H_2O_2 and UV/PDS*

Experiments with 0.15 mM of H_2O_2 or PDS in wastewater effluent spiked with 1 µg/L of each TOrC, resulted in significantly reduced percent removal compared to pure water experiments (e.g., <12% of degradation for group II and III compounds at 115 mJ/cm^2) (Figure S9, SI), indicating the strong scavenging effect of the water matrix (e.g., EfOM, inorganic species) on both radicals. The effect of the water matrix can be overcome by increasing the UV fluence and oxidant dose. Figure S10 (SI) presents the percent removal of TOrCs in wastewater effluent at 1,380 mJ/cm^2 and 0.6 mM of oxidant. Direct photolysis was effective for the degradation of group I compounds (>90%). UV/H_2O_2 and UV/PDS substantially enhanced the removal of group II and III compounds (except TCEP). TCEP was persistent to both UV/H_2O_2 and UV/PDS in wastewater effluent, and less than 4% removal was obtained for the highest fluence (1,380 mJ/cm^2) and oxidant dose (0.6 mM) applied. Ozonation was also reported to be inefficient for the elimination

of TCEP in municipal WWTP effluent (e.g., 25% of removal at 1.5 mg O_3/mg DOC), because of its low reaction rate constants with ozone and ·OH (Lee et al., 2013).

Figure 15 presents the fluence-based rate constants (k_{obs}) of TOrCs calculated for UV only (k_{obs-UV}), UV/H_2O_2 (k_{obs-UV/H_2O_2}) and UV/PDS ($k_{obs-UV/PDS}$) experiments performed in wastewater effluent (0.3 mM of oxidant). k_{obs} was not calculated for TCEP due to its low removal. The $k_{obs-UV}/k_{obs-UV/AOP}$ was calculated to be greater than 0.8 for group I compounds (except diclofenac in UV/PDS), indicating that their degradation was mainly attributed to direct photolysis. During UV/PDS, the removal rate of diclofenac was enhanced to $1.12 \cdot 10^{-2}$ cm²/mJ, suggesting that both direct photolysis and radical oxidation contributed to its elimination (i.e., $k_{obs-UV}/k_{obs-UV/PDS}$= 0.6). The removal of group II compounds followed both direct photodegradation and radical oxidation, whereas the radical oxidation was the dominant process for group III compounds.
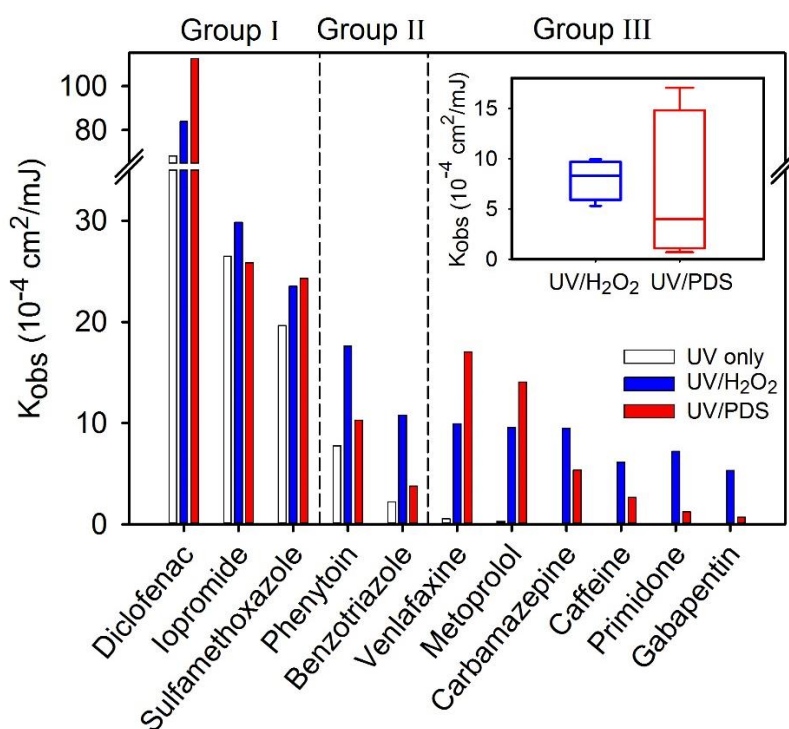
Figure 15. Fluence-based rate constants of TOrCs in wastewater effluent during UV only, UV/H_2O_2 and UV/PDS processes (fluence= 115–1,380 mJ/cm²; oxidants=0.3 mM). Inset boxplot shows the statistical evaluation of fluence-based rate constants of all group III compounds (except TCEP).

The inset boxplot in Figure 2 shows the fluence-based rate constants of group III compounds (except TCEP). The $k_{obs-UV/PDS}$ covered a wider range than k_{obs-UV/H_2O_2}, suggesting that UV/PDS showed higher selectivity towards TOrCs removal than UV/H_2O_2. Similar results were reported on UV/H_2O_2 and UV/PDS treatment of TOrCs in reverse osmosis brines (Yang et al., 2016b) and wastewater effluent (Lian et al., 2017). Moreover, the removal pattern of group III compounds during both processes was consistent with their second-order rate constants with ·OH and $SO_4^{·-}$ shown in Table 8. Group III compounds with high $k_{·OH}$ (>7 $\cdot 10^9$ M⁻¹s⁻¹) such as venlafaxine, metoprolol and

carbamazepine had similar k_{obs-UV/H_2O_2} (~1 ·10^{-3} cm²/mJ). Slightly lower removal rate was observed from caffeine (6.13 ·10^{-4} cm²/mJ) and primidone (7.20 ·10^{-4} cm²/mJ), which was consistent with their lower $k_{\bullet OH}$ (<7 ·10^9 M^{-1}s^{-1}). The k_{obs-UV/H_2O_2} of gabapentin was 5.31 ·10^{-4} cm²/mJ, suggesting that its $k_{\bullet OH}$ might have been overestimated previously (i.e., 9.1 ·10^9 M^{-1}s^{-1}) (Lee et al., 2014). Similarly, compounds with higher $k_{SO_4^{\bullet-}}$ (1.50-4.99 ·10^9 M^{-1}s^{-1}) such as venlafaxine, metoprolol, carbamazepine and caffeine showed higher removal rate than those with lower $k_{SO_4^{\bullet-}}$ (<1 ·10^9 M^{-1}s^{-1}), such as primidone and gabapentin.

Figure 16 shows the evolution of fluence-based rate constants of TOrCs as a function of initial oxidant dose. The k_{obs-UV/H_2O_2} and $k_{obs-UV/PDS}$ values of each TOrC (except for iopromide) gradually increased, suggesting that the radical exposure was promoted with increasing H₂O₂ and PDS dose (Rosario-Ortiz et al., 2010).
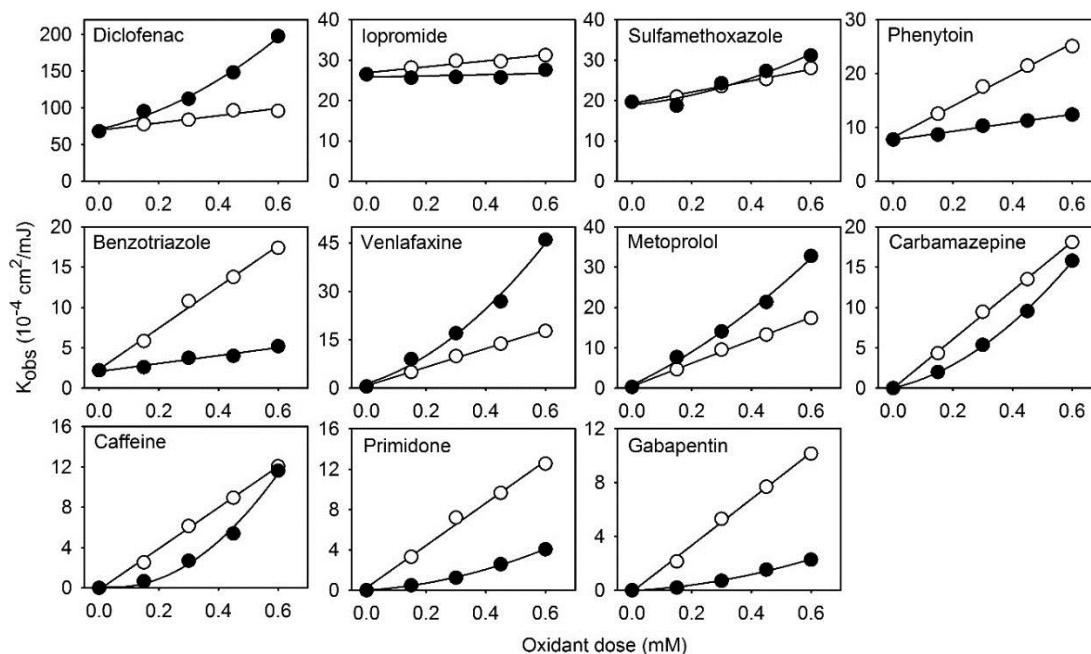
Figure 16. Fluence-based rate constants of TOrCs in wastewater effluent during UV/H₂O₂ (open circles) and UV/PDS (filled circles) (Fluence=115–1,380 mJ/cm2; Oxidants = 0, 0.15, 0.30, 0.45 and 0.60 mM)

During UV/H₂O₂, the k_{obs-UV/H_2O_2} values of TOrCs increased linearly as a function of initial H₂O₂ dose. Previous study showed that the log-transformation of TOrCs (i.e., log(C/C$_o$)) in wastewater effluent was linearly proportional to the initial H₂O₂ dose during UV/H₂O₂, which indicated that the competition between TOrCs and the wastewater effluent matrix for ·OH consumption remained constant during the oxidation process (Lee and von Gunten, 2010b). However, the $k_{obs-UV/PDS}$ values of TOrCs, especially those with high reactivity towards SO₄·⁻ (i.e., $k_{SO_4^{\bullet-}}$ >1 ·10^9 M^{-1}s^{-1}), such as diclofenac, sulfamethoxazole, venlafaxine, metoprolol, carbamazepine and caffeine, exhibited exponential increase with increasing of PDS dose.

Our results are comparable with previous studies on the treatment of TOrCs in wastewater effluent using selective oxidants (e.g., ozone, chlorine) (Lee and von Gunten, 2010b), which are highly reactive with the electron-rich organic moieties. When selective oxidants are applied, the degradation of TOrCs tends to have a "lag-phase" at low oxidant dose due to the high competition between the targeted TOrC and the wastewater effluent matrix (e.g., electron-rich site of EfOM). When the oxidant dose is increased to be above the initial water matrix demand, the degradation rates of TOrCs can be enhanced significantly (Lee and von Gunten, 2010b). To support our hypothesis, the fluorescence intensities of EEM regions (see Section 5.3.5) were progressively reduced with increasing initial PDS concentration during UV/PDS. About 62–76% fluorophores were degraded at 1,380 mJ/cm^2 and 0.6 mM of PDS (Figure S11, SI), indicating the large depletion of electron-rich organic moieties in EfOM at high PDS dose. Alternatively, more $SO_4^{\bullet-}$ will be available in solution to oxidize TOrCs. Although about 43–77% of the fluorescence intensity were removed during UV/H_2O_2 under the same experimental conditions (Figure S11, SI), $\bullet OH$ is a non-selective oxidant and it might react with all fractions of EfOM and the transformation products of EfOM as fast as their initial compounds, resulting in the constant scavenging rates of water matrix for $\bullet OH$ during the entire oxidation processes (Lee and von Gunten, 2010).

Diclofenac, venlafaxine and metoprolol were more efficiently eliminated by UV/PDS compared to UV/H_2O_2 because they can more easily overcome the scavenging impact of EfOM due to their high reactivity with $SO_4^{\bullet-}$. The UV/PDS process was also reported to be more efficient than UV/H_2O_2 for venlafaxine and metoprolol in wastewater effluent (Lian et al., 2017). Sulfamethoxazole was degraded faster in UV/PDS when PDS dose was above 0.3 mM. For caffeine and carbamazepine, $k_{obs-UV/PDS}$ was comparable with k_{obs-UV/H_2O_2} at 0.6 mM oxidant dose, thus UV/PDS is expected to outcompete UV/H_2O_2 for removal of these two compounds if higher PDS dose is applied (>0.6 mM). For phenytoin, benzotriazole, primidone and gabapentin, UV/H_2O_2 was more efficient as they have low reactivity with $SO_4^{\bullet-}$ to overcome the scavenging effect of the water matrix during UV/PDS. The k_{obs-UV/H_2O_2} of iopromide was only increased by less than 20% compared to k_{obs-UV} and its $k_{obs-UV/PDS}$ value was almost stable in various initial H_2O_2 and PDS doses, respectively. This can be explained by the low reactivity of iopromide with $\bullet OH$ and $SO_4^{\bullet-}$ (Table 8). Hence, direct photodegradation is mainly responsible for the removal of iopromide in wastewater effluent and upgrading UV process to UV/H_2O_2 or UV/PDS will not contribute substantially to its removal efficiency.

5.3.4 *Effect of wastewater matrix components*

The water matrix components (e.g., DOC, bicarbonate, nitrite and halides) react with $\bullet OH$ and $SO_4^{\bullet-}$, lowering the efficiency of UV/H_2O_2 and UV/PDS processes. Table 7 shows the water quality parameters of wastewater effluent used in this study. The exact concentration of chloride is not available, but the annual average concentration in this WWTP effluent is provided. The scavenging capacity of the known inorganic constituents were calculated by multiplying their concentrations with their second-order reaction rate

constants with ·OH and $SO_4^{·-}$ (rate constants and references are shown in Table S4). DOC and chloride were the most efficient scavengers for UV/H_2O_2 and UV/PDS, respectively.

The product radicals (e.g., $CO_3^{·-}$, $NO_2^{·}$ and $Cl_2^{·}$) generated from the reactions between inorganic components and ·OH or $SO_4^{·-}$ (Table S4) might also participate in the degradation of TOrCs (Wols and Hofman-Caris, 2012; Lian et al., 2017). The product radicals are moderate oxidants (i.e., 1.63 V, 1.03 V and 2.0 V for $CO_3^{·-}$, $NO_2^{·}$ and $Cl_2^{·}$, respectively) and even more selective than $SO_4^{·-}$ toward electron-rich moieties (e.g., activated aromatics like phenols and anilines) (Zuo et al., 1999; Guo et al., 2017; Ji et al., 2017). The impact of individual inorganic ions (i.e., bicarbonate, nitrite, nitrate and chloride) on the removal pattern of TOrCs during UV/H_2O_2 and UV/PDS was investigated in buffered pure water applying the concentration of each inorganic constituent in Table 1. The influence of chloride was simulated by applying 35 and 350 mg/L of chloride. The fluence-based rate constants of TOrCs are shown in Figure S12. The effect of nitrate (10.6 mg-N/L) was negligible for both processes. The k_{obs-UV/H_2O_2} and $k_{obs-UV/PDS}$ of TOrCs (except for diclofenac and sulfamethoxazole) in the presence of bicarbonate (307 mg/L) were lower than that in the presence of nitrite (0.028 mg-N/L), indicating that bicarbonate scavenged radicals more efficiently than nitrite. This is consistent with the calculated scavenging capacity of bicarbonate and nitrite shown in Table 1. However, nitrite was present at low concentration (0.028 mg-N/L) in this specific wastewater sample. The second-order rate constant of nitrite with ·OH ($1.0·10^{10}$ $M^{-1}s^{-1}$) (Coddington et al., 1999) and $SO_4^{·-}$ ($8.8·10^8$ $M^{-1}s^{-1}$) (Neta et al., 1988) is the highest among the known wastewater components in Table 1, suggesting that the scavenging capacity of nitrite can be significant at higher concentration. A previous study reported that the efficiency of TOrCs elimination during UV/H_2O_2 was strongly influenced by nitrite concentration fluctuations in WWTP effluent (Miklos et al., 2018a). Interestingly, sulfamethoxazole and diclofenac were degraded faster in bicarbonate containing solution than in the presence of nitrite during both processes, which suggests that $CO_3^{·-}$ contributed to their removal. Recent studies also reported the degradation of sulfamethoxazole and diclofenac by $CO_3^{·-}$ (Lu et al., 2017; Yang et al., 2017a). No significant reduction of k_{obs-UV/H_2O_2} was found for UV/H_2O_2 in the presence of chloride. This finding was expected because the reaction between chloride and ·OH is reversible and the rate constant of forward reaction ($4.3·10^9$ $M^{-1}s^{-1}$) is even lower than that for the backward reaction ($6.1·10^9$ $M^{-1}s^{-1}$) (Jayson et al., 1973) (Table S4). The concentration of TOrCs reached LOQ at 57.5 mJ/cm² during UV/PDS in the presence of 35 mg/L of chloride. When the chloride was increased to 350 mg/L, the removal rate of TOrCs decreased. Although the scavenging capacity of 350 mg/L of chloride (i.e., $3·10^6$ s^{-1}) is about two and three orders of magnitude higher than that of bicarbonate and nitrite, respectively, the $k_{obs-UV/PDS}$ values in the presence of chloride were comparable or even higher than those in the presence of bicarbonate and nitrite for most compounds, indicating that reactive chlorine species (e.g., $Cl_2^{·}$) might promote the degradation of TOrCs. Consequently, the presence of chloride in wastewater effluent reduces the steady-state concentration of $SO_4^{·-}$ during UV/PDS but might less affect the removal rate of TOrCs compared to bicarbonate and nitrite at similar scavenging capacity.

However, the importance of inorganic ions might be different in wastewater effluent compared to the buffered pure water with individual inorganic components. As shown in Table 7, DOC is a strong scavenger for $^{\cdot}$OH and $SO_4^{\cdot-}$, resulting in lower steady-state concentrations of primary radicals in wastewater effluent compared to pure water. Moreover, the product radicals can also be scavenged by the wastewater components. For instance, bicarbonate is reactive with $Cl^{\cdot}$ and $Cl_2^{\cdot}$ to produce more $CO_3^{\cdot-}$ (Table S4, SI). DOC was reported to scavenge $Cl^{\cdot}$ efficiently (i.e., $1.3 \cdot 10^4$ $(mg-C/L)^{-1} s^{-1}$) (Fang et al., 2014).

5.3.5 *Oxidative inactivation of fluorescent effluent organic matter components during UV/H₂O₂ and UV/PDS*

Figure S13 (SI) illustrates the EEM spectra of wastewater effluent during UV/H₂O₂ and UV/PDS processes. The EEM spectra of wastewater effluent (before AOP treatment) exhibited 4 characteristic regions with maximum fluorescence intensity identified as follows (Table S6, SI): aromatic protein-like peak (P_II, Excitation/Emission= 242/358 nm), fulvic-like peak (P_III, 242/430 nm), soluble microbial product-like peak (P_IV, 287/353 nm) and humic-like peak (P_V, 329/412 nm) (Chen et al., 2003).

The fluorescence intensity of P_IV was reduced by 15% during direct photolysis at 920 mJ/cm², suggesting the presence of relatively photo-sensitive fluorophores in soluble microbial product-like region. The intensity of the other fluorescence peaks was stable during direct photolysis (115–1,380 mJ/cm²). Once adding H₂O₂ and PDS, the fluorescence intensities of all the selected peaks decreased following first-order reaction kinetics, indicating the contribution of $^{\cdot}$OH and $SO_4^{\cdot-}$, respectively. Their fluence-based reaction rate constants (k_{obs-UV/H_2O_2} and ($k_{obs-UV/PDS}$) linearly increased as a function of initial oxidant dose (Figure 17a), except the $k_{obs-UV/PDS}$ of P_V, which appeared to increase exponentially. The fluorescence extinction of fulvic and humic-like fluorophores were much slower than that of soluble microbial product-like and aromatic protein-like fluorophores during UV/H₂O₂. This is in accordance with previous observation that some fluorophores in humic-like region might be more resistant to $^{\cdot}$OH attack than fluorophores from the protein-like region (Abdelmelek et al., 2011). Interestingly, unlike the removal of TOrCs, UV/PDS reduced the fluorescence intensities of all identified fluorophores and showed less selectivity toward fluorophores removal. This is consistent with the literature that $SO_4^{\cdot-}$ is a strong electrophile and preferentially oxidizes electron rich moieties (e.g., unsaturated and aromatic compounds) (Xiao et al., 2015), which is the primary characteristic of fluorescent compounds (Swietlik and Sikorska, 2004). The fluorescence loss of humic and fulvic-like fluorophores during UV/PDS were even faster than that during UV/H₂O₂. Addition and hydrogen abstraction are the main pathways for $^{\cdot}$OH, whereas electron transfer is predominant for $SO_4^{\cdot-}$ (Neta et al., 1988). During UV/H₂O₂, humic substances might mainly undergo hydroxylation and breakdown of macromolecules into smaller ones, but the main structural characteristic remains intact (González et al., 2013). The direct electron transfer from aromatic rings to $SO_4^{\cdot-}$ can follow hydroxylation in aqueous solution to generate similar hydroxylated aromatics as $^{\cdot}$OH (Olmez-Hanci and Arslan-Alaton, 2013). However, the electron transfer also can lead to the formation of unstable radical cation intermediates or the decarboxylation

following the oxidation of aromatic ring, which might induce the rapid ring cleavage during UV/PDS (Neta et al., 1977). Therefore, the prevalence of radical reactions with EfOM can impact differently on fluorescence during UV/H_2O_2 and UV/PDS.

Several studies investigated fluorescence as a surrogate to predict the elimination of TOrCs during various water treatment processes (Gerrity et al., 2012; Park et al., 2017). The possible correlation of fluence-based rate constants between selected fluorescence peaks and individual group III compounds (except TCEP) was examined in this study. Figure 17b presents venlafaxine as an example. Other group III compounds are shown in Figure S14 and Figure S15 in SI. The k_{obs-UV/H_2O_2} value of individual group III compounds was linearly correlated with that of selected fluorescence peaks, suggesting that fluorescence may be a useful indicator for group III compounds removal during UV/H_2O_2. The $k_{obs-UV/PDS}$ values of group III compounds exponentially increased with respect to $k_{obs-UV/PDS}$ of selected fluorescence peaks. Due to the selective oxidizing property of $SO_4^{\cdot-}$, the elimination of compounds that are less reactive with $SO_4^{\cdot-}$ can be eliminated much slower than fluorophores. For example, only about 28% of gabapentin was removed when 62-76% fluorophores were degraded during UV/PDS (Figure S10 and Figure S11, SI). Therefore, the development of compound-specific surrogate model on fluorescence would be required during UV/PDS.
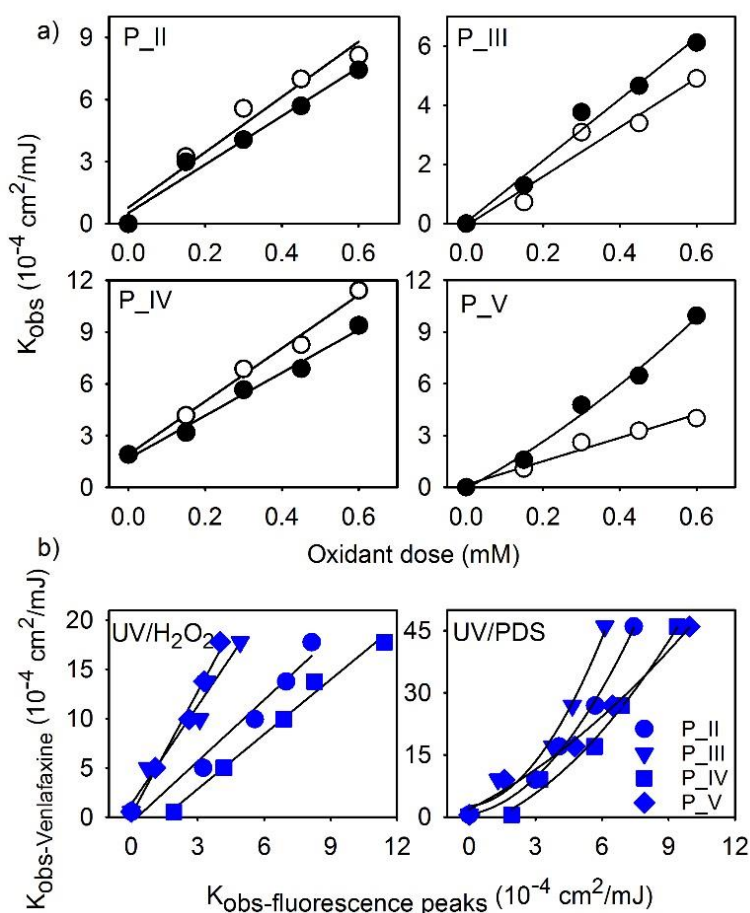
Figure 17. a) Fluence-based rate constants of selected fluorescence peaks in wastewater effluent during UV/H_2O_2 (open circles) and UV/PDS (filled circles). b) Correlations between the fluence-

based rate constants of venlafaxine and selected fluorescence peaks during UV/H$_2$O$_2$ and UV/PDS (Fluence=115–1,380 mJ/cm^2; Oxidants = 0, 0.15, 0.30, 0.45 and 0.60 mM).

5.3.6 *Degradation of TOrCs during pilot-scale UV/PDS*

Pilot-scale UV/PDS treatment of TOrCs was conducted at WWTP. The concentrations of TOrCs in WWTP effluent before UV/PDS treatment are shown in Table 2. Phenytoin (13±2 ng/L) and caffeine (71±32 ng/L) were present at very low initial concentrations, which were close to LOQ and consequently showing large uncertainties. Therefore, the elimination of phenytoin and caffeine was not monitored during pilot-testing. Figure 18 shows the relative removal of TOrCs during UV only and UV/PDS processes. Group I compounds were efficiently removed. More than 98% of diclofenac was degraded at 1,200 mJ/cm^2 when only UV was applied, with the addition of 0.6 mM of PDS, the same removal of 98% was already achieved at 800 mJ/cm^2. Comparable to lab-scale experiments, the elimination of iopromide and sulfamethoxazole was mainly caused by direct photolysis, with 94% and 91% removal at 1,200 mJ/cm^2, respectively. No significant contribution of SO$_4$$^{\cdot-}$ was observed to iopromide within experimental uncertainties due to its low $k_{SO_4^{\cdot-}}$ (i.e., <1 ·10^9 M^{-1}s^{-1}). Sulfamethoxazole is highly reactive with SO$_4$$^{\cdot-}$ (i.e., $k_{SO_4^{\cdot-}}$ 12.5 ·10^9 M^{-1}s^{-1}) (Mahdi Ahmed et al., 2012). Furthermore, the potential inner filter effect of PDS was excluded as the UV fluence was adjusted after PDS spiking during pilot-testing. However, the removal of sulfamethoxazole was slower during UV/PDS than direct UV photolysis for unknown reason. Venlafaxine and metoprolol were removed most efficiently among the group II and III compounds, which was consistent with the lab-scale experiments. About 77% of venlafaxine, 49% of metoprolol and 27% of carbamazepine were eliminated at 1,200 mJ/cm^2 and 0.6 mM PDS. Compounds showing low reactivity toward SO$_4$$^{\cdot-}$ were less removed. For instance, about 58% of benzotriazole and 11% of primidone were degraded at 1,200 mJ/cm^2 with 0.6 mM PDS. Similar to iopromide, the direct photodegradation was mainly responsible for the elimination of benzotriazole due to its low $k_{SO_4^{\cdot-}}$ (i.e., <1 ·10^9 M^{-1}s^{-1}) (Figure S16, SI). Gabapentin and TCEP appeared to be resistant to UV photolysis and UV/PDS in these experimental conditions.

The removal pattern of TOrCs during pilot-testing was comparable to lab-scale experiments, but their removal rates were lower. Higher concentrations of DOC and nitrite were observed during pilot-scale tests compared to lab-scale experiments, resulting in about 1.7 and 5.3 times higher scavenging capacity of the wastewater matrix on SO$_4$$^{\cdot-}$ (Table 7). Fluorescence intensity was reduced only by 35-54% at 1,200 mJ/cm^2 with 0.6 mM PDS (Figure S17 and Figure S18, SI), confirming the overall lower oxidation efficiency due to the scavengers during pilot-testing.
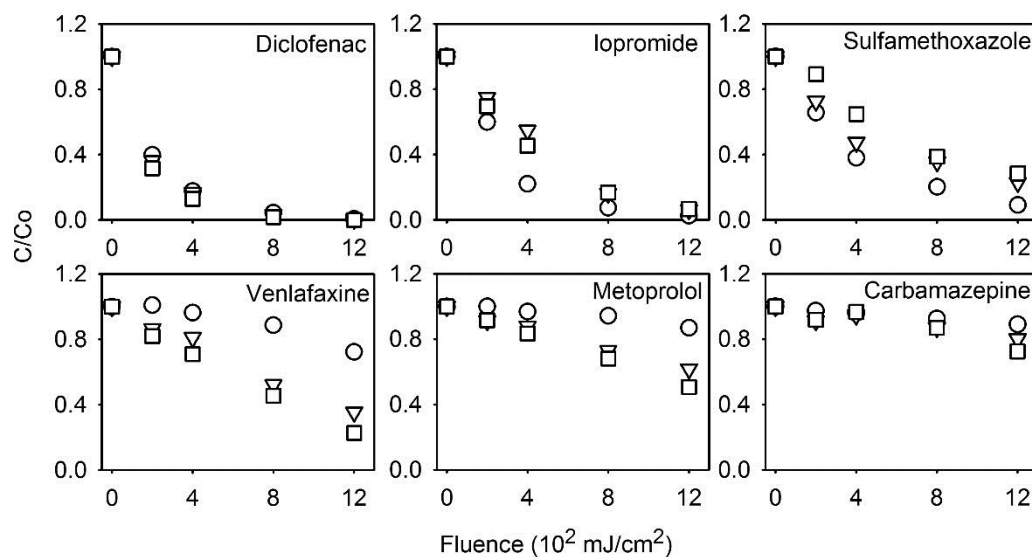
Figure 18. Relative removal of TOrCs in pilot-scale experiments by direct photolysis (circles) and UV/PDS (triangle: 0.3 mM of PDS; square: 0.6 mM of PDS) (Fluence= 0–1,200 mJ/cm²)

5.4 Conclusion

- When the same molar dose of PDS and H_2O_2 are applied, UV/PDS can eliminate all TOrCs more efficiently than UV/H_2O_2 in buffered pure water due to the higher yield of $SO_4^{\cdot-}$.

- $SO_4^{\cdot-}$ preferentially oxidizes TOrCs with electron-rich moieties (e.g., activated aromatic ring and amines) as well as the electron-rich site of EfOM (e.g., fluorophores), while $\cdot$OH reacts with almost all organic moieties with nearly diffusion-controlled rates.

- High competition between the target TOrCs and the electron-rich site of EfOM (scavenger) was observed at low PDS dose. However, the initial oxidant demand was followed by an exponential increase in the fluence-based rate constants of most compounds with increasing PDS dose. In contrast, the scavenging impact of the water matrix on $\cdot$OH was constant during UV/H_2O_2, leading to a linear increase of fluence-based rate constants with increasing H_2O_2 dose.

- Selectivity of $SO_4^{\cdot-}$ results in more efficient removal of TOrCs with electron-rich moieties by UV/PDS in wastewater effluent while UV/H_2O_2 better oxidizes compounds with less reactivity toward $SO_4^{\cdot-}$.

- The scavenging capacities of DOC and chloride were calculated to be the highest among the known water parameters during UV/H_2O_2 and UV/PDS, respectively. Experiments conducted in the presence of individual inorganic species indicated that $CO_3^{\cdot-}$ enhanced the degradation of diclofenac and sulfamethoxazole during both processes. Chlorine radicals might contribute to the degradation of most compounds during UV/PDS.

- The efficiency of pilot-scale UV/PDS was affected by the variation of DOC and nitrite in wastewater effluent. Higher UV fluences and oxidant doses are needed

to overcome the impact of the water matrix. However, the energy requirements and the effect of sulfate ion on the salinity of treated water should be evaluated prior to UV/PDS application in wastewater effluent.

Applying the radical promoter peroxodisulfate as a substitute for H_2O_2, a comparable oxidation performance of UV-AOPs can be achieved in municipal wastewater effluents, which supports hypothesis № 3 for operation with peroxodisulfate.

5.5 Acknowledgments

6. Comparison of UV-AOPs (UV/H₂O₂, UV/PDS and UV/Chlorine) for TOrC removal and surrogate model evaluation

Abstract

UV-based advanced oxidation processes (AOPs) have been widely explored as to remove organic contaminants from water streams. This lab-scale study demonstrates through direct comparison of UV/H₂O₂, UV/PDS and UV/Chlorine at equimolar radical promoter concentrations in municipal wastewater that the general oxidation performance of a wide range of TOrCs followed the order of UV/H₂O₂≈UV/PDS<UV/Chlorine while UV/PDS and UV/Chlorine exhibited higher compound selectivity than UV/H₂O₂. Evaluating potential optical surrogates to predict TOrC removal in UV-AOPs, nine parameters were selected representing chromophore and fluorophore features of DOM including components derived by parallel factor analysis (PARAFAC) of excitation-emission matrices. UVA, TF and the selected fluorescence peak P_IV revealed highest linear correlation coefficients and were therefore determined as surrogates representing underlying mechanistic reactions of each UV-AOP. Besides ·OH-based reactions in UV/H₂O₂ where P_IV showed highest R² values, best correlations were shown for UVA and TF, indicating that neither peak picking nor PARAFAC resulted in a higher informative value of selected optical surrogates. Although oxidation performance of UV/Chlorine is outstanding in comparison of the three UV-AOPs, it has to be noted that OBP formation potential might be substantially higher during both UV/PDS and UV/Chlorine compared to UV/H₂O₂. Therefore, OBP formation should be comparatively investigated in combined toxicological investigations to reveal potential drawbacks of each UV-AOP.

6.1 Introduction

UV irradiation combined with radical promoters such as hydrogen peroxide (H₂O₂), chlorine (HOCl/OCl⁻) and peroxodisulfate (PDS, S₂O₈²⁻) has been widely explored as UV-based advanced oxidation processes (AOPs) to remove organic contaminants and recently for the inactivation of antibiotic resistant genes from drinking water, wastewater, and reclaimed water (Watts and Linden, 2007; Sichel et al., 2011; Wols and Hofman-Caris, 2012; Zhang et al., 2015b; Wang et al., 2016; Wacławek et al., 2017; Yoon et al., 2017; Miklos et al., 2018a; Varanasi et al., 2018; Yoon et al., 2018). UV photolysis of these oxidants with low-pressure (LP) mercury lamps at a wavelength of λ=254 nm results in

the generation of highly reactive species such as hydroxyl radicals ($\cdot$OH), chlorine radicals (Cl$\cdot$), and sulfate radicals (SO$_4$$^{\cdot-}$). The photolysis rate of PDS is higher than that of H$_2$O$_2$ due to its higher quantum yield (i.e., 0.7 mol/E for PDS and 0.5 mol/E for H$_2$O$_2$) and higher molar absorption coefficient (i.e., 21.1 M^{-1} cm^{-1} for PDS and 18.6 M^{-1} cm^{-1} for H$_2$O$_2$) at 254 nm (Ike et al., 2018). Photolysis rate constants of HOCl/OCl$^-$ are slightly pH dependent (pK$_a$= 7.54) and even higher than those of PDS and H$_2$O$_2$ with quantum yields of 1.0 and 0.9 mol/E and molar absorption coefficients of 59 and 66 M^{-1} cm^{-1}, respectively (Feng et al., 2007). Besides $\cdot$OH and Cl$\cdot$, reactive chlorine species (RCS), such as Cl$_2$$^{\cdot-}$, ClO$\cdot$, and $\cdot$ClOH are abundant during UV/Chlorine AOP to oxidize target organic contaminants (Fang et al., 2014; Wang et al., 2016; Wu et al., 2017).

UV/H$_2$O$_2$ is the most frequently applied UV-AOP at full-scale and has been investigated at both laboratory (Wols et al., 2013) and pilot-scale (Miklos et al., 2018a) based on its low OBP formation potential (Linden et al., 2005) and primary formation of unselective and highly reactive $\cdot$OH (Neta et al., 1988). Application of UV/PDS for TOrC degradation has been receiving increasing attention in the past few years mainly due to its slightly higher radical yield by photolysis compared to UV/H$_2$O$_2$ and the selective reaction of SO$_4$$^{\cdot-}$ to organic molecules with electron rich functional groups (Wacławek et al., 2017; Ike et al., 2018). A considerable amount of research articles has been published about mechanisms and applications of UV/Chlorine in water treatment (Xiang et al., 2016; Guo et al., 2017; Wu et al., 2017; Rott et al., 2018). A first full-scale application of UV/Chlorine as part of an indirect potable reuse train recently started operation at the Los Angeles Terminal Island Water Reclamation Plant (Xylem, 2015) corroborating the applicability of this process. Based on the properties of $\cdot$OH, SO$_4$$^{\cdot-}$ and RCS, UV/PDS and UV/Chlorine reveal a higher sensitivity to water matrix changes and DOM composition compared to $\cdot$OH dominated processes (Varanasi et al., 2018). Based on the different oxidation mechanisms, oxidation by-product (OBP) formation should also be considered regarding UV-AOPs, since toxicological concerns about TOrCs might be shifted after oxidative water treatment to potential adverse effects of formed OBPs (Magdeburg et al., 2014). While UV/H$_2$O$_2$ does not results in relevant OBP formation (Linden et al., 2005), significant amounts of OBPs might be generated during UV/PDS (Fang and Shang, 2012; Lutze et al., 2014; Yuan et al., 2014) and UV/Chlorine (Sichel et al., 2011; Yang et al., 2016a; Wang et al., 2017b).

Comparison of UV-AOPs has already been approached by some studies that revealed the advantage of UV/PDS compared to UV/H$_2$O$_2$ in buffered pure water matrices (Khan et al., 2014; Zhang et al., 2015a; Xiao et al., 2016). However, this effect is significantly reduced if UV/PDS is applied to wastewater effluent (Nihemaiti et al., 2018). Another study confirmed the higher selectivity and oxidation performance of UV/PDS compared to UV/H$_2$O$_2$ by assessing fractions of natural organic matter (NOM) (Ahn et al., 2017). Higher TOrC removal efficiency of UV/Chlorine compared to UV/H$_2$O$_2$ has already been reported in a number of studies (Sichel et al., 2011; Yang et al., 2016a; Li et al., 2017; Pan et al., 2018; Pati and Arnold, 2018). A recent study indicated comparable removal of clofibric acid by UV/PDS and UV/Chlorine in phosphate buffer (Lu et al., 2018). The direct comparison of the three UV-AOPs has received little attention so far. Current investigations revealed the dependence of oxidation performance on water matrix and

target compounds: While Li et al. (2017) reported an oxidation performance of TOrCs in synthetic reverse osmosis permeate following the order of UV/PDS > UV/H$_2$O$_2$ > UV/Chlorine, investigations of Pati and Arnold (2018) in buffered pure water revealed highest removal performance for UV/Chlorine followed by UV/PDS and UV/H$_2$O$_2$. In a current study, transformation of a standard dissolved organic matter (DOM) by the three above mentioned UV-AOPs was investigated and revealed that UV/PDS is more affected by aromatic components of DOM while UV/H$_2$O$_2$ and UV/Chlorine are affected by aliphatic background DOM (Varanasi et al., 2018). Since $\cdot$OH, SO$_4$$^{\cdot-}$ and $\cdot$Cl are scavenged by inorganic ions and organic matter with different specific reactivities (Fang et al., 2014; Lutze et al., 2015b; Li et al., 2017), water quality not only affects the oxidation efficiency of UV-AOPs it also might already indicate which UV-AOP is the most effective for a given matrix. The above mentioned comparative studies reveal the importance of the water matrix on UV-AOPs performance. However, no comparative study investigated the TOrC removal performance of UV/H$_2$O$_2$, UV/PDS and UV/Chlorine, in real municipal wastewater matrices, so far, which is addressed in this study.

In addition to performance of TOrC removal, this study monitored various spectrophotometric parameters throughout different processes as potential surrogates which might be used for online monitoring or control of individual UV-AOPs. Today, extensive research has proved the correlation between UVA at 254 nm and TOrCs during (powdered) activated carbon (Anumol et al., 2015; Altmann et al., 2016), ozonation (Bahr et al., 2007; Dickenson et al., 2009; Altmann et al., 2014; Stapf et al., 2016; Park et al., 2017) and UV/H$_2$O$_2$ (Yu et al., 2015). Selected fluorescence peaks (e.g. fluorescence index (FI)) have been additionally investigated as surrogates for TOrC removal during water treatment (Chys et al., 2017; Yan et al., 2017). Different oxidation mechanisms of UV-AOPs result in a broad reactivity towards TOrCs and simultaneously in a differential depletion of DOM based on photolysis and additional reactions with radical species (Varanasi et al., 2018). The removal of photo-susceptible and photo-resistant TOrCs during UV-AOPs might therefore correlate with intensity changes of specific chromophore or fluorophore DOC components.

Instead of single surrogates that denote the overall AOP performance, the differentiated approach of this study aims to derive optical surrogates for AOPs that represent underlying mechanisms; i.e., photolysis and reactions with specific radical species. By expanding optical surrogates from single absorbance measurements (usually at λ=254 nm or λ=436 nm) to more differentiated parameters, i.e., fluorescence indices (FI), total fluorescence (TF), or statistically derived components by parallel factor analysis (PARAFAC) of excitation-emission matrices (EEMs), these parameters may enhance the reliability of predicting TOrC removal performance by representing specific oxidation mechanisms of UV-AOPs. Therefore, this study comparatively investigates the oxidation performance of UV/H$_2$O$_2$, UV/PDS and UV/Chlorine for TOrC removal from municipal wastewater effluent. In addition, optical surrogates namely total fluorescence (TF), fluorescence index (FI), UVA$_{254}$, and yellow color (measured as absorbance at 436 nm) as well as PARAFAC components derived from fluorescence EEMs are evaluated as potential surrogates to predict TOrC removal performance.

This study tested the hypothesis that application of the radical promoters peroxodisulfate and chlorine as substitutes for H_2O_2 result in a comparable oxidation performance of UV-AOPs in municipal wastewater effluents (Hypothesis № 3) and the removal of photo-susceptible and photo-resistant TOrCs during UV/AOPs correlate with intensity changes of specific chromophore or fluorophore DOC components (Hypothesis № 4).

6.2 Materials & Methods

6.2.1 Experimental set-up and procedure

The wastewater investigated in this study originated from the WWTP Gut Marienhof in Munich, which consists of a mechanical treatment stage including screens, aerated sand/fat traps and primary clarification, followed by a two-stage activated sludge process for biological carbon and nutrient removal (solids retention time of 2–3 and 6–8 days, respectively). The wastewater is subsequently filtered using tertiary granular media filters with a resulting UV-transmittance at 254 nm (UVT) of 65–75% prior to UV disinfection. In this study, a batch sample was collected directly after granular media filtration (08/21/2017). The water sample was stored in amber glass bottles at 4°C in the dark until experimental treatment. Before UV-exposure, the sample was filtered through a paper filter (MN 619, Machery-Nagel, Germany) and spiked with a mix of indicator TOrCs (i.e., benzotriazole, carbamazepine, caffeine, diclofenac, gabapentin, iopromide, metoprolol, phenytoin, primidone, sulfamethoxazole, TCEP, and venlafaxine) at a concentration of 1 µg/L each. The compounds sotalol, tramadol, trimethoprim, valsartan acid, and atenolol were not spiked and therefore occurred at ambient concentrations as reported in Table 9.

Laboratory-scale experiments were conducted in a self-constructed collimated beam device housing three low-pressure Hg UV-lamps at 15 W each (UV Technik Meyer, Germany). As a quasi-collimator, a 20 cm black PVC-tube with a diameter of 10 cm was used. UV-C irradiance at the sample position was determined as $1 - 1.4$ mW/cm² on average across the petri dish by a certified UV-C radiometer (sglux, Germany). More detailed information about the set-up can be found elsewhere (Miklos et al., 2018a).

Experimental procedure followed the standardized method for fluence determination (Bolton and Linden, 2003). Fluences of 50-800 mJ/cm² were applied to 30 mL of sample in a 100 mm glass petri dish. Oxidants were added at targeted concentrations of 0.075, 0.15, 0.3, and 0.45 mM directly before UV-exposure from stock oxidant solutions. Dark experiments were conducted with the same experimental set-up applying the same dosages as in UV-experiments (exposure time 13 minutes) to investigate direct TOrC attenuation by H_2O_2, peroxodisulfate and chlorine. Since significant oxidation was expected by chlorine, it was investigated over three different exposure times at 95, 379, and 758 sec. After reaction, residual oxidants were quenched with Na_2SO_3 (2:1 molar ratio). All samples were stored in amber glass bottles at 4°C and analyzed for 3D-fluorescence, DOC and TOrCs within 24 hours.

6.2.2   Analytics

6.2.2.1   General water parameters

General water parameters were measured using cuvette tests (acid capacity $K_{a\,4.3}$ (LCK 362, HACH, Germany), nitrate (LCK 340, HACH, Germany), and nitrite (LCK 341/342, HACH, Germany)). All cuvette tests as well as UVT_{254} and color (λ=436 nm) were analyzed using a DR6000 UV/Vis spectrophotometer (HACH, Germany). DOC was analyzed on a varioTOC cube (Elementar, Germany) after filtration through cellulose nitrate membrane filters with a pore size of 0.45 µm (Sartorius AG, Germany). H_2O_2 concentration in wastewater samples was determined according to DIN 38 409 H15 using titanium (IV) oxysulfate colorimetry (DIN 38 409, 1987). Titanium (IV) oxysulfate solution (2%) for H_2O_2-measurements in wastewater was purchased from Sigma-Aldrich. pH value was measured with a Sentix 60 glass electrode (WTW, Germany) according to Standard Method 4500-H+.

6.2.2.2   Trace organic chemicals

Quantification of TOrCs was conducted after filtration through 0.22 µm PVDF syringe filters (Berrytec, Germany) using a high-performance liquid chromatography (Knauer PLATINBLUE UHPLC) coupled with tandem mass spectrometry (LC-MS/MS) (SCIEX 6500) with direct injection. To account for matrix suppression and instrument variability, isotope dilution was used. A detailed description of the analytical method was recently published by Müller et al. (2017). Isotope labelled analytical standards for TOrCs analysis as well as TOrCs were purchased of analytical grade. All solvents used for liquid chromatography were HPLC-grade. Analyzed TOrCs are summarized in Table 9 along with previously reported kinetic data for the reaction with OH and sulfate radicals and their measured concentrations in wastewater effluent. Second-order rate constants for the reaction of TOrCs with chlorine radicals are only rarely available and therefore not included in Table 9.

Table 9: TOrC influent concentrations, limit of quantification (LOQ) and compound specific second-order reaction rate constants for OH radical oxidation

Compounds	LOQ [ng/L]	TOrC conc. before treatment [ng/L]	$k_{\cdot OH}$ [10^9 M^{-1} s^{-1}]	References	$k_{SO_4^{\cdot-}}$ [10^9 M^{-1} s^{-1}]	References	Direct UV photolysis			References
							ϕ [10^{-2} mol/E]	ε [m²/mol]	k_{UV} [10^{-5} m²/J]	
Atenolol	10	70	7.1	Wols et al., 2014	n/a		6.5	35	1.11	Wols et al. (2014)
Benzotriazole	50	5,800	8.0	Vel Leitner and Roshani (2010)	0.87	Nihemaiti et al. (2018)	1.6	614	4.8	Bahnmüller et al. (2015)
Caffeine	10	1,100	6.4	Wols and Hofman-Caris (2012)	2.39	Nihemaiti et al. (2018)	0.18	392	0.345	Rivas et al. (2011b)
Carbamazepine	5	1,240	8.2	Wols and Hofman-Caris (2012)	1.50	Nihemaiti et al. (2018)	0.06	607	0.178	Pereira et al. (2007b)
Diclofenac	5	1,960	8.2	Wols et al. (2014)	9.2	Mahdi Ahmed et al. (2012)	23	680	76.5	Wols et al. (2014)
Gabapentin	2.5	2,950	9.1	Lee et al. (2014)	<1.0	Lian 2017	n/a	n/a	-	
Iopromide	50	1,190	3.3	Huber et al. (2003)	0.36	Nihemaiti et al. (2018)	3.9	2,100	40	Canonica et al. (2008)
Metoprolol	2.5	1,300	8.1	Wols et al. (2014)	3.89	Nihemaiti et al. (2018)	6.6	33	1.06	Wols et al. (2014)
Phenytoin	5	1,240	6.28	Yuan et al. (2009)	0.62	Nihemaiti et al. (2018)	27.9	126	17.2	Yuan et al. (2009)
Primidone	25	1,150	6.7	Real et al. (2009)	0.53	Nihemaiti et al. (2018)	8.2	22	0.882	Real et al. (2009)
Sotalol	5	60	n/a	-			39	37	7.05	Wols et al. (2014)
Sulfamethoxazole	5	740	6.3	Wols et al. (2014)	12.5	Mahdi Ahmed et al. (2012)	8.4	1,300	53.4	Wols et al. (2014)
Tramadol	5	320	6.3	Zimmermann et al. (2012)			n/a	n/a	-	Zimmermann et al. (2012)
Trimethoprim	5	120	8.0	Wols et al. (2014)	n/a		0.09	1,600	0.704	Wols et al. (2014)
Tris (2-chloroethyl) phosphate (TCEP)	50	1,330	0.56	Watts and Linden (2009)	<1.0	Lian 20017	n/a	n./a	-	
Valsartan acid	5	1,870	7.9	Wols et al. (2014)	n/a		n/a	n/a	-	
Venlafaxine	2.5	1,380	8.8	Wols et al. (2014)	4.99	Nihemaiti et al. (2018)	9.7	38	1.8	Wols et al. (2014)

6.2.2.3   Fluorescence Analysis

Fluorescence excitation-emission matrices (EEM) were obtained using an Aqualog Fluorescence Spectrometer (Horiba Scientific, Germany). The fluorescence response of a blank solution (Milli-Q water) was subtracted from the EEM of each sample. The wastewater specific fluorescence signal was tested for linearity in a preliminary experiment using 5 dilutions with ultrapure water ranging from 2:1 to 10:1. Data processing included corrections using inner filter effects, Raman normalization, Rayleigh masking (Bahram et al., 2006), and diagram adjustments. The EEM were further quantitatively analyzed based on the PARAFAC method. PARAFAC analysis was carried out using the chemo-metrics software Solo (Eigenvector Inc.). Criteria were applied following the suggestions of Murphy et al. (2013) to examine the reliability of the PARAFAC model and to identify the number of fluorescence components: (1) the examination of the core consistency, (2) the evaluation of the shape of the spectral loading, (3) the leverage analysis regarding the influence of a specific sample or certain excitation and emission wavelengths, (4) the residuals analysis, and (5) the split half analysis. The generated model included an existing record of EEMs (n=417, effluent samples from WWTPs Munich II and Garching (Germany) from previous studies (Carvajal et al., 2017a; Hellauer et al., 2017; Miklos et al., 2018a; Nihemaiti et al., 2018; Ulliman et al., 2018b)), while validation of the PARAFAC model was applied on an independent data set obtained from this study (n=95). Excitation wavelengths <245 nm were excluded from all EEMs (n=512) since high fluorescence scatter in this area biased the modeling and obstructed a correct model calibration.

6.3 Results

6.3.1   UV/AOP comparison by TOrC removal performance

Seventeen TOrCs spanning a wide range of photolytic reactivities were selected based on diverse physicochemical characteristics and their occurrence in wastewater. Before investigations of UV-AOPs were commenced, preliminary experiments were conducted to evaluate water quality and direct oxidation of the 17 TOrCs with radical promoters and direct photolysis, separately. The batch wastewater sample used in lab-scale experiments was characterized by the following parameters: pH=7.5, 76.3% UVT, 0.022 mg-N/L NO$_2^-$, 12.7 mg-N/L NO$_3^-$, 118 mg/L HCO$_3^-$, and 6.0 mg/L DOC. Photolytic removal of the selected TOrCs is presented in Figure S20 and aligns well with experimental results obtained in previous studies (Miklos et al., 2018a; Nihemaiti et al., 2018; Ulliman et al., 2018b). Direct oxidation of TOrCs by the radical promoters H$_2$O$_2$ and PDS as well as the quencher Na$_2$SO$_3$ were investigated in these previous studies and resulted in negligible attenuation of <10% for all compounds. Dark reactions with chlorine were conducted within this study and resulted in a significant removal of 8 compounds at chlorine concentrations ranging from 0.075-0.45 mM and an exposure time of 12 min. During this reaction, gabapentin, tramadol, sotalol, venlafaxine, diclofenac, sulfamethoxazole and trimethoprim were oxidized by >95% and sotalol was attenuated by 70%. The TOrCs phenytoin, valsartan acid, carbamazepine, metoprolol and primidone were removed by

5-10% while iopromide, caffeine, atenolol, benzotriazole and TCEP did not exhibit substantial removal (<5%) (Figure S21).

The chemical structures of the 17 TOrCs investigated are presented in Table S10 (SI). TOrCs containing aniline groups (diclofenac, sulfamethoxazole), pyrimidine (trimethoprim), primary amines (gabapentin) or reduced sulfur groups (sulfamethoxazole, sotalol) are known to readily react with chlorine (Joo and Mitch, 2007; Deborde and von Gunten, 2008). High removal of venlafaxine and tramadol can be attributed to an electrophilic substitution on the tertiary amine. Tramadol additionally undergoes chlorine substitution at the activated aromatic ring (Cheng et al., 2015). In contrast, the aromatic ring of venlafaxine is substituted at the para position, which balances the increased electron density added by the ether group (Pinkston and Sedlak, 2004). However, removal of tramadol and venlafaxine is similarly high >90%. Amide groups (atenolol, phenytoin, primidone, carbamazepine, and iopromide), imide groups (caffeine) and azide groups (benzotriazole, valsartan acid) were reported to result in limited reactivity with chlorine (Pinkston and Sedlak, 2004; Deborde and von Gunten, 2008). TCEP does not carry any electron donating groups and is therefore resistant to chlorination. In contrast to our experiments, the β-blockers atenolol and metoprolol were reported to be highly reactive to chlorine based on the secondary amine (Deborde and von Gunten, 2008; DellaGreca et al., 2009; Postigo and Richardson, 2014). Another study aligns with our results reporting poor removal of atenolol in drinking water (Benotti et al., 2009). A back reaction of N-chlorinated atenolol with the quencher sulfite could explain this deviation since the primary transformation product of atenolol by chlorination is more resistant to chlorination than the parent compound (Lee and von Gunten, 2010a).

To compare the three selected UV-AOPs, chlorine resistant compounds (exhibiting removal by dark chlorination of <10%) were evaluated. These compounds characterized as resistant to direct chlorination were selected as indicators for the AOP comparison in this study: phenytoin, valsartan acid, carbamazepine, metoprolol, primidone, caffeine, atenolol and benzotriazole. TCEP did not result in any attenuation by photolysis, chlorination or AOP and is therefore excluded from further discussions. Iopromide could not be evaluated in most of the UV/chlorine samples due to efficient removal beyond the detection limit by RCS and is therefore also not discussed for comparison of UV-AOPs in this section.

In order to compare UV-based advanced oxidation of the eight radical indicators, the natural logarithm of the relative residual concentration c_0/c of each TOrC was plotted as a function of UV-fluence (n=6). Linear regression lines were determined (respective R^2 listed in Table S9) and the respective slopes (representing k_{obs}) were obtained. The observed pseudo first-order degradation rate constants of TOrCs (k_{obs}) from lab-scale UV/H_2O_2, UV/PDS and UV/Chlorine experiments are comparatively depicted in Figure 19. UV/Chlorine exhibited highest oxidation performance for all eight indicators with k_{obs} values ranging from $7.3 \cdot 10^{-4}$ - $1.4 \cdot 10^{-2}$ cm²/mJ. Increasing chlorine concentration from 0.075 to 0.45 mM resulted in a substantial increase of k_{obs} for all indicators except phenytoin and primidone, with no significant difference being observed. Since increasing chlorine concentrations yield in higher generation of RCS and ·OH (Wu et al., 2017), the

observed positive correlation between chlorine dose and removal of most compounds was expected. The different behavior of phenytoin and primidone cannot be explained based on mechanistic considerations. Analytical inaccuracies are unlikely, since each k_{obs} value comprises six experimentally derived values and respective R^2 were high ($R^2 > 0.97$) for both primidone and phenytoin.
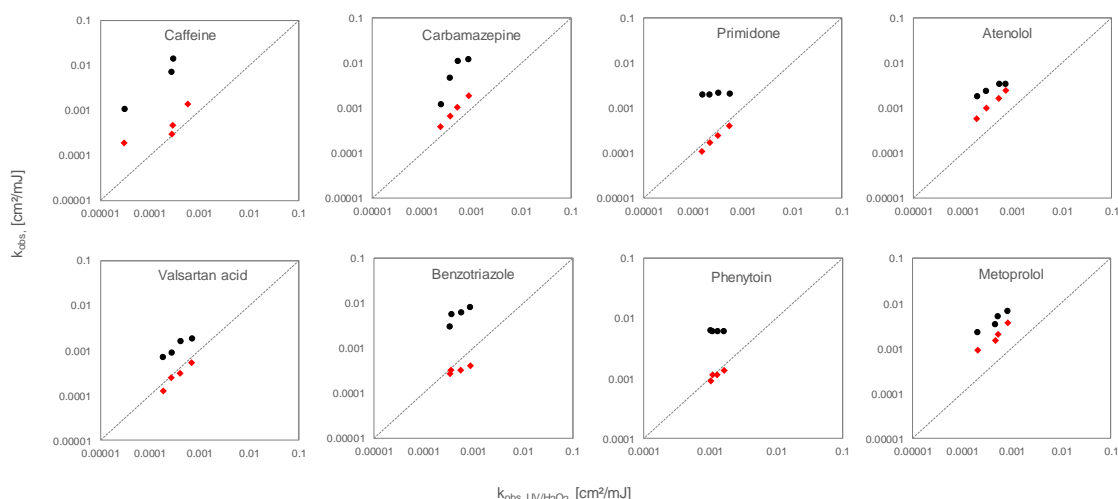
Figure 19: Comparative illustration (log-log plot) of observed rate constants (n=6) during UV/H₂O₂, UV/PDS (red diamonds) and UV/Chlorine (black dots) in wastewater effluent for different compounds at radical promoter concentrations of 0.075, 0.15, 0.3 and 0.45 mM and applied UV-doses of 50-800 mJ/cm². Dashed line represents the one-to-one line. Respective R^2 values are presented in Table S9 (SI).

Higher oxidation performance of UV/Chlorine compared to UV/H₂O₂ in tap water, sand-filtered natural water, reverse osmosis permeates, and buffered ultrapure water has already been reported (Sichel et al., 2011; Yang et al., 2016a; Li et al., 2017; Pan et al., 2018; Pati and Arnold, 2018) and is attributable to the higher photolysis rate constants of chlorine compared to H₂O₂ and PDS.

As depicted in Figure 19, UV/PDS exhibited k_{obs} values ranging from $0.11 \cdot 10^{-3}$ - $3.68 \cdot 10^{-3}$ cm²/mJ being higher than k_{obs} values of UV/H₂O₂ for caffeine, carbamazepine, atenolol, and metoprolol, while valsartan acid, benzotriazole, phenytoin, and primidone resulted in lower k_{obs} values by UV/PDS than UV/H₂O₂. This confirms previous results where benzotriazole, primidone and phenytoin resulted in lower and metoprolol in higher k_{obs} values during UV/PDS than UV/H₂O₂ (Nihemaiti et al., 2018). However, in contradiction to results in Figure 19, carbamazepine and caffeine exhibited lower k_{obs} values in UV/PDS compared to UV/H₂O₂ in the above-mentioned study, although wastewater effluent from the same WWTP and comparable oxidant doses were applied. Since second-order rate constants of carbamazepine and caffeine are 5.5 and 2.7 times higher for $k_{\bullet OH}$ compared to $k_{SO_4^{\bullet-}}$ (Table 9) and photolysis rate constants, molar absorption coefficient and quantum yield of PDS are slightly higher compared to H₂O₂ (13% and 40%, respectively), UV/H₂O₂ is expected to result in higher k_{obs} values as reported by Nihemaiti et al. (2018). However, slightly lower DOC concentrations in our study (6.0 mg/L compared to 6.8 mg/L) might have reduced the scavenging of SO₄•⁻ and resulted in a higher SO₄•⁻-exposure.

Interestingly, in Figure 19, the distance between $k_{obs,UV/Chlorine}$ and $k_{obs,UV/PDS}$ is constant for valsartan acid and metoprolol, while caffeine, carbamazepine and benzotriazole result in differences that increase with radical promoter dose. In contrast, atenolol exhibits smaller distances between $k_{obs,UV/Chlorine}$ and $k_{obs,UV/PDS}$ with increasing radical promoter dose. These observations indicate a non-linear correlation between k_{obs} values and radical promoter dose in at least one of the compared UV-AOPs. Process specific correlations are depicted in Figure S22 (SI). Application of UV/Chlorine in wastewater results in linear correlations between k_{obs} and chlorine dose for the compounds primidone, phenytoin, metoprolol and valsartan acid, while carbamazepine, benzotriazole, caffeine, and atenolol result in logarithmic correlations ($R^2 > 0.93$). However, Wang et al. (2016) reported a linear correlation of k_{obs} with increasing oxidant dose for the removal of carbamazepine in both ultrapure water and wastewater effluent at comparable chlorine doses. Since only four k_{obs} values are available in this study a deeper discussion of logarithmic relationships cannot be provided at this point.

UV/PDS results in linear correlations between k_{obs} and PDS dose for the compounds benzotriazole, valsartan acid, phenytoin and atenolol while carbamazepine, caffeine, primidone, and metoprolol exhibit exponential correlations ($R^2 > 0.96$, Figure S22b). A previous study resulted in an exponential relationship between oxidant dose and removal of some TOrCs for UV/PDS in wastewater effluent and described this observation with the high competition between the targeted TOrC and the wastewater effluent matrix (mainly electron-rich site of DOM) due to the selectivity of $SO_4^{\cdot-}$ (Nihemaiti et al., 2018). This is confirmed by Lee and von Gunten (2010), stating that when selective oxidants are applied, the removal of TOrCs exhibits a lag-phase at low radical promoter doses based on the high competition between the targeted TOrCs and electron-rich moieties of DOC. With increasing radical promoter concentrations, the degradation rates of TOrCs are significantly enhanced after the initial water matrix demand is met. This effect, however, is only observable if TOrCs are highly reactive towards the selective oxidant (i.e., $k_{SO_4^{\cdot-}} > 1 \times 10^9$ M^{-1}s^{-1}). Compounds that exhibit linear correlations between k_{obs} values and PDS dose are moderately reactive to $SO_4^{\cdot-}$ (Table 9). Based on the results of this study, the second-order rate constant $k_{SO_4^{\cdot-}}$ for atenolol and valsartan acid can be estimated as $<1 \cdot 10^9$ M^{-1}s^{-1}. As depicted in Figure S22c, linear correlations between k_{obs} and H_2O_2 dose were obtained for all eight indicator TOrCs applying UV/H_2O_2.

The negligible direct reaction of H_2O_2 and PDS with TOrCs enables a comparison of UV/PDS and UV/H_2O_2 with all compounds investigated as depicted in Figure S23. In contrast to UV/Chlorine, UV/PDS and UV/H_2O_2 exhibit oxidation performances of the same order of magnitude, while seven TOrCs are better attenuated by UV/PDS (tramadol, metoprolol, atenolol, carbamazepine, sulfamethoxazole, caffeine and venlafaxine), the removal of five TOrCs is favored by UV/H_2O_2 (gabapentin, primidone, phenytoin, valsartan acid and benzotriazole), and three compounds do not result in substantial differences (diclofenac, iopromide and trimethoprim). A recent study indicated that TOrCs with electron-donating groups (e.g., $-NH_2$, $-N=O$) have higher second-order rate constants with $SO_4^{\cdot-}$ than compounds with electron-withdrawing groups (e.g., $-COOH$, $-C(=O)N-$) (Ye et al., 2017). These structures apply to the substances listed above. Since diclofenac and iopromide are highly susceptible to photolysis, radical

oxidation does not significantly contribute to overall compound removal. Trimethoprim, however, is photo-resistant (Figure S20) and therefore its reactivity with $SO_4^{\bullet-}$ is expected to be comparable to $k_{\bullet OH}$ (no values available for $k_{SO_4^{\bullet-}, trimethoprim}$). The differences between k_{obs} values for the three UV/AOPs are ascribable to the different photolysis rate of radical promoters and the reactivity as well as selectivity of generated radicals to target TOrCs and the water matrix. While $\bullet$OH are known to react unselectively with organic water constituents (Neta et al., 1988), $SO_4^{\bullet-}$ and RCS have been described as selective oxidants favoring compounds with electron-rich moieties (Neta et al., 1977; Grebel et al., 2010; Wu et al., 2017; Varanasi et al., 2018). Consequently, the selective reaction of $SO_4^{\bullet-}$ and RCS resulted in a wider range of $k_{obs,UV/PDS}$ and $k_{obs,UV/Chlorine}$ compared to $k_{obs,UV/H_2O_2}$ as depicted in Figure 20. Similar results were reported on UV/H₂O₂ and UV/PDS oxidation of TOrCs in wastewater effluent (Lian et al., 2017) and reverse osmosis brines (Yang et al., 2016b). Median k_{obs} values as well as the range of k_{obs} values (difference between maximum and minimum value, Δk_{obs}) increase following the order of UV/H₂O₂ < UV/PDS < UV/Chlorine. While the range of $k_{obs,UV/H_2O_2}$ only slightly changes over H₂O₂ dose ($8.7 \cdot 10^{-4}$ - $1.1 \cdot 10^{-3}$ cm²/mJ), k_{obs} ranges for UV/PDS and UV/Chlorine remarkably increase with higher oxidant dose ($8 \cdot 10^{-4}$ - $3.3 \cdot 10^{-3}$ cm²/mJ for UV/PDS and $5.5 \cdot 10^{-3}$ - $1.3 \cdot 10^{-2}$ cm²/mJ for UV/Chlorine). While Δk_{obs}, in UV/PDS is directly attributed to the wide range of second-order rate constants of process indicator TOrCs with $SO_4^{\bullet-}$ ($0.53 \cdot 10^9$ - $3.89 \cdot 10^9$ M⁻¹s⁻¹, Table 9), in UV/Chlorine, generated $\bullet$OH are highly reactive ($k_{\bullet OH} \geq 6.28 \cdot 10^9$ M⁻¹s⁻¹, Table 9) and RCS are expected to result in higher $\Delta k_{obs,RCS}$ compared to $\Delta k_{obs,SO_4^{\bullet-}}$. For example, carbamazepine was reported to be highly reactive to Cl$\bullet$ ($k_{Cl\bullet} = 5.6 \cdot 10^{10}$ M⁻¹s⁻¹, Wang et al., 2016) and $\bullet$OH ($k_{\bullet OH} = 8.2 \cdot 10^9$ M⁻¹s⁻¹) while reactions with ClO$\bullet$ are significantly slower ($k_{ClO\bullet} = 9.2 \cdot 10^7$ M⁻¹s⁻¹, Guo et al., 2017). Direct reaction of $Cl_2^{\bullet-}$ with TOrCs is negligible since $Cl_2^{\bullet-}$ is reported to only play an important role in ClO$\bullet$ generation during UV/Chlorine (Guo et al., 2017).
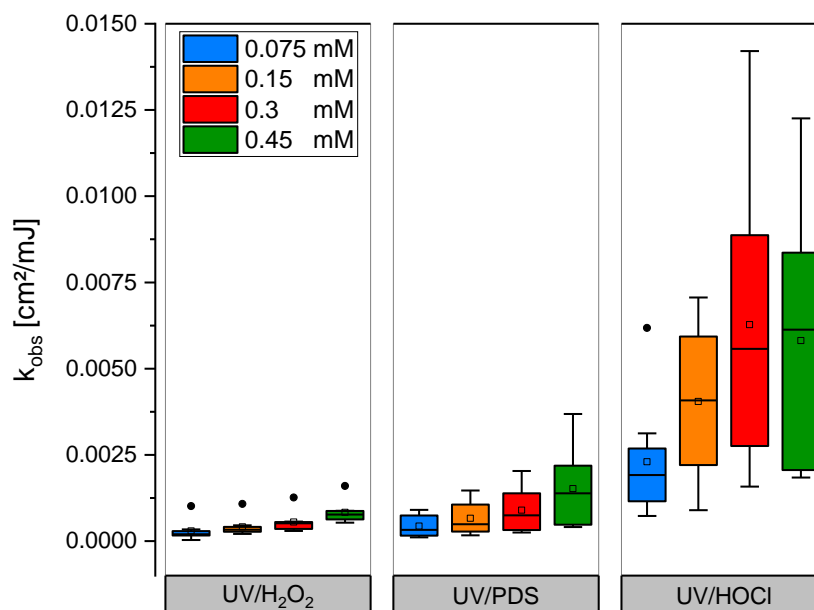
Figure 20: Box-plots of k_{obs} for indicator compounds (n=8) presented in Figure 19 indicating radical selectivity of $SO_4^{\cdot-}$ and RCS during UV/H_2O_2, UV/PDS and UV/Chlorine.

6.3.2 Surrogate evaluation

In addition to TOrC investigations, the progressive changes in selected optical surrogates during each UV-AOP was investigated to identify potential surrogate parameters. First, the sensitivity of surrogate parameters is tested for photolysis, dark chlorination, and the three UV-AOPs. Then, process indicator TOrCs, representing dominant reaction mechanisms in each AOP, are correlated with surrogates. Finally, linear correlations are determined, and best-fit parameters are selected for each process as potential optical surrogates.

6.3.2.1 Selection of surrogate parameters

The optical parameters of UV absorbance and fluorescence were chosen to represent the basic constituents of treated water and to serve as a surrogate parameter for the removal of TOrCs. The UV absorbance at 254 nm (UVA_{254}) was used to indicate the chromophores with conjugated double bond structures (C=O, C=C, C=N) and aromatic rings of DOM. The absorbance at 436 nm (Color) was used to indicate the yellowish color of chromophoric DOM, e.g., fulvic substances (Wert et al., 2009; Audenaert et al., 2013).

The specific fluorescence of a water sample was measured as a three-dimensional excitation-emission matrix (EEM), in which the fluorescent index (FI) with Excitation/Emission (Ex/Em) = 300/345 nm was chosen to determine the reduction of the soluble microbial by-product-like fluorescence (Chen et al., 2003). The total fluorescence (TF) intensity was integrated at excitation (245-600 nm) and emission (220-620 nm) to indicate the total fluorophores (Yu et al., 2015). Furthermore, the PARAFAC model with 2 components was validated (Figure S25). Component C1 exhibits a peak at Ex/Em=245/456 nm and component C2 Ex/Em=245/355 nm. EEM samples that were treated by chlorination or UV/Chlorine had to be excluded from the PARAFAC

model based on significantly higher residuals and consequently a lower core consistency. Residual analysis (measured EEM - modeled EEM) of irregular samples revealed an increase of fluorescence (P_Cl1 Ex/Em=248/345 and P_Cl2 Ex/Em=248/331, see Figure S26 and Figure S28) after chlorination which was already observed by other studies that explained this phenomenon by the transformation of phenolic groups into hydroquinone or catechol moieties (Cory and McKnight, 2005; Wenk et al., 2013). The above-mentioned peaks were therefore analyzed to additionally investigate fluorescence formation as a potential surrogate for UV/Chlorine in this study.

The resulting components from the PARAFAC analysis C1 and C2 were evaluated in UV/H$_2$O$_2$ and UV/PDS. Component C1 exhibited negative removal values with acceptable correlations to UV fluence (R^2>0.88) for both processes (Figure S30), however, the formation of a fluorescence component in the respective EEMs could not be confirmed by peak picking at the local peak of C1 (Ex/Em=245/445 nm). This observation can be explained by a mathematical artefact, since C1 might compensate overrated specific fluorescence areas of C2. C1 is therefore not considered as a potential surrogate for TOrC prediction in this study. In contrast to the formation of component C1, C2 is removed during UV-AOP application (R^2>0.92) and is therefore included in the following investigations. A total number of nine optical surrogates was selected to investigate their feasibility to predict TOrCs during the operation of three UV-AOPs. Two additional surrogates were evaluated to investigate the formation of fluorescence by UV/Chlorine.

6.3.2.2 *Impact of UV-AOPs on optical surrogates*

Dark chlorination at applied chlorine doses of 0.075-0.45 mM, exhibited a fast-initial reaction of all surrogates with chlorine and reached a plateau, indicating that not all chromophore and fluorophore features of DOM surrogates were reactive to chlorine. 0.075 mM chlorine at the lowest exposure time of 95 s resulted in highest removal of color (49.1%) and lowest removal of P_II (14.9%) followed by UVA (15.3%), while the remaining fluorophore surrogates were attenuated by 16.8% (P_II) – 30.3% (TF). Only a slight impact of exposure time (95-758 s) could be observed (Figure S27). The fluorophore surrogates P_Cl1 and P_Cl2 were constantly formed during dark chlorination with increasing oxidant dose, reaching 27.3% and 51.9% formation, respectively at 0.45 mM and 758 s (Figure S28). In contrast to surrogate depletion, both exposure time and oxidant dose had a substantial impact on the formation of P_Cl1 and P_Cl2.

No significant impact was detected from UV exposure up to 800 mJ/cm^2 which resulted in a removal of <16% for all surrogates (Figure S30) corroborating previous findings (Yu et al., 2015). Absorbance of UV-light by chromophore DOM may lead to molecule fragmentation and a subsequent loss of absorptivity/fluorescence. In addition, generation of reactive oxygen species by indirect photolysis can enhance the attenuation of chromophore and fluorophore properties of DOM (Thomson et al., 2004). However, correlations between surrogate removal and fluence resulted in low R^2 values (<0.7 for all surrogates, Figure S30), thus, the impact of direct photolysis is neglected below.

Oxidation of DOM by UV-AOPs resulted in substantial attenuation of all optical surrogates as depicted in Figure 21a-c for surrogates with lowest, moderate and highest reactivity in each AOP, respectively. Illustrations for all surrogates are provided in Figure S30 (SI) and respective R^2 values for linear correlations are presented in Table 10. DOC mineralization was negligible for all processes (<5%, data not shown). Linear correlation coefficients of surrogates over fluence were good at 0.45 mM radical promoter dose in UV/H_2O_2 (R^2>0.93) based on unselective reactions with ·OH, while R^2 values in UV/PDS and UV/Chlorine varied from 0.81-0.99 and 0.79-0.97, respectively (Table 10).
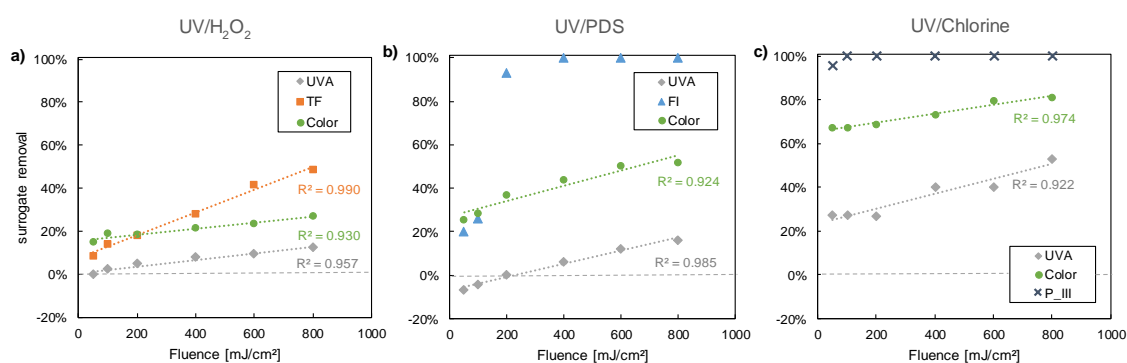
Figure 21: Degradation of selected surrogates in a) UV/H_2O_2, b) UV/PDS and c) UV/Chlorine at 0.45 mM radical promoter concentration. Illustrations for all surrogates are provided in Figure S30 (SI) and respective R^2 values are presented in Table 10.

Interestingly, at the highest process parameters applied, removal of all surrogates follows the order of UV/H_2O_2 < UV/PDS < UV/Chlorine. The higher attenuation of fluorescent surrogates in UV/PDS and UV/Chlorine (>99.99% at 400 mJ/cm² for FI and P_III, respectively) compared to UV/H_2O_2 (28% at 400 mJ/cm²) is additionally based on a higher radical yield in UV/PDS and UV/Chlorine compared to UV/H_2O_2, due to their respective quantum yields and molar absorption coefficients (Li et al., 2017). In addition, all three UV-AOPs exhibit UVA with lowest, color as moderate and a fluorescent surrogate with highest removal, revealing fastest attenuation of fluorescence being independent of radical speciation. Since fluorescence is ascribed to an extended π-electron system, the reaction of radicals with fluorophore groups might reduce fluorescence signals, while chromophore characteristics (e.g. UVA and color) of the compound are still present. However, while in UV/Chlorine all fluorophore surrogates were effectively removed to a greater extent than UVA and color, in UV/H_2O_2 and UV/PDS some fluorophore surrogates (C2, P_III, and P_V in UV/H_2O_2 and P_III and C2 in UV/PDS) only moderately reacted and resulted in removal rates that are lower than those of color, but still higher than those of UVA (Figure S30).

The fluorophore surrogates P_Cl1 and P_Cl2 that were formed during dark chlorination experiments resulted in effective degradation by UV/Chlorine (Figure S29), indicating that oxidation of P_Cl1 and P_Cl2 by RCS and ·OH was faster than formation of the two surrogates by chlorination of DOM. However, in comparison to the other fluorophore surrogates, P_Cl1 and P_Cl2 exhibited lowest reactivity but still reached >99.99% removal at 0.075 mM and 400 mJ/cm² applied. The PARAFAC component C2 was

removed by 26% and 15% by UV/H$_2$O$_2$ and UV/PDS, respectively, applying 800 mJ/cm² and 0.45 mM oxidant dose which is surprising, since the maximum peak of C2 (Ex/Em=245/355) is close to P_II (Ex/Em=245/358), but reactivity of the latter is substantially higher in both UV-AOPs.

Evaluating the fate of UVA during UV-AOPs in Figure 21a-c, surprising differences were observed: While low fluences at 50 mJ/cm² have no effect on UVA by UV/H$_2$O$_2$, UVA is formed in UV/PDS (6.5%) and UV/Chlorine results in a rapid decrease of UV absorbance (27.4%). Formation of UVA by UV/PDS might be attributed to transformation of aromatic groups of DOM exhibiting strong absorbance at higher wavelengths (e.g. 436 nm) into structures with absorption at lower wavelengths (e.g., phenols and quinones) (Korshin et al., 2002; Nöthe et al., 2009). Fast depletion of UVA during UV/Chlorine is most likely ascribed to direct chlorination of DOM. Subsequently, ·OH and RCS formed by photolytic chlorine activation linearly removed UVA with increasing fluence.

Table 10: Linear Correlation coefficients (R²) of surrogate parameters over fluence at an applied oxidant dose of 0.45 mM

	UVA	Color	TF	FI	P_II	P_III	P_IV	P_V	C2
UV/H$_2$O$_2$	0.957	0.930	0.990	0.995	0.999	0.954	0.996	0.986	0.971
UV/PDS	0.985	0.924	0.890	-	0.917	0.964	0.812	0.813	0.915
UV/Chlorine	0.922	0.974	0.825	0.790	-	-	0.807	0.881	-

6.3.2.3 *Correlations between surrogates and trace organic chemicals*

The diverse reactivity of TOrCs to different oxidants results in a unique correlation between selected surrogates and single targeted compounds during each AOP. However, the high number of chemicals and surrogates impedes the presentation of respective interrelations. Thus, based on dominant reaction pathways of each UV-AOP, indicator TOrCs were selected representing the underlying mechanistic processes. Iopromide served as an indicator for direct photolysis dominated removal in all AOPs, diclofenac represented dark chlorination and carbamazepine indicated TOrC removal by ·OH during UV/H$_2$O$_2$. For UV/PDS, benzotriazole and venlafaxine were selected indicating moderate ($k_{SO_4^{•-}}$ =8.7 ·10^8 M^{-1}s^{-1}) and high ($k_{SO_4^{•-}}$ = 4.99 ·10^9 M^{-1}s^{-1}) reactivity with SO$_4$$^{•-}$. For UV/Chlorine, primidone was defined as an ·OH indicator, based on its dominant reaction with ·OH while carbamazepine served as an indicator for RCS (Guo et al., 2017). Atenolol was additionally selected as a third indicator which is resistant to chlorination and equally reacts with ·OH and RCS (Guo et al., 2017). Compounds that are additionally susceptible to photolysis (i.e., diclofenac, iopromide and sulfamethoxazole) could not be evaluated during UV/Chlorine due to efficient removal >94% at 100 mJ/cm² and 0.075 mM.

Optical surrogate parameters, that resulted in highest linear correlation coefficients with each process specific indicator, are depicted in Figure 22a-c. R² values and respective slopes ($k_{surrogate}$) for linear correlations between all optical surrogates and process specific indicator TOrCs for UV/H$_2$O$_2$, UV/PDS and UV/Chlorine are reported in Table 11.
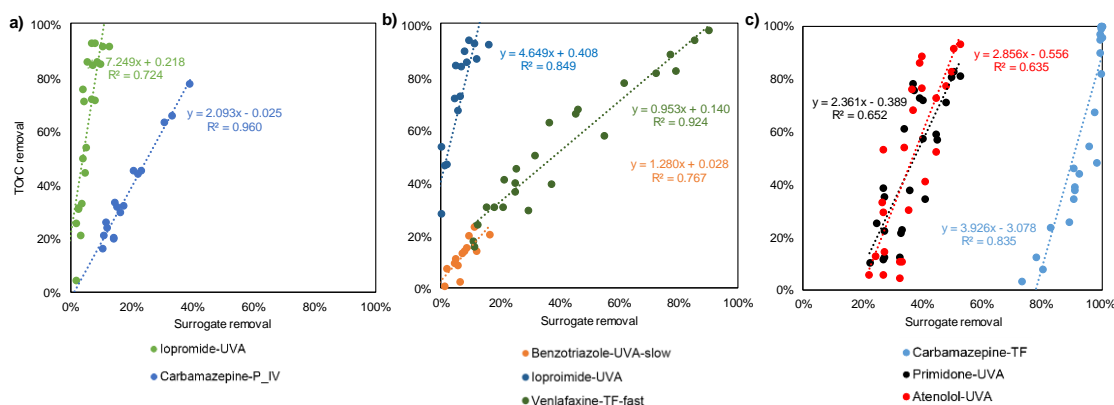
Figure 22: Selected correlations between indicator TOrC removal and surrogate removal depicted for a) UV/H₂O₂, b) UV/PDS and c) UV/Chlorine at radical promoter concentrations of 0.075, 0.15, 0.3 and 0.45 mM and applied UV-doses of 50-800 mJ/cm².

Evaluating UV/H₂O₂ data, UVA was found to represent the best surrogate for iopromide removal (R^2=0.72) and the fluorophore peak P_IV revealed highest correlation coefficients with carbamazepine (R^2=0.96). In UV/PDS, UVA could again be identified as a convenient surrogate for iopromide attenuation (R^2=0.85) and additionally for $SO_4^{\cdot-}$-based removal of the moderately reacting TOrC benzotriazole (R^2=0.77). Venlafaxine could be correlated with TF (R^2=0.92) representing high reactivity to $SO_4^{\cdot-}$. In UV/Chlorine, TF could be selected as a surrogate for carbamazepine indicating the reaction with RCS (R^2=0.84), while UVA was found to correlate well with primidone attenuation representing mainly reactions with $\cdot OH$ (R^2=0.65). Surprisingly, atenolol exhibits a similar correlation pattern to UVA (R^2=0.64) compared to primidone (Figure 22c).

Relationships between TOrC indicators and optical surrogates, including the slope and intercept of resulting linear correlation curves, represent the overall sensitivity of the selected surrogate parameter to reflect the change of indicator removal during UV-AOP. The slope of resulting linear correlation curves indicates differences in reactivity of indicator TOrCs and surrogates to the respective UV-AOP while R^2 values refer to the prediction reliability.

Linear correlation curves of $\cdot OH$ and $SO_4^{\cdot-}$ indicators in UV/H₂O₂ and UV/PDS pass through the origin, confirming that surrogates and indicator TOrCs are both predominantly susceptible to the respective radical. Iopromide removal over UVA attenuation results in linear correlations that exhibit an intercept on the y-axis in both UV/H₂O₂ and UV/PDS, which is explained by the high reactivity of iopromide to photolysis, while UVA is resistant to fluences >800 mJ/cm² (Figure S30). As formation of $\cdot OH$ and $SO_4^{\cdot-}$ decreases UVA, iopromide is already attenuated by 22% and 41%, respectively, indicating a higher fluence threshold in UV/PDS that is necessary to remove iopromide compared to UV/H₂O₂, most likely due to the substantially lower second-order rate constant with $SO_4^{\cdot-}$ compared to $\cdot OH$ (Table 9). However, more data would be needed to confirm this hypothesis. In UV/Chlorine, the horizontal intercepts of the correlation curves are ascribed to the direct chlorination of the surrogates UVA and TF

by 23% and 74%, respectively, while the indicator TOrCs exhibit <10% removal by direct chlorination at 0.45 mM chlorine and highest exposure time of 758 s.

The slope of the linear correlations in Figure 22a-c represents the differences in reactivity. In UV/H$_2$O$_2$, carbamazepine exhibits a 2.1-fold higher reactivity to ·OH compared to P_IV which represents tryptophan-like compounds of DOM. Comparing the second-order rate constants of carbamazepine ($k_{·OH} = 8.3 \cdot 10^9\,M^{-1}s^{-1}$, Wols and Hofman-Caris, 2012) and tryptophan ($k_{·OH} = 13 \cdot 10^9\,M^{-1}s^{-1}$, Solar et al., 1991), the opposite would have been expected. However, complex wastewater matrices might contain DOM with fluorophore characteristics with Ex/Em pattern that are similar to those of tryptophan (e.g. protein-like and microbial by-product-like, Chen et al., 2003) but are less reactive to ·OH. In UV/PDS, both radical indicators correlate well with a slope close to 1, indicating that the same oxidation mechanisms and comparable rate constants are involved in the degradation of these TOrCs and surrogates, i.e., predominant SO$_4$·$^-$-based oxidation.

The difference of indicator reactivity is not that emphasized in Figure 22c. Primidone and atenolol result in a comparable degradation range and reveal highest correlation coefficients with UVA, demonstrating predominant oxidation based on ·OH. Since primidone removal is dominated by ·OH and oxidation of atenolol is equally attributed to ·OH and RCS (Guo et al., 2017), evidence suggests that convenient correlations of these compounds with UVA rely on predominant oxidation based on ·OH. Compared to primidone and carbamazepine resulted in substantially higher k$_{obs}$ values at chlorine doses ≥0.3 mM (section 6.3.1) and exhibited highest R^2 values with TF which is most likely ascribed to the selective reaction with RCS.

Table 11: Respective R^2 values and slopes ($k_{surrogate}$) for linear correlation of surrogates with indicator TOrCs: iopromide (IOP), carbamazepine (CBZ), benzotriazole (BZT), venlafaxine (VLF), atenolol (ATL) and primidone (PMD).

		UV/H$_2$O$_2$		UV/PDS			UV/Chlorine		
		IOP	CBZ	IOP	BZT	VLF	ATL	PMD	CBZ
R^2	UVA	0.72	0.63	0.85	0.77	0.81	0.64	0.65	0.6
$k_{surrogate}$		7.25	5.14	4.65	1.28	3.84	2.86	2.36	3.01
R^2	Color	0.47	0.46	0.38	0.23	0.82	0.58	0.49	0.74
$k_{surrogate}$		4.0	4.08	1.74	0.34	2.18	2.63	1.97	3.21
R^2	TF	0.3	0.89	0.54	0.43	0.92	0.46	0.33	0.84
$k_{surrogate}$		1.32	1.67	0.86	0.19	0.95	2.67	1.86	3.93
R^2	FI	0.35	0.97	0.25	0.26	0.62	-	-	-
$k_{surrogate}$		2.03	2.03	0.5	0.1	0.55	-	-	-
R^2	P_II	0.57	0.94	0.46	0.58	0.73	-	-	-
$k_{surrogate}$		1.72	1.68	0.84	0.22	0.89	-	-	-
R^2	P_III	0.26	0.82	0.57	0.41	0.88	-	-	-
$k_{surrogate}$		2.41	3.28	1.80	0.37	1.91	-	-	-
R^2	P_IV	0.49	0.96	0.4	0.23	0.75	-	-	-
$k_{surrogate}$		2.12	2.09	0.64	0.12	0.73	-	-	-
R^2	P_V	0.24	0.79	0.33	-	0.58	-	-	-
$k_{surrogate}$		2.69	3.52	0.44	-	0.49	-	-	-
R^2	C2	0.74	0.84	0.78	0.63	0.47			
$k_{surrogate}$		3.60	2.93	4.85	1.14	3.19			

This study revealed the applicability of chromophore or fluorophore DOC components as surrogates for different indicator TOrCs that represent dominant reaction pathways in UV-AOPs. Photo-resistant TOrCs correlated well with selected chromophore or fluorophore surrogates in the three UV-AOPs as discussed above. The applicability of optical surrogates for photo-susceptible TOrCs, however, could only be proven for UV/H$_2$O$_2$ and UV/PDS, since the compounds diclofenac, iopromide and sulfamethoxazole were shown to be highly reactive to both direct chlorination and RCS. Correlations representing photolysis as an underlying oxidation mechanism could not be determined since direct photolysis did not result in substantial surrogate removal.

However, since no surrogate was found to represent direct photolysis, some limitations have to be considered: correlations between photo-susceptible TOrCs and optical surrogates during UV/H$_2$O$_2$ and UV/PDS are biased since radical generation by radical promoter addition has a higher effect on surrogate removal in comparison to photolysis indicator TOrCs which are predominantly attenuated by photolysis. This trend can be observed in Figure S31, where increasing oxidant dose substantially reduces the slope of the linear correlation between iopromide and UVA removal while the slopes of linear correlations between radical indicators and surrogates remain constant (Figure S31b). Therefore, applicability of surrogates for photo-susceptible TOrCs is limited to a narrow concentration range of radical promoters (0.075-0.45 mM), since higher concentrations are expected to significantly lower linear correlation coefficients. Further studies are needed to determine the full concentration range that is applicable for this purpose.

Besides ·OH-based reactions in UV/H$_2$O$_2$ where P_IV showed highest R^2 values, best correlations were shown for UVA and TF, indicating that neither peak picking nor PARAFAC resulted in a higher informative value. UVA and TF are well investigated surrogates in numerous publications (e.g., Yu et al., 2015; Park et al., 2017) and could be emphasized in this study as useful parameters to predict TOrC removal in different UV-AOPs. TF, however, requires the recording of a complete EEM that is not yet available as a viable online measurement, while UVA or selected fluorescence peaks are straightforward to implement. Therefore, if correlations are acceptable, alternative parameters should be selected as surrogates based on Table 11. In UV/PDS, venlafaxine could also be correlated to P_III (R^2=0.88) or UVA (R^2=0.81) instead of TF (R^2=0.92). In UV/Chlorine, carbamazepine could alternatively be predicted by color (R^2=0.74).

6.4 Conclusion

This lab-scale study demonstrates through direct comparison of UV-AOPs in municipal wastewater that the general oxidation performance of a wide range of TOrCs followed the order of UV/H$_2$O$_2$≈UV/PDS<UV/Chlorine while UV/PDS and UV/Chlorine exhibited higher compound selectivity than UV/H$_2$O$_2$. Evaluating potential optical surrogates to predict TOrC removal in UV-AOPs, nine parameters were selected representing chromophore and fluorophore features of DOM. UVA, TF and the selected fluorescence peak P_IV revealed highest linear correlation coefficients and were therefore determined as surrogates representing underlying mechanistic reactions of each UV-AOP. Besides ·OH-based reactions in UV/H$_2$O$_2$ where P_IV showed highest R^2 values, best correlations were shown for UVA and TF, indicating that neither peak picking nor PARAFAC resulted in a higher informative value of selected optical surrogates. In future research, the revealed surrogates should be tested in continuous pilot experiments treating municipal wastewater effluent to verify the applicability under real conditions including water matrix fluctuations. Although oxidation performance of UV/Chlorine is outstanding in comparison of the three UV-AOPs, it has to be noted that OBP formation potential might be substantially higher during both UV/PDS and UV/Chlorine compared to UV/H$_2$O$_2$ (Miklos et al., 2018b). Therefore, OBP formation should be comparatively investigated in combined toxicological investigations to reveal potential drawbacks of each UV-AOP.

The tested hypothesis that application of the radical promoters peroxodisulfate and chlorine as substitutes for H$_2$O$_2$ results in a comparable oxidation performance of UV-AOPs in municipal wastewater effluents (Hypothesis № 3) can be accepted. In addition, the hypothesis that the removal of photo-susceptible and photo-resistant TOrCs during UV/AOPs correlate with intensity changes of specific chromophore or fluorophore DOC components can likewise be accepted for photo-resistant TOrCs (Hypothesis № 4.2). However, applicability of optical surrogates for photo-susceptible TOrCs could only be proven for UV/H$_2$O$_2$ and UV/PDS, since the compounds diclofenac, iopromide and sulfamethoxazole were shown to be highly reactive in UV/Chlorine to both direct chlorination and RCS. Consequently, Hypothesis № 4.1 is accepted for UV/H$_2$O$_2$ and UV/PDS and rejected for UV/Chlorine.

6.5 Acknowledgements

7. Retrofitting of the Full-Scale UV Disinfection System at WWTP Munich II for Advanced Removal of TOrCs

7.1 Introduction

In recent years there has been a growing public debate about the emission of anthropogenic trace substances into the water cycle and potential adverse effects for aquatic organisms (Barbosa et al., 2016; Chu et al., 2016). Most important emitters have been identified as municipal wastewater treatment plants, in which TOrCs usually receive insufficient removal during conventional wastewater treatment (Lim, 2008; Gros et al., 2010; Luo et al., 2014). Many substances, including primarily pharmaceutical and endocrine disruptors, but also household and industrial chemicals as well as cosmetics, are regularly detected in wastewater treatment plants and surface waters (Luo et al., 2014). Ecotoxicological studies have shown that drugs such as the analgesic diclofenac can negatively affect aquatic organisms (Vieno and Sillanpää, 2014; Lonappan et al., 2016). Therefore, monitoring and regulation of TOrCs in the aquatic environment is crucial following the precautionary principle which might result in adoption of environmental quality standards (see Section 1.1). In order to comply with potential EQS, advanced wastewater treatment has to be considered for effective attenuation of TOrCs. Demonstration plants employing advanced processes are currently in operation throughout Germany to investigate the removal efficiency of anthropogenic trace substances. The majority of the processes investigated are based on adsorption onto activated carbon (powdered or granulated activated carbon) and oxidation with ozone (Miehe and Stapf, 2015).

In a study initiated by the LfU, the combination of ozonation with subsequent activated carbon filtration was identified as the most promising process for TOrC removal from municipal wastewater effluents (Günthert, 2013). This process combination is currently being tested at a demonstration-scale facility at the WWTP Weissenburg. Furthermore, the LfU has commissioned a georeference model for the entire Bavarian river network to identify exceedances of proposed EQS for selected TOrCs in certain river sections. In this model, the WWTP Munich II was revealed as a major emitter of TOrCs into the river Isar. Furthermore, diclofenac was identified as the most relevant TOrC in the river with occurrences close to the PNEC level downstream of the discharge of Munich II (Klasmeier et al., 2011). Alternative treatment options for the removal of TOrCs, such as advanced biological treatment or advanced oxidation processes are currently receiving little attention in Germany. UV-based oxidation processes can be an alternative to ozonation, especially if a UV system is already being employed for disinfection and could potentially be retrofitted. Advanced oxidation with UV irradiation and hydrogen peroxide (UV/H_2O_2) is already being used in other countries such as the USA or Australia for advanced wastewater treatment (Traves et al., 2008; Drewes and Khan, 2011). In contrast to the selective removal of TOrCs in activated

carbon and ozone treatment, $^{\bullet}OH$ formed in UV/H_2O_2 react unspecifically, resulting in oxidative removal of substances that neither adsorb to activated carbon nor can be effectively removed by ozone (e.g., iopromide).

Chapter 4 of this dissertation investigated the removal of TOrCs during UV/H_2O_2 and presented a kinetic model to estimate removal efficiencies during advanced oxidation of municipal wastewater effluent. TOrCs were grouped based on photolytic reactivity in photo-susceptible ($k_{UV}>10^{-3}$ cm²/mJ; like diclofenac, iopromide and sulfamethoxazole), moderately photo-susceptible ($10^{-4}<k_{UV}<10^{-3}$ cm²/mJ; like climbazole, tramadol, sotalol, citalopram, benzotriazole, venlafaxine and metoprolol), and photo-resistant ($k_{UV}<10^{-4}$ cm²/mJ; like primidone, carbamazepine and gabapentin) compounds.

While UV disinfection systems are operated to meet microbial targets, simultaneous degradation of less than 30% of photo-susceptible TOrCs has been observed (Nick et al., 1992; Canonica et al., 2008; Gagnon et al., 2008). However, based on the current mode of operation, fluences can potentially be enhanced by reducing flow rates or maximizing UV intensity by adjusting lamp power. Therefore, the objective of this study was to investigate the applicability of existing UV disinfection plants for enhanced removal of TOrCs by adapting process parameters or by retrofitting the existing infrastructure. This objective has been investigated at the WWTP Munich II.

For the scenario of UV/H_2O_2 oxidation the objective was divided into photolytic and $^{\bullet}OH$-based degradation of TOrCs to consider compound specific reactivity. Diclofenac and primidone were selected as indicator compounds for photo-susceptible and photo-resistant TOrCs, respectively. Based on kinetic information presented in Table 8, diclofenac is the most photo-susceptible compound, while primidone has the lowest reactivity with $^{\bullet}OH$ ($6.7 \cdot 10^9$ M⁻¹s⁻¹) compared to other photo-resistant compounds that were investigated in this study. In addition, since diclofenac has shown the highest toxicity potential in the river Isar (Klasmeier et al., 2011), the impact of wastewater discharge on resulting diclofenac concentrations in the river and mitigation potential by UV photolysis were examined. Two specific target definitions were set and investigated by a sampling campaign on-site and by kinetic modeling to identify modification and retrofitting possibilities of the full-scale disinfection facility:

(i) Compliance with proposed diclofenac thresholds (50 and 100 ng/L) in the river Isar by UV photolysis of wastewater effluent

(ii) Additional removal of primidone by 50% as indicator for radical-based oxidation cby UV/H_2O_2 AOP.

Investigations for these objectives were conducted during the following steps (a) to (c):

(a) As a first approach, to determine the status quo of the full-scale UV disinfection facility at Munich II, occurrence of TOrCs was evaluated prior to and after UV-disinfection as well as in the river Isar up- and down-stream of the wastewater discharge point.

(b) Subsequently, the impact of UV photolysis of diclofenac has been modeled to determine resulting concentrations in the river Isar after discharge and required

process parameters are specified to meet the proposed target concentrations in the river.

(c) Site-specific implementation options were suggested to meet the different specific water quality targets for diclofenac and primidone:
- Calculation of fluence enhancement potential in the current system
- Determination of retrofitting potential of the existing lamp technology
- Technical design of a full-scale UV/H_2O_2 system

This study tested the hypotheses that (i) the UV disinfection system at the WWTP Munich II can be modified to achieve a significant attenuation of photo-susceptible TOrCs by enhanced photolysis (Hypothesis 1.2) and (ii) achieve a radical indicator removal of 50% by retrofitting the disinfection system and applying H_2O_2 as a radical promoter (Hypothesis 1.3).

7.2 Materials and Methods

7.2.1 Description of the wastewater treatment plant Munich II

The WWTP Munich II is one of two large wastewater treatment plants in the city of Munich, which are jointly responsible for the entire wastewater treatment of the state capital. The joint capacity of both facilities is designed for a population equivalent of three million people. Based on weather conditions, between 1 and 6 m³/s of wastewater are received by Munich II, which corresponds to approximately one million population equivalents. The treatment plant is comprised of a mechanical treatment stage including screens, aerated sand-/fat traps and primary clarification. It is followed by a two-stage activated sludge process for biological carbon and nutrient removal with an intermediate clarification stage. After two-stage secondary clarification, the water is filtered using tertiary granular media filters with a resulting UV transmittance at 254 nm of 65-75%. During summer months, methanol is added to 8 out of 24 granular media filter cells as an external carbon source to achieve denitrification. Furthermore, the filter effluent is disinfected by a low-pressure (LP) UV system at a targeted fluence of 45 mJ/cm² from May-September to maintain microbial bathing water quality in the receiving river Isar. The disinfection system was designed for a maximum flow rate of 6 m³/s. With two WEDECO TAK-55 series irradiation benches (Xylem, Germany) per channel and a total of six irradiation channels, 1,296 LP-UV lamps are installed in the whole system. The total output of 466 kW leads to a specific energy consumption of 22 Wh/m³. A schematic diagram of the UV disinfection system is shown in Figure 23.
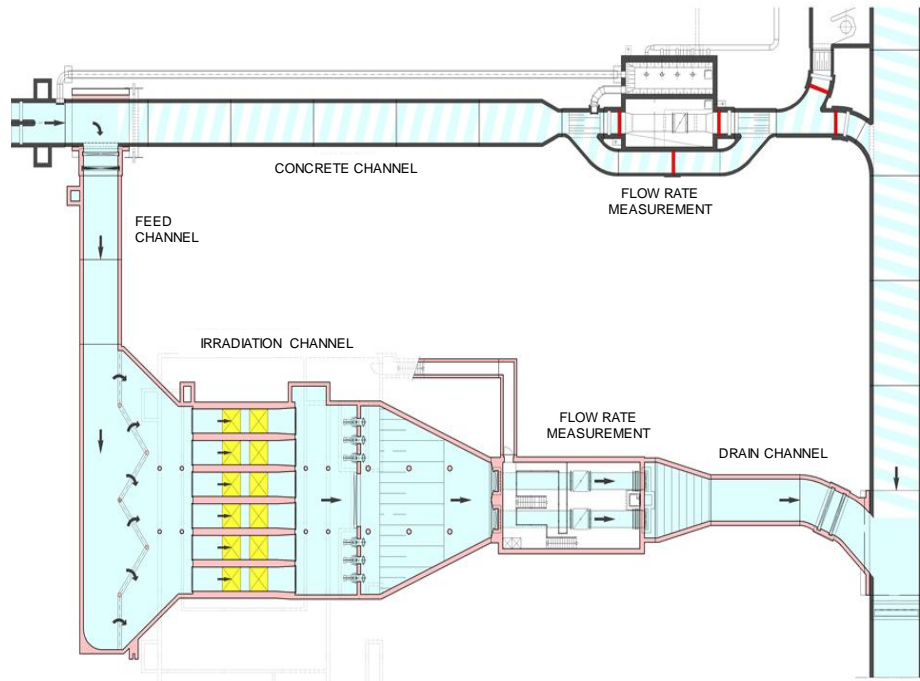
Figure 23: Schematic diagram of the UV disinfection system (Munich II). Adapted from *Münchner Stadtentwässerung*

7.2.2 *Sampling procedure and analysis*

All work in this study has been conducted within the framework of Chapter 4. Sampling procedure and analysis of bulk water parameters and TOrCs were conducted analogously to descriptions in Section 4.2. Sampling points for sand filter effluent, UV disinfection effluent, and river water samples up- and down-stream of the wastewater discharge are depicted in a simplified scheme in Figure 24. Up-stream river water samples were collected 200 m above the wastewater discharge point and down-stream samples were taken 2 km down-stream. Both river water samples were taken using a 3-meter sampling rod directly from the western riverbank. Wastewater samples were taken by automatic sample collectors directly from the wastewater channels. To assess fluctuation of TOrC photolysis in the UV system as a function of naturally varying feed water conditions, two independent experiments were conducted over a period of five days each (Section 4.2). Each day, influent and effluent samples were taken at 6 and 9 a.m. and 12, 3, 6 and 8 p.m., resulting in 30 samples per week and sampling point.
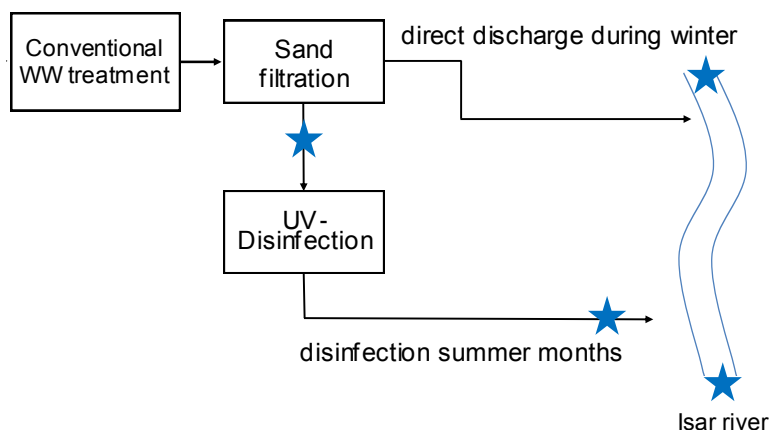
Figure 24: Simplified scheme of the WWTP Munich II after secondary clarification. The blue stars highlight the sampling locations

7.3 Results

7.3.1 *Sampling campaign to characterize current TOrC removal performance at the full-scale UV disinfection system*

Based on the sampling campaign at the WWTP Munich II TOrC removal performance during regular disinfection was investigated. Median UVT of the sand filter effluent samples was measured as 72.9% and the fluence applied is reported at a median of 45.2 mJ/cm². Removal performance of 15 indicator TOrCs during regular disinfection is depicted as boxplots in Figure 25 following the order of photolytic reactivity as presented in Section 4.3.1. The general trend of decreasing median percent removal from diclofenac to TCEP in Figure 25 is similar compared to the trend in Figure 8, however, iopromide and gabapentin have higher median values and consequently received higher degradation during regular disinfection than expected by the photolytic rate constants presented in Chapter 4. Significant TOrC removal was observed for the compounds diclofenac, iopromide, sulfamethoxazole, and gabapentin with median values of 39%, 45%, 23%, and 27%, respectively, while other compound removal scatters around zero which indicates no considerable reduction by photolysis. These removal values confirm data reported by Gagnon et al. (2008), who determined 20% diclofenac and 3% carbamazepine removal at a disinfection dose of 25 mJ/cm². Based on previous investigations in Chapter 4, removal of gabapentin cannot be explained by UV photolysis. Comprehensive TOrC concentration data is presented in Table 12.
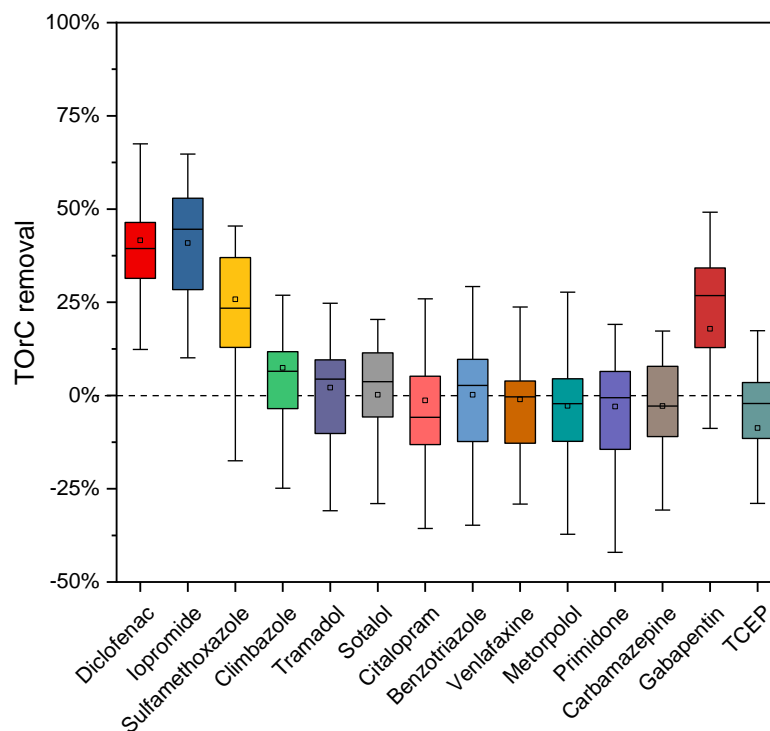
Figure 25: Boxplots indicating photolytic indicator TOrC removal during regular UV disinfection at the WWTP Munich II

For a more detailed analysis of diclofenac removal during UV disinfection, the fate of diclofenac during regular UV disinfection is discussed in more detail. Measured concentrations were plotted as boxplots for each sampling point in the WWTP Munich II and the river. As depicted in Figure 26, the median concentration of diclofenac is measured at 2.0 µg/L after sand filtration and 1.4 µg/L after UV disinfection. In the river, up-stream concentrations were determined as 9.5 ng/L while down-stream of the wastewater discharge point median concentrations of 110 ng/L were detected. The latter value confirms exceedance predictions of both potential diclofenac thresholds (50 and 100 ng/L) reported by Klasmeier et al. (2011).
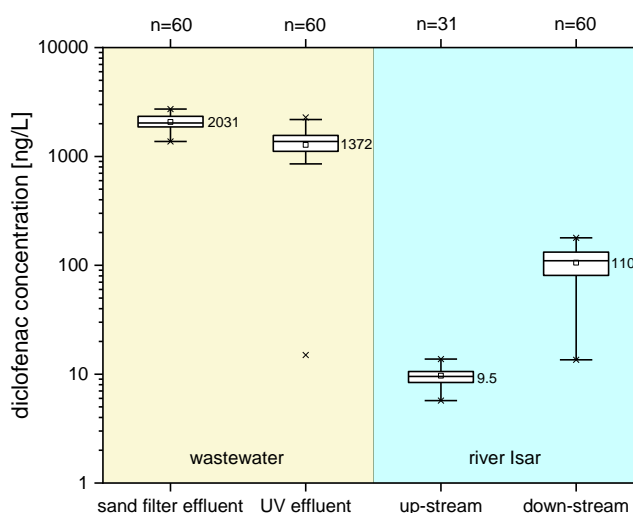
Figure 26: Boxplots of the diclofenac concentration in the WWTP Munich II and in the river Isar

Based on the presented concentration values of diclofenac, the wastewater percentage (WWP) in the river after discharge can be calculated by Equation 16 as 7.5%. This value also represents the median of all calculated WWPs based on different indicator TOrCs (Table 12) and applies as a calculated estimation for the two separate weeks of sampling.

$$WWP \; [\%] = \frac{C_{down-stream} - C_{up-stream}}{C_{UV-effluent}} \cdot 100 \qquad\qquad (\,16\,)$$

Table 12: Average TOrC concentrations, standard deviation (STD) and number of data points (n) obtained from two single weeks of sampling at WWTP Munich II.

TOrCs	Sand filter effluent			UV effluent			Upstream Isar			Downstream Isar			WWP
	average [ng/L]	STD [ng/L]	n	average [ng/L]	STD [ng/L]	n	average [ng/L]	STD [ng/L]	n	average [ng/L]	STD [ng/L]	n	[%]
Benzotriazole	6991	1518	60	6564	2226	60	51	33	46	585	261	60	8.1
Caffeine	51	66	60	70	46	60	55	58	60	154	669	60	-
Carbamazepine	498	160	60	528	233	60	14	2	30	42	21	48	5.3
Citalopram	194	49	60	171	44	60	2	1	30	12	6	58	5.8
Climbazole	150	29	60	130	27	60	16	3	60	24	5	60	6.5
Diclofenac	2069	341	60	1277	525	60	10	2	31	106	38	60	7.5
Erythromycin	254	151	60	253	146	60	3	2	13	34	30	53	12.4
Gabapentin	3522	661	60	2811	311	60	31	9	32	220	72	60	6.7
Iopromide	2804	1520	60	1909	1203	60	34	10	30	195	106	59	8.5
Metoprolol	408	92	60	368	83	60	3	0	30	30	8	58	7.4
Primidone	125	34	60	118	27	60	2	1	29	12	8	34	8.6
Sotalol	61	12	60	55	9	60	1	0	30	5	1	39	8.1
Sulfamethoxazole	258	87	60	215	75	60	7	1	30	23	7	60	7.2
TCEP	125	34	60	120	17	60	2	1	2	6	3	27	3.4
Tramadol	367	90	60	325	79	60	7	1	30	39	14	60	9.7
Venlafaxine	396	102	60	357	80	60	6	1	60	33	9	60	7.7

7.3.2   Modeling of UV photolysis and UV/H₂O₂ impact on TOrC removal

7.3.2.1   Modeling of UV photolysis impact on diclofenac concentrations in the river Isar

Diclofenac was identified as the only substance with measured concentration in the Isar that could require legally binding action in the future. As a photolytically degradable substance, diclofenac can sufficiently be removed from the wastewater treatment plant effluent with relatively simple adjustments of UV system parameters. Figure 27 depicts measured removal of diclofenac during lab-scale experiments and expected removal calculated by applying the kinetic model presented in Section 4.2.4. The model was fed with scavenger concentrations presented in Table 6. Resulting concentrations in the river Isar downstream of the discharge site were predicted using Equation 17 with WWP and median diclofenac concentrations from Section 7.3.1.

$$C_{downstream}\left[\frac{ng}{L}\right] = 7.5\% \ \cdot 2031\left[\frac{ng}{L}\right] \cdot \frac{C}{C_{0}}_{modeled} + 9.5\left[\frac{ng}{L}\right] \qquad (17)$$

Experimental and modeled removal of diclofenac show good agreement. The median diclofenac removal (39%) obtained from the sampling campaign represents a higher value than modeled. This deviation could be explained by variances of fluence in each irradiation channel of the full-scale disinfection system during sampling. Since specific fluence data were not accessible during sampling, a median diclofenac removal was assigned to median fluence data from 2016 (Table 13). Graphical evaluation of Figure 27 reveals fluences, which are necessary to comply with the proposed thresholds of 50 or 100 ng/L diclofenac in the river. For the compliance with 100 ng/L diclofenac in the Isar, a fluence of 99 mJ/cm² is required. The Federal Environment Agency's proposed EQS of 50 ng/L coul be achieved at a fluence of 255 mJ/cm².
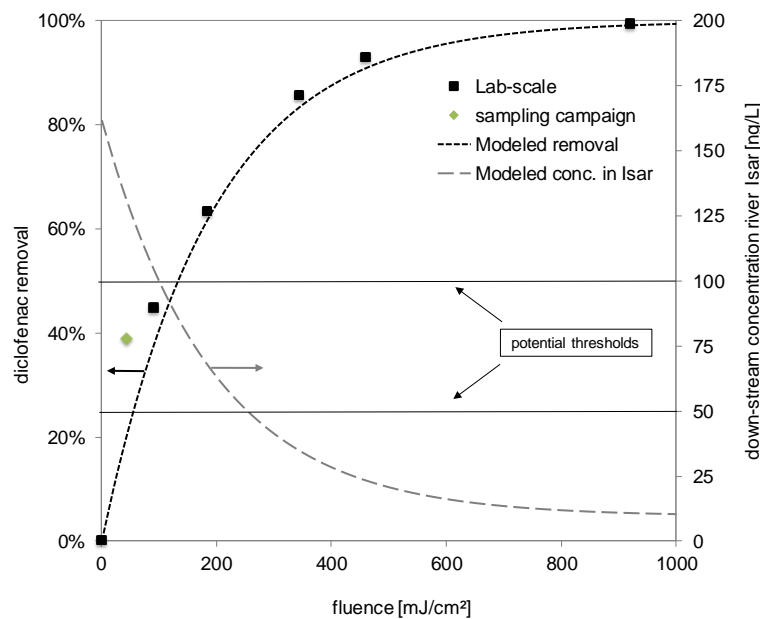
Figure 27: Modeled and experimental removal of diclofenac by UV photolysis and calculated resulting concentration in the river Isar.

7.3.2.2   *Modeling of UV/H₂O₂ oxidation impact on primidone removal*

To assess the general oxidation potential of UV/H_2O_2, the radical indicator chemical primidone was chosen since it has the lowest second-order rate constant with ·OH ($6.7 \cdot 10^9$ M^{-1}s^{-1}) compared to the other photo-resistant TOrCs carbamazepine and gabapentin (see Table 4) studied in this thesis. Consequently, besides TCEP, all TOrCs considered in this dissertation are expected to exhibit higher removal by UV/H_2O_2. As depicted in Figure 28, dosing of H_2O_2 to the photolysis of primidone substantially enhances the removal performance. When 5 or 10 mg/L H_2O_2 are added to the system, a fluence of 2,030 or 1,145 mJ/cm² should be applied, respectively, to meet the removal target of 50%.
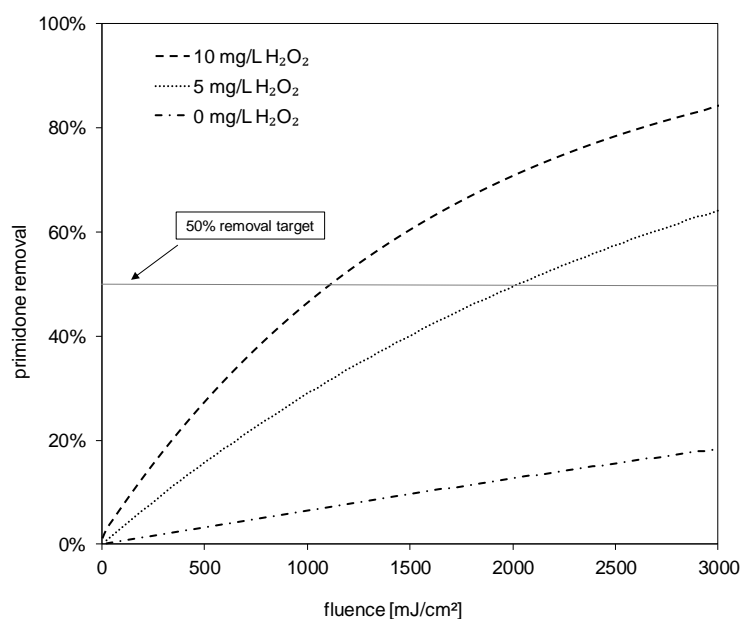
Figure 28: Modeled removal of primidone by UV/H_2O_2 AOP to comply with the target definition of 50% removal.

7.3.3   *Site-specific implementation of the UV/H₂O₂ process to meet target thresholds*

To reveal evidence of potential fluence enhancement, system parameters of the full-scale UV disinfection system were collected. An annual data set was provided by the Munich II WWTP staff consisting of daily average values from 2016 that represent UV intensity (n=1836) and fluence (n=918) of the six full-scale irradiation channels as well as daily average total flow rates of the UV disinfection system (n=153). Summarized descriptive statistical information of this dataset is provided in Table 13. The specific energy consumption during regular disinfection is 22 Wh/m³.

Table 13: Annual descriptive statistical values (2016) of the UV disinfection system for daily averages summarized for all six irradiation channels of the full-scale disinfection system.

	15th percentile	median	85th percentile
Total flow rate [m³/s]	1.4	1.9	2.4
Lamp power [%]	24.1	43.5	60.2
Fluence [mJ/cm²]	27.2	45.2	63.9

The existing full-scale UV disinfection system can be modified under certain conditions to achieve advanced TOrC attenuation. In the following three scenarios are distinguished:

1. Modification of operational parameters of the existing UV disinfection system,
2. Retrofitting of the existing UV lamp technology,
3. Design of a full-scale UV/H_2O_2 AOP system.

7.3.3.1 *Modification of operational parameters of the existing UV disinfection system*

Modification options of the full-scale UV disinfection system at WWTP Munich II for TOrC removal enhancement are restricted by the current infrastructure and technical system installations. Two parameters can be adjusted to enhance the resulting fluence in the UV system, namely flow rate per irradiation channel (exposure time) and lamp power (UV intensity). In current system operation, the wastewater influent is divided to all channels (see detailed description below) and lamp power in the respective channel is adjusted based on actual flow rate and UVT. Considering lamp power adjustments only, the potential maximized fluence can be calculated based on the average daily fluence which is multiplied by the lamp power enhancement factor (the maximum lamp power (100%) divided by daily average lamp power values) as presented in Equation 18.

$$Potential\ fluence \left[\frac{mJ}{cm^2}\right] = average\ fluence\ \left[\frac{mJ}{cm^2}\right] \cdot \frac{100\ \%}{lamp\ power\ (t)\ [\%]} \qquad (\ 18\ )$$

Resulting potential fluences are illustrated in Figure 29 as a histogram with a median value of 102 mJ/cm² (n=153). These data reveal the capability to improve photolytic diclofenac removal from modeled 20% at a disinfection dose of 45 mJ/cm² to 41%, slightly exceeding the 99 mJ/cm² that are required for complying with the threshold of 100 ng/L diclofenac in the river Isar (Section 7.3.2.1). Since energy consumption is linear with lamp power applied in the system, specific energy data during regular disinfection (22 Wh/m³) can be multiplied by the lamp power enhancement factor resulting in 50 Wh/m³ for 102 mJ/cm².
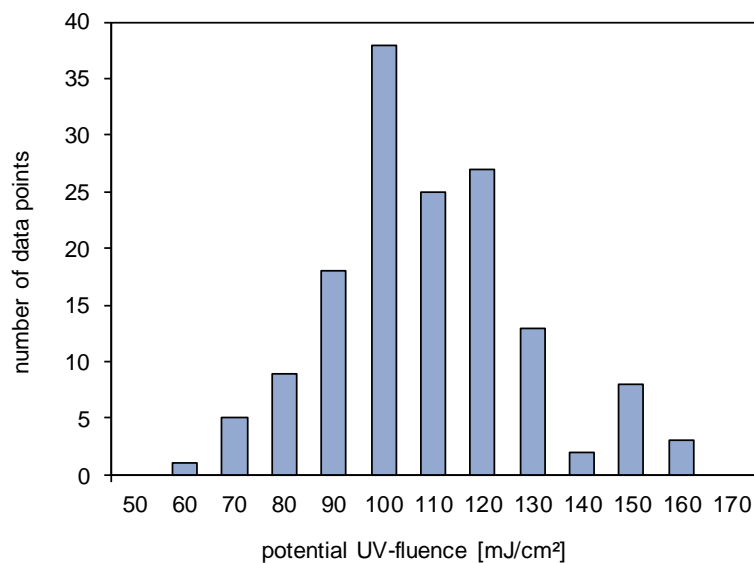
Figure 29: Histogram for potential fluences obtained by lamp power modification in the existing UV system at Munich II.

Reducing the flow rate in each irradiation channel increases exposure time and consequently the applied fluence. Current system operation is realized by a flow-proportional control unit. During the summer season, an irradiation channel is permanently in operation. For total flow rates above 0.5 m³/s, another channel is connected per 1 m³/s. Based on the data presented in Table 13, a continuous operation of a maximum of three irradiation channels can be assumed for the 85th percentile of the annual data (<3 m³/s). Consequently, operation of the three additional irradiation channels can be realized for 85% of the seasonal operating period. With this modification, exposure times in the full-scale UV disinfection system could theoretically be doubled. With the assumption that the changed flow pattern does not influence the irradiance distribution due to reduced flow velocity in the irradiation channels, the applied fluence also doubles. A considerable temperature increase of the wastewater effluent can be neglected, as the increased energy input of 100 W/m³ coupled with the efficiency of LP mercury vapor lamps (30-40%) can be neglected compared to the specific heat capacity of water (4,182 kJ/(kg-K)).

If both modification options (exposure time and lamp power) are combined, a theoretical fluence of <204 mJ/cm² can be achieved resulting in a specific energy consumption of 100 Wh/m³. This corresponds to a photolytic diclofenac removal of about 65% and a resulting concentration in the Isar of 63 ng/L. Compliance with the target diclofenac concentration of 50 ng/L in the river cannot be obtained by modifications of the UV system operation. In addition, a sufficiently high fluence which is needed for radical promoter activation in UV-based AOPs (usually >400 mJ/cm²) cannot be reached by lamp power adjustments and exposure time extension only. Therefore, the addition of radical promoters is not considered to lead to considerable removal enhancements by modification of operational parameters.

7.3.3.2   *Retrofitting of the existing UV lamp technology*

Besides operational modifications of the existing UV system, retrofitting of the current lamp technology to systems with higher UV output was investigated. For this purpose, potential alternatives were explored in cooperation with *Xylem Water Solutions Deutschland GmbH*. Suitability of the alternative lamp technology in the existing irradiation channel was set as a major requirement. The technical design in this investigation is based on a flow rate of 2.4 m³/s (85th percentile, 2016) and a UV transmittance of 70%. Replacing the current lamp technology (WEDECO TAK-55 series) by the WEDECO Duron UV disinfection system equipped with 806 lamps (600 W, each), a maximum fluence of 290 mJ/cm² could be achieved without applying any of the modification options proposed in Section 7.3.3.1. This would correspond to a photolytic diclofenac removal of 82% and a resulting diclofenac concentration in the Isar of 43 ng/L. Additionally, a retrofitted system could also be modified if operated at the median flow rate of 1.9 m³/s. In this case, fluence could potentially be enhanced by <20%. Adding 10 mg/L H_2O_2 to a fluence of 290 mJ/cm², primidone could be attenuated by 18%.

7.3.3.3   *Implementation of a full-scale UV/H_2O_2 system*

Another scenario for retrofitting the full-scale UV disinfection system at WWTP Munich II for advanced removal of TOrCs is the technical implementation of a full-scale UV/H_2O_2 process. The full-scale UV/H_2O_2 process is designed considering a flow rate of 2.4 m³/s and a wastewater UVT of 70%. Based on the results in Section 7.3.2.2, the target definition was set as 50% primidone removal. The full-scale UV/H_2O_2 process was designed in cooperation with *Xylem Water Solutions Deutschland GmbH* applying the Duron system. To achieve a desired fluence of 1,145 mJ/cm², 3,181 Duron lamps (600W each) have to be installed with an overall capacity of 2,099 kW. Due to the number of UV sources required, an extension of the existing irradiation channels must be considered for the implementation of this scenario.

In addition to UV lamp technology, dosing of H_2O_2 has to be designed. The "blue grotto" (see Figure 30) was identified as an appropriate dosing point in the WWTP Munich II which provides thorough mixing by combining the effluents of all sand filter cells in one concrete channel. In this scenario, the daily requirement of H_2O_2 at a stock concentration of 30% and a targeted concentration in wastewater (flow rate of 2.4 m³/s) of 10 mg/L H_2O_2 has been determined as 6.2 m³/d. H_2O_2 is delivered by tanker trucks and stored in a stainless-steel tank near the dosing point (Figure 30). To provide dosing at 10 mg/L H_2O_2 over a period of 15 days, the tank capacity is designed with a volume of 100 m³.
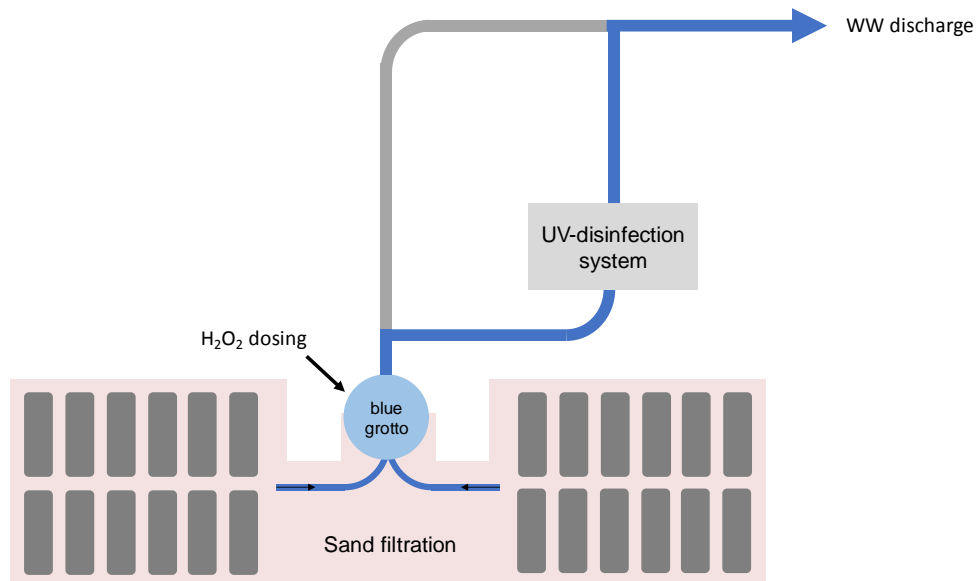
Figure 30: Schematic diagram of the channel flow between sand filtration and wastewater discharge to the river Isar to identify appropriate dosing of H_2O_2.

H_2O_2 is dosed proportionally to the wastewater flow rate into the blue grotto. Due to the turbulent flow at the dosing point, a homogeneous concentration profile can be assumed in the UV disinfection system. However, to ensure thorough mixing, installation of static mixers in the concrete feed channel of the UV system is recommended.

7.4 Conclusion

This chapter investigated the applicability of existing UV disinfection plants for enhanced removal of TOrCs by adapting process parameters or by retrofitting the existing infrastructure. Advanced removal of photo-susceptible TOrCs from wastewater effluents could theoretically be carried out in wastewater treatment plants which have an existing UV disinfection system. As presented above, photo-susceptible compounds can be removed by relatively minor modifications of process operation. Process parameters and plant-specific energy data from Sections 7.3.2 and 7.3.3 serve as the basis for the overall comparison of the respective scenarios. Table 14 summarizes target definitions, modeled indicator compound removal and system parameters from modifications and retrofitting of the full-scale UV disinfection system.

The target threshold of 100 ng/L diclofenac in the river Isar can be achieved by enhancing lamp power by a factor of 2.26. This procedure increases the specific energy consumption from 22 to 49.6 Wh/m³. Additionally, extending the exposure time in the irradiation channels results in a diclofenac removal of 65% and a diclofenac concentration of 63 ng/L with a specific energy consumption of 100 Wh/m³. Therefore, the targeted threshold of 50 ng/L cannot be achieved by system modification. The retrofitting potential of the existing UV disinfection system was theoretically investigated by calculating fluence after replacing the current TAK-55 irradiation system by a WEDECO Duron system. This option revealed a modeled diclofenac removal of 82% complying with the potential threshold of 50 ng/L with a specific energy consumption of 99 Wh/m³. Investigating the target threshold of 50% primidone removal, required

fluences of 1,145 mJ/cm² at a peroxide dose of 10 mg/L were calculated and a full-scale UV/H$_2$O$_2$ system was designed.

Table 14: Target threshold, modeled indicator removal and system parameters from modifications and retrofitting of the full-scale UV disinfection system.

Target threshold	Modeled indicator removal	Modification investigated	Fluence [mJ/cm²]	Specific energy consumption [kWh/m³]
Regular disinfection	20 %	none	45.2	0.022
100 ng/L diclofenac in Isar	41 %	lamp power enhancement	102	0.05
100 ng/L diclofenac in Isar	65%	lamp power enhancement + exposure time extension	204	0.1
50 ng/L diclofenac in Isar	82%	retrofitting lamp technology	290	0.099
50% primidone removal		full-scale AOP design	1,145*	0.23

*Dosing of 10 mg/L H$_2$O$_2$ needed to comply with the target definition.

Accounting for all-year operation and a flow rate of 2.4 m³/s, specific energy consumption can be converted to annual energy consumption expressed in GWh/a as depicted in Figure 31. The annual energy consumption meeting target thresholds represents a large range from 0.8 to 15.8 GWh/a. System compatibility could be improved if disinfection fluences are only increased to higher values if high TOrC loads are expected (e.g. during dry-weather operation).
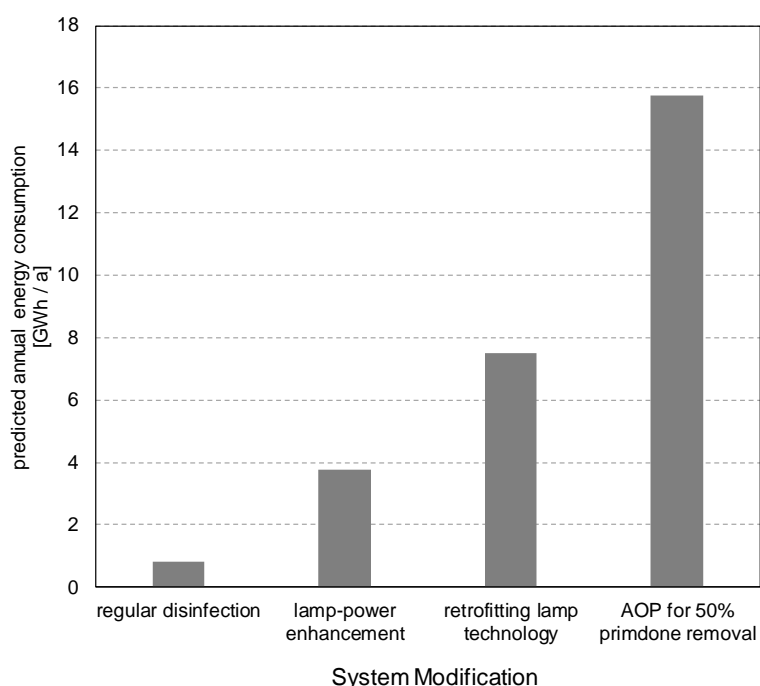
Figure 31: Annual energy consumption for the investigated modification options of the full-scale disinfection facility at WWTP Munich II.

Besides energy needs, modification of operational parameters leads to an increased maintenance requirement for the UV system since continuous operation of all irradiation channels reduces the maximum lifetime of UV lamps. Moreover, in contrast to seasonal disinfection, compliance with potential TOrC thresholds would have to be realized by continuous operation throughout the year and therefore result in doubling of annual operation time, additionally increasing annual energy needs.

Transferability of investigation results from this study to other WWTPs with existing full-scale UV disinfection systems is limited since UV systems are designed and operated at different site-specific targets. Individual investigation of operational system parameters is needed on-site to evaluate potential modification and retrofitting possibilities. This chapter represents a basic procedure of investigation steps that reveal modification options for each WWTP.

The tested hypothesis that the UV disinfection system at the WWTP Munich II can be modified to achieve a significant attenuation of photo-susceptible TOrCs by enhanced photolysis (Hypothesis 1.2) can be accepted while Hypothesis 1.3, stating that a radical indicator removal of 50% can be achieved by retrofitting the disinfection system and applying H_2O_2 as a radical promoter, is rejected.

8. Overall Discussion and Future Research Needs

The current availability of 12,600 UV systems worldwide that are installed to disinfect the effluent of WWTPs, indicates that UV installations could potentially be used for advanced oxidation of TOrCs from wastewater effluents. Therefore, this study was initiated to investigate the TOrC removal potential by the combination of UV light with radical promoters in municipal wastewater effluents. Five detailed research objectives were derived to explore the general objective of this study and four hypotheses (cf. Chapter 2) were developed and tested by a series of experiments with results being presented in Chapters 3–7. A literature study was performed to review the state-of-the-art of emerging and established AOPs and to compare the energy efficiency of these processes which supports the evaluation of AOP applicability for advanced wastewater treatment (cf. Chapter 3). Beyond the literature study, experiments were conducted (i) to investigate the modification potential of full-scale UV disinfection facilities for advanced TOrC removal by UV/H_2O_2 and evaluate process resilience towards water quality changes at pilot-scale (cf. Chapter 4), (ii) to study alternative radical promoters for advanced treatment of wastewater effluent by UV-based AOPs at lab- and pilot-scale (cf. Chapter 5 and 6), (iii) to investigate optical surrogates for UV-AOPs to predict photo-susceptible and photo-resistant TOrCs (cf. Chapter 6), and (iv) to explore the modification and retrofitting potential of the full-scale UV disinfection system at the WWTP Munich II for advanced TOrC attenuation (cf. Chapter 7).

Based on these results, a preliminary assessment on the applicability of UV-AOPs for TOrC removal from municipal wastewater effluent is provided in the following sections additionally addressing current knowledge gaps and future research needs. In this context, applicability of UV/H_2O_2 for TOrC removal from municipal wastewater effluent is discussed referring to water matrix effects on oxidation performance of UV-AOPs and kinetic modeling of TOrC removal as well as retrofitting potential of existing UV infrastructures. Then, alternative radical promoters are discoursed and finally, dynamic process control opportunities are being comprehensively discussed to provide a direct application perspective for municipal and industrial wastewater treatment plant operators.

8.1 Applicability of UV/H_2O_2 for TOrC Removal from Municipal Wastewater Effluent

UV/H_2O_2 could successfully be operated to attenuate TOrCs from municipal wastewater effluents. Already moderate fluences (<200 mJ/cm²) resulted in significant removal of photo-resistant TOrCs by radical oxidation. Thus, based on the results presented in Chapters 4-6, UV/H_2O_2 is a promising treatment option to attenuate TOrCs from wastewater effluents. The hypothesized applicability of UV/H_2O_2 for advanced TOrC removal by UV/H_2O_2 (***Hypothesis № 1.1***) could be accepted.

8.1.1   UV disinfection system modification for TOrC removal

At the full-scale UV disinfection facility at Munich II, exposure time extension (by reduction of flow rate) and lamp power enhancement were determined as major control variables for fluence augmentation resulting in fluences of ≤204 mJ/cm². Thus, **Hypothesis № 1.2,** stating that the UV disinfection system at Munich II can be modified to achieve a significant attenuation of photo-susceptible TOrCs by enhanced photolysis, could be accepted. In addition, retrofitting the existing infrastructure with more powerful lamps revealed the possibility to improve UV fluence up to 290 mJ/cm². However, system retrofitting did not result in sufficiently high fluences for primidone oxidation (<20%) by UV/H_2O_2 resulting in the rejection of **Hypothesis № 1.3**. Implementation of a full-scale UV/H_2O_2 process at Munich II would have been necessary to achieve a 50% primidone removal threshold by applying 1,145 mJ/cm² and 10 mg/L H_2O_2. Such an option would, in any case, require major infrastructural changes of the existing system. In 2014, a study suggested that UV disinfection systems are not suitable for the attenuation of TOrCs without supplementing technologies (Pinnekamp et al., 2014). Results discussed above, however, emphasize the opposite. Modification and retrofitting of existing UV-systems is a considerable option to attenuate photo-susceptible TOrCs while the application of existing systems for radical-based oxidation is limited. The current relevance of this topic is also evident in an upcoming project in Germany: The Wupperverband has launched an investigation into the applicability of a full-scale UV disinfection system for advanced removal of TOrCs[1]. Since the removal of TOrCs during regular disinfection has already been investigated in literature (Nick et al., 1992; Canonica et al., 2008; Gagnon et al., 2008) and in the document-on-hand, future investigations could focus on full-scale evaluation of TOrC removal during enhanced application of UV disinfection systems as modeled in Chapter 7 to confirm the applicability of modified and/or retrofitted UV disinfection systems.

8.1.2   Water matrix effects on UV/H_2O_2

The major challenge of UV-AOPs applied to wastewater effluent is the highly complex wastewater matrix that barely exceeds 70% UVT at 254 nm and contains considerable amounts of DOC, as well as substantial concentrations of inorganic scavengers. Significant scavenging of ·OH has already been reported to be mainly attributed to DOC (Rosario-Ortiz et al., 2010; Keen et al., 2014), nitrite (Sharpless and Linden, 2001; Keen et al., 2012), and HCO_3^-/CO_3^{2-} (Liao et al., 2001). Comprehensive experimental data of continuous UV/H_2O_2 operation presented in Chapter 4 have underlined the significant influence of radical scavenging particularly by NO_2^- and DOC on AOP performance. NO_2^- concentrations considerably fluctuated in our study reaching unexpectedly high values of ≤2 mg-N/L, resulting in significant reduction of ·OH exposure. In contrast, the comparison of TOrC removal in ten different wastewater effluents stated DOC as a major scavenger (DOC accounted for 62% of scavenging) in a recent study (Gerrity et al., 2016) supporting findings of other studies on UV/H_2O_2 (Rosario-Ortiz et al., 2008; Keen et al.,

---

[1] Personal correspondence with Philipp Pyro, Wupperverbandsgesellschaft für integrale Wasserwirtschaft mbH, Wuppertal, Germany.

2014). By depicting the removal of single compounds as a function of fluence/DOC [(mJ/cm²)/(mg-C/L)], in the above-mentioned study, results were adjusted for DOC scavenging and aligned well from different WWTPs, indicating the minor role of other radical scavengers. However, Gerrity et al. (2016) conducted all experiments in lab-scale batch reactors and NO_2^- concentrations in wastewaters were measured as ≤0.45 mg-N/L. Since usually low nitrite concentrations are expected in municipal wastewater effluents, DOC is certainly the scavenger with the highest relevance, which has been confirmed by our study for dry-weather conditions (cf. Chapter 4). Nevertheless, nitrite should be monitored at full-scale UV-AOP applications in WWTPs ideally being implemented in a dynamic system operation to avoid oxidation performance losses during nitrite peaks. Besides the negative impact of water matrix scavenging on ·OH exposure in UV/H_2O_2, a recent study revealed enhanced compound degradation in the presence of low iron concentrations (<0.3 mg/L) due to participating photo-Fenton reactions (Ulliman et al., 2018a) which should be evaluated in more detail in future studies.

8.1.3 *Improving UV/H_2O_2 performance following tertiary treatment of municipal wastewater*

Water quality has been shown to play a significant role in radical generation and consequently energy efficiency of AOPs (cf. Chapter 3, 4 & 5). In addition, the influence of water matrix changes on ·OH radical exposure was presented in Section 4.3.4. Pre-treatment of UV-AOP feed water might therefore be beneficial to reduce radical scavenging effects. However, few studies have investigated the effect of treatment processes added post conventional wastewater treatment as strategies to increase subsequent UV-AOP performance. Therefore, as part of this dissertation, four different pre-treatment processes were investigated as options for improving water quality conditions of secondary treated wastewater effluents just prior to UV treatment, with and without added H_2O_2 (**Paper V, Chapter 9.6 (SI)**). The pre-treatment options included single-stage biofiltration, sequential biofiltration, coagulation-flocculation-sedimentation-filtration (CFSF), and nanofiltration (NF) and mainly aimed to reduce DOC and increase UVT to subsequently enhance the photolysis rate of UV-susceptible TOrCs and radical promoters. Lab-scale investigations revealed NF treatment to produce the most favorable water quality conditions for UV/H_2O_2 and direct photolysis. When comparing CFSF, single-stage biofiltration and sequential biofiltration, CFSF treatment exhibited the highest increase in UVT (12%) and all three technologies reduced scavenging capacity by ~24%. Scavenging capacity results were further analyzed and the percent contributions of individual scavengers to the overall scavenging capacity was evaluated. While DOC was the predominant scavenger in CFSF, single-stage biofiltration and sequential biofiltration treated water, the scavenging capacity of NF effluent exhibited equal contribution by DOC and bicarbonate. Interestingly, oxidation performance measured as steady-state ·OH concentration substantially increased by 36% for sequential biofiltration, 55% for single-stage biofiltration, 59% for CFCF and 164% for NF revealing significant optimization potentials of UV/H_2O_2 by tertiary treatment of municipal wastewater.

Similar results were achieved in a recent study applying anion exchange before UV/H_2O_2 treatment which increased the UVT from 38% to 85% and simultaneously decreased the energy demand for the UV/H_2O_2 process by 84% (Hofman-Caris et al., 2017). Adding one (or a combination) of the above-mentioned processes with the exception of CFSF as a pre-treatment step prior to UV-AOP, besides increasing the oxidation potential, another barrier against TOrCs and pathogens would be provided reducing their presence in wastewater effluent.

Future studies could focus on economic analyses to determine if the savings in UV-AOP operational costs offset the expenses of chemicals, energy, installation and equipment required for an additional treatment step before the UV-AOP system.

8.1.4 Modeling UV/H₂O₂ oxidation performance

The effect of scavenging on ·OH formation was also investigated in this study by kinetic modeling (cf. Chapter 4) supporting **Hypothesis № 2**, stating that the removal of TOrCs during UV/H_2O_2 in treated wastewater can be predicted by mathematical models. Early time-based modeling investigations of UV/H_2O_2 included relevant radical species (·OH, $O_2^{\cdot-}$, $CO_3^{\cdot-}$) and scavengers (DOC, $H_2PO_4^-$/HPO_4^{2-} HCO_3^-/CO_3^{2-}) (Glaze et al., 1995) and were complemented with additional oxidants ($HO_2^\cdot$, $HPO_4^{\cdot-}$) increasing model accuracy in buffered distilled water (Crittenden et al., 1999). Other fluence-based approaches limited their model to the most important ·OH-based oxidation pathway and relevant scavengers, i.e., DOC, NO_2^-, HCO_3^-/CO_3^{2-} (Pereira et al., 2007b) or DOM, HCO_3^-/CO_3^{2-}, Fe(II), Mn(II) (Yao et al., 2013), and likewise resulted in convenient prediction accuracies. However, modeling accuracy (under- or overprediction) was found to be significantly affected by the modeled TOrC and applied water matrix (Yao et al., 2013; Lee et al., 2016) which was also observed in this study (cf. Chapter 4). Potential reasons for modeled deviations were ascribed to uncertainties of the applied photolysis or second-order rate constants from literature or accelerated (indirect) photolysis due to formation and reactions of triplet excited states of DOM (3DOM*) with activated aromatic structures of TOrCs (Lee et al., 2016). In a recent study, several models, that included specific concepts to calculate TOrC removal, were applied to 10 different wastewaters (Gerrity et al., 2016). The authors investigated the ·OH exposure concept (steady-state ·OH concentration over time) and the R·$_{OH,UV}$-concept (·OH exposure/fluence, Rosenfeldt and Linden, 2007) which resulted in nearly congruent results based on the same kinetic equation for ·OH generation from UV/H_2O_2 that was also applied in the present study. Thus, implementation of ·OH exposure or R•$_{OH,UV}$ did not result in a higher prediction accuracy than the model presented in equation 13 and 14 (Chapter 4). However, kinetic models always rely on experimentally derived second-order rate constants which always contain uncertainties that are not considered in modeling approaches. Future research could thus focus on refining kinetic models including uncertainties of these rate constants which might subsequently enhance prediction accuracy as shown elsewhere for water disinfection with chlorine (Carvajal et al., 2017b).

8.2 Potential of Alternative Radical Promoters for UV-AOP Application in Wastewater Effluents

If different radical promoters are applied in UV-AOPs, radical speciation and consequently, the importance of single radical scavengers might change. Especially, since $SO_4^{\cdot-}$ and RCS are known to react more selectively with organic water constituents than $\cdot OH$ (Li et al., 2017), UV/PDS and UV/Chlorine are expected to be more responsive to water matrix changes than UV/H_2O_2. Therefore, this dissertation hypothesized that UV/PDS and UV/Chlorine achieve a comparable oxidation performance to UV/H_2O_2 if applied to wastewater effluent (**Hypothesis № 3**). Thus, the application of peroxodisulfate and chlorine as alternative radical promoters for UV-AOPs was investigated in Chapters 5 and 6 comparing their respective oxidation performance to UV/H_2O_2 in municipal wastewater effluents.

UV/H_2O_2 and UV/PDS were comparatively investigated in buffered ultrapure water and wastewater to reveal water matrix impacts on $SO_4^{\cdot-}$ and $\cdot OH$ (Chapter 5). Experimental investigations in pure water revealed moderate removal of TOrCs in UV/H_2O_2, while the concentration of all TOrCs reached the limit of quantification during UV/PDS within the same applied fluence and molar oxidant dose. Significantly higher TOrC removal during UV/PDS in buffered pure water was attributed to the higher photolysis rate of PDS at 254 nm and the lower scavenging effect of the pure water matrix on $SO_4^{\cdot-}$, which led to a higher steady-state concentration of $SO_4^{\cdot-}$ than $\cdot OH$ (Chapter 5). Another study reported a 3.7 times higher degradation rate constant for UV/PDS compared to UV/H_2O_2 for atrazine removal in pure water corroborating our results (Khan et al., 2014). When applied to municipal wastewater effluent, both AOPs resulted in significantly reduced percent removal compared to pure water experiments indicating the strong scavenging effect of the water matrix. Interestingly, in the wastewater matrix UV/PDS exhibited a similar removal of TOrCs in comparison to UV/H_2O_2, which could be reproduced in Chapter 6, confirming **Hypothesis № 3** for PDS. However, $SO_4^{\cdot-}$-based oxidation displayed higher selectivity than the $\cdot OH$-based process which confirms previous findings (Ahn et al., 2017; Lian et al., 2017). The removal pattern of photo-resistant compounds during both processes was consistent with their second-order rate constants with $\cdot OH$ and $SO_4^{\cdot-}$. To assess the wastewater matrix impact on oxidation performance of the two UV-AOPs, additional experiments conducted in the presence of individual inorganic species indicated that the formation of $CO_3^{\cdot-}$ enhanced the degradation of diclofenac and sulfamethoxazole during both processes which support findings from a previous study (Zhang et al., 2015a).

In Chapter 6, the UV-AOP comparison was complemented by UV/Chlorine. UV/H_2O_2, UV/PDS, and UV/Chlorine were comparatively investigated in municipal wastewater effluent. Oxidation performance of a wide range of TOrCs (measured as observed first-order rate constants) revealed highest oxidation performance of UV/Chlorine for all TOrCs, followed by UV/H_2O_2 and UV/PDS which exhibited comparable k_{obs} values, confirming **Hypothesis № 3** for operation with peroxodisulfate and chlorine. UV/PDS and UV/Chlorine exhibited higher compound selectivity than UV/H_2O_2 based on the

selective reaction of $SO_4^{\cdot-}$ and RCS (Li et al., 2017). Higher oxidation performance of UV/Chlorine compared to UV/H_2O_2 has already been reported in a number of previous studies (Sichel et al., 2011; Yang et al., 2016a; Li et al., 2017; Pan et al., 2018; Pati and Arnold, 2018). However, the comparison of UV/PDS and UV/Chlorine received less attention. A recent study indicated comparable removal of c acid by UV/PDS and UV/Chlorine in phosphate buffer (Lu et al., 2018), which corroborates our findings in Chapter 5, where UV/PDS yielded significantly higher $SO_4^{\cdot-}$ compared to experiments in wastewater. The comparison of UV/H_2O_2, UV/PDS, and UV/Chlorine has been approached by some researchers (Li et al., 2017; Pati and Arnold, 2018; Varanasi et al., 2018) revealing a significant impact of water matrix on oxidation performance. While Li et al. (2017) reported an oxidation performance of TOrCs in synthetic reverse osmosis permeate following the order of UV/PDS > UV/H_2O_2 > UV/Chlorine, investigations of Pati and Arnold (2018) in buffered pure water revealed highest removal performance for UV/Chlorine followed by UV/PDS and UV/H_2O_2. Results presented in Chapters 5 and 6 are also biased by the specific batch wastewater sample that was used for all experiments. To reveal the specific effect of water matrix composition on the respective UV-AOPs, continuous pilot-scale operation is suggested for future investigations since those reveal statistically significant impact of water matrix changes on radical generation. Alternatively, comprehensive investigations applying the three UV-AOPs to numerous different wastewaters would allow a detailed insight into water matrix effects on process specific oxidation performance as investigated elsewhere for UV/H_2O_2, O_3/H_2O_2 and UV/O_3 (Lee et al., 2016).

Although oxidation performance of UV/Chlorine is outstanding in comparison of the three different UV-AOPs, it has to be noted that oxidation by-product formation potential might be substantially higher during both UV/PDS and UV/Chlorine compared to UV/H_2O_2 (Section 3.3). Several studies have already investigated OBP formation during $SO_4^{\cdot-}$-based AOPs (Yuan et al., 2011b; Lutze et al., 2014; Yuan et al., 2014; Lutze et al., 2015b) and a mechanistic summary is provided in Section 3.3. A recent study indicated significant AOX formation if $SO_4^{\cdot-}$-based AOP is applied in saline wastewater (Fang et al., 2017). BrO_3^- as well as ClO_3^- formation by a direct reaction of Br^- with $SO_4^{\cdot-}$ was reported to be negligible if DOM is present in the treated water (Lutze et al., 2014; Hou et al., 2018). In UV/Chlorine, main formation pathways of halogenated organic OBPs (e.g., THM, HAN and HAA) are based on reactions between $HOCl/OCl^-$ and DOM (von Gunten, 2003b). Consequently, UV/Chlorine process may involve formation of AOX. However, to the best of our knowledge, as of today no literature is available targeting the OBP formation potential of UV/PDS and UV/Chlorine in municipal wastewater.

Some limitations of UV/PDS need to be considered despite the promising results on the oxidation of TOrCs. Unlike H_2O_2 and chlorine, dosing of peroxodisulfate increases the salinity of treated water by sulfate ions, which should be evaluated prior to UV/PDS application in wastewater effluent. In addition, PDS molar mass, which is 5.6 times higher than the molecular mass of H_2O_2, results in considerably higher chemical requirements. Further research is needed to investigate OBP formation-potential and corresponding toxicological effects applying UV/H_2O_2, UV/PDS, and UV/Chlorine to

municipal wastewater effluent. If toxicological effects can be neglected, UV/Chlorine might be a reasonable AOP for retrofitting existing UV disinfection systems, since a moderate AOP-fluence of 400 mJ/cm² and an oxidant dose of 0.45 mM chlorine result in remarkable attenuation of all TOrCs (>51%) with the exception of TCEP (cf. Chapter 6).

Besides H_2O_2, PDS and chlorine, other radical promoters are being investigated for UV-AOPs in literature. UV/O_3 was discussed in Section 3.2.2.2 as a process combination that is mostly limited due to high energy demands since both UV lamps and ozone generator need large amounts of electrical energy. ClO_2 received little attention as a radical promoter in UV-based processes most likely because the photolysis at 254 nm (molar absorption coefficient $\varepsilon=61$ $M^{-1}s^{-1}$) does not yield in radical species but chloride and chlorate formation as the major products of the photo-decomposition reaction (Karpel Vel Leitner et al., 1992). In addition, the quantum yield at 254 nm was reported to be moderate at 0.42 (Cosson and Ernst, 1994). An underestimated radical promoter is peroxymonosulfate (PMS) which is activated by LP-UV radiation into a $SO_4^{\cdot-}$ and a $^{\cdot}OH$ with a quantum yield for $SO_4^{\cdot-}$ of 0.52 at pH 7 and molar absorption coefficients ranging from 13.8–149.5 $M^{-1}cm^{-1}$ at pH 6-12, respectively (Guan et al., 2011). TOrC removal efficiency by UV/PMS in buffered pure water was reported to be lower than UV/PDS but higher than UV/H_2O_2. However, the presence of transition metals (e.g., iron or copper) resulted in highest TOrC removal efficiency by UV/PMS followed by UV/PDS and UV/H_2O_2 if applied to tap water (He et al., 2013). In wastewater, UV/PMS revealed likewise to be the most effective process followed by UV/PDS and UV/H_2O_2 (Mahdi-Ahmed and Chiron, 2014). Future research could therefore aim to evaluate PMS as a potential alternative to the radical promoters H_2O_2, peroxodisulfate and chlorine that were investigated in the document-on-hand.

8.3 Dynamic process control

Comprehensive data about radical scavenging on AOP performance (cf. Chapter 3 & 4) have underlined the necessity of dynamic AOP operation based on water matrix fluctuations. Oxidation performance losses that are caused by water matrix changes during continuous AOP operation should be compensated by adjustment of process parameters (e.g., fluence and oxidant dose in UV-AOPs). This procedure likewise applies if water matrix fluctuates towards lower scavenging and higher UVT, demanding to lower AOP parameters in order not to exceed targeted TOrC removal. Full-scale UV-AOP systems are usually operated with a flow-proportional oxidant dosing towards a constant targeted dose and a radiometer-based UV intensity control for fluence adjustment. A dynamic process control, however, could optimize both energy and chemical consumption and account for oxidation performance losses due to water matrix changes. Below, surrogates (cf. Chapter 6) and mathematical models (cf. Chapter 4) are discussed as two fundamentally different options that could be implemented at full-scale AOP operation control systems.

Surrogate approaches apply bulk water parameters such as UVA or fluorescence to track performance measures of treatment processes (Dickenson et al., 2009; Chys et al., 2018),

which was investigated in Chapter 6 for UV/H_2O_2, UV/PDS, and UV/Chlorine. A total number of 11 optical surrogate parameters derived from fluorescence and absorbance measurements were correlated to the attenuation of 15 indicator TOrCs. It was hypothesized that the removal of photo-susceptible and photo-resistant TOrCs during UV/AOPs correlate with intensity changes of specific chromophore or fluorophore DOC components (***Hypothesis № 4***) since underlying mechanisms of TOrC degradation should be reflected in DOM transformation.

Selection of optical surrogate parameters resulted in UVA and color (measured as absorbance at 436 nm), total fluorescence, fluorescence index and four additionally selected fluorescence peaks (P_II – P_V) that represent fluorescence regions previously defined by Chen et al. (2003). In addition, two PARAFAC components (C1 and C2) were statistically derived from fluorescence EEMs. The diverse reactivity of TOrCs to different oxidants resulted in a unique correlation between selected surrogates and single targeted compounds during each AOP. However, the multiplicity of 15 TOrCs and 11 surrogates was not depictable and, thus, based on dominant reaction pathways of each UV-AOP, indicator TOrCs were selected representing the underlying mechanistic processes, i.e., oxidation dominated by photolysis and oxidation dominated by reactions with radicals ($\cdot OH$, $SO_4^{\cdot -}$, RCS).

UVA, TF and the selected fluorescence peak P_IV revealed highest linear correlation coefficients with process indicator TOrCs of each UV-AOP. Besides $\cdot OH$-based reactions in UV/H_2O_2 where P_IV showed highest R^2 values, best correlations were shown for UVA and TF indicating that neither peak picking nor PARAFAC resulted in a higher informative value of selected optical surrogates. Including oxidation mechanisms into surrogate evaluation, the underlying mechanistic reactions can be reflected revealing good correlations between indicator TOrCs and selected optical surrogates. ***Hypothesis № 4.2*** could thus be accepted representing correlations between photo-resistant TOrCs and selected chromophore or fluorophore DOC components in the three UV-AOPs. The applicability of optical surrogates for photo-susceptible TOrCs, however, could only be proven for UV/H_2O_2 and UV/PDS, since the compounds diclofenac, iopromide, and sulfamethoxazole were shown to be highly reactive to both direct chlorination and RCS. Consequently, **Hypothesis № 4.1** is accepted for UV/H_2O_2 and UV/PDS and rejected for UV/Chlorine.

However, since no surrogate was found to represent direct photolysis, some limitations of **Hypothesis № 4.1** need to be considered: correlations between photo-susceptible TOrCs and optical surrogates during UV/H_2O_2 and UV/PDS are biased since radical generation by radical promoter addition has a higher effect on surrogate removal in comparison to photolysis indicator TOrCs which are predominantly attenuated by photolysis. Therefore, applicability of surrogates for photo-susceptible TOrCs is limited to a narrow concentration range of radical promoters (0.075-0.45 mM), since higher concentrations are expected to significantly lower linear correlation coefficients. Further studies are needed to determine the full concentration range that is applicable for this purpose.

UVA and TF are well investigated surrogates in numerous research investigations (e.g., Yu et al., 2015; Gerrity et al., 2016) and could be emphasized as useful parameters to predict TOrC removal in different UV-AOPs in Chapter 6. Further experimental investigations are needed on testing these surrogates in continuous pilot experiments treating municipal wastewater effluent to verify the applicability under real conditions including water matrix fluctuations. If the sensitivity of the surrogates is considered sufficient, such models could be implemented at full-scale AOP operation control systems. Chys et al. (2018) recently studied wastewater quality fluctuations over time in 15 WWTPs to assess the applicability of surrogates for application in an ozonation system and revealed stable occurrence of TOrCs and spectral measurements (UVA and fluorescence parameters) between different locations, corroborating the applicability of optical surrogates for UV-AOP control in WWTPs. However, sampling was not coordinated to weather lowering the general transferability of the above-mentioned study. The applicability of TF or PARAFAC components, however, is limited since it requires the recording of a complete EEM that is not yet available as a viable online measurement. In contrast, UVA or selected fluorescence peaks are straightforward to measure by optical sensors which are already commercially available. Therefore, if correlations are acceptable, alternative parameters to TF should be selected as surrogates based on the findings presented in Chapter 6.

Besides TOrC prediction, surrogate models are also subject to research aiming to predict OBP formation. A number of studies have shown evidence that formation of total organic halides (TOX), e.g., THM or HAA, during chlorination, can be correlated to the differential absorbance of UVA at 272 nm (ΔUVA_{272}) in surface water and drinking water (Korshin et al., 2002; Roccaro et al., 2008; Roccaro and Vagliasindi, 2009). However, this approach has not yet been investigated for wastewater and UV-AOP applications, which could be targeted in future studies.

Apart from surrogate models, kinetic models as presented in Chapter 4 for UV/H_2O_2 can be used to predict the change of TOrC removal caused by water matrix fluctuations during continuous operation or to dynamically control UV/H_2O_2 based on TOrC removal targets. However, this method relies on dependable online measurement of the relevant matrix components which are not always procurable as reliable online systems. Especially online measurements of the critical scavenger nitrite by UV spectral sensors (e.g. NiCaVis® 700 IQ NI, WTW, Germany) have shown to be restrictedly reliable due to sensor failures[2]. In addition, established online-sensors (e.g. TOC, UVT, conductivity, pH) also reveal minor challenges during operation in real wastewater matrix due to biofouling of the sensor probes that results in signal shifts or sensor failures (Bourgeois et al., 2001). Thus, approaches predicting scavenging in real-time are needed to overcome these challenges. Virtual or software sensors are advanced tools to predict target parameters by other available, reliable sensors (Jacobsen and Lynggaard Jensen, 1998; Fernandez de Canete et al., 2016) and are promising solutions to overcome real-time scavenger monitoring limitations. Especially, since general monitoring at WWTPs

---

[2] Personal correspondence with Jürgen Terstappen, head of laboratory at WWTP Gut Marienhof (Munich II), Munich Sewage Company (Münchner Stadtentwässerung)

is often accomplished for hundreds of hydraulic and qualitative parameters, including both online and offline measurements which, in modern WWTPs, are combined in a supervisory control and data acquisition (SCADA) system, advanced statistical methods can be used to extract hidden information in these existing data to predict real-time scavenger concentrations (Dürrenmatt, 2011).

In the framework of experimental investigations for Chapter 4, data driven machine-learning methods (including data mining and data-driven modelling) were investigated as software sensors to predict radical scavenger concentrations that cannot be measured in reasonable quality and time resolution (*Paper VI*). 30 attributes were evaluated as potential predictors for single scavenger concentrations mainly including typical WWTP parameters such as flow parameters (e.g. numerous recirculation flow rates) and water quality data such as Total Kjeldahl Nitrogen (TKN), turbidity, phosphate, pH or biochemical oxygen demand (BOD) across the treatment train of the WWTP Munich II. In addition, methanol dosage was selected as an attribute, which is a strong mechanistic trigger for the occurrence of effluent nitrite (Böhm, 2002). While the focus of *Paper VI* was on model development and applicability comparison of eight different machine-learning classifiers, which resulted in selection of the Tree Augmented Naïve Bayes (TAN) algorithm, prediction of the water parameters UVT, pH, nitrite, alkalinity, and TOC could be performed. In contrast to kinetic models, that calculate exact removal percentages of TOrCs (cf. Chapter 4), the TAN algorithm applied in this study provides probabilistic associations between attributes and target scavengers in partitioned ranges (five bins representing discretized data) as a visualized graph model. With an additional evidence sensitivity analysis, more detailed insights into the relation of attributes and target parameters could be enabled considering the impact of individual discrete states of the attributes on the target scavenger. In short, at real-time attribute values, the model outputs a range of scavenger concentrations that is most likely to occur based on previous system operation modes. Consequently, the model developed in *Paper VI* could be applied to predict real-time scavenger concentrations at Munich II based on monitoring procedures that are already implemented. However, machine-learning techniques are based on probabilistic associations instead of causality and thus must be combined with expert knowledge to be reliable. As an example, highest nitrite concentrations were revealed to be vastly associated with high recirculation flow rates and moderately associated to methanol dosage, while the model also stated dependencies between mid-range nitrite concentrations and flow rates of UV disinfection channel 5. The latter can be neglected since nitrite formation by nitrate photolysis is negligible with LP-UV lamps at a fluence of $45\,\mathrm{mJ/cm^2}$. The model therefore needs to be readjusted by expert knowledge. Interestingly, methanol dose exhibits contradictory results since high methanol dose is associated with high nitrite concentrations, while in practice, methanol is dosed to improve nitrate removal in the granular media filters. Nitrite formation in the granular media filter is probably related to stoichiometry between nitrate and methanol (Böhm, 2002). Nitrite mitigation could thus be addressed in Munich II by e.g. adjusting recirculation flow rates. The model developed in this study is consequently not only applicable for scavenging prediction as a software sensor, but also provides the first knowledge discovery tool for WWTPs enabling deeper process insights which might reveal unforeseen parameter associations.

Both, data driven machine-learning models for scavenger prediction and kinetic models for TOrC removal prediction were presented in this dissertation as promising methods supporting AOP control systems. Especially the combination of these models could result in a resilient AOP control system that dynamically adapts system parameters (fluence and radical promoter dose) to water matrix changes meeting oxidation targets. Apart from predicting scavenger concentrations, for a subsequent kinetic model, machine-learning approaches could also be applied to model TOrC removal performance during AOP operation, including surrogate and scavenger information. This holistic approach would cover uncertainties that are unavoidable in the application of kinetic or surrogate models, since both models include deviations that are based on experimental procedures.

Applicability testing needs to be carried out in further studies to confirm scavenger prediction accuracy and TAN model applicability in combination with kinetic models to control UV-AOPs. In addition, development of a holistic approach could be targeted in future investigations.

8.4 Final Remarks

The evidence from this dissertation suggests the general applicability of UV-AOPs for advanced oxidation of TOrCs in municipal wastewater effluent. UV/H_2O_2 proved effective in attenuating TOrCs over a wide range of photolytic and $\cdot OH$ reactivities exhibiting considerably high energy demands. However, pre-treatment of the AOP feed water and use of alternative radical promoters (i.e., peroxodisulfate, chlorine) displayed potential to improve UV-AOP efficiency. Since oxidation process efficiency generally relies on radical scavenger concentrations, a water matrix-coupled process control is a reasonable solution which can be approached by surrogate, kinetic or data-driven machine-learning models. Future research should be conducted to evaluate other alternative radical promoters and investigate the applicability of dynamic AOP control applying the above-mentioned approaches. Finally, OBP formation potential and overall ecotoxicity assessment should be studied further to allow a more comprehensive assessment of UV/PDS and UV/Chlorine application in municipal wastewater effluents.

9. Supplemental Information

9.1 List of Publications

9.1.1 Topic Related Peer-Reviewed Journal Articles

Paper I: Miklos, D.B.; Remy, C.; Jekel, M.; Linden, K.G.; Drewes, J.E.; Hübner, U. (2018). Evaluation of advanced oxidation processes for water and wastewater treatment – A critical review. Water Research 139, 118–131.
Author contribution:
Miklos, D.B. (55%); Remy, C. (20%); Jekel, M. (5%); Linden, K.G. (5%); Drewes, J.E. (5%); Hübner, U. (10%)

Paper II: Miklos, D.B.; Hartl, R.; Michel, P.; Linden, K.G.; Drewes, J.E.; Hübner, U. (2018). UV/H_2O_2 process stability and pilot-scale validation for trace organic chemical removal from wastewater treatment plant effluents. Water Research 136, 169–179.
Author contribution:
Miklos, D.B. (60%); Hartl, R. (10%); Michel, P. (10%); Linden, K.G. (5%); Drewes, J.E. (5%); Hübner, U. (10%)

Paper III: Nihemaiti, M.; **Miklos, D.B**.; Hübner, U.; Linden, K.G.; Drewes, J.E.; Croué, J.-P. (2018). Removal of Trace Organic Contaminants in Wastewater Effluent by UV/H_2O_2 and UV/PDS. Water Research 145, 487–497.
Author contribution:
Nihemaiti, M. (60%); Miklos, D.B. (20%); Hübner, U. (5%); Linden, K.G. (5%); Drewes, J.E. (5%); Croué, J.-P. (5%)

Paper IV: Miklos, D.B.; Wang, W.-L.; Linden, K.G.; Drewes, J.E.; Hübner, U. (2018). Comparison of UV-AOPs (UV/H_2O_2, UV/PDS and UV/Chlorine) for TOrC removal and surrogate model evaluation. Submitted to Chemical Engineering Journal (under review).
Author contribution:
Miklos, D.B. (70%); Wang, W.-L. (15%); Linden, K.G. (5%); Drewes, J.E. (5%); Hübner, U. (5%)

Paper V: Ulliman, S.; **Miklos, D.B.**; Drewes, J.E.; Hübner, U.; Linden, K.G. (2018). Evaluation of pretreatment technologies for improved UV/H_2O_2 performance in municipal wastewater. Environmental Science: Water Research & Technology 4, 1321-1330.
Author contribution:
Ulliman, S. (70%); Miklos, D.B. (15%); Drewes, J.E. (5%); Hübner, U. (5%); Linden, K.G. (5%)

Paper VI: Michel P., Ortega G., **Miklos D.B.**, Khan S.J., Drewes J.E. (2018). Benchmarking data driven machine-learning algorithms for advanced wastewater treatment to predict a wastewater matrix by real data. (in progress)
Targeted journal: Environmental Science and Modelling

9.1.2 Conference Contributions and Posters

International contributions

Miklos, D.B.; Wang, W.-L.; Linden, K.G.; Drewes, J.E.; Hübner U. (2018). UV-LED based water disinfection: Characterization and irradiance measurement of lab-scale LED irradiation systems. International Conference on UV-LED Technologies & Applications (ICULTA 2018), April 22.-24. 2018, Berlin.

Fajnorová S., Hübner U., Herzog B., Müller J., Hellauer K., **Miklos D.B.**, Drewes J.E., Wanner J. (2018). Fate of antibiotic resistance during advanced wastewater treatment. Conference proceedings from: Vodárenská biologie (Water Supply Biology), February 6.-7. 2018, 53-60, Prague.

Miklos, D.B.; Hartl, Rebecca; Michel, Philipp; Kletke, Thomas; Linden, Karl G.; Drewes, Jörg. E.; Hübner, Uwe (2017). UV/H_2O_2 pilot-scale process validation and process stability evaluation for trace organic chemical removal from WWTP effluents. IUVA World Congress, September 18.-20. 2017, Dubrovnik.

Wang, W.-L.; **Miklos, D.B.**; Hu, H.-Y.; Linden, K.G.; Drewes, J.E.; Hübner, U. (2017). Degradation of trace organic chemicals by LED-UV/chlorine: synergistic effects. IUVA World Congress, September 18.-20. 2017, Dubrovnik.

Hübner, U., **Miklos, D.B.,** Müller, J., Fajnarova, S., Herzog, B., Drewes, J.E (2017). Evaluation of alternative concepts for removal of trace organic chemicals from secondary effluents. IWA 10th Micropol & Ecohazard Conference, 17.-20. September 2017, Vienna.

Miklos, D.B.; Hübner, U.; Remy, C.; Jekel, M.; Drewes, J.E. (2016). The OH radical Exposure Concept as a Promising Assessment Tool to Compare Advanced Oxidation Processes (AOPs). IUVA World Congress & Exhibition, February 28. – March 2. 2016, Vancouver, BC, Canada.

German contributions

Miklos, D.B., Hartl, R.; Kletke, T.; Hübner, U.; Drewes, J.E. (2017). Entfernung anthropogener Spurenstoffe mittels UV/H2O2 aus dem Kläranlagenablauf der Großkläranlage Gut Marienhof (München II) - eine Pilotstudie. Jahrestagung der Wasserchemischen Gesellschaft, Wasser 2017, 22.-24. Mai 2017. Donaueschingen.

Miklos, D.B.; Eitzen, L.; Hübner, U.; Drewes, J.E. (2016). Entfernung anthropogener Spurenstoffe durch weitergehende Oxidationsverfahren: Die Hydroxyl-Radikalexposition als neues Vergleichskonzept für AOPs. Jahrestagung der Wasserchemischen Gesellschaft, Wasser 2016, 2.-4. Mai. Bamberg.

9.2 SI for Paper I

Table S1: References for the data illustrated in Figure 4.

AOP Process	References
O_3/H_2O_2	(Müller, 1998; Safarzadeh-Amiri, 2001; Sutherland et al., 2004; Westerhoff et al., 2009; Katsoyiannis et al., 2011; Lester et al., 2011; Sarkar et al., 2014)
O_3/UV	(Leitzke, 1992; Müller, 1998; Müller et al., 2001; Müller and Jekel, 2001; Alaton et al., 2002; Sona et al., 2006; Lester et al., 2011; Pisarenko et al., 2012; Sarkar et al., 2014)
UV/H_2O_2	(Festger et al; Welshans et al., 1990; EPA, 1993; Giggy, C., Winkler, H., 1993; EPA, 1994; Müller, 1998; Cater et al., 2000; Müller et al., 2001; Müller and Jekel, 2001; Safarzadeh-Amiri, 2001; Alaton et al., 2002; Kruithof et al., 2002; Sutherland et al., 2004; Tuhkanen, 2004; Kruithof et al., 2005; Rosenfeldt et al., 2005; Kusic et al., 2006; Sona et al., 2006; Toor and Mohseni, 2007; Olmez-Hanci et al., 2009; Yasar and Tabinda, 2010; Hofman-Caris, C.H.M., Beerendonk, E.F., 2011; Katsoyiannis et al., 2011; Sichel et al., 2011; Hansen and Andersen, 2012; Liu et al., 2012; Zoschke et al., 2012; Shu et al., 2013; Ureña de Vivanco et al., 2013; Sarkar et al., 2014; Wang, 2015; Xiao et al., 2016)
UV-Catalyst	(Bolton et al., 1998; Mills and Lee, 2004; Daneshvar et al., 2005; Martínez et al., 2013; Shirzad-Siboni et al., 2014; Mohagheghian et al., 2015; Vishnuganth et al., 2016)
UV/PDS	(Anipsitakis, 2005; Lin and Wu, 2014; Gao et al., 2015; Xiao et al., 2016; Tan et al., 2017)
UV/Chlorine	(Festger et al; Wang, 2015)
Photo-Fenton	(Safarzadeh-Amiri, 2001; Ureña de Vivanco et al., 2013)
Ultrasound	(Kalumuck and Chahine, 2000; Goel et al., 2004; Mahamuni and Adewuyi, 2010; Behnajady and Vahid, 2016)
eAOP	(Bewersdorf, 2005; Malpass et al., 2008; Zhuo et al., 2011; Niu et al., 2012; Lin et al., 2013; Ureña de Vivanco et al., 2013; Vahid and Khataee, 2013; Abdessamad et al., 2015; Escudero et al., 2016; Niu et al., 2016; Armijos-Alcocer et al., 2017; Benito et al., 2017)
Plasma	(Even-Ezra et al., 2009; Gerrity et al., 2010)
Electron Beam	(Bolton et al., 1998; Cooper et al., 2004; Kim et al., 2012)
Micro wave	(Karthikeyan and Gopalakrishnan, 2011)
Ozone	(Baus et al., 2008; Pisarenko et al., 2012)

9.2.1 Influence of compound reactivity

Figure S1: Reviewed compound specific E_{EO} values for UV/H_2O_2 in drinking water illustrated over respective second order rate constants k_{OH} (n=44).

9.2.2 Influence of dissolved organic carbon
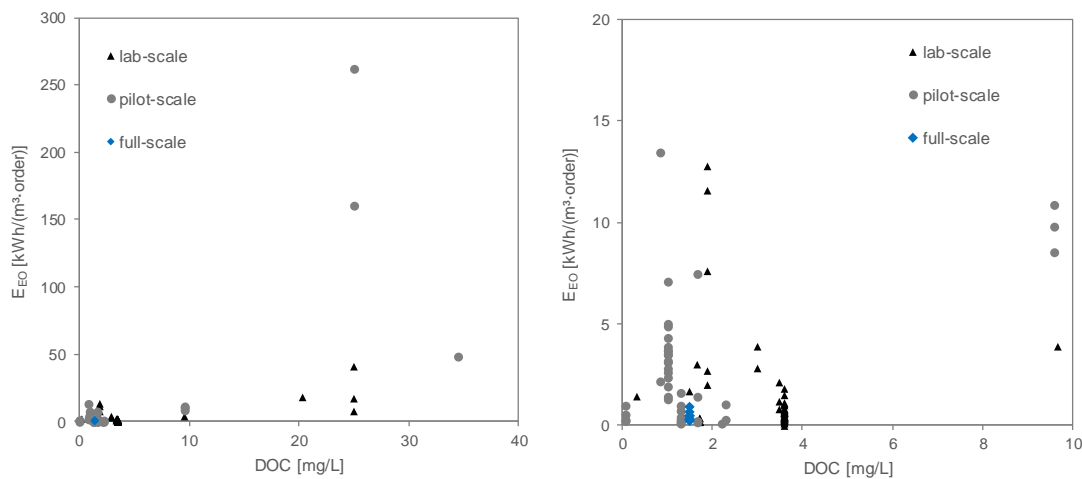
Figure S2: Reviewed compound specific E_{EO} values for UV/H_2O_2 in drinking water illustrated over DOC concentrations on different scales (n=124).

9.2.3 *Influence of UV transmittance and turbidity*
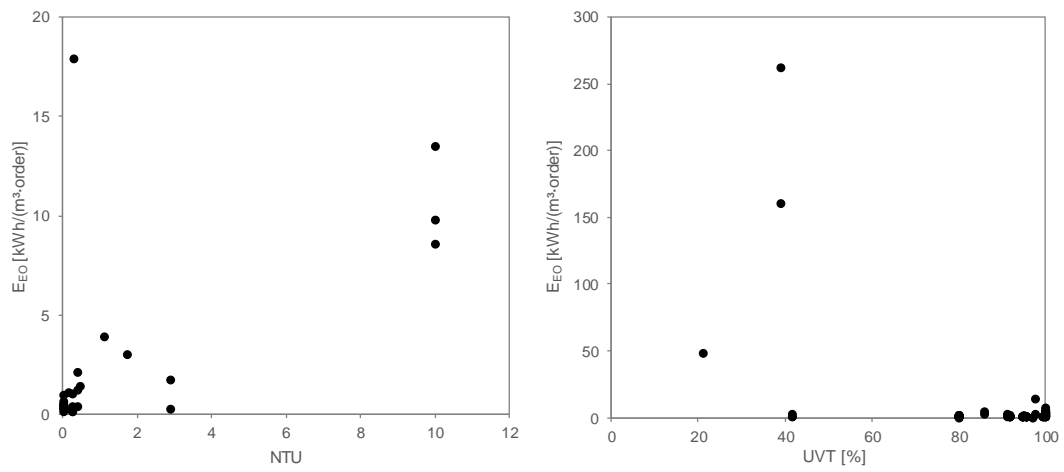
Figure S3: Reviewed E_{EO} values for UV/H_2O_2 illustrated over UV transmittance (n=116) and NTU (n=31).

9.3 SI for Paper II

Table S2: Observed first-order rate constants (k_{app}) in lab- and pilot-scale with 0 and 10 mg H_2O_2/L, respective R^2 values and calculated ratio for $k_{app,pp}/k_{app,CBD}$.

Substance	H_2O_2 [mg/l]	Pilot plant k_{obs} ($\cdot 10^{-4}$ cm²/mJ)	R^2	Collimated beam device k_{obs} ($\cdot 10^{-4}$ cm²/mJ)	R^2	Ratio $k_{app,pp}/k_{app,CBD}$
Benzotriazole	0	7.32	0.98	1.98	0.93	3.7
	10	11.7	0.99	6.5	0.99	1.8
Carbamazepine	0	0.52	0.66	-	-	
	10	6.02	0.98	6.06	0.97	1.0
Citalopram	0	1.39	0.95	2.11	0.89	0.7
	10	8.5	0.99	7.14	0.99	1.2
Climbazole	0	3.53	0.98	4.78	0.97	0.7
	10	8.14	0.99	8.93	0.98	0.9
Diclofenac	0	48.6	0.98	67.3	0.99	0.7
	10	53.3	0.98	74.8	0.999	0.7
Gabapentin	0	0.08	0.11	-	-	
	10	3.29	0.98	3.14	0.97	1.0
Iopromide	0	29.2	0.98	24.6	0.99	1.2
	10	25.7	0.98	28	0.98	0.9
Metoprolol	0	1.02	0.94	1	0.62	1.0
	10	7.97	0.99	6.05	0.98	1.3
Primidone	0	-	-	0.47	0.75	
	10	4.77	0.97	4.44	0.98	1.1
Sotalol	0	16.8	0.8	3.48	0.8	4.8
	10	5.97	0.95	20.5	0.96	0.3
Sulfamethoxazole	0	18.9	0.93	14.1	0.99	1.3
	10	16.7	0.93	13.3	0.99	1.3
Tramadol	0	5.47	0.11	3.62	0.97	1.5
	10	9.69	0.99	8.57	0.99	1.1
Venlafaxine	0	1.77	0.97	1.52	0.55	1.2
	10	7.5	0.99	6.73	0.91	1.1
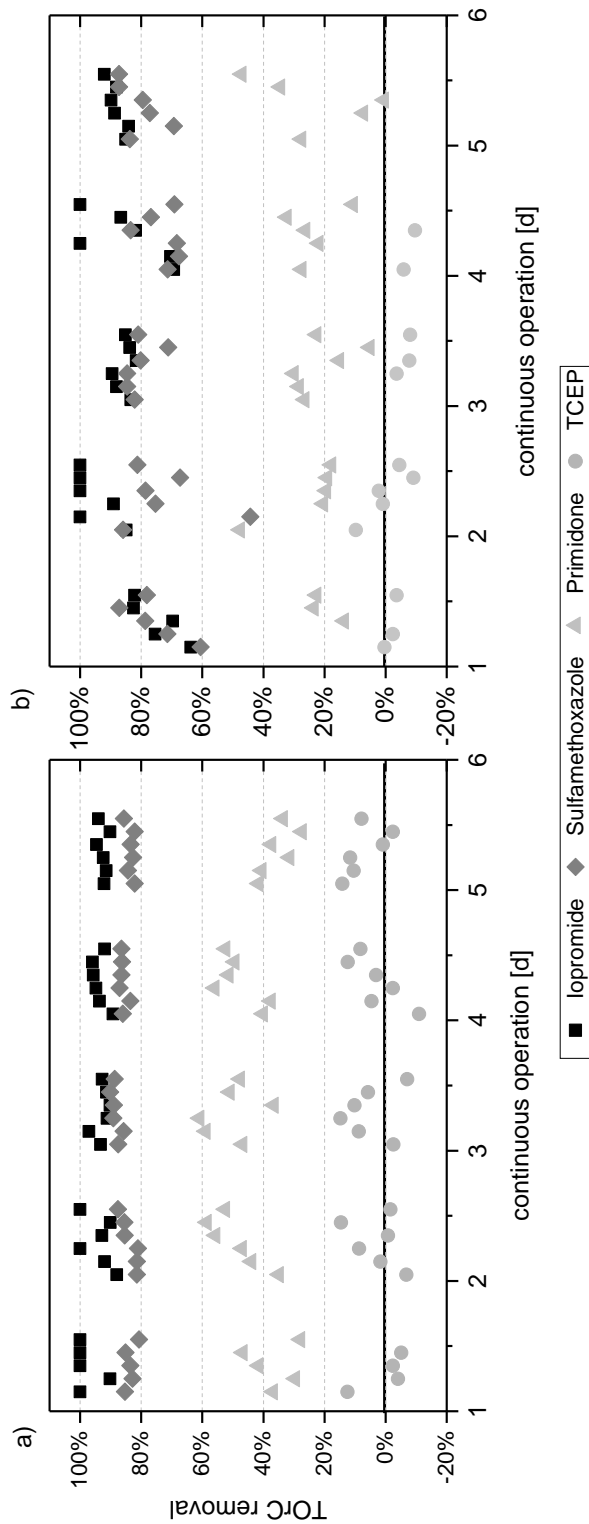
Figure S4: Oxidative removal of iopromide, sulfamethoxazole, primidone and TCEP from WWTP effluent during continuous operation in pilot-scale UV/H$_2$O$_2$ process during dry weather (a) and rain-event (b). Application of constant process parameters at 800 mJ/cm² and 10 mg/L H$_2$O$_2$.

LBX 10

$$y = -8.0742x^3 + 18.173x^2 - 13.361x + 5.189$$

LBXe 90

$$y = -23.022x^3 + 51.628x^2 - 39.275x + 12.532$$
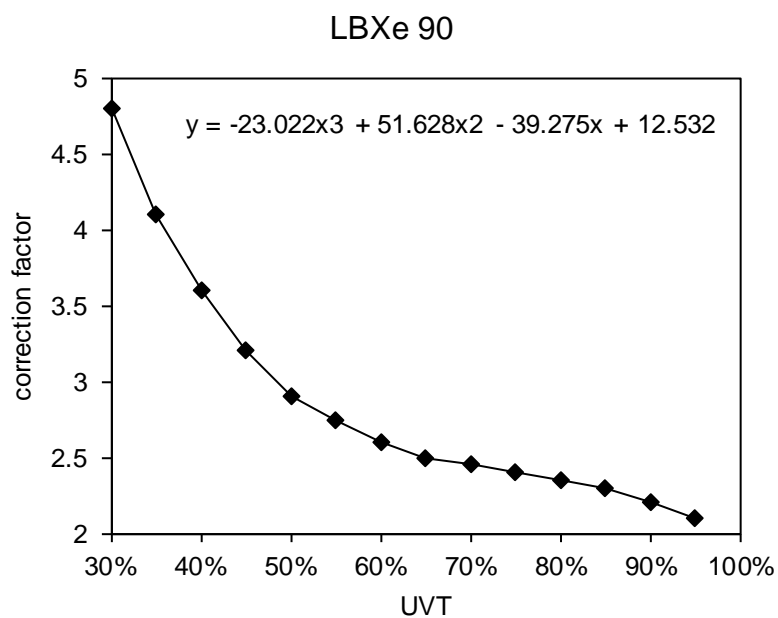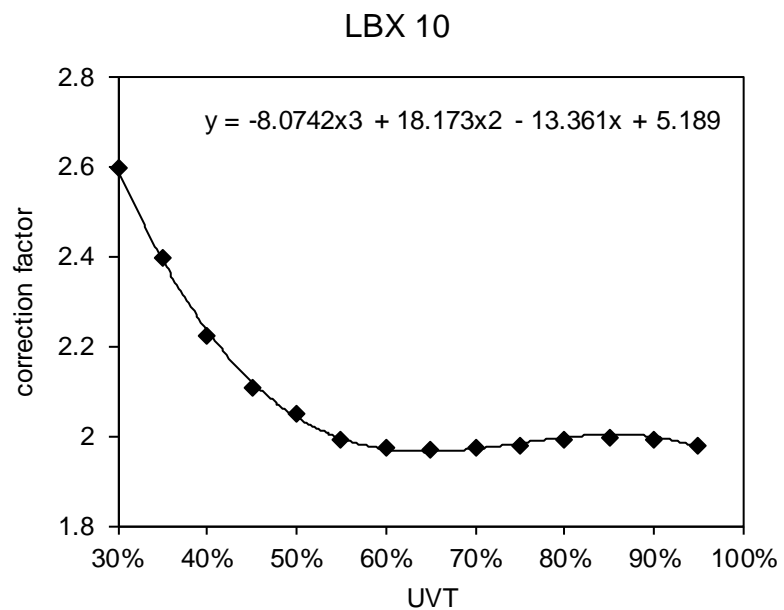
Figure S5: UVT-based intensity correction factors for measured UV intensity in respective reactors provided by WEDECO (Xylem).

Modeling was obtained by combining equation 13 and 14 in equation 15:

$$\int OH\, dt = 2 \ln(10) \frac{\varepsilon_{H2O2} * \Phi_{H2O2}}{U_{254}} * c_{H2O2} * F' * \frac{1}{\sum(c_i * k_{OH,i}) + k_{H2O2} * c_{H2O2}} \quad (19)$$

This equation was used to calculate °OH exposure in Figure 13

9.4 SI for Paper III

Table S3: TOrCs investigated in this study

TOrCs	CAS Number	Purity	Source	Product Number
Benzotriazole	95-14-7	99.8%	Cimachem	BTA-99
Caffeine	58-08-2	> 99%	Sigma Aldrich	C7050
Carbamazepine	298-46-4	>98%	Sigma Aldrich	C4024
Diclofenac	15307-86-5	>99%	Caymanchem	70680
Gabapentin	60142-96-3	European Pharmacopoeia (EP) Reference Standard	Sigma Aldrich	Y0001280
Iopromide	73334-07-3	98.7%	Sigma Aldrich	Y0001020
Metoprolol	56392-17-7	>98%	Sigma Aldrich	M5391
Phenytoin	57-41-0	HPLC grade	Sigma Aldrich	PHR1139
Primidone	125-33-7	HPLC grade	Sigma Aldrich	P7295
Sulfamethoxazole	723-46-6	HPLC grade	Sigma Aldrich	S7507
TCEP	51805-45-9	97%	Sigma Aldrich	119660
Venlafaxine	99300-78-4	>98% (HPLC)	Sigma Aldrich	V7264

Table S4: Reactions of the wastewater matrix with $^{\cdot}OH$ and $SO_4^{\cdot-}$

	Reactions	Rate constant	Reference
1	$^{\cdot}OH + EfOM \rightarrow products$	$3.3 \cdot 10^4 \, (mg\text{-}C/L)^{-1} \, s^{-1}$	Yang et al., 2016b
2	$SO_4^{\cdot-} + EfOM \rightarrow products$	$9.4 \cdot 10^3 \, (mg\text{-}C/L)^{-1} \, s^{-1}$	Yang et al., 2016b
3	$^{\cdot}OH + HCO_3^- \rightarrow CO_3^{\cdot-} + H_2O$	$8.6 \cdot 10^6 \, M^{-1} \, s^{-1}$	Buxton et al., 1988
4	$SO_4^{\cdot-} + HCO_3^- \rightarrow CO_3^{\cdot-} + HSO_4^-$	$2.8 \cdot 10^6 \, M^{-1} \, s^{-1}$	Huie and Clifton, 1990
5	$^{\cdot}OH + NO_2^- \rightarrow {^{\cdot}NO_2} + OH^-$	$1.0 \cdot 10^{10} \, M^{-1} \, s^{-1}$	Coddington et al., 1999
6	$SO_4^{\cdot-} + NO_2^- \rightarrow {^{\cdot}NO_2} + SO_4^{2-}$	$8.8 \cdot 10^8 \, M^{-1} \, s^{-1}$	Neta et al., 1988
7	$^{\cdot}OH + NO_3^- \rightarrow products$	$<1 \cdot 10^5 \, M^{-1} \, s^{-1}$	Keen et al., 2012
8	$SO_4^{\cdot-} + NO_3^- \rightarrow NO_3^{\cdot} + SO_4^{2-}$	$3.0 \cdot 10^4 \, M^{-1} \, s^{-1}$	Buxton et al., 1988
9	$^{\cdot}OH + Cl^- \rightarrow ClOH^{\cdot-}$	$4.3 \cdot 10^9 \, M^{-1} \, s^{-1}$	Jayson et al., 1973
10	$ClOH^{\cdot-} \rightarrow {^{\cdot}OH} + Cl^-$	$6.1 \cdot 10^9 \, M^{-1} \, s^{-1}$	Jayson et al., 1973
11	$SO_4^{\cdot-} + Cl^- \rightarrow Cl^{\cdot} + SO_4^{2-}$	$3.0 \cdot 10^9 \, M^{-1} \, s^{-1}$	Das, 2001
12	$Cl^{\cdot} + Cl^- \rightarrow Cl_2^{\cdot-}$	$8.5 \cdot 10^9 \, M^{-1} \, s^{-1}$	Yu and Barker, 2003
13	$Cl^{\cdot} + HCO_3^- \rightarrow CO_3^{\cdot-} + Cl^- + H^+$	$2.2 \cdot 10^8 \, M^{-1} \, s^{-1}$	Matthew and Anastasio, 2006
14	$Cl_2^{\cdot-} + HCO_3^- \rightarrow CO_3^{\cdot-} + 2Cl^- + H^+$	$8.0 \cdot 10^7 \, M^{-1} \, s^{-1}$	Matthew and Anastasio, 2006

Table S5: The scavenging capacity of the main water matrix components during buffered pure water experiments

Component	Concentration M	Second-order rate constants $(M^{-1} s^{-1})$		Scavenging capacity (s^{-1}) [a]	
		$k_{\bullet OH}$	$k_{SO_4^{\bullet-}}$	UV/H_2O_2	UV/PDS
HPO_4^{2-}	$2.5 \cdot 10^{-3}$	$1.5 \cdot 10^{5}$[b]	$1.2 \cdot 10^{6}$[c]	$3.8 \cdot 10^2$	$3.0 \cdot 10^3$
$H_2PO_4^-$	$2.5 \cdot 10^{-3}$	$2.0 \cdot 10^{4}$[b]	$5 \cdot 10^{4}$[c]	50.0	$1.3 \cdot 10^3$
H_2O_2	$1.5 \cdot 10^{-4}$	$2.7 \cdot 10^{7}$[c]	n.a.	$4.1 \cdot 10^3$	n.a.
PDS	$1.5 \cdot 10^{-4}$	n.a.	$6.5 \cdot 10^{5}$[c]	n.a.	97.5
TOrCs[d]	1 µg/L each	see Table 2[e]		$3.6 \cdot 10^2$	$1.5 \cdot 10^2$
SUM				$4.8 \cdot 10^3$	$3.4 \cdot 10^3$

[a] Calculated by multiplying the molar concentration of each component with its second-order reaction rate constants with radicals; [b] Crittenden et al. (1999); [c] Yang et al. (2016b); [d] Sum of the scavenging capacity of each TOrC; [e] The rate constants of TCEP and gabapentin with $SO_4^{\bullet-}$ were estimated to be $1.0 \cdot 10^9$ $M^{-1}s^{-1}$.

Table S6: Fluorescence EEM regions and the Excitation/Emission wavelengths of the selected peaks

Region[a]	Dissolved organic matter components	Selected peaks		
		Name	Excitation wavelength (nm)	Emission wavelength (nm)
II	aromatic proteins, tryptophan-like	P_II	242	358
III	Fulvic acid-like	P_III	242	430
IV	soluble microbial by-product-like	P_IV	287	353
V	Humic acid-like	P_V	329	412

[a] From Chen et al. (2003).

Table S7: HPLC-UV parameters[a] for the detection of *p*CBA and TOrCs

Compounds	Mobile phase	Flow rate (mL/min)	Wavelength (nm)
*p*CBA	60% Methanol+40% MQ (0.1% phosphoric acid)	1	238
phenytoin	50% Methanol+50% MQ (0.1% phosphoric acid)	1	230
caffeine	25% Methanol+75% MQ (0.1% phosphoric acid)	1	273
benzotriazole	25% Methanol+75% MQ (0.1% phosphoric acid)	1	273
primidone	25% Methanol+75% MQ (0.1% phosphoric acid)	1	218
metoprolol	30% Methanol+70% MQ (0.1% phosphoric acid)	1	225
venlafaxine	25% Acetonitrile+75% MQ (0.1% phosphoric acid)	1	225
carbamazepine	50% Methanol+50% MQ (0.1% phosphoric acid)	1	285
Iopromide	4% Acetonitrile+96% MQ (0.3% phosphoric acid)	1	238[b]

[a] Compounds were separated on a XDB-C18 column (5 μm, 4.6 ·150 mm, Agilent).

[b] The sum of the peak areas of 2 isomers were followed for quantification.

Text S1. Fluorescence excitation-emission matrix analysis

Fluorescence EEM were measured using an Aqualog Fluorescence Spectrometer (Horiba Scientific, Germany). Samples were filtered through 0.45 μm cellulose nitrate membrane filters (Sartorius, Germany) and measured using a 10 mm quartz cuvette. The fluorescence response of a blank solution (Milli-Q water) was subtracted from the EEM of each sample. The wastewater specific fluorescence signal was tested for linearity in a preliminary experiment using 5 dilutions with ultrapure water ranging from 2:1 to 10:1. Data processing included corrections using inner filter effects, Raman normalization, Rayleigh masking and diagram adjustments.

Four fluorescence peaks were selected from different regions on fluorescence spectra previously defined by Chen et al. (2003). The fluorescence intensities of selected peaks were used as representative indices of dissolved organic matter in wastewater to study the effect of radical exposure on effluent organic matter (EfOM) during UV/H$_2$O$_2$ and UV/PDS (Sgroi et al., 2017). The excitation and emission wavelengths of selected peaks are presented in Table S6.

Text S2. Second-order rate constants of TOrCs with SO$_4^{\cdot-}$

The second-order rate constants for the reaction of TOrCs with SO$_4^{\cdot-}$ were determined by competition kinetics based on the methods published before (Lutze et al., 2015; Lian et al., 2017). *para*-chlorobenzoic acid (*p*CBA) was used as a probe compound, K (SO$_4^{\cdot-}$ + *p*CBA) = 3.6 ·10^8 M^{-1}s^{-1} (Neta et al., 1977). Experiments were conducted in phosphate buffer (2.5 mM) at pH=7 with 20 μM of *p*CBA and target compound. SO$_4^{\cdot-}$ was generated by UV photolysis of PDS (1 mM). 10 mM of *tert*-Butanol was also added into the solution as the ·OH scavenger. For benzotriazole, iopromide and phenytoin, the degradation by direct photolysis was considered when calculating their second-order rate constants with SO$_4^{\cdot-}$. The concentrations of *p*CBA and TOrCs were followed analyzed by a HPLC (Agilent 1100) coupled with a DAD detector. Compounds were separated on a XDB-C18 column (5 μm, 4.6 ·150 mm, Agilent). Mobile phase composition followed various isocratic mixtures of methanol (or acetonitrile) and water (0.1% or 0.3% phosphoric acid). All compounds were analyzed on their maximum UV absorption. HPLC-UV parameters are listed in Table S7.

Text S3. Estimation of the second-order rate constants of gabapentin and TCEP with $SO_4^{\cdot-}$

The $K_{SO_4^{\cdot-}}$ values of gabapentin and TCEP were estimated based on the steady-state concentration of $SO_4^{\cdot-}$ (i.e., $[SO_4^{\cdot-}]_{ss}$) during UV/PDS treatment of TOrCs in pure water (Fluence=7.5-57.5 mJ/cm^2 and PDS=0.15 mM). Primidone was used to calculated $[SO_4^{\cdot-}]_{ss}$. The pseudo-first order degradation of a TOrC can be expressed as following:

$$-\frac{d[TOrC]}{dt} = K\ (TOrC + SO_4^{\bullet-})[TOrC][SO_4^{\bullet-}]_{ss} \qquad (S1)$$

$$ln\frac{[TOrC]_0}{[TOrC]} = K\ (TOrC + SO_4^{\bullet-})[SO_4^{\bullet-}]_{ss}t = k_{obs,TOrC}\ t \qquad (S2)$$

As shown in Figure S14, the k_{obs} of primidone, gabapentin and TCEP was 0.142 (s^{-1}), 0.106 (s^{-1}) and 0.005 (s^{-1}). The second-order rate constant of primidone with $SO_4^{\cdot-}$ is $5.29 \cdot 10^8$ (M^{-1}s^{-1}) (Table 8). Thus $[SO_4^{\cdot-}]_{ss}$ was calculated to be $2.6 \cdot 10^{-10}$ M. According to equation S2, the second-order rate constant of gabapentin and TCEP with $SO_4^{\cdot-}$ was calculated to be $4.1 \cdot 10^8$ (M^{-1}s^{-1}) and $1.92 \cdot 10^7$ (M^{-1}s^{-1}), which were lower than $1 \cdot 10^9$ (M^{-1}s^{-1}).
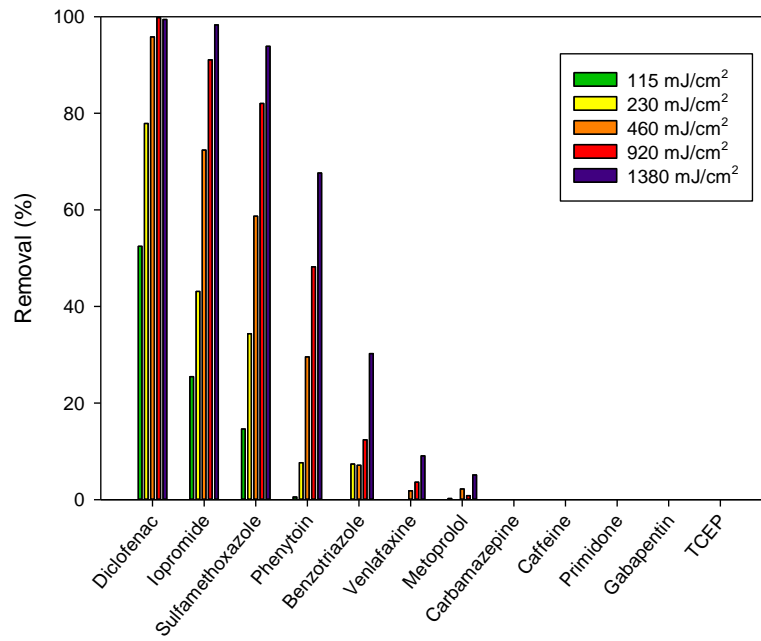
Figure S6: Percent removal of TOrCs in wastewater effluent by direct UV photolysis (Fluence=115–1,380 mJ/cm²)
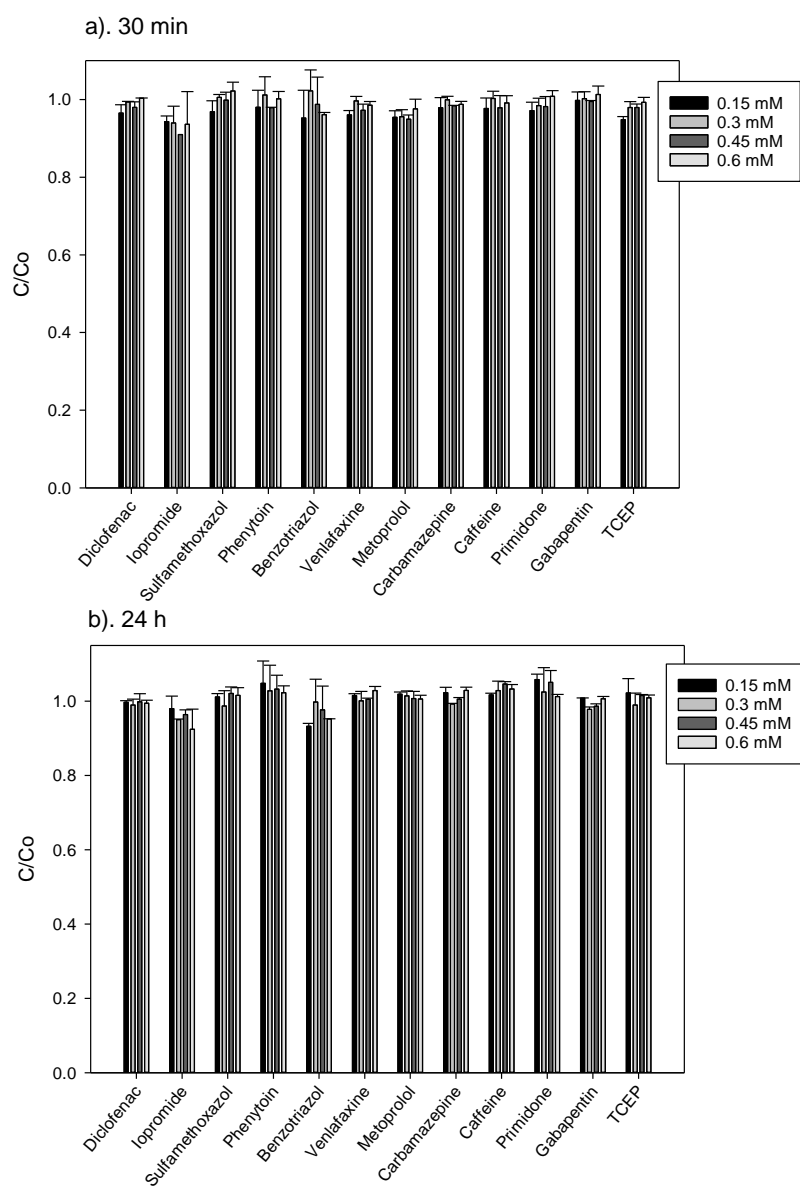
Figure S7: Effect of PDS on the removal of TOrCs in the dark within a) 30 min and b) 24 h of contact time (5 mM phosphate buffer, pH 7, PDS=0.15, 0.3, 0.45 and 0.6 mM)
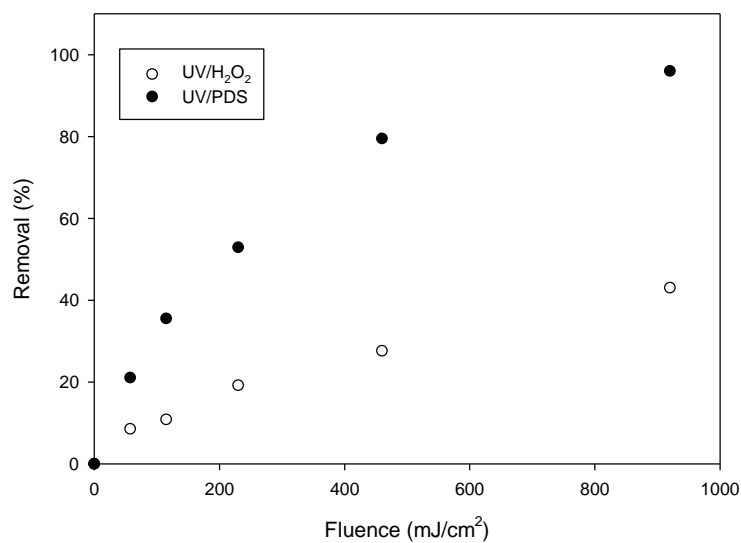
Figure S8: Relative removal of TCEP in pure water during UV/H$_2$O$_2$ and UV/PDS (pH=7, 5 mM phosphate buffer; oxidants=0.15 mM)
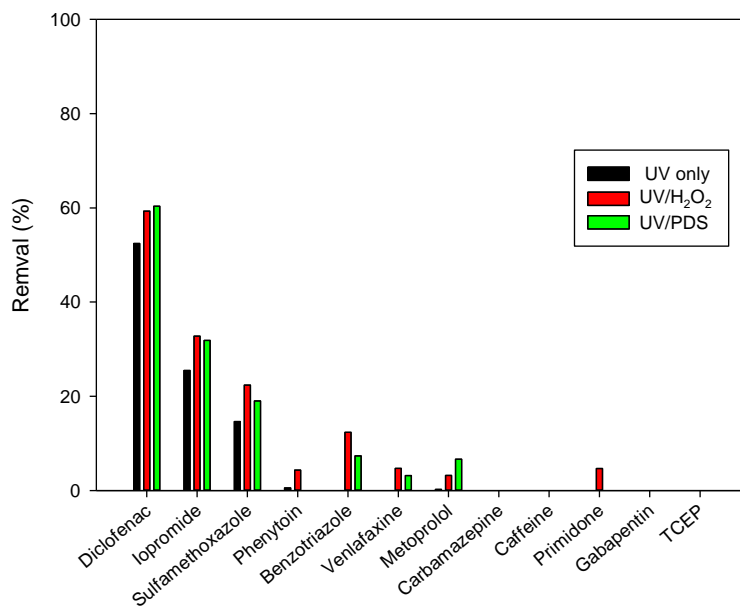
Figure S9: Relative removal of TOrCs in wastewater effluent during UV/H$_2$O$_2$ and UV/PDS (Fluence=115 mJ/cm²; Oxidant=0.15 mM).
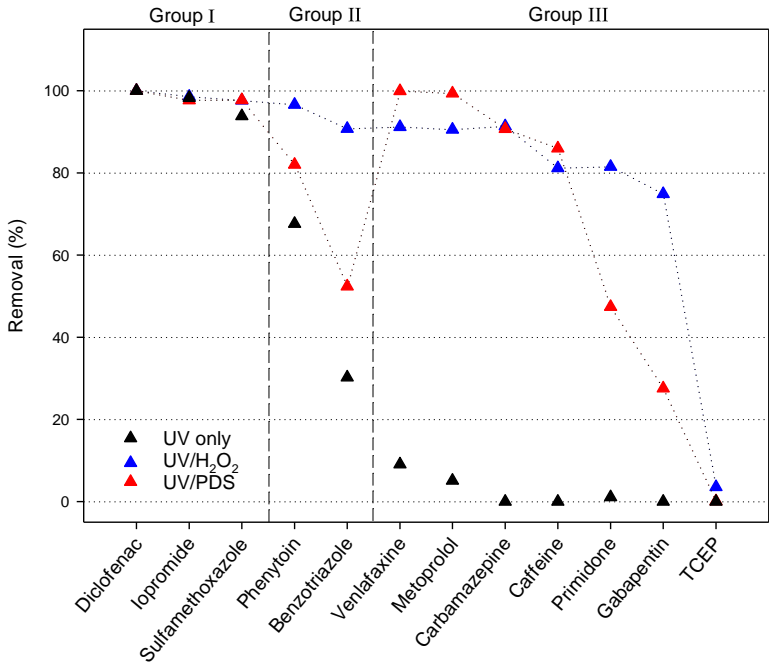
Figure S10: Percent removal of TOrCs in wastewater effluent during UV/H$_2$O$_2$ and UV/PDS (Fluence=1380 mJ/cm^2; Oxidant=0.6 mM).
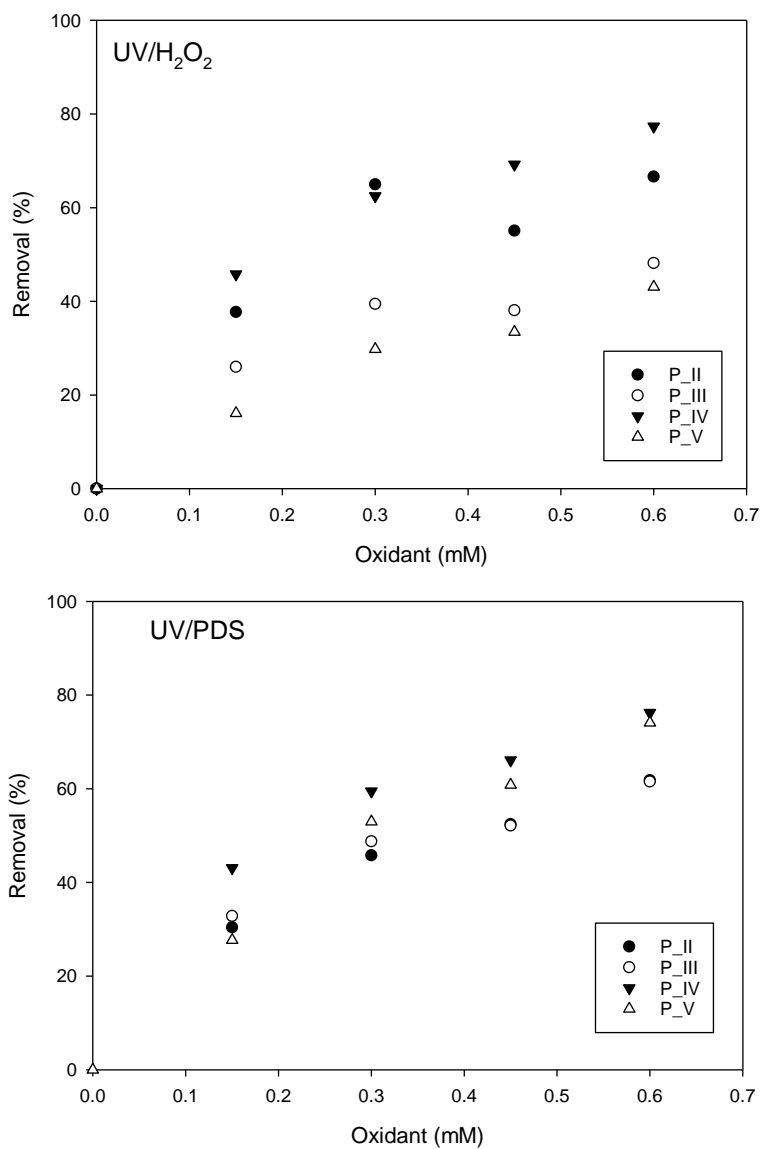
Figure S11: Relative removal of fluorescence intensities of selected peaks in wastewater effluent during UV/H$_2$O$_2$ and UV/PDS (Fluence =1,380 mJ/cm^2; Oxidant= 0.15, 0.3, 0.45 and 0.6 mM)

a). UV/H$_2$O$_2$
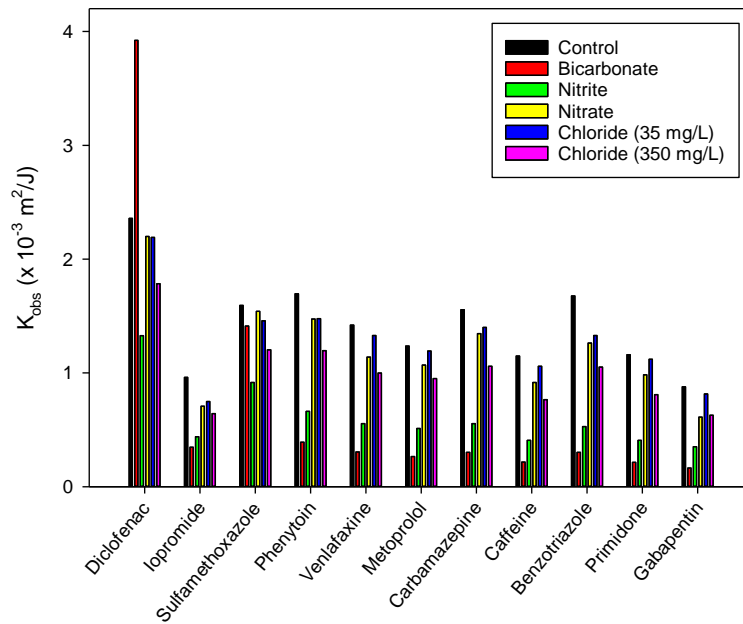
b). UV/PDS
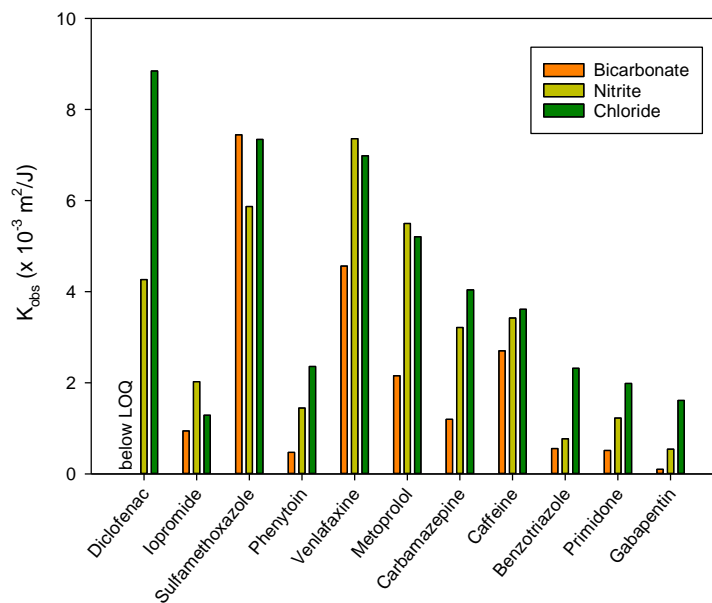
Figure S12: Effect of individual inorganic compounds on the efficiency of UV/H$_2$O$_2$ and UV/PDS processes in phosphate buffer at pH 7. Experimental conditions: Fluence= 57.5-920 mJ/cm^2; Oxidant=0.15 mM; Bicarbonate=300 mg/L; Nitrite=0.028 mg-N/L; Nitrate=10.6 mg-N/L; Chloride= 35 mg/L and 350 mg/L (The concentration of TOrCs were below LOQ during the control experiments as well as in the presence of nitrate and 35 mg/L of chloride during UV/PDS; the concentration of diclofenac was below LOQ during UV/PDS in the presence of bicarbonate).
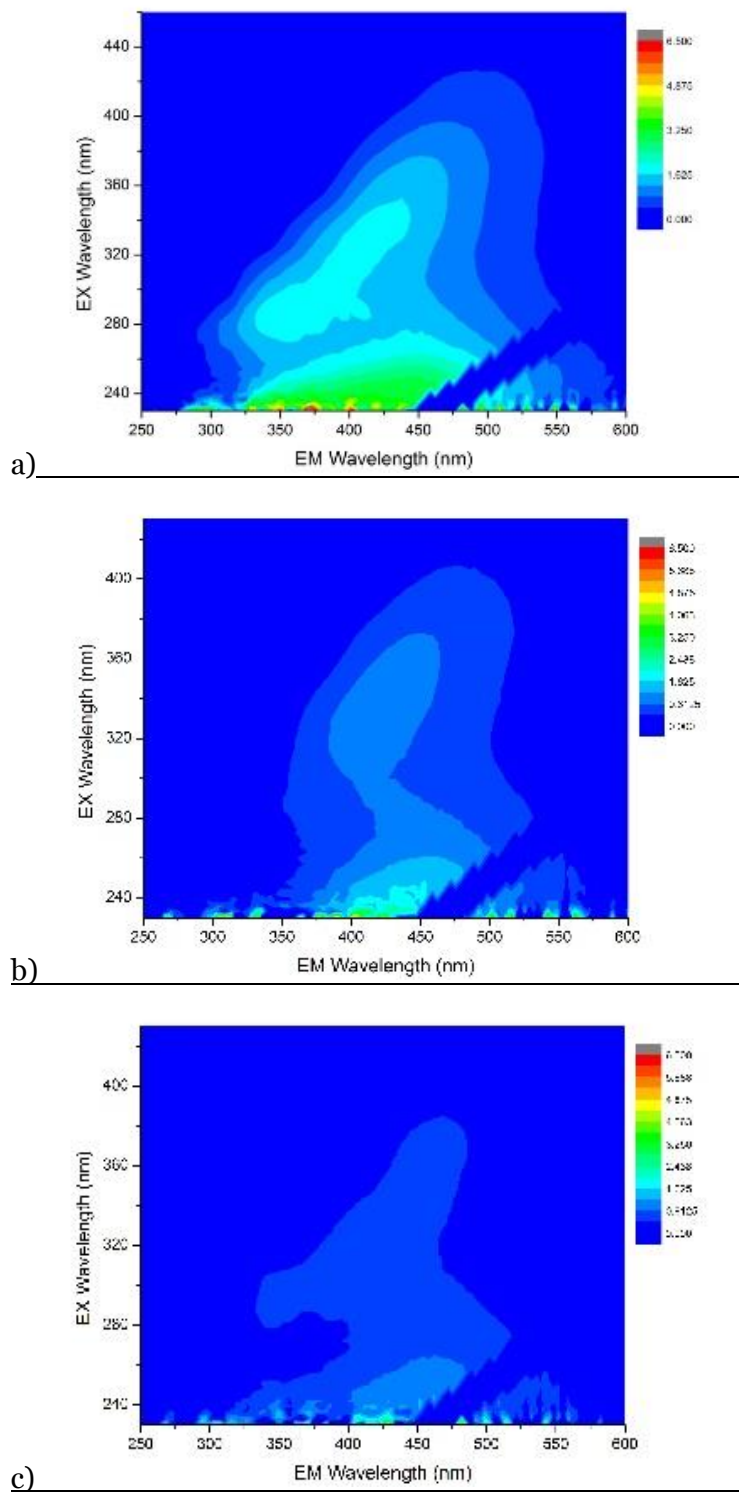
Figure S13: Fluorescence excitation–emission matrices (EEMs) of wastewater effluent before treatment (a), after UV/H$_2$O$_2$ (b) and UV/PDS (c) treatment. (Experimental conditions for UV/H$_2$O$_2$ and UV/PDS: oxidants=0.6 mM; fluence=1,380 mJ/cm^2)
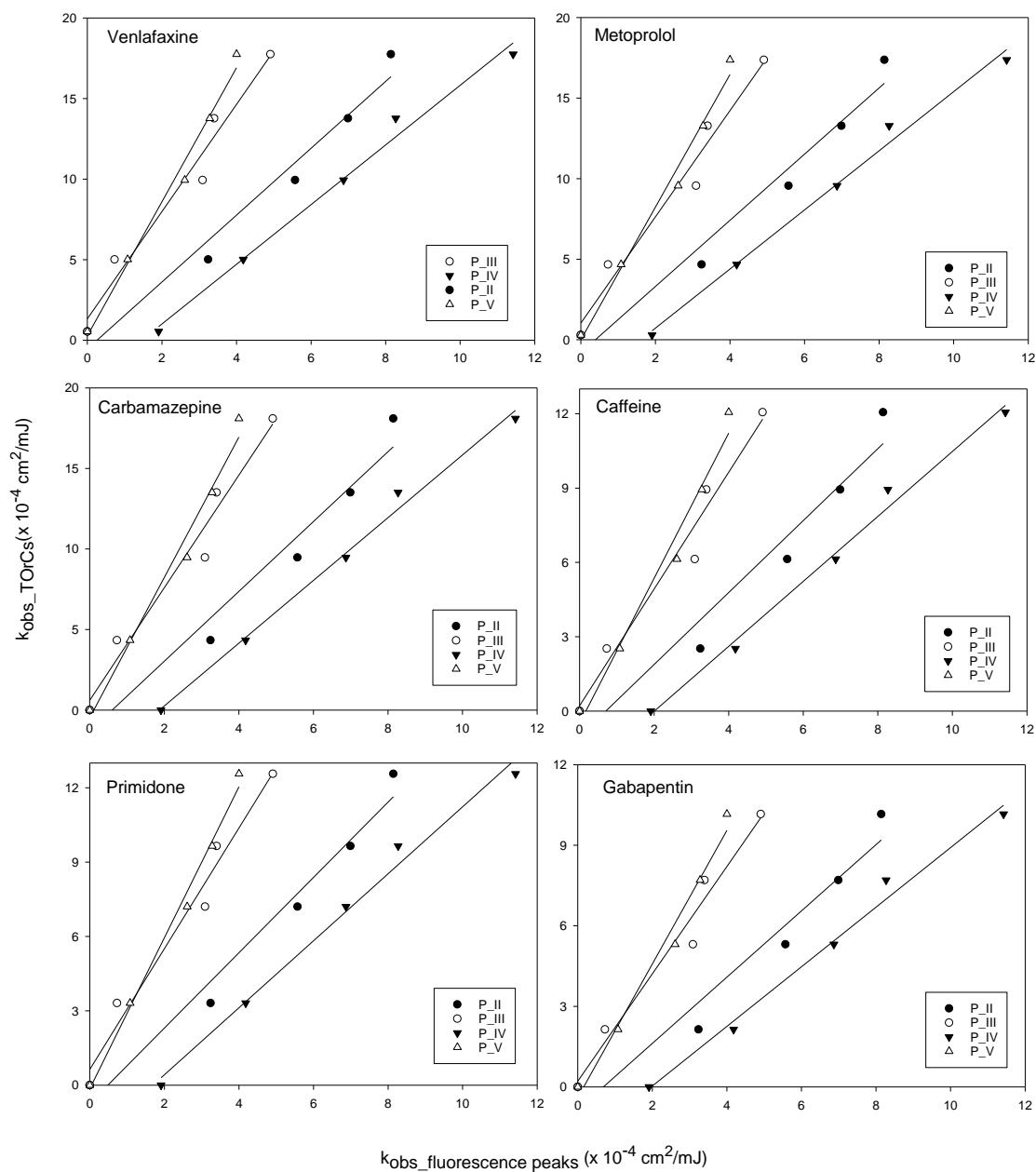
Figure S14: Correlations between the fluence-based rate constants of group III compounds (except TCEP) and selected fluorescence peaks during UV/H₂O₂ (Fluence=115–1,380 mJ/cm²; Oxidants = 0, 0.15, 0.3, 0.45 and 0.6 mM).
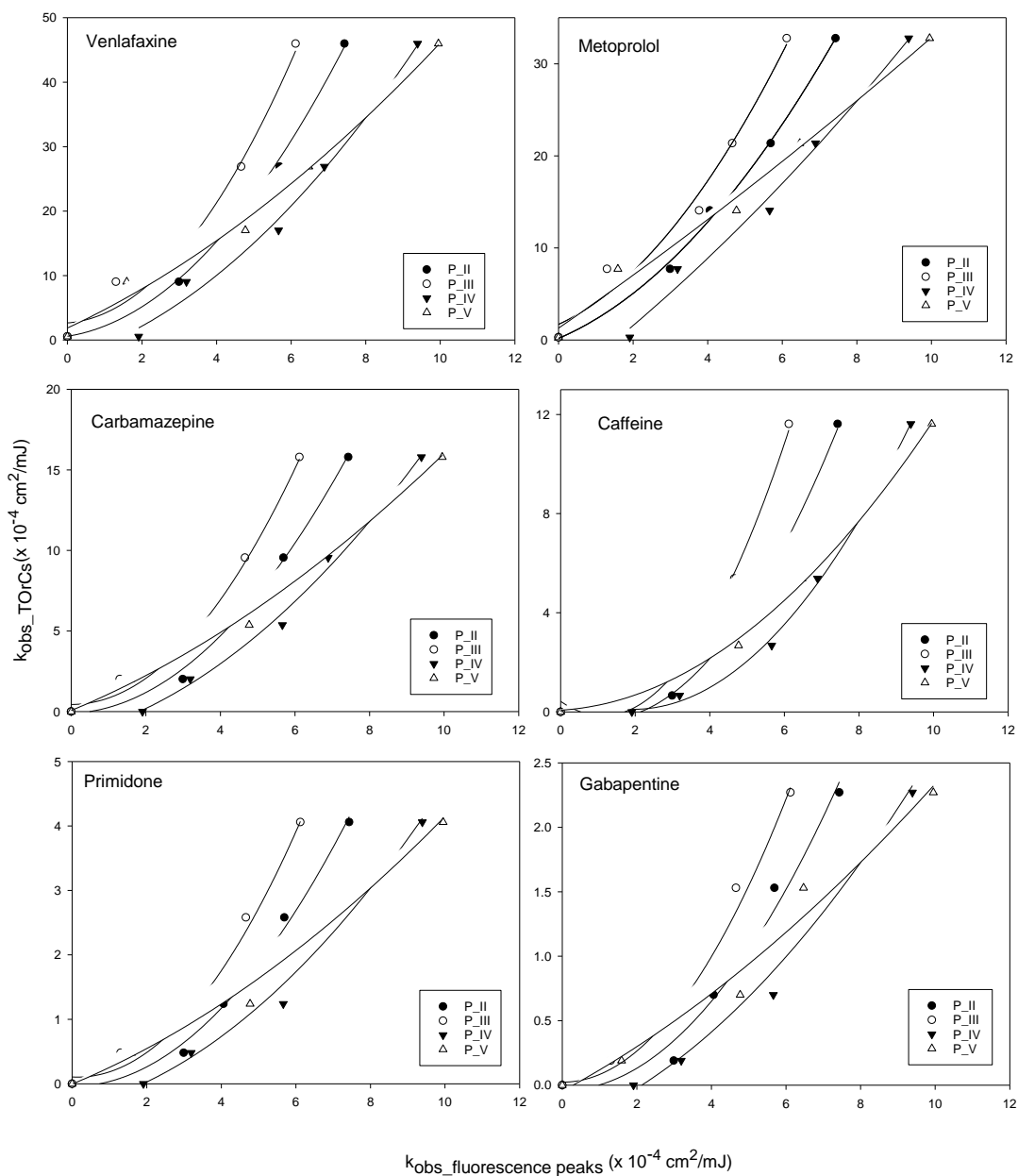
Figure S15: Correlations between the fluence-based rate constants of group III compounds (except TCEP) and selected fluorescence peaks during UV/PDS (Fluence=115–1,380 mJ/cm²; Oxidants = 0, 0.15, 0.3, 0.45 and 0.6 mM).
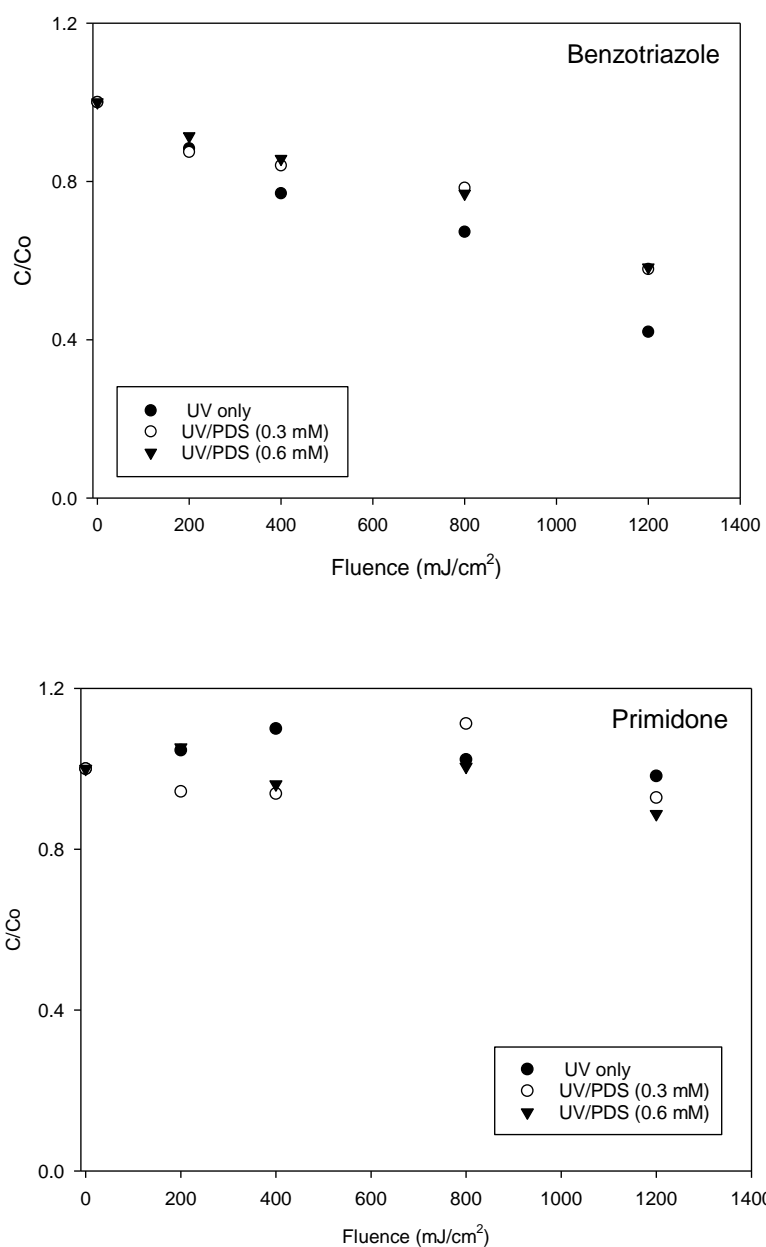
Figure S16: Relative removal of benzotriazole and primidone in pilot-scale experiments by direct photolysis and UV/PDS (PDS=0.3 and 0.6 mM)

a).
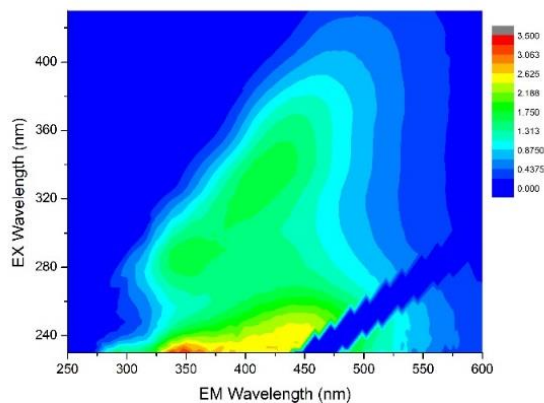
b).
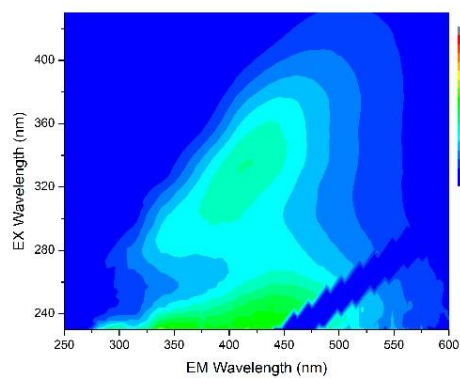
c).
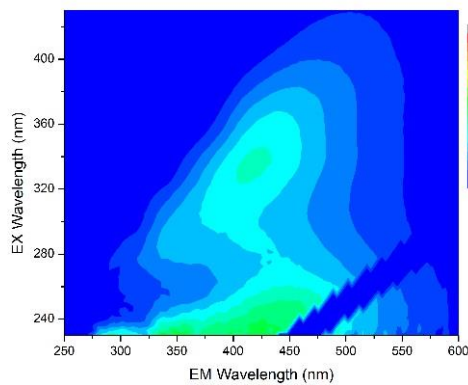
Figure S17: Fluorescence excitation−emission matrices (EEMs) of wastewater effluent before treatment (a) and after UV/PDS at 1,200 mJ/cm² (b. PDS= 0.3 mM; c. PDS=0.6 mM) in pilot scale experiments
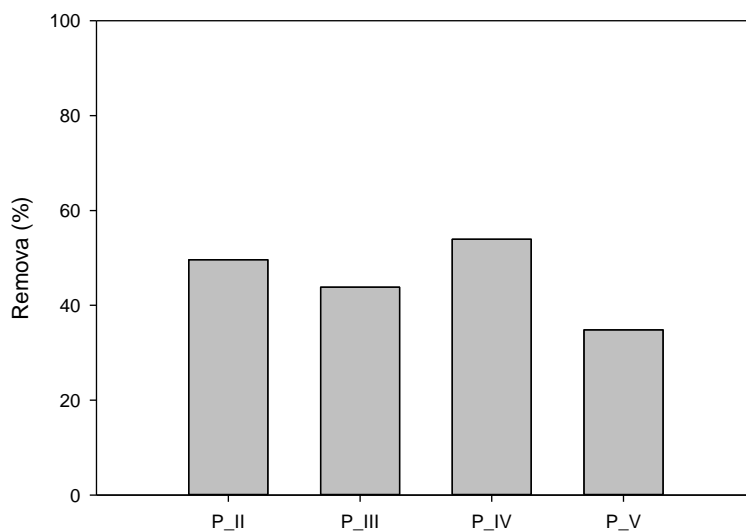
Figure S18: Relative removal of fluorescence intensities of selected peaks in wastewater effluent during UV/PDS pilot-tests (Fluence =1,200 mJ/cm²; Oxidant= 0.6 mM)
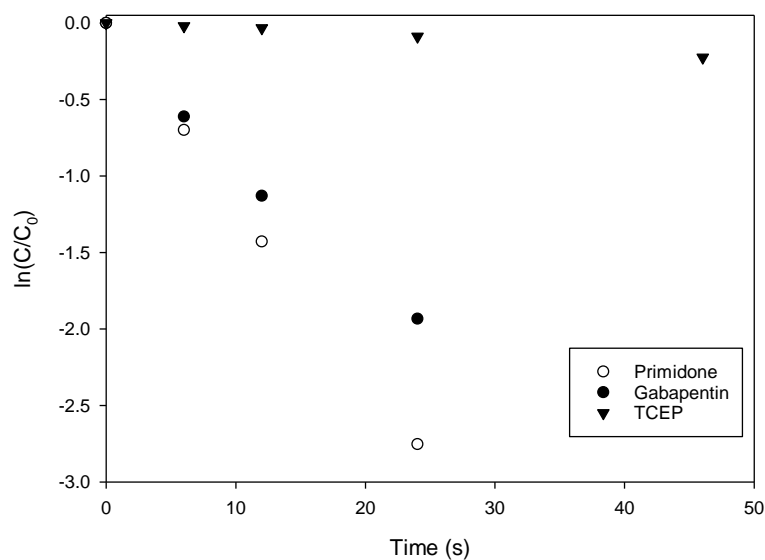
Figure S19: Pseudo-first order removal of primidone, gabapentin and TCEP during UV/PDS in ultrapure water at pH 6 (Fluence= 7.5-57.5 mJ/cm²; PDS= 0.15 mM)

9.5 SI for Paper IV

9.5.1   Supporting figures
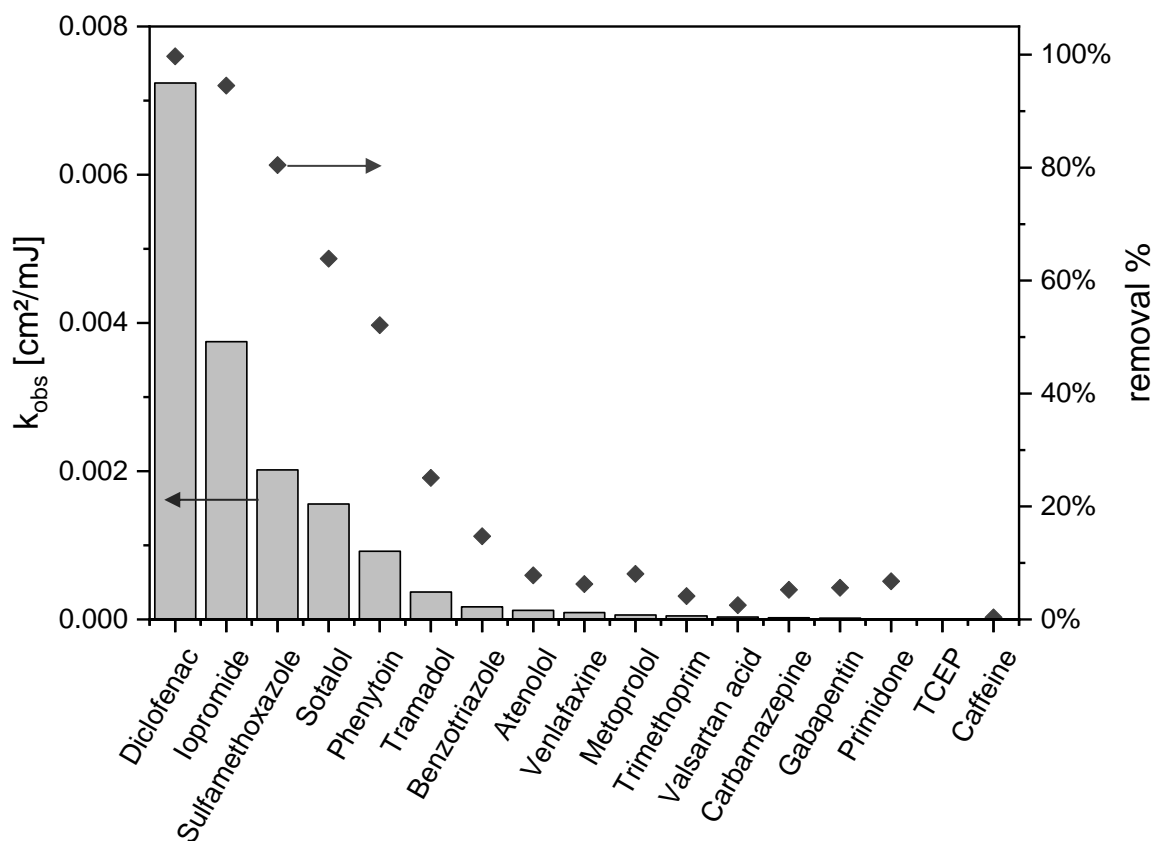
Figure S20: Observed reaction rate constant (grey bars) and % removal (diamonds) at 800 mJ/cm² by direct photolysis of target TOrCs in wastewater effluent (no addition of radical promoters).
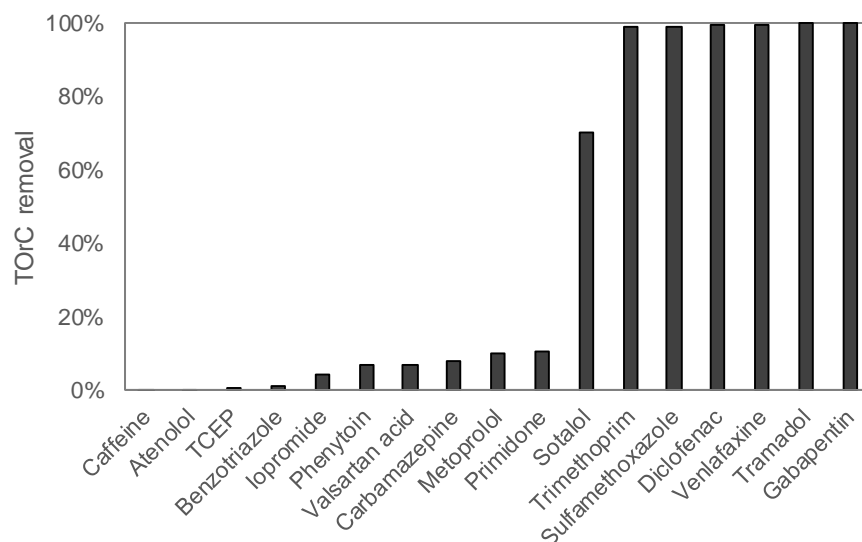
Figure S21: Direct oxidation of target TOrCs in wastewater effluent during dark chlorination (no UV-treatment) with 0.45 mM chlorine and an exposure time of 758 s for UV/Chlorine indicator TOrC determination.
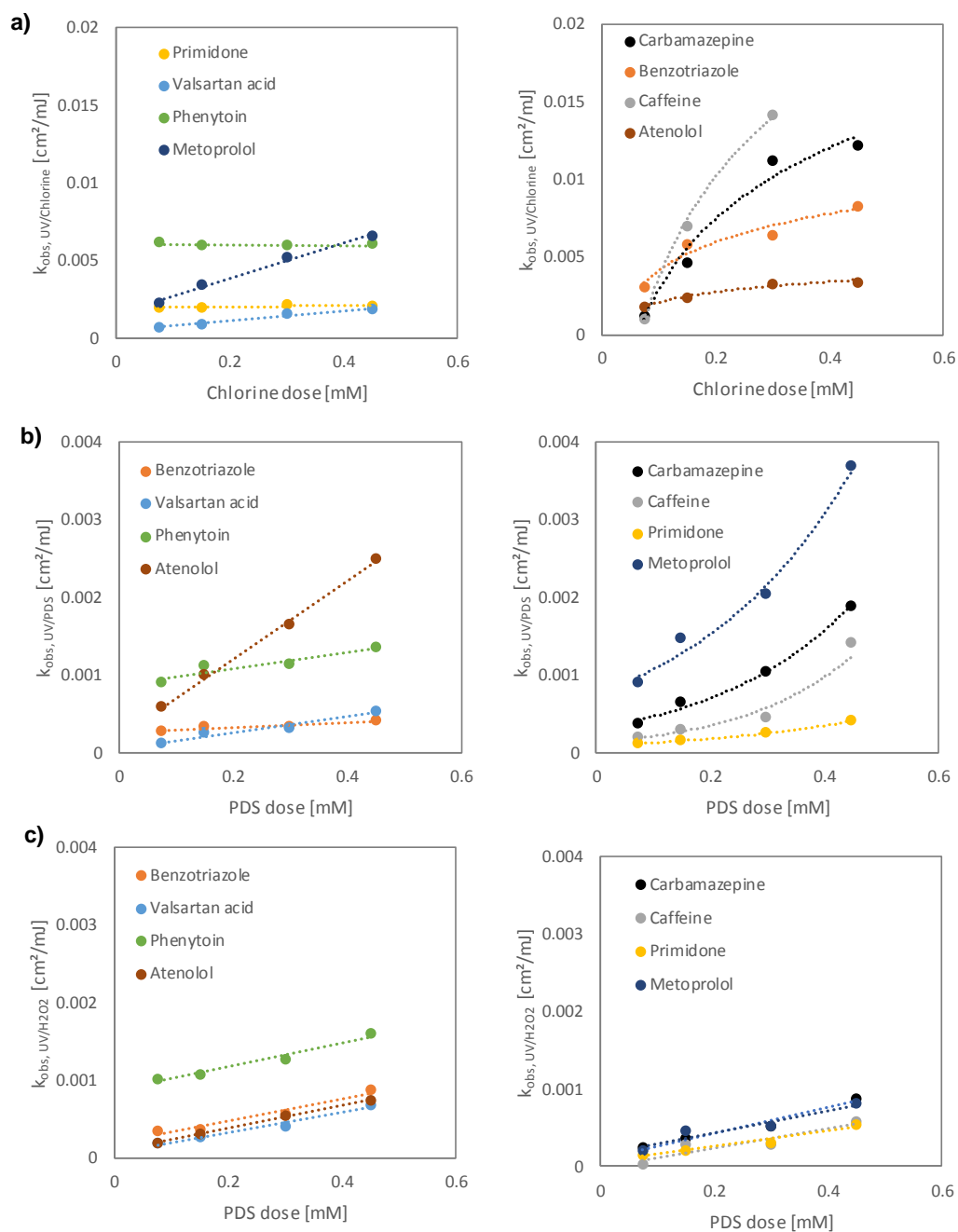
Figure S22: Observed pseudo first-order reaction reaction rate constant during a) UV/Chlorine, b) UV/PDS and c) UV/H₂O₂ in wastewater effluent for different compounds at radical promoter concentrations of 0.075, 0.15, 0.3 and 0.45 mM and applied fluences of 50-800 mJ/cm².
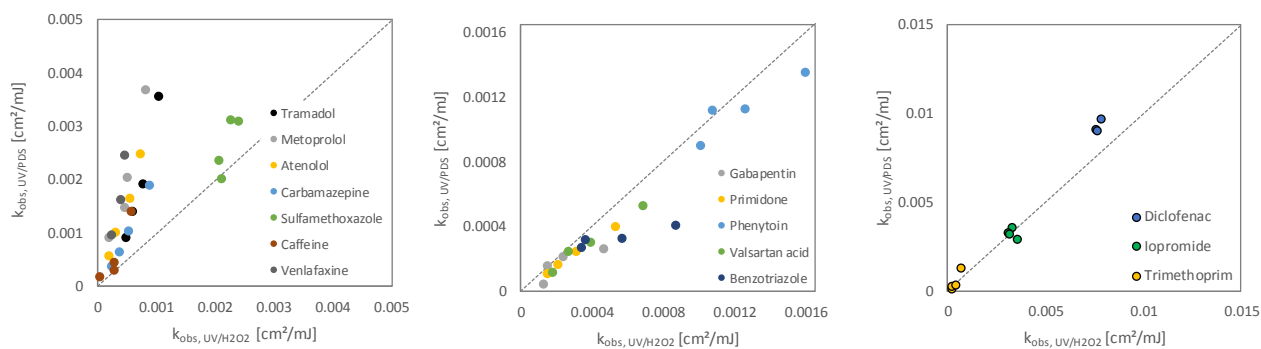
Figure S23: Comparative illustration of observed reaction rate constants in UV/H₂O₂ and UV/PDS in wastewater effluent for different compounds at radical promoter concentrations of 0.075, 0.15, 0.3 and 0.45 mM. Dashed line represents the one-to-one line.
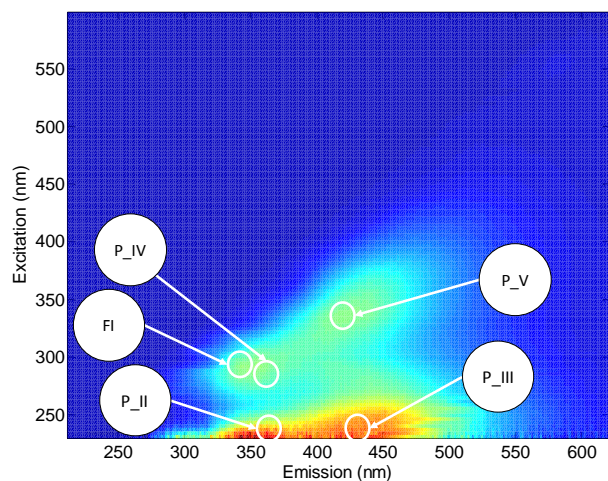
Figure S24: Illustration of selected fluorescence features by peak-picking method as stated in Table S8.
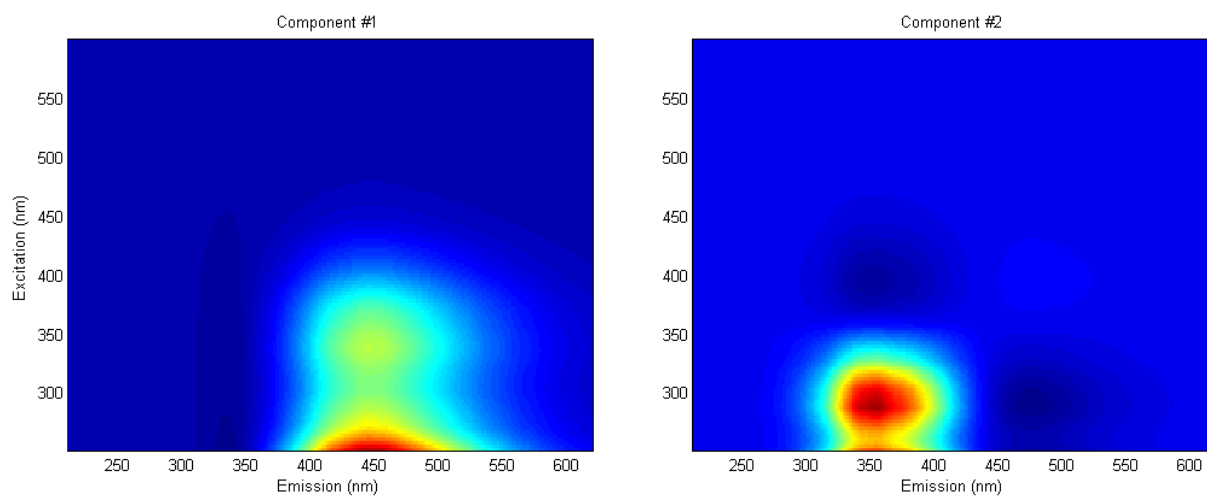
Figure S25: PARAFAC components C1 (left) and C2 (right) (model data n=417, validation data (this study, n=95))
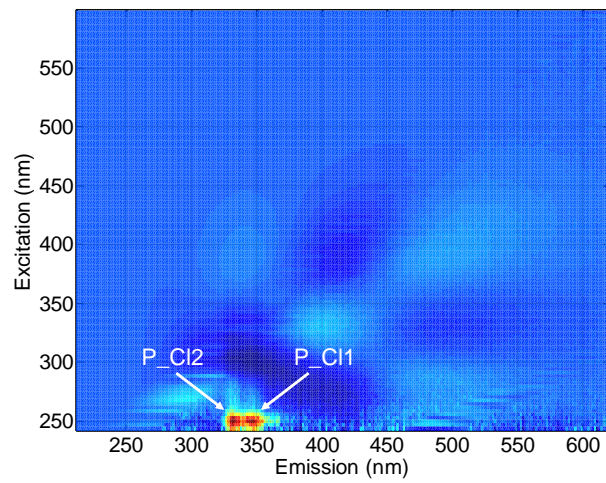
Figure S26: Fluorescence peaks (P_Cl1 and P_Cl2) formed during UV/Chlorine AOP at 0.4 mM chlorine and 400 mJ/cm².
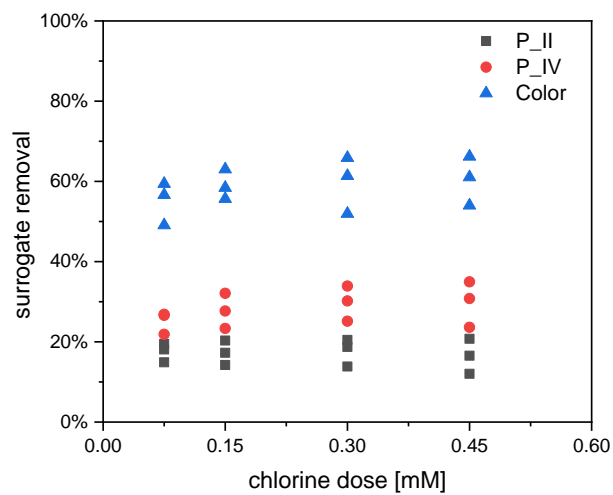
Figure S27: Removal of selected surrogates (lowest, moderate and highest reactivity) by dark chlorination in wastewater effluent with 0.075-0.45 mM chlorine and 95-758 s exposure time applied.
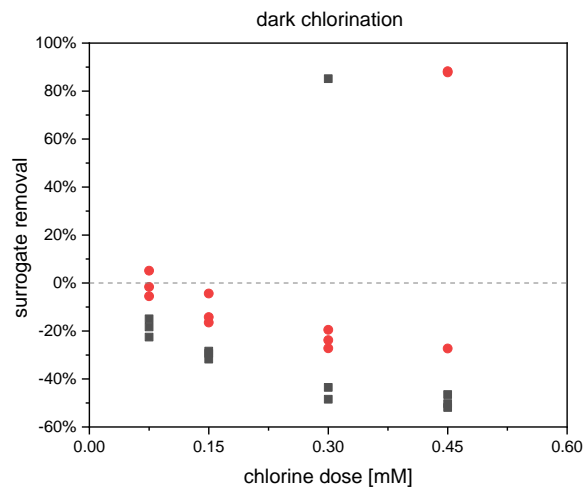
Figure S28: Fluorescence peak P_Cl1 (dots) and P_Cl2 (squares) formation during dark chlorination in wastewater effluent with 0.075-0.45 mM chlorine and 95-758 s exposure time applied.
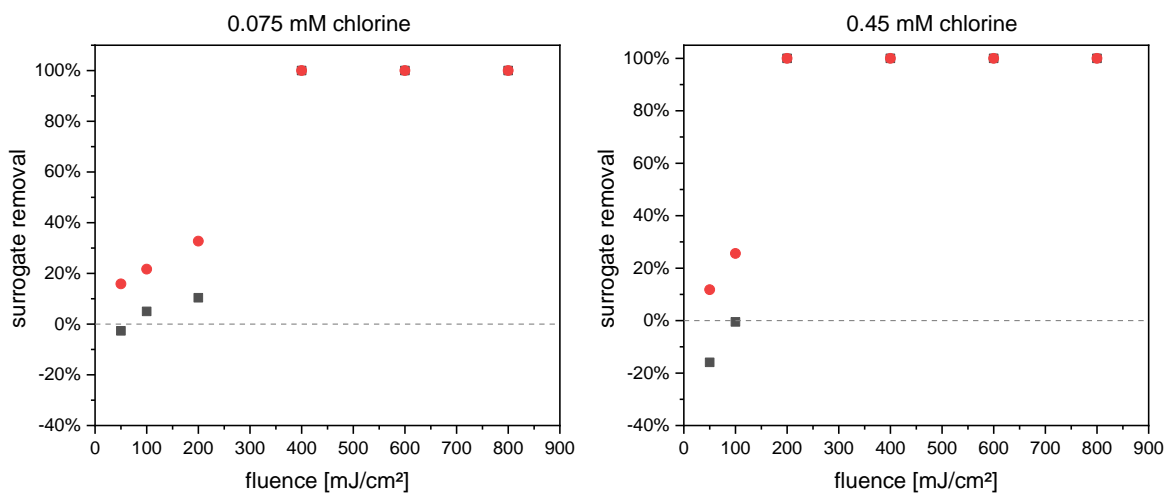
Figure S29: Fluorescence peak P_Cl1 (dots) and P_Cl2 (squares) formation and degradation during UV/Chlorine AOP in wastewater effluent with 0.075 mM and 0.45 mM chlorine applied.
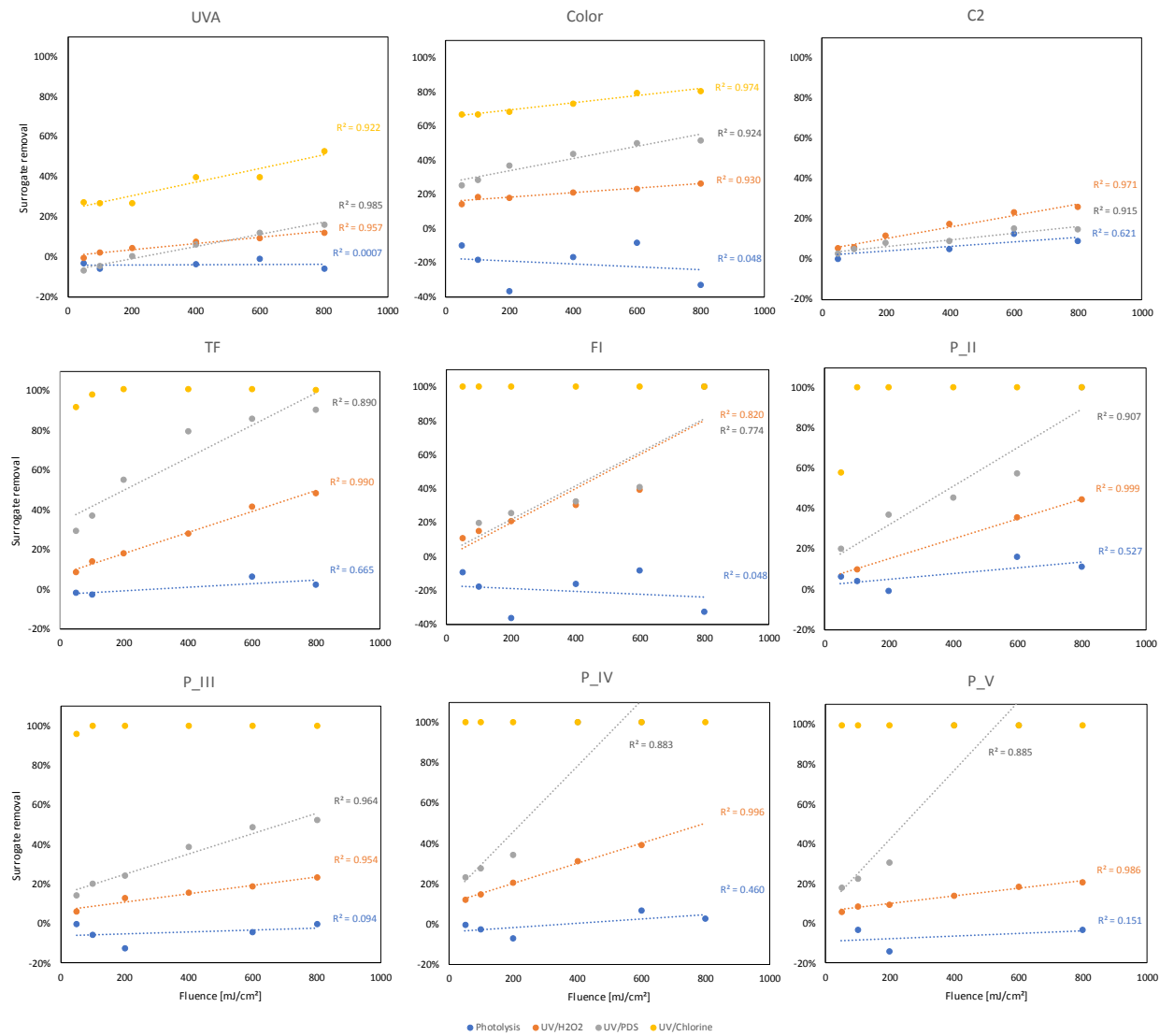
Figure S30: Removal of all optical surrogate parameters by UV-photolysis, UV/H$_2$O$_2$, UV/PDS and UV/Chlorine (0.45 mM of radical promoters).
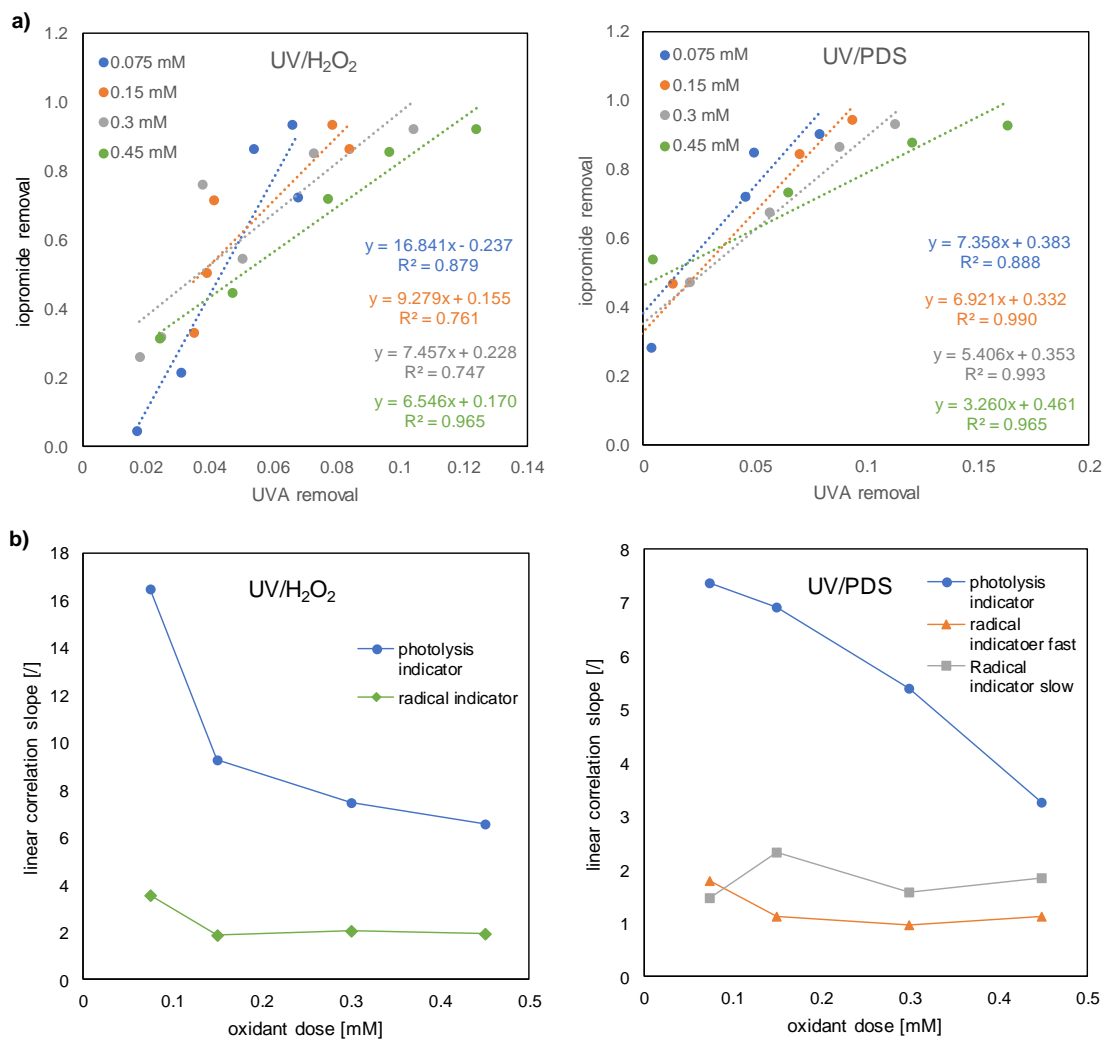
Figure S31: Linear correlations between the photolysis indicator iopromide and UVA during UV/H₂O₂ and UV/PDS at different radical promoter doses (0.075-0.45 mM) (a), slope of correlation curves over oxidant dose for photolysis and radical indicators (slow reactivity with sulfate radicals: benzotriazole; fast reactivity with sulfate radicals: venlafaxine) (b).

9.5.2 *Supporting Tables*

Table S8: Fluorescence EEM regions and Excitation/Emission wavelengths of the selected peaks

Region[a]	EfOM components	Selected peaks		Suggested peak area	
		Λ Excitation (nm)	Λ Emission (nm)	Λ Excitation (nm)	Λ Emission (nm)
I	aromatic proteins	-	-	200-250	280-330
II	aromatic proteins, tryptophan-like	245	358	200-250	330-380
III	Fulvic acid-like	245	430	200-250	380-550
IV	soluble microbial by-product-like	287	353	250-340	250-380
V	Humic acid-like	329	412	250-400	380-550

[a]From Chen et al. (2003)

Table S9: Observed first-order rate constants (k_{app}) and respective R^2 from lab-scale experiments with 0.075, 0.15, 0.3 and 0.45 mM radical promoters and applied UV-fluences of 50-800 mJ/cm²,

		oxidant dose (mM)	Benzotriazole	Caffeine	Carbamazepine	Diclofenac	Gabapentin	Iopromide	Metoprolol	Phenytoin	Primidone	Sulfamethoxazole	Tramadol	Venlafaxine	Trimethoprim	Valsartan acid	Atenolol
UV/H2O2	kobs	0.075	3.39E-04	3.05E-05	2.39E-04	7.55E-03	1.27E-04	3.54E-03	2.03E-04	1.01E-03	1.48E-04	2.10E-03	4.94E-04	2.41E-04	1.64E-04	1.78E-04	1.93E-04
		0.15	3.64E-04	2.74E-04	3.65E-04	7.78E-03	1.55E-04	3.29E-03	4.59E-04	1.08E-03	2.11E-04	2.07E-03	5.96E-04	3.87E-04	2.04E-04	2.67E-04	2.98E-04
		0.3	5.68E-04	2.93E-04	5.21E-04	7.58E-03	2.39E-04	3.05E-03	5.16E-04	1.26E-03	3.13E-04	2.27E-03	7.70E-04	4.72E-04	4.21E-04	3.96E-04	5.42E-04
		0.45	8.69E-04	5.72E-04	8.79E-04	7.86E-03	4.66E-04	3.15E-03	8.09E-04	1.60E-03	5.35E-04	2.39E-03	1.05E-03	8.59E-04	6.75E-04	6.86E-04	7.29E-04
	R²	0.075	0.976	0.606	0.944	0.99996	0.909	0.998	0.921	0.989	0.892	0.999	0.992	0.918	0.824	0.868	0.621
		0.15	0.923	0.983	0.819	0.99975	0.846	0.997	0.963	0.978	0.817	0.995	0.975	0.815	0.778	0.822	0.807
		0.3	0.997	0.962	0.994	0.999	0.984	0.996	0.986	1.000	0.948	0.999	0.999	0.996	0.958	0.987	0.981
		0.45	0.993	0.936	0.990	0.998	0.980	0.998	0.992	0.994	0.988	0.998	0.999	0.996	0.995	0.988	0.978
UV/PDS	kobs	0.075	2.73E-04	1.90E-04	3.82E-04	9.12E-03	4.47E-05	2.89E-03	9.04E-04	9.08E-04	1.10E-04	2.02E-03	9.08E-04	9.72E-04	1.47E-04	1.24E-04	5.82E-04
		0.15	3.26E-04	3.00E-04	6.51E-04	9.69E-03	1.58E-04	3.61E-03	1.47E-03	1.12E-03	1.66E-04	2.37E-03	1.39E-03	1.62E-03	2.48E-04	2.49E-04	1.00E-03
		0.3	3.31E-04	4.60E-04	1.03E-03	9.01E-03	2.15E-04	3.27E-03	2.03E-03	1.13E-03	2.49E-04	3.11E-03	1.93E-03	2.46E-03	3.71E-04	3.10E-04	1.64E-03
		0.45	4.16E-04	1.41E-03	1.89E-03		2.64E-04	3.22E-03	3.68E-03	1.36E-03	4.06E-04	3.09E-03	3.56E-03	5.01E-03	1.33E-03	5.36E-04	2.49E-03
	R²	0.075	0.923	0.928	0.867	0.991	0.520	0.996	0.910	0.995	0.889	0.997	0.938	0.884	0.798	0.856	0.875
		0.15	0.987	0.994	0.967	0.919	0.962	0.992	0.991	0.998	0.914	0.9996	0.992	0.998	0.902	0.993	0.992
		0.3	0.961	0.905	0.996	0.826	0.959	0.990	0.998	0.998	0.880	0.992	0.995	0.995	0.963	0.997	0.998
		0.45	0.976	0.981	0.991		0.957	0.997	0.990	0.995	0.939	0.921	0.986	0.991	0.929	0.959	0.998
UV/Chlorine	kobs	0.075	3.13E-03	1.10E-03	1.21E-03				2.24E-03	6.18E-03	1.97E-03					7.27E-04	1.86E-03
		0.15	5.86E-03	7.06E-03	4.74E-03				3.42E-03	6.00E-03	2.01E-03					8.96E-04	2.40E-03
		0.3	6.42E-03	1.42E-02	1.13E-02				5.18E-03	5.97E-03	2.17E-03					1.58E-03	3.35E-03
		0.45	8.36E-03		1.23E-02				6.63E-03	6.13E-03	2.06E-03					1.84E-03	3.42E-03
	R²	0.075	0.938	0.922	0.983				0.992	0.999	0.974					0.925	0.993
		0.15	0.997	0.997	0.990				0.999	0.998	0.998					0.934	0.983
		0.3	0.998	0.979	0.994				0.997	1.000	0.998					0.955	0.993
		0.45	0.977		0.953				1.000	1.000	1.000					0.999	0.996

Table S10: Chemical structures of the 17 TOrCs investigated

Chlorine sensitive		Chlorine moderately persistent		Chlorine persistent	
Compound	Structure	Compound	Structure	Compound	Structure
Sulfamethoxazole*		Valsartan Acid		Atenolol	
Gabapentin		Phenytoin*		Caffeine	
Diclofenac*		Metoprolol		Benzotriazole	
Trimethoprim		Primidone		Iopromide*	
Venlafaxine		Carbamazepine		TCEP	
Tramadol		Sotalol			
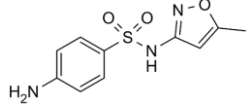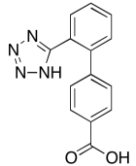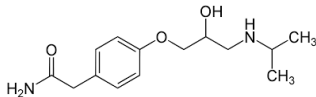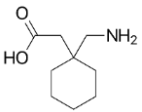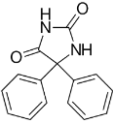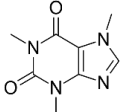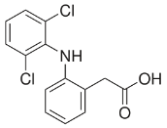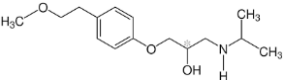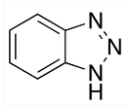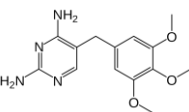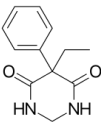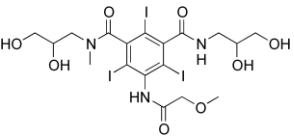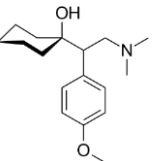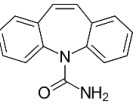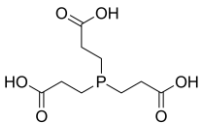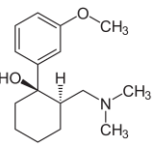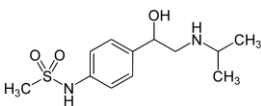
9.6 Paper V – Improving UV/H₂O₂ performance following tertiary treatment of municipal wastewater
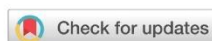
Check for updates

Improving UV/H₂O₂ performance following tertiary treatment of municipal wastewater†

Sydney L. Ulliman, [ID] [a] David B. Miklos, [ID] [b] Uwe Hübner, [ID] [b] Jörg E. Drewes [ID] [b] and Karl G. Linden [ID] *[a]

The ability of UV/AOP to treat trace organic contaminants (TOrCs) in wastewater is inhibited by (1) UV light-absorbing species and (2) hydroxyl radical ($^{\bullet}$OH) scavenging species. We address these challenges by investigating four diverse technologies, single-stage biofiltration, sequential biofiltration, coagulation–floc-culation–sedimentation–filtration (CFSF), and nanofiltration, as options for improving water quality conditions just prior to UV treatment, with and without added hydrogen peroxide (H_2O_2). By evaluating UV_{254} transmittance (UVT), $^{\bullet}$OH scavengers, and $^{\bullet}$OH steady-state concentrations, we found nanofiltration treatment to produce the most favorable pre-UV and UV/H_2O_2 water quality conditions. In comparing CFSF, single-stage biofiltration and sequential biofiltration treatment, CFSF treatment resulted in the highest increase in UVT and all three technologies reduced the scavenging capacity by ~24% despite differences in removal of typical $^{\bullet}$OH scavengers. UV and UV/H_2O_2 performance were evaluated by tracking the degradation rates of 11 targeted TOrCs for each pre-UV/H_2O_2 treatment scenario. Applying the additional treatment, average pseudo first-order degradation rates of TOrCs under UV/H_2O_2 increased by 20 to 92%, informing potential strategies to increase the oxidation potential of UV/AOP systems applied to wastewater.

Water impact

Converting UV disinfection systems into UV/AOP systems is a potential strategy to decrease the concentration of trace organic contaminants discharged into natural water systems by municipal WWTPs. This study investigates the use of tertiary and advanced treatment processes to improve the water quality prior to, and increase the oxidation potential during, UV/AOP treatment of wastewater effluents.

1 Introduction

Numerous research studies[1–5] have demonstrated that conventional municipal wastewater treatment plants (WWTPs), consisting of preliminary treatment (screening and grit removal), primary treatment (sedimentation), secondary treatment (biological treatment like activated sludge), and tertiary treatment (filtration), are ineffective at removing pharmaceutical residuals, endocrine disrupting compounds and other pollutants that have low sorption coefficients and are recalcitrant to biodegradation.[2,6] Despite the increased toxicity and concentration of pollutants entering municipal WWTPs,[6] most countries require secondary treatment as the final treatment step prior to discharging into surface water.[7,8] Subse-quently, discharging wastewater effluent into natural water systems has resulted in adverse health effects of aquatic eco-systems,[6] dispersion of trace-levels (ng L^{-1} to μg L^{-1}) of various contaminants of emerging concern[9] and compromised source water for drinking water treatment facilities located downstream of wastewater discharges.[10]

To decrease the concentration of pollutants in wastewater effluent, implementing advanced treatment technologies might be a viable option for existing and future WWTPs. A class of treatment technologies well-recognized for their ability to destroy a wide range of organic pollutants are advanced oxidation processes (AOPs). AOPs are defined by their capacity to generate powerful (2.8 eV) and reactive (10^8 to 10^{10} M^{-1} s^{-1}) $^{\bullet}$OH *in situ*.[11] The most common industry-used AOPs for advanced wastewater treatment are ozone or UV coupled with an added oxidant, which is commonly H_2O_2.[12] An advantage of ozone- and UV-based AOPs is their ability to simultaneously destroy TOrCs and inactivate microorganisms.

Today, there are over 7300 UV systems installed at WWTPs in the United States and over 12 600 UV systems installed

^{a} *Department of Civil, Environmental, and Architectural Engineering, University of Colorado at Boulder, 4001 Discovery Drive, Boulder, CO 80303 USA.*
E-mail: Karl.Linden@colorado.edu; Fax: +1 303 492 7317; Tel: +1 303 492 4798
^{b} *Chair of Urban Water Systems Engineering, Technical University of Munich, Am Coulombwall 3, 85748 Garching, Germany*
† Electronic supplementary information (ESI) available. See DOI: 10.1039/ c8ew00233a

Paper

worldwide. Although the UV dose required for disinfection (~30 to 40 mJ cm^{-2}) is significantly lower than design doses for UV/AOP applications (>500 mJ cm^{-2}), most UV reactors have the capacity to increase their UV intensity up to 4 times during average daily flow conditions. This is because UV reactors are often designed to achieve disinfection doses for peak flow conditions. Alternatively, increased UV intensity can be achieved by adding banks of lamps or another UV reactor in series (information above provided through personal correspondence with three independent UV manufacturers). Thus, there is opportunity to convert UV disinfection systems operating at WWTPs into UV/AOP systems which could result in capital cost savings compared to installing a new UV/AOP system or an alternative AOP system.

While it is common practice for municipalities to disinfect wastewater with UV light, UV/AOPs are not typically utilized for treatment of conventionally treated municipal wastewater effluent. Compared to drinking water sources, wastewater effluents contain higher concentrations of UV-absorbing species and ˙OH scavengers which can decrease the performance of UV/AOP and result in increased operating costs. Low UVT conditions can inhibit the photolysis of UV-degradable contaminants and H$_2$O$_2$. The latter results in the reduction of ˙OH production. Additionally, the ability of ˙OH radicals to react with target pollutants can be inhibited by the competing reactions (scavenging) of ˙OH with organic and inorganic constituents, such as dissolved organic matter (DOM), carbonate species, and NO$_2^-$.

The effect of water quality on ˙OH scavenging has extensively been investigated,[13–15] and UV and UV/AOP performance has been evaluated in diverse effluents collected from established water and wastewater treatment processes (e.g., CFSF, activated sludge, moving bed bioreactor, ion exchange, filtration and others).[16–18] However, few studies have evaluated the effect of treatment processes added post conventional tertiary filtration treatment as strategies to increase the oxidation potential of subsequent UV/AOP systems in WWTPs even though evidence suggests that UV/AOP systems are a viable solution to reduce pollutant discharge.[17,19] For example, a recent study conducted by Hofman-Caris et al.[17] reported that the addition of an anion exchange system before UV/H$_2$O$_2$ treatment increased the UVT from 38% to 85% and decreased the humic acid fractions of DOM which enabled the degradation of pharmaceutical compounds at UV doses <300 mJ cm^{-2}.

For this study, a single batch of tertiary-treated wastewater effluent collected from the WWTP in Garching, Germany was further treated with four technologies, single-stage biofiltration, sequential biofiltration, CFSF and nanofiltration, to improve water quality prior to UV and UV/H$_2$O$_2$ treatment. These treatment technologies were selected because they utilize different processes (e.g., biological, physical and chemical) to remove organic matter and absorbing constituents that affect UV and UV/AOP efficiency. Wastewater effluents were compared before and after treatment of the tertiary effluent by quantifying changes in UVT, ˙OH scavenging rates,

and steady-state ˙OH concentrations. The efficiency of UV and UV/H$_2$O$_2$ following post-treatment of tertiary effluent was evaluated by determining the degradation rates of 11 spiked TOrCs with varied susceptibility to photolysis and oxidation. TOrC removal was investigated over a range of UV doses, including well below those typically used for UV/H$_2$O$_2$ application.

2 Experimental methods

2.1 Wastewater effluent collection

A single 3 m^3 batch of wastewater effluent that was collected after tertiary filtration at the Garching WWTP, Germany which served as the test water for all bench-scale experiments. This WWTP employs conventional biological nutrient removal with full nitrification and denitrification and tertiary filtration. During the period from May to September, when this study was conducted, the plant operates a seasonal UV system (~50 mJ cm^{-2}) to provide disinfection prior to discharging to the Isar river. Minimal differences in water quality before and after UV disinfection were observed (data not provided). While the biological nutrient removal system is designed to achieve nitrogen concentration <10 mg L^{-1}-N, low-levels of nitrite were occasionally measured (<0.2 mg L^{-1}-N) in tertiary effluent (Table 1).

2.2 Post-treatment of tertiary effluent

A two-stage sequential biofiltration system comprised of an anthracite filter followed by a sand filter was operated under saturated top-down flow conditions with tertiary effluent (see Müller et al. (2017)[20] for detailed description of the system). Samples were collected after the first stage anthracite filter (empty bed contact time (EBCT) = 90 min, single-stage biofiltration) and after the second stage sand filter (EBCT = 200 min, sequential biofiltration). The first-stage effluent was aerated prior to sand filtration to promote aerobic biofilm growth at the surface of the sand media with the goal of improving DOC removal. The system was operated for approximately 2 years before sampling.

The CFSF treatment was simulated using a programmable jar tester (Microfloc Pty Ltd, Australia) with aluminum sulfate (Al$_2$(SO$_4$)$_3$·16 H$_2$O, Sigma Aldrich, Germany). After testing a range of alum concentrations (100–240 mg L^{-1}), a dose of 160 mg L^{-1} was determined as an optimum dose for DOC removal. (Mixing conditions are presented in the ESI,† Table S1.) The supernatant was filtered through a 0.45 μm filter (Sartorius AG, Germany) prior to water quality analysis and UV and UV/H$_2$O$_2$ experiments to remove particulates and simulate water quality conditions after rapid sand filtration.

Nanofiltration experiments were performed using a bench-scale cross-flow nanofiltration system (Sepa II, Osmonics), equipped with a feed tank, sensors to monitor conductivity, pressure and temperature, and a heat exchanger used to maintain a temperature of 20 °C. A flat-sheet test cell encased a nanofiltration membrane (NF270, Dow Filmtec™), with an active membrane area of 139 cm^2 and a cross sectional area

Table 1 Water quality characteristics of water matrices prior to UV and UV/H₂O₂ experiments

Parameter	Units	Tertiary	Single-stage biofiltration	Sequential biofiltration	CFSF	Nanofiltration
COD	mg L^{-1}	16.5	11.9	10.4	9.8	2.4
DOC	mg L^{-1}	5.3	4.0	4.0	4.2	0.3
NO$_3^-$	mg L^{-1} as N	10.8	11.5	11.4	10.7	9.7
NO$_2^-$	mg L^{-1} as N	0.110	DL^a	DL^a	0.021	0.019
UV$_{254}$ (UVT)	m^{-1} (%)	13.0 (74.1)	11.3 (77.1)	10.8 (78.0)	8.3 (82.7)	1.0 (97.7)
SUVA	L mg$_\text{C}^{-1}$ m^{-1}	2.5	2.8	2.7	2.0	3.3
HCO$_3^-$	mg L^{-1} as CaCO$_3$	231	231	231	155	119
CO$_3^{2-}$	mg L^{-1} as CaCO$_3$	2.12	2.38	3.50	0.33	0.83
pH	—	8.19	8.21	8.20	7.25	7.80

^{a} DL of NO$_2^-$ is 0.015 mg L^{-1}-N.

of 0.92 cm^2. Tertiary effluent was fed to the system at a cross-flow velocity of 0.22 m s^{-1} across the membrane surface and a flux of 20 L m^{-2} h^{-1} was maintained during permeate collection. The test unit was monitored and controlled using LabVIEW™ software.

2.3 UV and UV/H₂O₂ treatment

A 1 L sample from each pre-UV treated water matrix was spiked with TOrCs (discussed in section 2.5) to achieve a concentration of 1 μg L^{-1} of each TOrC. The purpose of spiking in TOrCs rather than using native TOrCs (additional information on native TOrC concentrations in this wastewater effluent can be found elsewhere[20] was to achieve an initial concentration well above the instrument limit of detection. This allowed for TOrCs measurement after UV exposures >1200 mJ cm^{-2} which was used to develop degradation curves. Water quality was measured prior to UV and UV/H₂O₂ experiments to ensure it was not changing over holding times of <3 days.

Bench-scale UV and UV/H₂O₂ irradiation experiments were performed using a collimated beam device equipped with three low-pressure UV lamps (15 W, UV Technik Meyer GmbH, Germany) emitting at 254 nm. An incident irradiance of 1.1 mW cm^{-2} was consistently measured before and after exposure using a UV-C surface radiometer (sglux GmbH, Germany). 30 mL aliquots of wastewater effluent were continuously mixed (~200 rpm) in a 100 mm glass Petri dish (Petri factor > 0.9) to ensure uniform sample irradiation. The delivered UV fluence was determined following protocols outlined in Bolton and Linden (2003).[21] A total of nine discrete samples were taken for each pre-UV treated water matrix at fluence values ranging from 0 to 1200 mJ cm^{-2} (up to 1180 s exposure time). Directly before UV/H₂O₂ treatment, H₂O₂ was added at a concentration of 10 mg L^{-1}. Based on previous studies,[19,22] 10 mg L^{-1} H₂O₂ in the absence of UV irradiation was assumed to have minimal (0 to <10%) impact on TOrC degradation at the exposure times studied herein.

2.4 Determination of scavenging rate, pseudo first-order degradation rate constants, and ˙OH steady-state concentration

To quantify the reaction potential of ˙OH with scavengers (*e.g.*, DOC, HCO$_3^-$, CO$_3^{2-}$, and NO$_2^-$) for each pre-UV treat-

ment scenario, the scavenging rate (SR) was estimated by multiplying the scavenger concentration by established second order ˙OH reaction rate constants ($k_{\cdot\text{OH}}$) as shown in eqn (1).

$$\text{SR} = \sum k_{\cdot\text{OH,scavenger}}[\text{Scavenger}] \tag{1}$$

The following $k_{\cdot\text{OH}}$ values were used: $k_{\cdot\text{OH,DOC}}$ = 5.8 × 10^8 M^{-1} s^{-1} for DOC,[23] $k_{\cdot\text{OH,HCO}_3^-}$ = 8.5 × 10^6 M^{-1} s^{-1} for HCO$_3^-$,[24] $k_{\cdot\text{OH,CO}_3^{2-}}$ = 3.9 × 10^8 M^{-1} s^{-1} for CO$_3^{2-}$,[24] and $k_{\cdot\text{OH,NO}_2^-}$ = 1.0 × 10^{10} M^{-1} s^{-1} for NO$_2^-$.[24]

The degradation of target compounds was assessed by determining the pseudo first-order rate constant (k') which is the slope of the natural logarithm of the ratio of the compound concentration at an exposure time (t) to the concentration at t = 0, $\ln\left(\dfrac{C}{C_0}\right)$ plotted against exposure time (t) (eqn (2)). The k' plots were developed using seven discrete samples (Table S4†) taken at fluence values ranging from 0 to 1200 mJ cm^{-2} for each pre-UV treated water matrix.

$$k' = \frac{\ln\left(\dfrac{C}{C_0}\right)}{t} \tag{2}$$

The formation and scavenging of ˙OH was evaluated in each water matrix by applying eqn (3) to determine the steady-state concentration of ˙OH, [˙OH]$_{\text{ss}}$.

$$[\text{˙OH}]_{\text{ss}} = -\frac{k'}{k_{\cdot\text{OH}}} \tag{3}$$

Probe compounds carbamazepine and primidone were selected because of their low quantum yields and fast second-order rate of reaction with ˙OH (Table 2).

2.5 TOrC selection

Selection of TOrCs was based on their presence and persistence in municipal wastewater[3,25–29] as well as analytical capabilities. TOrCs were grouped according to Miklos *et al.* (2018)[19] and categorized based on their sensitivity to

Table 2 Kinetic parameters of selected TOrCs. Standard deviation is given in parentheses as reported

Group	TOrC	$\Phi_{254} \times 10^{-2}$ (mol Einstein^{-1})	$\varepsilon_{254} \times 10^3$ (M^{-1} cm^{-1})	$k_{OH} \times 10^9$ (M^{-1} s^{-1})
Photo-susceptible	Diclofenac	23 ($\pm$1.6)[a]	6.8 ($\pm$0.27)[a]	8.2 ($\pm$2.6)[a]
	Iopromide	3.9[b]	21[b]	3.3[c]
	Sulfamethoxazole	8.4 ($\pm$0.95)[a]	13 ($\pm$0.097)[a]	6.3 ($\pm$0.55)[a]
Moderately photo-susceptible	Benzotriazole	1.6[d]	6.14 ($\pm$19)[d]	8.34 ($\pm$0.37)[d]
	Caffeine	0.18[e]	3.92[e]	6.4 ($\pm$0.71)[e]
	Metoprolol	6.6 ($\pm$4.7)[a]	0.33 ($\pm$0.0011)[a]	8.1 ($\pm$0.98)[a]
	Phenytoin	27.9[e]	1.26[e]	6.28[e]
	Venlafaxine	9.7 ($\pm$5.7)[a]	0.38 ($\pm$0.019)[a]	8.8 ($\pm$1.5)[a]
Photo-resistant	Carbamazepine	0.33 ($\pm$0.1)[a]	5.8 ($\pm$0.0089)[a]	9.5 ($\pm$1)[a]
	Gabapentin	—	—	9.1[f]
	Primidone	8.2[e]	0.22[e]	6.7[e]

[a] Wols *et al.* (2014).[52] [b] Canonica *et al.* (2008).[53] [c] Huber *et al.* (2003).[54] [d] Bahnmüller *et al.* (2015).[55] [e] Wols and Hofman-Caris (2012).[34] [f] Lee *et al.* (2014).[56]

degradation by photolysis (Φ_{254}) and $\cdot$OH oxidation (k_{OH}): photo-susceptible (diclofenac, iopromide, and sulfamethoxazole), moderately photo-susceptible (benzotriazole, caffeine, metoprolol, and venlafaxine), and photo-resistant (carbamazepine, gabapentin, and primidone) compounds (Table 2).

2.6 Analytical methods

The H$_2$O$_2$ (Bernd Kraft GmbH, Germany) concentration was verified before and after UV/H$_2$O$_2$ treatment using the titanium IV oxysulfate (Sigma-Aldrich) colorimetry method (DIN 38 409, part 15, DEV-18). The following methods and instruments were used to measure bulk water quality parameters: Hach cuvette tests for nitrate (LCK 340), nitrite (LCK 341/342), and acid capacity $K_{a4,3}$ (LCK 362), DR6000 UV/vis spectrophotometer (Hach Lange, Germany) for UVT$_{254}$ measurement, and varioTOC cube (Elementar Analysensysteme, Germany) for DOC measurement of 0.45 μm cellulose nitrate membrane (Sartorius AG, Germany) filtered samples.

Samples collected for TOrC analysis were filtered through 0.22 μm PVDF syringe filters (Berrytec, Germany) and stored in amber glass vials at 4 °C before analysis. TOrC measurement was performed using a high performance liquid chromatography (Knauer PLATINBLUE UHPLC) coupled with tandem mass spectrometry (LC-MS/MS) (SCIEX QTRAP 6500) with direct injection as described in Müller *et al.* (2017).[20] Analytical grade TOrCs and isotope labelled standards were used.

3 Results and discussion

3.1 Effect of tertiary treatment on UV transmittance and scavenging rate

Table 1 presents the relevant water quality data of water types used for the UV and UV/H$_2$O$_2$ experiments. The UV transmittance (% UVT = 100 × 10$^{-UVA_{254}}$) and scavenging rate were the selected parameters to compare the water quality after treatment of tertiary effluent (Fig. 1) because of their impact on UV and UV/H$_2$O$_2$ performance. For example, absorbing species, including suspended solids and DOM, can shield UV light and inhibit the photolysis of target pollutants and H$_2$O$_2$,

which results in decreased $\cdot$OH production. Radical scavengers consume generated $\cdot$OH and, subsequently, decrease the reaction potential of $\cdot$OH with target pollutants.

Overall, nanofiltration treatment resulted in the most improved water quality conditions, producing water with a 98% UVT and decreasing the scavenging rate by 86%. CFSF treatment increased the UVT by 12% while UVT was only marginally improved (4–5%) after biofiltration treatment (single-stage and sequential). The scavenging rates of CFSF and biofiltration (single-stage and sequential) treatment were similar and ranged from 2.27 × 10^5 s^{-1} to 2.44 × 10^5 s^{-1} (Fig. 1).

To further analyze the scavenging rate results, the percent contribution of individual scavengers to the overall scavenging rate was evaluated (Fig. 2). The radical scavengers evaluated in this study were: $k_{OH,DOC} = 5.8 \times 10^8$ M^{-1} s^{-1}, $k_{OH,NO_2^-} = 1.0 \times 10^{10}$ M^{-1} s^{-1}, and $k_{OH,CO_3^{2-}} = 3.9 \times 10^8$ M^{-1} s^{-1} and $k_{OH,HCO_3^-} = 8.5 \times 10^6$ M^{-1} s^{-1}. The contribution of NO$_3^-$ to the overall scavenging demand was found to be negligible which is explained by its low reaction rate with $\cdot$OH ($k_{OH,NO_3^-} < 1.0 \times 10^5$ M^{-1} s^{-1} ref. 30). Although chloride and sulfate are often present in wastewater and known scavengers of $\cdot$OH ($k_{OH,Cl^-} = 4.3 \times 10^9$ M^{-1} s^{-1} ref. 31) and $k_{OH,SO_4^{\cdot-}} = 1.0 \times 10^{10}$
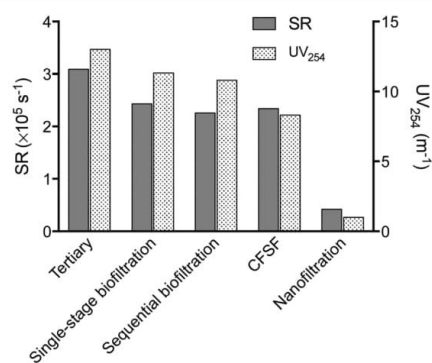
Fig. 1 Scavenging rate (primary *y*-axis) and UV absorbance (secondary *y*-axis) of pre-UV/H$_2$O$_2$ water quality scenarios.
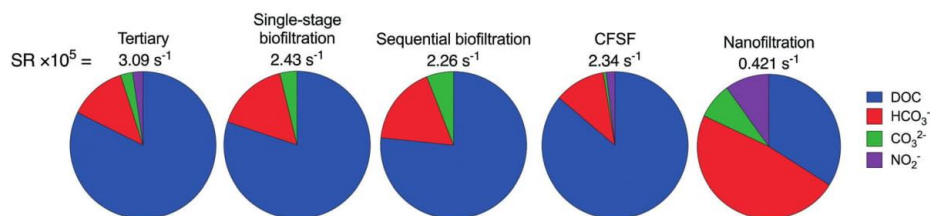
Fig. 2 Percent contribution of individual scavengers to the overall scavenging demand. $SR \times 10^5$ values represent the total scavenging capacity of the water matrix. Scavenging by DOC is calculated using rate constant from literature which may not represent reactivity in every post-treated effluent as explained in section 3.1.

M^{-1} s^{-1} (ref. 32)), their scavenging potential has been shown to be offset by the production of radicals through intermediate reactions. Liao *et al.*[33] explains that at a pH >6 (for all wastewaters the pH was >7) the $\cdot$OH scavenged by Cl^- is replaced by $\cdot$OH generated during the dissociation of $HOCl^{\cdot-}$ (ref. 33) thus is inconsequential at the pH of the wastewater in this study. Photolysis of sulfate generates the sulfate radical which is more selective then $\cdot$OH but has similar oxidizing power.[33] Therefore, chloride and sulfate were not considered major scavengers of $\cdot$OH.

Within the literature, there is a high variance between $k_{OH,DOC}$ values reported ranging from 3.5×10^8 M^{-1} s^{-1} to 9.2×10^8 M^{-1} s^{-1}.[34] This is because $\cdot$OH reactivity with DOC is a function of organic matter composition, and organic matter present in aqueous environments is continuously changed from natural and anthropogenic inputs and processes. The $k_{OH,DOC}$ (5.8×10^8 M^{-1} s^{-1}) value used to calculate the scavenging rate was previously determined for WWTP effluent[23] and, therefore, was assumed to be a good representative of the tertiary-treated WWTP effluent used for this study. Because differences in organic matter composition have been shown to affect the reactivity of $\cdot$OH,[35,36] it is important to consider that the $k_{OH,DOC}$ used to determine the scavenging rate of tertiary effluent may not accurately represent the reactivity of $\cdot$OH with DOC in every post-treated tertiary effluent. While $k_{OH,DOC}$ values were not experimentally determined in this study, section 3.3 investigates whether the reactivity of organic matter is changed as a result of treatment of tertiary effluent by comparing modeled and experimentally-determined $\cdot$OH steady state concentrations.

Interestingly, CFSF and biofiltration (single-stage and sequential) treatment achieved similar DOC removal (21 to 24%) which resulted in comparable calculated scavenging rates (Fig. 2). This result was unexpected since CFSF and biofiltration utilize different mechanisms for DOC removal: CFSF combines chemical and physical processes to remove organic matter whereas biofiltration simultaneously removes organic matter through adsorption, filtration and biodegradation. However, analysis of specific UV absorbance at 254 nm (SUVA, calculated by dividing the 254 nm absorbance (UVA_{254}) by DOC) values reveal CFSF and biofiltration treatment may have preferentially removed different organic matter components. CFSF treatment decreased the SUVA value by

20% indicating larger molecular weight or aromatic DOC fractions were removed, which has been observed in previous coagulation work.[37,38] In comparison, SUVA was increased by 15 and 8% after single-stage and sequential biofiltration, respectively, indicating preferential biodegradation of aliphatic and lower molecular weight compounds.[39,40]

In comparing single-stage and sequential biofiltration, the removal of DOC was not enhanced by the additional biofiltration step. Similar results were observed in a recent study by Müller *et al.* (2017)[20] where it was explained that the first biofiltration stage likely consumed the readily available organic substrate and the second biofiltration stage resulted in minor structural changes as well as minimal mineralization of the remaining slowly biodegradable organic substrate.

Removal of carbonate species and NO_2^- was shown to vary with treatment. While alkalinity was unchanged after biofiltration (single-stage and sequential) treatment, CFSF and nanofiltration treatment removed 33% and 49%, respectively. It was also observed that CFSF treatment decreased the pH from 8.2 to 7.3 which resulted in the shift of carbonate (CO_3^{2-}) to bicarbonate (HCO_3^-) and an overall reduction in carbonate scavenging potential. In contrast, oxic biofiltration (single-stage and sequential) removed NO_2^- to levels below the method detection limit (<0.015 mg L^{-1}-N) likely due to biological oxidation of NO_2^- to NO_3^-. These findings demonstrate that biofiltration treatment, while maintaining oxic conditions, can be an effective barrier for NO_2^- when WWTPs are experiencing sporadic elevated NO_2^- emissions from secondary treatment.

Because nanofiltration treatment reduced the DOC concentration to <0.3 mg L^{-1}, the contribution of HCO_3^- (48%) and NO_2^- (10%) were found to have a higher impact on the scavenging rate as compared to the other wastewater effluents (Fig. 2). Nanofiltration systems have been shown to physically reject compounds with a molecular weight compounds down to 200 Da through repulsive forces at the membrane surface.[41–43] However, inorganic nitrogen molecules have been shown to pass through nanofiltration membranes.[43]

3.2 Degradation rates of TOrCs

Presented in Fig. 3 are time-based pseudo first-order degradation kinetics (noted as k') of selected TOrCs. Time-based

units were selected because they do not correct the fluence for absorbance and water depth (embedded in Beers law) and therefore illustrate the impact of UV transmittance on UV degradation. For instance, for an exposure of 600 s the delivered fluence was 606 mJ cm^{-2} for tertiary effluent and 674 mJ cm^{-2} for nanofiltration permeate (irradiance was constant at 1.1 mW cm^{-2} for all experiments).

With respect to individual treatment technologies, average TOrC degradation rates (n = 11) were improved by 27%, 18%, 30%, and 98% after single-stage biofiltration, sequential biofiltration, CFSF, and nanofiltration treatment, respectively. Although a consistent trend of $k'_{nanofiltration} > k'_{CFSF} > k'_{single-stagebiofiltration} > k'_{sequentialbiofiltration} > k'_{tertiary}$ for average k' values of TOrCs can be observed for most compounds (Fig. 3), k' values generated for single-stage biofiltration, sequential biofiltration and CFSF were not statistically different ($p > 0.05$, one-tailed student's t-test) which corroborates scavenging rate results.

Resulting from treatment of tertiary effluent, the average TOrC degradation rates of photo-resistant compounds (n = 3) were most improved (75% ± 33%, reported as averages followed by the standard error of the mean), followed closely by moderately photo-susceptible compounds (n = 5) (71% ± 26%) and finally photo-susceptible compounds (n = 3) which were least improved (34% ± 21%). With relatively low quantum yields or molar absorption coefficients (Table 2), moderately photo-susceptible and photo-resistant compounds degrade primarily through $^{\bullet}$OH oxidation and are therefore more sensitive to changes in $^{\bullet}$OH scavengers.

The changes in scavenging capacity and UVT from tertiary treatment on TOrC degradation rates can be investigated by comparing fluence-based k' values to time-based k' values (Table S3†). UV-fluence-based pseudo first-order degradation kinetics correct the fluence for absorbance and depth effects, therefore normalizing differences between waters,[21] however, the impact of the water matrix on scavenging of $^{\bullet}$OH radicals is present in both time and fluence based units.[21] To illustrate this point, the variability (based on the standard deviation, n = 4) of time-based k' values (s = 4.29 × 10^{-4} s^{-1}) after treatment was almost double that of fluence-based k' values (s = 2.62 × 10^{-4} cm^2 mJ^{-1}) for the photo-amenable compound iopromide. In comparison, the variability of time- and

fluence-based k' after treatment were similar (s = 6.29 × 10^{-4} s^{-1} and 5.14 × 10^{-4} cm^2 mJ^{-1}) for photo-resistant compound Primidone, and the variability of fluence-based k' values is notably higher than Iopromide. Similar trends were observed for the other photo-susceptible and photo-resistant compounds studied. Overall, these results show that photo-amenable compounds are primarily affected by absorbing species,[44] as demonstrated by the relatively low variability of fluence-based degradation rates after treatment, whereas nonphoto-amenable TOrCs will not only be affected by absorbing species, but also vary because of treatment due to known and unknown effects of scavenging as well as other radicals that may form during UV photolysis.

3.3 Hydroxyl radical production

To compare the oxidation potential of water quality conditions prior to UV/H$_2$O$_2$ treatment, steady-state $^{\bullet}$OH concentrations, [$^{\bullet}$OH]$_{ss}$, were determined. As shown in Fig. 4, treatment of tertiary effluent significantly increased the [$^{\bullet}$OH]$_{ss}$ by 55% for single-stage biofiltration, 36% for sequential biofiltration, 59% for CFCF and 164% for nanofiltration. $^{\bullet}$OH production is a function of the UVT since UVT controls the rate of light absorption by H$_2$O$_2$. Therefore, it is not surprising that the [$^{\bullet}$OH]$_{ss}$ level correlated well with the TOrC degradation rates and scavenging rates (inversely correlated) for each pre-UV/H$_2$O$_2$ water quality scenario.

As discussed in section 3.1, differences in SUVA values (Table 1) indicate organic matter composition was changed as a result of tertiary effluent treatment. While $^{\bullet}$OH are widely recognized as a non-selective oxidant, studies have observed that $^{\bullet}$OH react more quickly with electron rich carbon–carbon double and triple bonds, as compared to aliphatic structures[24] and, in general, $^{\bullet}$OH reaction rates increase with increasing SUVA and molecular size of DOM.[36] To understand if $^{\bullet}$OH reactivity changed after tertiary effluent treatment, modeled [$^{\bullet}$OH]$_{ss}$ were calculated from literature k_{OH} values of scavengers and probe compounds (additional information provided in ESI†), and compared to the experimentally-determined [$^{\bullet}$OH]$_{ss}$ (Fig. S1†). Experimental [$^{\bullet}$OH]$_{ss}$ values of sequential biofiltration and CFSF aligned well with the modeled [$^{\bullet}$OH]$_{ss}$ (<7% difference between experimental and
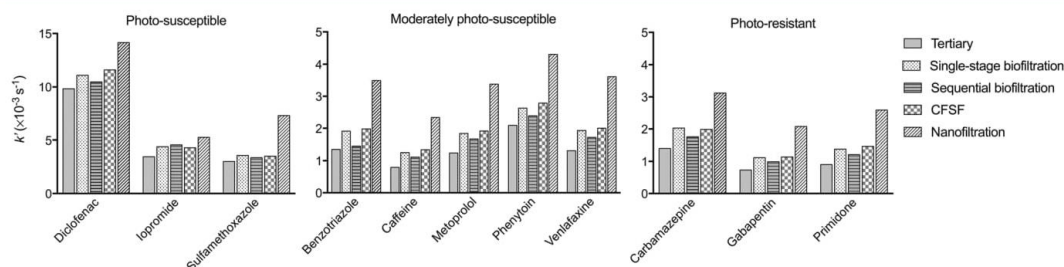
Fig. 3 Time-based pseudo first-order degradation rate constants of selected TOrCs (using an incident irradiance = 1.1 mW cm^{-2} and 10 mg L^{-1} H$_2$O$_2$). The y-axis was scaled to fit the data.
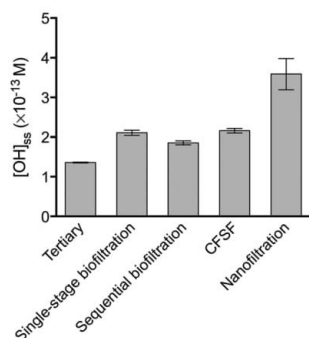
Fig. 4 Steady-state ·OH production determined using probe compounds primidone and carbamazepine with 10 mg L^{-1} H$_2$O$_2$. Error bars represent the standard deviation between probe compound results.

modeled values) and were below the percent difference (13%) between modeled and experimental [·OH]$_{ss}$ values for tertiary effluent. However, modeled [·OH]$_{ss}$ of single-stage biofiltration and nanofiltration were respectively 26% higher and 36% lower than experimental [·OH]$_{ss}$. These results suggest that organic matter reactivity, $k_{OH,DOC}$, may have increased after nanofiltration, as indicated by the 32% increase in SUVA, and decreased after single-stage biofiltration.

Whether the organic matter reactivity was changed as a result of treatment cannot be reliably determined from this analysis; in future work, it would be valuable to study organic matter reactivity as a function of wastewater treatment by employing more advanced characterization techniques (such as ^{13}C-NMR, FT-IR spectroscopy).

3.4 Comparison of UV and UV/H$_2$O$_2$ treatment

TOrC degradation was evaluated at UV exposure times (100 s and 600 s) resulting in UV doses of 100 ± 3 mJ cm^{-2} to 600 ± 20 mJ cm^{-2}, well below those typically used for UV/AOP applications. 100 mJ cm^{-2} represents a UV dose achievable by existing UV disinfection systems during average daily flow conditions and 600 mJ cm^{-2} represents the lower limit of UV design doses for UV/AOP applications. In Fig. 5, the average percent degradation of TOrCs after 100 s and 600 s of UV exposure, with and without H$_2$O$_2$ addition of 10 mg L^{-1}, is depicted for photo-susceptible, moderately photo-susceptible and photo-resistant compounds. Results from individual compounds are illustrated in Fig. S2.†

Treatment of tertiary effluent simultaneously reduced the concentration of ·OH scavengers and increased the UVT which resulted in improvement of the percent degradation of TOrCs by direct photolysis and oxidation. For example, after 100 s of UV exposure and with added H$_2$O$_2$, treatment of tertiary effluent increased the TOrC degradation by 77% ± 14% for photo-susceptible compounds, 89% ± 30% for moderately photo-susceptible compounds and 95 ± 40% for photo-resistant compounds (Fig. 5).

As expected and observed in past work,[16,18,45] photo-susceptible compounds were degraded more efficiently by UV photolysis than moderately photo-susceptible and photo-resistant compounds. After only 100 s of exposure, compounds were degraded by 29 to 43% and increased UV exposure (600 s) resulted in up to 100% degradation. In contrast, UV alone was not sufficient to degrade compounds with relatively low quantum yields or molar absorption coefficients (Table 2). Moderately photo-susceptible compounds were
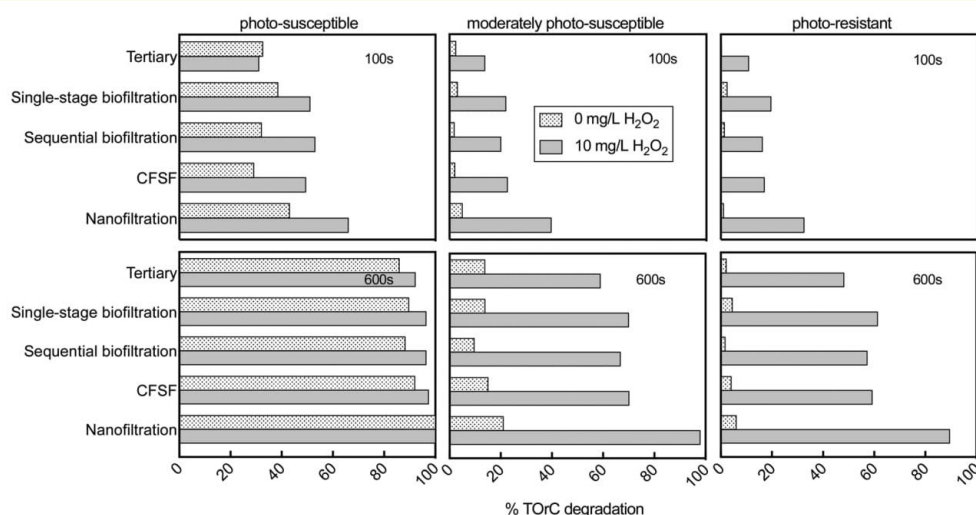
Fig. 5 Average percent degradation of TOrCs after 100 s and 600 s of UV exposure (incident irradiance 1.1 mW cm^{-2}) with and without 10 mg L^{-1} H$_2$O$_2$.

Paper

minimally degraded (<5% after 100 s, <21% after 600 s) and photo-resistant compounds were not removed. While past work[46] has demonstrated that the photolysis of DOM can produce ˙OH, our results indicate ˙OH were not being produced at detectible levels during UV exposure following any of the treatments, based on decay results for non-photolyzable compound gabapentin (additional information provided in ESI†). In addition to ˙OH, other reactive intermediates (*e.g.* singlet oxygen and excited triplet state DOM) can be generated during DOM photolysis,[47] however, these radicals were not measured in this study.

What can clearly be seen in Fig. 5 are the significant increases in the degradation profiles of moderately photo-susceptible and photo-resistant compounds because of ˙OH produced from the added H_2O_2. Importantly, without added H_2O_2, and at the exposure times studied herein, photo-resistant compounds would not have been significantly degraded. Lastly, few studies have evaluated the efficiency of low-pressure UV/H_2O_2 to degrade TOrCs in municipal wastewater using fluence values <300 mJ cm^{-2}.[17] While full degradation of the TOrC would require much higher UV doses, our results show that UV doses as low as 100 mJ cm^{-2} with added H_2O_2 can partially photolyze selected TOrCs in diverse wastewater matrices, produce ˙OH and potentially improve the treatment of tertiary effluent *via* TOrC degradation by UV/H_2O_2.

4 Broader impact

Apart from improved efficiency of UV/AOP for the degradation of TOrCs, there are several other advantages of 1) adding a treatment step prior to UV/AOP and 2) operating UV system at doses >100 mJ cm^{-2}. Additional treatment steps, such as biofiltration, CFSF, and nanofiltration, would provide another barrier against TOrCs and pathogens and thereby reduce their presence in wastewater effluent. From a regulatory standpoint, increasing the UV dose to above 186 mJ cm^{-2} can meet a 4 log virus requirement;[48] and filtration followed by UV disinfection at a design dose (often based on MS2 bioassay results) of 100 mJ cm^{-2} can meet California's Title 22 water recycling disinfection criteria of 5-log inactivation of viruses.[49] Lastly, improved water quality as a result of added treatment processes would potentially decrease operating costs of UV/AOP systems as shown in previous work.[17] In future studies, it would be worthwhile to conduct an economic analysis to determine if the savings in UV/AOP energy costs offset the cost of energy, chemicals, installation and equipment required for an additional treatment step before the UV/AOP system.

While the focus of this study was on evaluating strategies to improve UV/H_2O_2 performance in municipal wastewater, it is important to consider that toxicity levels may change after UV/H_2O_2 treatment of TOrCs and effluent organic matter. Reports on toxicity levels post UV/H_2O_2 treatment have been shown to vary based on the toxicity test used and site-specific water quality conditions.[50,51] Whether toxicity levels are decreased or increased from advanced oxidation treatment is under active investigation.

5 Conclusion

This study evaluated four treatment technologies as strategies to improve water quality for, and TOrC degradation during, UV and UV/H_2O_2 processes for TOrC degradation. Overall, treatment of tertiary effluent increased the UVT and decreased the concentration of radical scavengers which resulted in improved ˙OH production and degradation of targeted TOrCs. In comparing the four pretreatment technologies, nanofiltration treatment achieved the highest UVT, lowest scavenging demand and, subsequently, the highest ˙OH production and TOrC degradation rates. The scavenging rates of biofiltration and CFSF treatment were similar despite preferentially removing different scavengers: CFSF treatment reduced carbonate scavengers where as biofiltration decreased NO_2^- to levels below detection. Differences in SUVA values and modeled and experimental [˙OH]$_{ss}$ indicate treatment of tertiary effluent changed the organic matter composition and reactivity with ˙OH, however, more research is required to fully understand ˙OH reactivity of organic matter as a function of treatment. Finally, treatment of tertiary effluent helped increase removal of all TOrCs at UV doses well below those typically used for UV/AOP applications.

Conflicts of interest

There are no conflicts to declare.

Acknowledgements

Notes and references

1 Y. Luo, W. Guo, H. H. Ngo, L. D. Nghiem, F. I. Hai, J. Zhang, S. Liang and X. C. Wang, A Review on the Occurrence of Micropollutants in the Aquatic Environment and Their Fate and Removal during Wastewater Treatment, *Sci. Total Environ.*, 2014, 473–474, 619–641.

2 N. H. Tran, M. Reinhard and K. Y.-H. Gin, Occurrence and Fate of Emerging Contaminants in Municipal Wastewater Treatment Plants from Different Geographical Regions-a Review, *Water Res.*, 2018, 133, 182–207.

3 J. T. Yu, E. J. Bouwer and M. Coelhan, Occurrence and Biodegradability Studies of Selected Pharmaceuticals and

Personal Care Products in Sewage Effluent, *Agric. Water Manag.*, 2006, **86**(1–2), 72–80.

4 Y. Zhang, S.-U. Geißen and C. Gal, Carbamazepine and Diclofenac: Removal in Wastewater Treatment Plants and Occurrence in Water Bodies, *Chemosphere*, 2008, **73**(8), 1151–1161.

5 M. J. Benotti, R. A. Trenholm, B. J. Vanderford, J. C. Holady, B. D. Stanford and S. A. Snyder, Pharmaceuticals and Endocrine Disrupting Compounds in U.S. Drinking Water, *Environ. Sci. Technol.*, 2009, **43**(3), 597–603.

6 B. Subedi and B. Loganathan, Environmental Emission of Pharmaceuticals from Wastewater Treatment Plants in the U.S.A. in *ACS Symposium Series*, ed. B. G. Loganathan, J. S. Khim, P. R. S. Kodavanti and S. Masunaga, American Chemical Society, Washington, DC, 2016, vol. 1244, pp. 181–202.

7 EPA, *Clean Watersheds Needs Survey: Report to Congress 2012; EPA: 830-F-15-002*, Environmental Protection Agency, 2016.

8 J. Mateo-Sagasta, L. Raschid-Sally and A. Thebo, Global Wastewater and Sludge Production, Treatment and Use, in *Wastewater*, ed. P. Drechsel, M. Qadir and D. Wichelns, Springer Netherlands, Dordrecht, 2015, pp. 15–38.

9 R. P. Schwarzenbach, B. I. Escher, K. Fenner, T. B. Hofstetter, C. A. Johnson, U. von Gunten and B. Wehrli, The Challenge of Micropollutants in Aquatic Systems, *Science*, 2006, **313**(5790), 1068–1072.

10 J. Rice and P. Westerhoff, High Levels of Endocrine Pollutants in US Streams during Low Flow Due to Insufficient Wastewater Dilution, *Nat. Geosci.*, 2017, **10**(8), 587–591.

11 R. P. Schwarzenbach, P. M. Gschwend and D. M. Imboden, *Environmental Organic Chemistry*, Wiley, New York [u.a.], 2nd edn, 2003.

12 W. Yang, H. Zhou and N. Cicek, Treatment of Organic Micropollutants in Water and Wastewater by UV-Based Processes: A Literature Review, *Crit. Rev. Environ. Sci. Technol.*, 2014, **44**(13), 1443–1476.

13 J. C. Crittenden, S. Hu, D. W. Hand and S. A. Green, A Kinetic Model for H2O2/UV Process in a Completely Mixed Batch Reactor, *Water Res.*, 1999, **33**(10), 2315–2328.

14 O. S. Keen, G. McKay, S. P. Mezyk, K. G. Linden and F. L. Rosario-Ortiz, Identifying the Factors That Influence the Reactivity of Effluent Organic Matter with Hydroxyl Radicals, *Water Res.*, 2014, **50**, 408–419.

15 T. Sultan and J. Cho, Optimization of a UV/H$_2$O$_2$ AOP System Using Scavenger Radicals and Response Surface Methodology, *Chem. Eng. Commun.*, 2016, **203**(8), 1093–1104.

16 S. Giannakis, F. A. Gamarra Vives, D. Grandjean, A. Magnet, L. F. De Alencastro and C. Pulgarin, Effect of Advanced Oxidation Processes on the Micropollutants and the Effluent Organic Matter Contained in Municipal Wastewater Previously Treated by Three Different Secondary Methods, *Water Res.*, 2015, **84**, 295–306.

17 C. H. M. Hofman-Caris, W. G. Siegers, K. van de Merlen, A. W. A. de Man and J. A. M. H. Hofman, Removal of Pharmaceuticals from WWTP Effluent: Removal of EfOM Followed by Advanced Oxidation, *Chem. Eng. J.*, 2017, **327**, 514–521.

18 F. L. Rosario-Ortiz, E. C. Wert and S. A. Snyder, Evaluation of UV/H2O2 Treatment for the Oxidation of Pharmaceuticals in Wastewater, *Water Res.*, 2010, **44**(5), 1440–1448.

19 D. B. Miklos, R. Hartl, P. Michel, K. G. Linden, J. E. Drewes and U. Hübner, UV/H2O2 Process Stability and Pilot-Scale Validation for Trace Organic Chemical Removal from Wastewater Treatment Plant Effluents, *Water Res.*, 2018, **136**, 169–179.

20 J. Müller, J. E. Drewes and U. Hübner, Sequential Biofiltration – A Novel Approach for Enhanced Biological Removal of Trace Organic Chemicals from Wastewater Treatment Plant Effluent, *Water Res.*, 2017, **127**, 127–138.

21 J. R. Bolton and K. G. Linden, Standardization of Methods for Fluence (UV Dose) Determination in Bench-Scale UV Experiments, *J. Environ. Eng.*, 2003, **129**(3), 209–215.

22 S. L. Ulliman, G. McKay, F. L. Rosario-Ortiz and K. G. Linden, Low Levels of Iron Enhance UV/H2O2 Efficiency at Neutral PH, *Water Res.*, 2018, **130**(Supplement C), 234–242.

23 P. M. Nagarnaik and B. Boulanger, Advanced Oxidation of Alkylphenol Ethoxylates in Aqueous Systems, *Chemosphere*, 2011, **85**(5), 854–860.

24 G. V. Buxton, C. L. Greenstock, W. P. Helman, A. B. Ross and W. Tsang, Critical Review of Rate Constants for Reactions of Hydrated Electrons Chemical Kinetic Data Base for Combustion Chemistry. Part 3: Propane, *J. Phys. Chem. Ref. Data*, 1988, **17**(2), 513.

25 I. J. Buerge, T. Poiger, M. D. Müller and H.-R. Buser, Caffeine, an Anthropogenic Marker for Wastewater Contamination of Surface Waters, *Environ. Sci. Technol.*, 2003, **37**(4), 691–700.

26 C. G. Daughton and T. A. Ternes, Pharmaceuticals and Personal Care Products in the Environment: Agents of Subtle Change?, *Environ. Health Perspect.*, 1999, **107**(Suppl 6), 907.

27 P. C. Rúa-Gómez and W. Püttmann, Occurrence and Removal of Lidocaine, Tramadol, Venlafaxine, and Their Metabolites in German Wastewater Treatment Plants, *Environ. Sci. Pollut. Res.*, 2012, **19**(3), 689–699.

28 N. H. Tran, H. Chen, M. Reinhard, F. Mao and K. Y.-H. Gin, Occurrence and Removal of Multiple Classes of Antibiotics and Antimicrobial Agents in Biological Wastewater Treatment Processes, *Water Res.*, 2016, **104**, 461–472.

29 S. Weiss, J. Jakobs and T. Reemtsma, Discharge of Three Benzotriazole Corrosion Inhibitors with Municipal Wastewater and Improvements by Membrane Bioreactor Treatment and Ozonation, *Environ. Sci. Technol.*, 2006, **40**(23), 7193–7199.

30 O. S. Keen, N. G. Love and K. G. Linden, The Role of Effluent Nitrate in Trace Organic Chemical Oxidation during UV Disinfection, *Water Res.*, 2012, **46**(16), 5224–5234.

31 G. G. Jayson, B. J. Parsons and A. J. Swallow, Some Simple, Highly Reactive, Inorganic Chlorine Derivatives in Aqueous Solution. Their Formation Using Pulses of Radiation and Their Role in the Mechanism of the Fricke Dosimeter, *J. Chem. Soc., Faraday Trans. 1*, 1973, **69**(0), 1597.

Paper

32 T. N. Das, Reactivity and Role of $SO_5^{\cdot-}$ Radical in Aqueous Medium Chain Oxidation of Sulfite to Sulfate and Atmospheric Sulfuric Acid Generation, *J. Phys. Chem. A*, 2001, **105**(40), 9142–9155.

33 C.-H. Liao, S.-F. Kang and F.-A. Wu, Hydroxyl Radical Scavenging Role of Chloride and Bicarbonate Ions in the H2O2/UV Process, *Chemosphere*, 2001, **44**(5), 1193–1200.

34 B. A. Wols and C. H. M. Hofman-Caris, Review of Photochemical Reaction Constants of Organic Micropollutants Required for UV Advanced Oxidation Processes in Water, *Water Res.*, 2012, **46**(9), 2815–2827.

35 M. M. Dong, S. P. Mezyk and F. L. Rosario-Ortiz, Reactivity of Effluent Organic Matter (EfOM) with Hydroxyl Radical as a Function of Molecular Weight, *Environ. Sci. Technol.*, 2010, **44**(15), 5714–5720.

36 P. Westerhoff, G. Aiken, G. Amy and J. Debroux, Relationships between the Structure of Natural Organic Matter and Its Reactivity towards Molecular Ozone and Hydroxyl Radicals, *Water Res.*, 1999, **33**(10), 2265–2276.

37 M. Edwards, Predicting DOC Removal during Enhanced Coagulation, *Journal AWWA*, 1977, **89**(5), 78–89.

38 J. A. Korak, F. L. Rosario-Ortiz and R. Scott Summers, Evaluation of Optical Surrogates for the Characterization of DOM Removal by Coagulation, *Environ. Sci.: Water Res. Technol.*, 2015, **1**(4), 493–506.

39 A. M. Hansen, T. E. C. Kraus, B. A. Pellerin, J. A. Fleck, B. D. Downing and B. A. Bergamaschi, Optical Properties of Dissolved Organic Matter (DOM): Effects of Biological and Photolytic Degradation, *Limnol. Oceanogr.*, 2016, **61**(3), 1015–1032.

40 J. E. Drewes, M. Reinhard and P. Fox, Comparing Microfiltration-Reverse Osmosis and Soil-Aquifer Treatment for Indirect Potable Reuse of Water, *Water Res.*, 2003, **37**(15), 3612–3621.

41 C. Bellona and J. E. Drewes, The Role of Membrane Surface Charge and Solute Physico-Chemical Properties in the Rejection of Organic Acids by NF Membranes, *J. Membr. Sci.*, 2005, **249**(1), 227–234.

42 K. Boussu, B. Van der Bruggen, A. Volodin, C. Van Haesendonck, J. A. Delcour, P. Van der Meeren and C. Vandecasteele, Characterization of Commercial Nanofiltration Membranes and Comparison with Self-Made Polyethersulfone Membranes, *Desalination*, 2006, **191**(1–3), 245–253.

43 B. Xu, D.-P. Li, W. Li, S.-J. Xia, Y.-L. Lin, C.-Y. Hu, C.-J. Zhang and N.-Y. Gao, Measurements of Dissolved Organic Nitrogen (DON) in Water Samples with Nanofiltration Pretreatment, *Water Res.*, 2010, **44**(18), 5376–5384.

44 C. M. Sharpless and K. G. Linden, Experimental and Model Comparisons of Low- and Medium-Pressure Hg Lamps for the Direct and H_2O_2 Assisted UV Photodegradation of N-Nitrosodimethylamine in Simulated Drinking Water, *Environ. Sci. Technol.*, 2003, **37**(9), 1933–1940.

45 M. Neamțu, D. Grandjean, A. Sienkiewicz, S. Le Faucheur, V. Slaveykova, J. J. V. Colmenares, C. Pulgarín and L. F. de Alencastro, Degradation of Eight Relevant Micropollutants in Different Water Matrices by Neutral Photo-Fenton Process under UV254 and Simulated Solar Light Irradiation – A Comparative Study, *Appl. Catal., B*, 2014, **158–159**, 30–37.

46 M. M. Dong and F. L. Rosario-Ortiz, Photochemical Formation of Hydroxyl Radical from Effluent Organic Matter, *Environ. Sci. Technol.*, 2012, **46**(7), 3788–3794.

47 S. Canonica, U. Jans, K. Stemmler and K. Hoigne, Transformation Kinetics of Phenols in Water Photosensitization by Dissolved Organic Material and Aromatic Ketones, *Environ. Sci. Technol.*, 1995, **29**(7), 1822–1831.

48 EPA, *Occurance and Monitoring Document for the Final Ground Water Rule*, 2006, No. EPA 815-R-06-012.

49 *Ultraviolet Disinfection Guidelines for Drinking Water and Water Reuse*, National Water Research Institute, 3rd edn, 2012, www.NWRI-USA.org.

50 B. I. Escher, M. Allinson, R. Altenburger, P. A. Bain, P. Balaguer, W. Busch, J. Crago, N. D. Denslow, E. Dopp and K. Hilscherova, *et al.*, Benchmarking Organic Micropollutants in Wastewater, Recycled Water and Drinking Water with In Vitro Bioassays, *Environ. Sci. Technol.*, 2014, **48**(3), 1940–1956.

51 H. Mestankova, A. M. Parker, N. Bramaz, S. Canonica, K. Schirmer, U. von Gunten and K. G. Linden, Transformation of Contaminant Candidate List (CCL3) Compounds during Ozonation and Advanced Oxidation Processes in Drinking Water: Assessment of Biological Effects, *Water Res.*, 2016, **93**, 110–120.

52 B. A. Wols, D. J. H. Harmsen, E. F. Beerendonk and C. H. M. Hofman-Caris, Predicting Pharmaceutical Degradation by UV (LP)/H2O2 Processes: A Kinetic Model, *Chem. Eng. J.*, 2014, **255**, 334–343.

53 S. Canonica, L. Meunier and U. von Gunten, Phototransformation of Selected Pharmaceuticals during UV Treatment of Drinking Water, *Water Res.*, 2008, **42**(1), 121–128.

54 M. M. Huber, S. Canonica, G.-Y. Park and U. von Gunten, Oxidation of Pharmaceuticals during Ozonation and Advanced Oxidation Processes, *Environ. Sci. Technol.*, 2003, **37**(5), 1016–1024.

55 S. Bahnmüller, C. H. Loi, K. L. Linge, U. Gunten and S. Canonica, Degradation Rates of Benzotriazoles and Benzothiazoles under UV-C Irradiation and the Advanced Oxidation Process UV/H2O2, *Water Res.*, 2015, **74**, 143–154.

56 Y. Lee, L. Kovalova, C. S. McArdell and U. von Gunten, Prediction of Micropollutant Elimination during Ozonation of a Hospital Wastewater Effluent, *Water Res.*, 2014, **64**, 134–148.

9.7 Review on published reaction rate constants of TOrCs

Compound	CAS-N°	k_OH [M⁻¹s⁻¹]	Reference	Quantum yield (mol/E)	Molar absorption coefficient (m²/mol)	k_UV [m²/J]	Reference
1,2,3-trichlorobenzene	(87-61-6)	6.10E+09	Real et al., 2007	1.90E-01	3.08E+01	2.86E-05	Real et al., 2007
1,4-dichlorobenzene	(106-46-7)	7.95E+09	Wols and Hofman-Caris, 2012	6.00E-01	1.18E+01	3.46E-05	Real et al., 2007
2,4-Dichlorophenoxyacetic acid	(94-75-7)	3.24E+09	Wols and Hofman-Caris, 2012	9.50E-03	1.73E+01	8.03E-07	Benitez et al., 2004b
2,6-Dinitrotoluene	(606-20-2)	7.50E+08	Beltrán et al., 1998	2.20E-02	6.64E+02	7.14E-05	Beltrán et al., 1998
4-t-Octylphenol	(140-66-9)	4.20E+09	Błędzka et al., 2010	1.60E-02	6.75E+01	5.28E-06	Błędzka et al., 2010
5-Methyl-Benzotriazole	(136-85-6)	4.00E+09	Lutze, 2005				
Acenaphthene	(83-32-9)	8.80E+09	Beltrán et al., 1996	5.20E-02	1.22E+02	3.10E-05	Beltrán et al., 1996 Beltran et al., 1995
Acesulfam-K	(55589-62-3)	4.55E+09	Kaiser et al., 2013				
Acetovanillone	(498-02-2)	5.62E+09	Benitez et al., 2005	2.33E-02			Benitez et al., 2005
Acetylsulfamethoxazol	(21312-10-7)	6.80E+09	Dodd et al., 2006				
Alachlor	(15972-60-8)	5.30E+09	Wols and Hofman-Caris, 2012	1.48E-01	4.79E+01	3.47E-05	Wols and Hofman-Caris, 2012
Amoxicillin	(26787-78-0)	5.43E+09	Wols and Hofman-Caris, 2012	3.72E-01	1.20E+02	2.18E-04	Wols and Hofman-Caris, 2012
amidotrizoic acid	(117-96-4)	5.40E+08	Real et al., 2009				
Anthracene	(120-12-7)			1.49E-01	1.07E+02	7.79E-05	Wols and Hofman-Caris, 2012
Atenolol	(29122-68-7)	7.10E+09	Wols et al., 2014	6.50E-02	3.50E+01	1.11E-05	Wols et al., 2014

Compound	CAS-N°	k_{OH} $[M^{-1}s^{-1}]$	Reference	Quantum yield (mol/E)	Molar absorption coefficient (m²/mol)	k_{UV} $[m²/J]$	Reference
Atrazine	(1912-24-9)	5.00E+09	Wols et al., 2014	1.30E-02	2.40E+02	1.53E-05	Wols et al., 2014
Azithromycin	(83905-01-5)	2.90E+09	Dodd et al., 2006				
Bezafibrate	(41859-67-0)	7.40E+09	Huber et al., 2003				Wols et al., 2014
Benzene	(71-43-2)	6.72E+09	Real et al., 2007	8.80E-01	2.50E+01	1.08E-04	Wols and Hofman-Caris, 2012
Benzo[a]anthracene	(56-55-3)			1.21E-03	6.94E+03	4.11E-05	Lehto et al., 2000
Benzo[a]pyrene	(50-32-8)	2.51E+10	Wols and Hofman-Caris, 2012	1.64E-01	1.08E+02	8.66E-05	Wols and Hofman-Caris, 2012
Benzotriazole	(95-14-7)	9.90E+09	Hübner et al., 2015b	1.60E-02	6.14E+02	4.80E-05	Bahnmüller et al., 2015
Bis(2-ethylhexyl) phthalate	(117-81-7)	3.40E+08	Jin et al., 2012				
Bisphenol A	(80-05–7)	8.0E+09	Wols and Hofman-Caris, 2012	6.55E-03	7.50E+01	2.40E-06	Wols and Hofman-Caris, 2012
Boldenone	(846-48-0)			6.10E-01	1.46E+03	4.35E-03	Błędzka et al., 2010
Bromoxynil	(1689-84-5)		Chelme-Ayala et al., 2010b	4.00E-02	4.97E+02	9.72E-05	Chelme-Ayala et al., 2010a
Butachlor	(23184-66-9)	7.40E+09	Acero et al., 2003	8.20E-01	4.10E+01	1.64E-04	Benitez et al., 2004a
Butylbenzyl phthalate	(85-68-7)	4.00E+09	Jin et al., 2012				
Butylated hydroxyanisole	(25013-16-5)	7.40E+09	Jin et al., 2012				
Caffeine	(58-08-2)	6.40E+09	Wols and Hofman-Caris, 2012	1.80E-03	3.92E+02	3.45E-06	Rivas et al., 2011b
Carbamazepine	(298-46-4)	8.02E+09	Wols and Hofman-Caris, 2012	6.00E-04	6.07E+02	1.78E-06	Pereira et al., 2007b
Carbendazime	(10605-21-7)	2.20E+09	Mazellier et al., 2002a	2.30E-03	4.47E+02	5.03E-06	Mazellier et al., 2002b

Compound	CAS-N°	k_{OH} [M^{-1}s^{-1}]	Reference	Quantum yield (mol/E)	Molar absorption coefficient (m²/mol)	k_{UV} [m²/J]	Reference
Carbofuran	(1563-66-2)	2.46E+09	Wols and Hofman-Caris, 2012	1.66E-02	8.00E+01	6.49E-06	Benitez et al., 1995
Carbomethoxyfenitrothion	(54812-31-6)			8.40E-04	5.02E+02	2.06E-06	Wan et al., 1994
Chloramphenicol	(56-75-7)	5.80E+09	Zeegers et al., 1992	8.40E-02	4.33E+02	1.78E-04	Zhou et al., 2010
Chlorfenvinphos	(470-90-6)	1.09E+10	Wols and Hofman-Caris, 2012	7.25E-02	7.97E+02	2.82E-04	Wols and Hofman-Caris, 2012
Chlorotetracycline	(57-62-5)			2.95E-02	1.68E+03	2.42E-04	Wols and Hofman-Caris, 2012
Chlorotoluron	(15545-48-9)	4.30E+09	De Laat et al., 1996	3.19E-02	6.08E+02	9.48E-05	Benitez et al., 2006
Chlorpyrifos	(2921-88-2)	4.54E+09	Wols and Hofman-Caris, 2012	1.60E-02	6.50E+01	5.08E-06	Wan et al., 1994
Chrysene	(218-01–9)	9.82E+09	Ledakowicz et al., 1999	3.15E-03			Miller and Olejnik, 2001
Ciprofloxacin	(85721-33-1)	5.94E+09	Wols and Hofman-Caris, 2012	1.18E-02	1.72E+03	9.92E-05	Wols and Hofman-Caris, 2012
Citalopram	(59729-32-7)			2.60E-04	4.00E+02	5.08E-07	Kwon and Armbrust, 2005
Climbazole	(38083-17-9)			1.72E-01	6.16E+01	5.17E-05	Liu et al., 2016a
Clofibric acid	(882-09-7)	5.03E+09	Wols and Hofman-Caris, 2012	4.10E-01	3.50E+01	7.02E-05	Wols et al., 2015
Coumaphos	(56-72-4)			2.70E-03	2.40E+02	3.17E-06	Wan et al., 1994
Cortisol	(50-23-7)	8.0E+09	Wols et al., 2014	3.20E-02	1.60E+03	2.50E-04	Wols et al., 2014
Cortisone	(53-06-5)	6.30E+09	Wols et al., 2014	1.10E-02	1.40E+03	7.53E-05	Wols et al., 2014
Cyclophosphamide	(50-18-0)	3.20E+09	Wols et al., 2014	4.60E-02	3.10E-01	6.97E-08	Wols et al., 2014

Compound	CAS-N°	k_{OH} [$M^{-1}s^{-1}$]	Reference	Quantum yield (mol/E)	Molar absorption coefficient (m^2/mol)	k_{UV} [m^2/J]	Reference
DBCP (1,2-Dibrom-3-chlorpropane)	(96-12-8)	1.50E+08	Wols and Hofman-Caris, 2012	4.90E-01	1.50E+00	3.59E-06	Glaze et al., 1995
DNOC (2-Methyl-4,6-dinitrophenol)	(534-52-1)			4.80E-04	6.83E+02	1.60E-06	Wan et al., 1994
Desethylatrazine	(6190-65-4)	1.20E+09	Laat et al., 1994	5.90E-02	3.44E+02	9.92E-05	Nick et al., 1992
Desethyldesisopropylatrazine	(3397-62-4)	5.00E+07	Laat et al., 1994	1.80E-02	2.20E+02	1.94E-05	Nick et al., 1992
Desisopropylatrazine	(1007-28-9)	1.80E+09	Laat et al., 1994	5.90E-02	3.60E+02	1.04E-04	Nick et al., 1992
Diatrizoic acid	(737-31-5)	6.30E+08	Wols et al., 2014	3.90E-02	1.90E+03	3.62E-04	Wols et al., 2014
Diazinon	(333-41-5)	8.75E+09	Wols and Hofman-Caris, 2012	6.53E-02	2.94E+02	9.39E-05	Wols and Hofman-Caris, 2012
Dibenz[a,h]anthracene	(53-70-3)			2.22E-03	1.26E+03	1.37E-05	Lehto et al., 2000
Dicamba	(1918-00-9)	3.50E+09					
Diclofenac	(15307-86-5)	8.20E+09	Wols et al., 2014	2.30E-01	6.80E+02	7.65E-04	Wols et al., 2014
Dicofol	(115-32-2)	3.70E+09	Jin et al., 2012				
DEET	(134-62-3)	5.00E+09	Song et al., 2009				
Dimetridazole	(551-92-8)	5.60E+10	Sánchez-Polo et al., 2008	3.20E-03	2.24E+02	3.50E-06	Prados-Joya et al., 2011
Diphenhydramine	(147-24-0)	5.42E+09	Wols and Hofman-Caris, 2012	1.25E-01	3.88E+01	2.37E-05	Yuan et al., 2009
Disulfoton	(298-04-4)			1.60E-01	1.60E+01	1.25E-05	Zamy et al., 2004
Diuron	(330-54-1)	4.60E+09	De Laat et al., 1996	1.43E-02	1.61E+03	1.13E-04	Wols and Hofman-Caris, 2012
Doxycycline	(564-25-0)	7.74E+09	Wols and Hofman-Caris, 2012	1.15E-02	4.99E+03	2.81E-04	Wols and Hofman-Caris, 2012
EPN	(2104-64-5)			8.10E-03	4.36E+02	1.73E-05	Wan et al., 1994

Compound	CAS-N°	k_{OH} [M^{-1}s^{-1}]	Reference	Quantum yield (mol/E)	Molar absorption coefficient (m²/mol)	k_{UV} [m²/J]	Reference
Equilenin	(517-09-9)	1.70E+10	Jin et al., 2012				
Erythromycin	(114-07-8)	3.80E+09	Wols et al., 2014				
Estradiol (β) (E2)	(50-28-2)	1.41E+10	Rosenfeldt and Linden, 2004	5.50E-02	4.03E+01	1.08E-05	Wols and Hofman-Caris, 2012
Estriol (E3)	(50-27-1)				2.34E+01		Li Puma et al., 2010
Estrone (E1)	(53-16-7)				3.95E-02		Li Puma et al., 2010
(17a-)Ethinylestradiol EE2	(57-63-6)	9.80E+09	Huber et al., 2004	4.83E-02	1.04E+02	2.46E-05	Wols and Hofman-Caris, 2012
Etridiazole	(2593-15-9)			4.60E-01	7.20E+01	1.62E-04	Liu et al., 2009
Fenchlorfos	(299-84-3)			7.10E-01	6.35E+01	2.20E-04	Wan et al., 1994
Fenitrothion	(122-14-5)			9.10E-03	4.66E+02	2.07E-05	Wan et al., 1994
Fenoterol	(13392-18-2)	3.90E+09	Jin et al., 2012				
Fensulfothion	(115-90-2)			4.90E-02	1.74E+02	4.17E-05	Wan et al., 1994
Fenthion	(55-38-9)			9.20E-02	1.03E+03	4.63E-04	Wan et al., 1994
Fluoranthene	(206-44-0)			4.47E-01	3.11E+01	6.80E-05	Sanches et al., 2011
Fluorene	(86-73-7)	6.34E+09	Beltrán et al., 1996	5.65E-03	1.67E+03	4.61E-05	Wols and Hofman-Caris, 2012
Fluoxetine	(54910-89-3)	9.00E+09	Wols et al., 2014	4.10E-01	7.90E+01	1.58E-04	Wols et al., 2014
Furosemide	(54-31-9)	1.10E+10	Wols et al., 2014	2.20E-02	6.70E+02	7.21E-05	Wols et al., 2014
Gabapentin	(60142-96-3)	9.10E+09	Lee et al., 2014				
Geosmin	(19700-21-1)	1.40E+10	Wright, 2017				
Gemfibrozil	(25812-30-0)	6.80E+09	Shu et al., 2013	9.20E-02	3.70E+01	1.66E-05	Wols et al., 2014
Hexachlorobenzene	(118-74-1)	2.40E+08	Jin et al., 2012				
Hydrochlorothiazide	(58-93-5)	5.70E+09	Real et al., 2010	4.10E-02	6.65E+02	1.33E-04	Real et al., 2010
Ibuprofen	(15687-27-1)	7.04E+09	Wols and Hofman-Caris, 2012	1.92E-01	2.56E+01	2.40E-05	Yuan et al., 2009

Compound	CAS-N°	k_{OH} [M^{-1}s^{-1}]	Reference	Quantum yield (mol/E)	Molar absorption coefficient (m²/mol)	k_{UV} [m²/J]	Reference
Ifosfamide	(3778-73-2)	**3.60E+09**	Wols et al., 2014				
Imazalil	(35554-44-0)						
Iohexol	(66108-95-0)	**3.81E+09**	Pereira et al., 2007b	4.03E-02	2.76E+03	**5.44E-04**	Pereira et al., 2007b
Iomeprol	(78649-41-9)	**2.03E+09**	Cooper et al., 2010				
Iopamidol	(62883-00-5)	**2.80E+09**	Baus et al., 2005				
Iopromide	(73334-07-3)	**3.30E+09**	Huber et al., 2003	3.90E-02	2.10E+03	**4.00E-04**	Canonica et al., 2008
Isazofos	(42509-80-8)			2.70E-02	7.00E+00	**9.24E-07**	Zamy et al., 2004
Isofenfos	(25311-71-1)			4.95E-02	1.05E+02	**2.54E-05**	Wols and Hofman-Caris, 2012
Isoproturon	(34123-59-6)	**3.00E+09**	De Laat et al., 1996	2.85E-03	6.01E+02	**8.37E-06**	Wols and Hofman-Caris, 2012
Ketoprofen	(22071-15-4)	**1.50E+10**	Wols et al., 2014	2.20E-01	3.80E+03	**4.09E-03**	Wols et al., 2014
Ketorolac	(74103-06-3)			6.00E-03	6.54E+02	**1.92E-05**	Rivas et al., 2011b
Linuron	(330-55-2)	**4.30E+09**	De Laat et al., 1996	3.60E-02	1.34E+03	**2.36E-04**	Benitez et al., 2006
MCPA	(94-74-6)	**4.55E+09**	Wols and Hofman-Caris, 2012	1.50E-01	3.52E+01	**2.58E-05**	Benitez et al., 2004b
Mecoprop	(7085-19-0)	**1.90E+09**	Beltran et al., 1994				
Mefenamic acid	(61-68-7)	**4.00E+09**	Kimura et al., 2012		5.50E+02		Rivas et al., 2010
Methicillin	(61-32-5)	**1.00E+10**	Jin et al., 2012				
Methyl chlorpyrifos	(5598-13-0)			1.30E-02	6.10E+01	**3.88E-06**	Wan et al., 1994
Methyl parathion	(298-00-0)			4.30E-04	4.58E+02	**9.63E-07**	Wan et al., 1994
Metformin	(657-24-9)	**1.40E+09**	Wols et al., 2014	1.40E-02	9.40E+01	**6.43E-06**	Wols et al., 2014

Compound	CAS-N°	k_{OH} [$M^{-1}s^{-1}$]	Reference	Quantum yield (mol/E)	Molar absorption coefficient (m^2/mol)	k_{UV} [m^2/J]	Reference
Metolachlor	(51218-45-2)	**6.96E+09**	Wols and Hofman-Caris, 2012	4.55E-01	5.64E+01	**1.25E-04**	Wols and Hofman-Caris, 2012
Metoprolol	(56392-17-7)	**8.10E+09**	Wols et al., 2014	6.60E-02	3.30E+01	**1.06E-05**	Wols et al., 2014
Metoxuron	(19937-59-8)			2.00E-02			Boulkamh et al., 2001
Metronidazole	(443-48-1)	**5.00E+09**	Wols et al., 2014	1.00E-02	2.20E+02	**1.08E-05**	Wols et al., 2014
MTBE	(1634-04-4)	**1.90E+09**	Acero et al., 2001				
NDMA	(62-75-9)	**3.80E+08**	Wols and Hofman-Caris, 2012	2.48E-01	1.65E+02	**2.00E-04**	Wols and Hofman-Caris, 2012
Naproxen	(22204-53-1)	**1.00E+10**	Wols et al., 2014	1.40E-02	4.80E+02	**3.29E-05**	Wols et al., 2014
Niacin	(59-67-6)	**1.70E+09**	Wols et al., 2014				
Nitrobenzene	(98-95-3)	**3.40E+09**	Wols and Hofman-Caris, 2012	7.00E-03	5.56E+02	**1.90E-05**	Beltrán et al., 1998
Nonylphenol	(104-40-5)						
Norfloxacin	(70458-96-7)	**1.00E+09**	Rivas et al., 2011a	3.40E-03	1.54E+03	**2.56E-05**	Rivas et al., 2011a
Oxamyl	(23135-22-0)	**2.00E+09**	Haag and Yao, 1992	5.50E-01	5.32E+02	**1.43E-03**	Mazellier et al., 2002b
Oxalic acid	(144-62-7)	**1.40E+06**	Legube and Karpel Vel Leitner, 1999				
Oxytetracycline	(79-57-2)	**6.96E+09**	Yuan et al., 2011a	1.15E-02	1.58E+03	**8.88E-05**	Wols and Hofman-Caris, 2012
pCBA	(74-11-3)	**5.20E+09**	Yao and Haag, 1991	1.30E-02	2.37E+02	**1.51E-05**	Rosenfeldt and Linden, 2007
PFOA	(335-67-1)			1.00E-05			Park, 2010
PFOS	(1763-23-1)			1.70E-04			Park, 2010

Compound	CAS-N°	k_{OH} [M⁻¹s⁻¹]	Reference	Quantum yield (mol/E)	Molar absorption coefficient (m²/mol)	k_{UV} [m²/J]	Reference
Paracetamol/Acetaminophen	(103-90-2)	**5.85E+09**	Wols and Hofman-Caris, 2012	1.80E-03	6.64E+02	**5.84E-06**	Wols and Hofman-Caris, 2012
Parathion	(56-38-2)	**9.70E+09**	Wu and Linden, 2010	6.00E-04			Mok et al., 1987
Paroxetine	(61869-08-7)	**9.60E+09**	Wols et al., 2014	2.10E-01	2.50E+01	**2.57E-05**	Wols et al., 2014
Pentachlorophenol	(87-86-5)	**9.00E+09**	Sanches et al., 2010	2.50E-02	7.40E+02	**9.04E-05**	Sanches et al., 2010
Pentoxifylline	(6493-05-6)	**6.80E+09**	Wols et al., 2014	3.90E-03	4.40E+02	**8.39E-06**	Wols et al., 2014
Phenacetin	(62-44-2)	**4.00E+09**	Benitez et al., 2009	4.60E-03	9.10E+02	**2.05E-05**	Benitez et al., 2009
Phenanthrene	(85-01–8)	**1.34E+10**	Beltrán et al., 1996	6.90E-03	4.05E+03	**1.37E-04**	Beltrán et al., 1996 Beltran et al., 1995
Phenazone	(60-80-0)	**8.90E+09**	Wols et al., 2014	5.90E-02	8.90E+02	**2.57E-04**	Wols et al., 2014
Phenol	(108-95-2)	**1.03E+10**	Wols and Hofman-Caris, 2012	2.55E-02	7.50E+01	**9.35E-06**	Wols and Hofman-Caris, 2012
Phenytoin	(57-41-0)	**6.28E+09**	Yuan et al., 2009	2.79E-01	1.26E+02	**1.72E-04**	Yuan et al., 2009
Prednisolone	(50-24-8)	**1.60E+10**	Wols et al., 2014	1.30E-01	7.10E+03	**4.51E-03**	Wols et al., 2014
Primidone	(125-33-7)	**6.70E+09**	Real et al., 2009	8.20E-02	2.20E+01	**8.82E-06**	Real et al., 2009
Profenofos	(41198-08-7)			2.60E-02	4.60E+01	**5.85E-06**	Zamy et al., 2004
Progesterone	(57-83-0)			2.20E-02	1.70E+03	**1.83E-04**	Meite et al., 2010
Propachlor	(1918-16-7)	**4.45E+09**	Wols and Hofman-Caris, 2012	1.27E-01	4.21E+01	**2.61E-05**	Benitez et al., 2004a
Propazine	(139-40-2)	**1.65E+09**	Wols and Hofman-Caris, 2012	9.90E-02	3.37E+02	**1.63E-04**	Nick et al., 1992
Propranolol	(525-66-6)	**1.10E+10**	Wols et al., 2014	3.20E-02	1.30E+02	**2.03E-05**	Wols et al., 2014

Compound	CAS-N°	k_{OH} [M^{-1}s^{-1}]	Reference	Quantum yield (mol/E)	Molar absorption coefficient (m²/mol)	k_{UV} [m²/J]	Reference
Prothiofos	(34643-46-4)			1.10E+00	1.21E+01	6.51E-05	Wan et al., 1994
Pyrene	(129-00-0)	1.40E+09	Jin et al., 2012	3.85E-03	1.82E+03	3.43E-05	Lehto et al., 2000
Pyridaphenthion	(119-12-0)			3.20E-04	1.87E+02	2.93E-07	Wan et al., 1994
Ronidazole	(7681-76-7)	1.39E+10	Sánchez-Polo et al., 2008	2.21E-03	2.26E+02	2.44E-06	Prados-Joya et al., 2011
Roxithromycin	(80214-83-1)	5.40E+09	Dodd et al., 2006				
Simazine	(122-34-9)	2.90E+09	Wols and Hofman-Caris, 2012	8.30E-02	3.33E+02	1.35E-04	Nick et al., 1992
Sotalol	(3930-20-9)	7.90E+09	Wols et al., 2014	3.90E-01	3.70E+01	7.05E-05	Wols et al., 2014
Sulfachloropyridazine	(80-32-0)	1.10E+10	Wols et al., 2014	5.80E-03	2.20E+03	6.24E-05	Wols et al., 2014
Sulfadiazine	(68-35-9)	1.10E+10	Wols et al., 2014	4.80E-03	2.30E+03	5.40E-05	Wols et al., 2014
Sulfadimidine	(57-68-1)	6.32E+09	Wols and Hofman-Caris, 2012	8.70E-03	1.40E+03	5.95E-05	Wols and Hofman-Caris, 2012
Sulfamethazine	(57-68-1)	5.00E+09	Huber et al., 2003				
Sulfamethoxazole	(723-46-6)	6.30E+09	Wols et al., 2014	3.80E-02	1.30E+03	2.42E-04	Wols et al., 2014
Sulfapyridine	(144-83-2)						
Sulfaquinoxalin	(59-40-5)	1.10E+10	Wols et al., 2014	2.60E-03	3.90E+03	4.96E-05	Wols et al., 2014
TCEP	(51805-45-9)	5.60E+08	Watts and Linden, 2009				
Terbuthylazine	(5915-41-3)	2.80E+09	Laat et al., 1994	9.40E-02	3.83E+02	1.76E-04	Nick et al., 1992
Testosterone	(58-22-0)			3.30E-02	1.51E+03	2.44E-04	Meite et al., 2010
Tetracycline	(60-54-8)	7.70E+09	Dodd et al., 2006	3.80E-03	8.82E+02	1.64E-05	Wols and Hofman-Caris, 2012
Tinidazole	(19387-91-8)	4.50E+10	Sánchez-Polo et al., 2008	1.96E-03	2.34E+02	2.24E-06	Prados-Joya et al., 2011
Tolclofos	(57018-04–9)			1.70E-02	7.74E+01	6.43E-06	Wan et al., 1994

Compound	CAS-N°	k_{OH} [M^{-1}s^{-1}]	Reference	Quantum yield (mol/E)	Molar absorption coefficient (m²/mol)	k_{UV} [m²/J]	Reference
Toluene	(108-88-3)						
Tramadol	(27203-92-5)	**6.30E+09**	Zimmermann et al., 2012				
Trenbolone	(10161-33-8)	**4.30E+09**	Błędzka et al., 2010		2.90E-03	**6.30E+02**	Gryglik et al., 2010
Trichloroethylene	(79-01–6)	**2.90E+09**	Getoff, 1991	3.54E-01			Li et al., 2004
Triclosan	(3380-34-5)	**6.00E+09**	Jin et al., 2012				
Trifluralin	(1582-09-8)	**1.30E+09**	Jin et al., 2012	6.00E-01	4.97E+02	**1.46E-03**	Chelme-Ayala et al., 2010a
Trimethoprim	(738-70-5)	**8.00E+09**	Wols et al., 2014	9.00E-04	1.60E+03	**7.04E-06**	Wols et al., 2014
Triphenyl phoshate	(115-86-6)			2.90E-01	6.44E+01	**9.13E-05**	Wan et al., 1994
Triphenyltin hydroxide	(76-87-9)	**9.40E+09**	Palm et al., 2003	1.25E+00	5.82E+01	**3.56E-04**	Palm et al., 2003
m-cresol	(203-39-4)			5.70E-02	3.02E+01	**8.42E-06**	Wan et al., 1994
m-nitrophenol	(554-84-7)			1.90E-04	3.41E+02	**3.17E-07**	Wan et al., 1994
n-Butylparaben	(94-26-8)	**4.80E+09**	Błędzka et al., 2010	3.30E-03	1.54E+03	**2.48E-05**	Błędzka et al., 2010
o-nitrophenol	(88-75-5)			2.00E-03	4.31E+02	**4.21E-06**	Wan et al., 1994
Valsartan	(137862-53-4)	**1.00E+11**	Lee et al., 2014				
Venlafaxin	(93413-69-5)	**8.80E+09**	Wols et al., 2014	9.70E-02	3.80E+01	**1.80E-05**	Wols et al., 2014

References

Abdelmelek, S.B., Greaves, J., Ishida, K.P., Cooper, W.J., Song, W., 2011. Removal of pharmaceutical and personal care products from reverse osmosis retentate using advanced oxidation processes. Environmental Science & Technology 45 (8), 3665–3671.

Abdessamad, N., Akrout, H., Bousselmi, L., 2015. Anodic oxidation of textile wastewaters on boron-doped diamond electrodes. Environmental Technology 36 (24), 3201–3209.

Acero, J.L., Benitez, F.J., Real, F.J., Maya, C., 2003. Oxidation of Acetamide Herbicides in Natural Waters by Ozone and by the Combination of Ozone/Hydrogen Peroxide: Kinetic Study and Process Modeling. Industrial & Engineering Chemistry Research 42 (23), 5762–5769.

Acero, J.L., Haderlein, S.B., Schmidt, T.C., Suter, M.J.-F., Gunten, U. von, 2001. MTBE Oxidation by Conventional Ozonation and the Combination Ozone/Hydrogen Peroxide: Efficiency of the Processes and Bromate Formation. Environmental Science & Technology 35 (21), 4252–4259.

Ahn, Y., Lee, D., Kwon, M., Choi, I.-H., Nam, S.-N., Kang, J.-W., 2017. Characteristics and fate of natural organic matter during UV oxidation processes. Chemosphere 184, 960–968.

Alaton, I.A., Balcioglu, I.A., Bahnemann, D.W., 2002. Advanced oxidation of a reactive dyebath effluent: Comparison of O3, H2O2/UV-C and TiO2/UV-A processes. Water Research 36 (5), 1143–1154.

Altmann, J., Massa, L., Sperlich, A., Gnirss, R., Jekel, M., 2016. UV254 absorbance as real-time monitoring and control parameter for micropollutant removal in advanced wastewater treatment with powdered activated carbon. Water Research.

Altmann, J., Ruhl, A.S., Zietzschmann, F., Jekel, M., 2014. Direct comparison of ozonation and adsorption onto powdered activated carbon for micropollutant removal in advanced wastewater treatment. Water Research 55, 185–193.

Andrzejewski, P., Kasprzyk-Hordern, B., Nawrocki, J., 2008. N-nitrosodimethylamine (NDMA) formation during ozonation of dimethylamine-containing waters. Water Research 42 (4-5), 863–870.

Anipsitakis, G.P., 2005. Cobalt/peroxymonosulfate and related oxidizing reagents for water treatment: Doctoral dissertation. University of Cincinnati, Cincinnati.

Antoniou, M.G., La Cruz, A.A. de, Dionysiou, D.D., 2010. Degradation of microcystin-LR using sulfate radicals generated through photolysis, thermolysis and e– transfer mechanisms. Applied Catalysis B: Environmental 96 (3-4), 290–298.

Anumol, T., Sgroi, M., Park, M., Roccaro, P., Snyder, S.A., 2015. Predicting trace organic compound breakthrough in granular activated carbon using fluorescence and UV absorbance as surrogates. Water Research 76, 76–87.

Ao, X., Liu, W., 2016. Degradation of sulfamethoxazole by medium pressure UV and oxidants: Peroxymonosulfate, persulfate, and hydrogen peroxide. Chemical Engineering Journal.

Armijos-Alcocer, K.G., Espinoza-Montero, P.J., Frontana-Uribe, B.A., Barrera-Diaz, C.E., Nevárez-Martínez, M.C., Fierro-Naranjo, G.C., 2017. Electrochemical Degradation of Nonylphenol Ethoxylate-7 (NP7EO) Using a DiaClean® Cell Equipped with Boron-Doped Diamond Electrodes (BDD). Water Air Soil Pollut 228 (8), 1131.

Audenaert, W.T.M., Vandierendonck, D., van Hulle, S.W.H., Nopens, I., 2013. Comparison of ozone and HO· induced conversion of effluent organic matter (EfOM) using ozonation and UV/H2O2 treatment. Water Research 47 (7), 2387–2398.

Audenaert, W.T.M., Vermeersch, Y., van Hulle, S.W.H., Dejans, P., Dumoulin, A., Nopens, I., 2011. Application of a mechanistic UV/hydrogen peroxide model at full-scale: Sensitivity analysis, calibration and performance evaluation. Chemical Engineering Journal 171 (1), 113–126.

Autin, O., Romelot, C., Rust, L., Hart, J., Jarvis, P., MacAdam, J., Parsons, S.A., Jefferson, B., 2013. Evaluation of a UV-light emitting diodes unit for the removal of micropollutants in water for low energy advanced oxidation processes. Chemosphere 92 (6), 745–751.

Bae, W., Won, H., Hwang, B., Toledo, R.A. de, Chung, J., Kwon, K., Shim, H., 2015. Characterization of refractory matters in dyeing wastewater during a full-scale Fenton process following pure-oxygen activated sludge treatment. Journal of Hazardous Materials 287, 421–428.

Bagastyo, A.Y., Batstone, D.J., Kristiana, I., Gernjak, W., Joll, C., Radjenovic, J., 2012. Electrochemical oxidation of reverse osmosis concentrate on boron-doped diamond anodes at circumneutral and acidic pH. Water Research 46 (18), 6104–6112.

Bahnmüller, S., Loi, C.H., Linge, K.L., von Gunten, U., Canonica, S., 2015. Degradation rates of benzotriazoles and benzothiazoles under UV-C irradiation and the advanced oxidation process UV/H2O2. Water Research 74, 143–154.

Bahr, C., Schumacher, J., Ernst, M., Luck, F., Heinzmann, B., Jekel, M., 2007. SUVA as control parameter for the effective ozonation of organic pollutants in secondary effluent. Water Science and Technology 55 (12), 267.

Bahram, M., Bro, R., Stedmon, C., Afkhami, A., 2006. Handling of Rayleigh and Raman scatter for PARAFAC modeling of fluorescence data using interpolation. J. Chemometrics 20 (3-4), 99–105.

Bai, Z., Yang, Q., Wang, J., 2016. Catalytic ozonation of sulfamethazine antibiotics using Ce0.1Fe0.9OOH: Catalyst preparation and performance. Chemosphere 161, 174–180.

Barbosa, M.O., Moreira, N.F.F., Ribeiro, A.R., Pereira, M.F.R., Silva, A.M.T., 2016. Occurrence and removal of organic micropollutants: An overview of the watch list of EU Decision 2015/495. Water Research 94, 257–279.

Baus, C., Brauch, J.H., Schick, R., Hörner, D., 2005. Removal of Iodinated X-Ray Contrast Media by Ozonation-A Lab Scale and Pilot Scale Investigation. Conference Proceedings of the World congress and exibition of the International Ozone Association, IOA, 17, Strasbourg.

Baus, C., Ehmann, M., Graf, C., Sacher, F., Muriel, S., Thoma, A., Bergheim, M., Günther, A., Hädrich, C., Trautwein, C., 2008. Pharmaceuticals in the aquatic

environment - Identification and assessment of sources and measures to reduce inputs for the protection of drinking water, using the Freiburg region as an example (Arzneimittel in der aquatischen Umwelt–Identifizierung und Bewertung von Quellen und Maßnahmen zur Reduzierung der Einträge für den Schutz des Trinkwassers am Beispiel der Region Freiburg). University Hospital Freiburg; DVGW Water Technology Centre, Karlsruhe.

Baycan, N., Thomanetz, E., Sengül, F., 2007. Influence of chloride concentration on the formation of AOX in UV oxidative system. Journal of Hazardous Materials 143 (1-2), 171–176.

Bazri, M.M., Barbeau, B., Mohseni, M., 2012. Impact of UV/H_2O_2 advanced oxidation treatment on molecular weight distribution of NOM and biostability of water. Water Research 46 (16), 5297–5304.

Behnajady, M.A., Vahid, B., 2016. Development of an Empirical Kinetics Model for Sono-Degradation of Malachite Green: Evaluation of Electrical Energy Per Order. Jundishapur Journal of Health Sciences 8 (1).

Bejan, D., Malcolm, J.D., Morrison, L., Bunce, N.J., 2009. Mechanistic investigation of the conductive ceramic Ebonex® as an anode material. Electrochimica Acta 54 (23), 5548–5556.

Belhaj, D., Baccar, R., Jaabiri, I., Bouzid, J., Kallel, M., Ayadi, H., Zhou, J.L., 2015. Fate of selected estrogenic hormones in an urban sewage treatment plant in Tunisia (North Africa). The Science of the total environment 505, 154–160.

Beltran, F.J., Gonzalez, M., Rivas, J., Marin, M., 1994. Oxidation of mecoprop in water with ozone and ozone combined with hydrogen peroxide. Industrial & Engineering Chemistry Research 33 (1), 125–136.

Beltran, F.J., Ovejero, G., Garcia-Araya, J.F., Rivas, J., 1995. Oxidation of Polynuclear Aromatic Hydrocarbons in Water. 2. UV Radiation and Ozonation in the Presence of UV Radiation. Ind. Eng. Chem. Res. 34 (5), 1607–1615.

Beltrán, F.J., 2004. Ozone reaction kinetics for water and wastewater systems. Lewis Publishers, Boca Raton, Fla.

Beltrán, F.J., Encinar, J.M., Alonso, M.A., 1998. Nitroaromatic Hydrocarbon Ozonation in Water. 2. Combined Ozonation with Hydrogen Peroxide or UV Radiation. Industrial & Engineering Chemistry Research 37 (1), 32–40.

Beltrán, F.J., Ovejero, G., Rivas, J., 1996. Oxidation of Polynuclear Aromatic Hydrocarbons in Water. 3. UV Radiation Combined with Hydrogen Peroxide. Industrial & Engineering Chemistry Research 35 (3), 883–890.

Benitez, F.J., Acero, J.L., Real, F.J., Maya, C., 2004a. Modeling of photooxidation of acetamide herbicides in natural waters by UV radiation and the combinations UV/H2O2 and UV/O3. Journal of Chemical Technology & Biotechnology 79 (9), 987–997.

Benitez, F.J., Acero, J.L., Real, F.J., Roman, S., 2004b. Oxidation of MCPA and 2,4- d by UV Radiation, Ozone, and the Combinations UV/H2O2 and O3 /H2O2. Journal of Environmental Science and Health, Part B 39 (3), 393–409.

Benitez, F.J., Beltran-Heredia, J., Gonzalez, T., Real, A.F., 1995. Photooxidation of Carbofuran by a Polychromatic UV Irradiation without and with Hydrogen Peroxide. Industrial & Engineering Chemistry Research 34 (11), 4099–4105.

Benitez, F.J., Real, F., Acero, J., Garcia, C., 2006. Photochemical oxidation processes for the elimination of phenyl-urea herbicides in waters. Journal of Hazardous Materials 138 (2), 278–287.

Benitez, F.J., Real, F.J., Acero, J.L., Leal, A.I., Cotilla, S., 2005. Oxidation of acetovanillone by photochemical processes and hydroxyl radicals. Journal of Environmental Science and Health, Part A 40 (12), 2153–2169.

Benitez, F.J., Real, F.J., Acero, J.L., Roldan, G., 2009. Removal of selected pharmaceuticals in waters by photochemical processes. Journal of Chemical Technology and Biotechnology 84 (8), 1186–1195.

Benito, A., Penadés, A., Lliberia, J.L., Gonzalez-Olmos, R., 2017. Degradation pathways of aniline in aqueous solutions during electro-oxidation with BDD electrodes and UV/H2O2 treatment. Chemosphere 166, 230–237.

Benotti, M.J., Trenholm, R.A., Vanderford, B.J., Holady, J.C., Stanford, B.D., Snyder, S.A., 2009. Pharmaceuticals and Endocrine Disrupting Compounds in U.S. Drinking Water. Environ. Sci. Technol. 43 (3), 597–603.

Bergmann, M.E.H., Iourtchouk, T., Rollin, J., 2011. The occurrence of bromate and perbromate on BDD anodes during electrolysis of aqueous systems containing bromide: First systematic experimental studies. Journal of Applied Electrochemistry 41 (9), 1109–1123.

Bergmann, M.H., Rollin, J., 2007. Product and by-product formation in laboratory studies on disinfection electrolysis of water using boron-doped diamond anodes. Catalysis Today 124 (3-4), 198–203.

Bewersdorf, I., 2005. Investigations on the effect of boron-doped diamond electrodes for advanced water treatment. Diploma thesis submitted at the Technical University of Berlin, Department of Water Quality Control, Berlin.

Blake, D.M., 2001. Bibliography of work on the heterogeneous photocatalytic removal of hazardous compounds from water and air (NREL/TP-510-31319). National Renewable Energy Laboratory, Colorado.

Błędzka, D., Gmurek, M., Gryglik, M., Olak, M., Miller, J.S., Ledakowicz, S., 2010. Photodegradation and advanced oxidation of endocrine disruptors in aqueous solutions. Catalysis Today 151 (1-2), 125–130.

Blum, K.M., Norstrom, S.H., Golovko, O., Grabic, R., Jarhult, J.D., Koba, O., Soderstrom Lindstrom, H., 2017. Removal of 30 active pharmaceutical ingredients in surface water under long-term artificial UV irradiation. Chemosphere 176, 175–182.

Bo, L., Quan, X., Chen, S., Zhao, H., Zhao, Y., 2006. Degradation of p-nitrophenol in aqueous solution by microwave assisted oxidation process through a granular activated carbon fixed bed. Water Research 40 (16), 3061–3068.

Böhm, B., 2002. Nitrite formation during denitrification in biofilters with external carbon sources (Nitritbildung bei der Denitrifikation in Biofiltern mit externen Kohlenstoffquellen). Dissertation, Technichal University of Munich (TUM), Germany.

Bokare, A.D., Choi, W., 2014. Review of iron-free Fenton-like systems for activating H2O2 in advanced oxidation processes. Journal of Hazardous Materials 275, 121–135.

Bolton, J.R., Bircher, K.G., Tumas, W., Tolman, C.A., 1996. Figures-of merit for the technical development and application of advanced oxidation processes. Journal of Advanced Oxidation Technologies 1, 13–17.

Bolton, J.R., Bircher, K.G., Tumas, W., Tolman, C.A., 2001. Figures-of-merit for the technical development and application of advanced oxidation technologies for both electric- and solar-driven systems (IUPAC Technical Report). Pure and Applied Chemistry 73 (4).

Bolton, J.R., Linden, K.G., 2003. Standardization of Methods for Fluence (UV Dose) Determination in Bench-Scale UV Experiments. Journal of Environmental Engineering 129 (3), 209–215.

Bolton, J.R., Stefan, M.I., 2002. Fundamental photochemical approach to the concepts of fluence (UV dose) and electrical energy efficiency in photochemical degradation reactions. Research on Chemical Intermediates 28 (7-9), 857–870.

Bolton, J.R., Valladares, J.E., Zanin, J.P., Cooper, W.J., Nickelsen, M.G., Kajdi, D.C., Waite, Kurucz, C.N., 1998. Figures-of-Merit for Advanced Oxidation Technologies: A Comparison of Homogeneous UV/H2O2, Heterogeneous UV/TiO2 and Electron Beam Processes. Journal of Advanced Oxidation Technologies 3 (2), 174–181.

Bonfatti, F., 1999. Electrochemical Incineration of Glucose as a Model Organic Substrate. I. Role of the Electrode Material. Journal of The Electrochemical Society 146 (6), 2175.

Bonnefille, B., Gomez, E., Courant, F., Escande, A., Fenet, H., 2018. Diclofenac in the marine environment: A review of its occurrence and effects. Marine pollution bulletin 131 (Pt A), 496–506.

Boulkamh, A., Harakat, D., Sehili, T., Boule, P., 2001. Phototransformation of metoxuron [3-(3-chloro-4-methoxyphenyl)-1,1-dimethylurea] in aqueous solution. Pest Management Science 57 (12), 1119–1126.

Bourgeois, W., Burgess, J.E., Stuetz, R.M., 2001. On-line monitoring of wastewater quality: A review. J. Chem. Technol. Biotechnol. 76 (4), 337–348.

Bourgin, M., Beck, B., Boehler, M., Borowska, E., Fleiner, J., Salhi, E., Teichler, R., Gunten, U. von, Siegrist, H., McArdell, C.S., 2018. Evaluation of a full-scale wastewater treatment plant upgraded with ozonation and biological post-treatments: Abatement of micropollutants, formation of transformation products and oxidation by-products. Water Research 129, 486–498.

Bourgin, M., Borowska, E., Helbing, J., Hollender, J., Kaiser, H.-P., Kienle, C., McArdell, C.S., Simon, E., von Gunten, U., 2017. Effect of operational and water quality parameters on conventional ozonation and the advanced oxidation process O3/H2O2: Kinetics of micropollutant abatement, transformation product and bromate formation in a surface water. Water Research 122, 234–245.

Braslavsky, S.E., 2007. Glossary of terms used in photochemistry, 3rd edition (IUPAC Recommendations 2006). Pure and Applied Chemistry 79 (3), 293–465.

Brausch, J.M., Connors, K.A., Brooks, B.W., Rand, G.M., 2012. Human pharmaceuticals in the aquatic environment: A review of recent toxicological studies and considerations for toxicity testing. Reviews of environmental contamination and toxicology 218, 1–99.

Brodin, T., Fick, J., Jonsson, M., Klaminder, J., 2013. Dilute concentrations of a psychiatric drug alter behavior of fish from natural populations. Science 339 (6121), 814–815.

Brun, G.L., Bernier, M., Losier, R., Doe, K., Jackman, P., Lee, H.-B., 2006. Pharmaceutically active compounds in atlantic canadian sewage treatment plant effluents and receiving waters, and potential for environmental effects as measured by acute and chronic aquatic toxicity. Environmental Toxicology and Chemistry 25 (8), 2163.

Buchanan, W., Roddick, F., Porter, N., 2006. Formation of hazardous by-products resulting from the irradiation of natural organic matter: Comparison between UV and VUV irradiation. Chemosphere 63 (7), 1130–1141.

Buffle, M.-O., Schumacher, J., Meylan, S., Jekel, M., von Gunten, U., 2006. Ozonation and Advanced Oxidation of Wastewater: Effect of O3 Dose, pH, DOM and HO• - Scavengers on Ozone Decomposition and HO• Generation. Ozone: Science & Engineering 28 (4), 247–259.

Buffle, M.-O., von Gunten, U., 2006. Phenols and Amine Induced HO• Generation During the Initial Phase of Natural Water Ozonation. Environmental Science & Technology 40 (9), 3057–3063.

Burns, J.M., Cooper, W.J., Ferry, J.L., King, D.W., DiMento, B.P., McNeill, K., Miller, C.J., Miller, W.L., Peake, B.M., Rusak, S.A., Rose, A.L., Waite, T.D., 2012. Methods for reactive oxygen species (ROS) detection in aqueous environments. Aquatic Sciences 74 (4), 683–734.

Bustillo-Lecompte, C.F., Ghafoori, S., Mehrvar, M., 2016. Photochemical degradation of an actual slaughterhouse wastewater by continuous UV/H2O2 photoreactor with recycle. Journal of Environmental Chemical Engineering 4 (1), 719–732.

Buxton, G.V., Greenstock, C.L., Helman, W.P., Ross, A.B., Tsang, W., 1988. Critical Review of rate constants for reactions of hydrated electrons, hydrogen atoms and hydroxyl radicals (·OH/·O−) in Aqueous Solution. Journal of Physical and Chemical Reference Data 17 (2), 513.

Calderara, V., Jekel, M., Zaror, C., 2002. Ozonation of 1-naphthalene, 1,5-naphthalene, and 3-nitrobenzene sulphonic acids in aqueous solutions. Environmental Technology 23 (4), 373–380.

Canonica, S., Hellrung, B., Müller, P., Wirz, J., 2006. Aqueous Oxidation of Phenylurea Herbicides by Triplet Aromatic Ketones. Environmental Science & Technology 40 (21), 6636–6641.

Canonica, S., Meunier, L., von Gunten, U., 2008. Phototransformation of selected pharmaceuticals during UV treatment of drinking water. Water Research 42 (1-2), 121–128.

Cardoso, J.C., Bessegato, G.G., Boldrin Zanoni, M.V., 2016. Efficiency comparison of ozonation, photolysis, photocatalysis and photoelectrocatalysis methods in real textile wastewater decolorization. Water Research 98, 39–46.

Carvajal, G., Branch, A., Michel, P., Sisson, S.A., Roser, D.J., Drewes, J.E., Khan, S.J., 2017a. Robust evaluation of performance monitoring options for ozone disinfection in water recycling using Bayesian analysis. Water Research 124, 605–617.

Carvajal, G., Roser, D.J., Sisson, S.A., Keegan, A., Khan, S.J., 2017b. Bayesian belief network modelling of chlorine disinfection for human pathogenic viruses in municipal wastewater. Water Research 109, 144–154.

Cater, S.R., Stefan, M.I., Bolton, J.R., Safarzadeh-Amiri, A., 2000. UV/H2O2 Treatment of Methyl tert -Butyl Ether in Contaminated Waters. Environmental Science & Technology 34 (4), 659–662.

Cedat, B., Brauer, C. de, Metivier, H., Dumont, N., Tutundjan, R., 2016. Are UV photolysis and UV/H2O2 process efficient to treat estrogens in waters? Chemical and biological assessment at pilot scale. Water Research 100, 357–366.

Chang, T.-B., Lin, T.-M., 2014. Water and energy conservation for a counterflow cooling tower using UV light disinfection and variable speed fan. Proceedings of the Institution of Mechanical Engineers, Part E: Journal of Process Mechanical Engineering 230 (3), 235–243.

Chaplin, B.P., 2014. Critical review of electrochemical advanced oxidation processes for water treatment applications. Environmental Science. Processes & Impacts 16 (6), 1182–1203.

Chaplin, B.P., Hubler, D.K., Farrell, J., 2013. Understanding anodic wear at boron doped diamond film electrodes. Electrochimica Acta 89, 122–131.

Chelme-Ayala, P., El-Din, M.G., Smith, D.W., 2010a. Degradation of bromoxynil and trifluralin in natural water by direct photolysis and UV plus H2O2 advanced oxidation process. Water Research 44 (7), 2221–2228.

Chelme-Ayala, P., El-Din, M.G., Smith, D.W., 2010b. Kinetics and mechanism of the degradation of two pesticides in aqueous solutions by ozonation. Chemosphere 78 (5), 557–562.

Chen, J., Loeb, S., Kim, J.-H., 2017. LED revolution: Fundamentals and prospects for UV disinfection applications. Environmental Science: Water Research & Technology 3 (2), 188–202.

Chen, W., Westerhoff, P., Leenheer, J.A., Booksh, K., 2003. Fluorescence Excitation?: Emission Matrix Regional Integration to Quantify Spectra for Dissolved Organic Matter. Environmental Science & Technology 37 (24), 5701–5710.

Cheng, H., Song, D., Chang, Y., Liu, H., Qu, J., 2015. Chlorination of tramadol: Reaction kinetics, mechanism and genotoxicity evaluation. Chemosphere 141, 282–289.

Chu, W., Gao, N., Yin, D., Krasner, S.W., Mitch, W.A., 2014. Impact of UV/H2O2 pre-oxidation on the formation of haloacetamides and other nitrogenous disinfection byproducts during chlorination. Environmental Science & Technology 48 (20), 12190–12198.

Chu, W., Li, D., Gao, N., Templeton, M.R., Tan, C., Gao, Y., 2015. The control of emerging haloacetamide DBP precursors with UV/persulfate treatment. Water Research 72, 340–348.

Chu, X., Xiao, Y., Hu, J., Quek, E., Xie, R., Pang, T., Xing, Y., 2016. Pilot-scale UV/H2O2 study for emerging organic contaminants decomposition. Reviews on Environmental Health 31 (1), 71–74.

Chys, M., Audenaert, W.T.M., Deniere, E., Mortier, S.T.F.C., van Langenhove, H., Nopens, I., Demeestere, K., van Hulle, S.W.H., 2017. Surrogate-Based Correlation

Models in View of Real-Time Control of Ozonation of Secondary Treated Municipal Wastewater-Model Development and Dynamic Validation. Environmental Science & Technology 51 (24), 14233–14243.

Chys, M., Demeestere, K., Nopens, I., Audenaert, W.T.M., van Hulle, S.W.H., 2018. Municipal wastewater effluent characterization and variability analysis in view of an ozone dose control strategy during tertiary treatment: The status in Belgium. Science of The Total Environment 625, 1198–1207.

Cizmas, L., Sharma, V.K., Gray, C.M., McDonald, T.J., 2015. Pharmaceuticals and personal care products in waters: Occurrence, toxicity, and risk. Environmental Chemistry Letters 13 (4), 381–394.

Cleuvers, M., 2004. Mixture toxicity of the anti-inflammatory drugs diclofenac, ibuprofen, naproxen, and acetylsalicylic acid. Ecotoxicology and Environmental Safety 59 (3), 309–315.

Coble, P.G., 1996. Characterization of marine and terrestrial DOM in seawater using excitation-emission matrix spectroscopy. Marine Chemistry 51 (4), 325–346.

Coday, B.D., Yaffe, B.G.M., Xu, P., Cath, T.Y., 2014. Rejection of trace organic compounds by forward osmosis membranes: A literature review. Environmental Science & Technology 48 (7), 3612–3624.

Coddington, J.W., Hurst, J.K., Lymar, S.V., 1999. Hydroxyl Radical Formation during Peroxynitrous Acid Decomposition. Journal of the American Chemical Society 121 (11), 2438–2443.

Collins, J., Bolton, J.R., 2016. Advanced oxidation handbook, First edition ed. American Water Works Association, Denver, CO.

Comninellis, C., Kapalka, A., Malato, S., Parsons, S.A., Poulios, I., Mantzavinos, D., 2008. Advanced oxidation processes for water treatment: Advances and trends for R&D. Journal of Chemical Technology & Biotechnology 83 (6), 769–776.

Cooper, W., Gehringer, P., Pikaev, A., Kurucz, C., Mincher, B., 2004. Radiation processes. IWA Publishing. Advanced Oxidation Processes for Water and Wastewater Treatment, pp. 209–246.

Cooper, W.J., Snyder, S.A., Mezyk, S.P., Peller, JR, Nickelsen, M.G., 2010. Reaction rates and mechanisms of advanced oxidation processes for water reuse. WateReuse Foundation Project Number: WRF-04-017. WateReuse Foundation, Alexandria, VA, USA.

Cory, R.M., McKnight, D.M., 2005. Fluorescence Spectroscopy Reveals Ubiquitous Presence of Oxidized and Reduced Quinones in Dissolved Organic Matter. Environmental Science & Technology 39 (21), 8142–8149.

Cosson, H., Ernst, W.R., 1994. Photodecomposition of Chlorine Dioxide and Sodium Chlorite in Aqueous Solution by Irradiation with Ultraviolet Light. Industrial & Engineering Chemistry Research 33 (6), 1468–1475.

Cristóvão, R.O., Botelho, C.M., Martins, R.J.E., Loureiro, J.M., Boaventura, R.A.R., 2015. Fish canning industry wastewater treatment for water reuse – a case study. Journal of Cleaner Production 87, 603–612.

Crittenden, J.C., Hu, S., Hand, D.W., Green, S.A., 1999. A kinetic model for H2O2/UV process in a completely mixed batch reactor. Water Research 33 (10), 2315–2328.

References

Daneshvar, N., Salari, D., Niaei, A., Rasoulifard, M.H., Khataee, A.R., 2005. Immobilization of TiO 2 Nanopowder on Glass Beads for the Photocatalytic Decolorization of an Azo Dye C.I. Direct Red 23. Journal of Environmental Science and Health, Part A 40 (8), 1605–1617.

Das, T.N., 2001. Reactivity and Role of SO5•- Radical in Aqueous Medium Chain Oxidation of Sulfite to Sulfate and Atmospheric Sulfuric Acid Generation. The journal of physical chemistry. A 105 (40), 9142–9155.

De La Cruz, N., Esquius, L., Grandjean, D., Magnet, A., Tungler, A., Alencastro, L.F. de, Pulgarin, C., 2013. Degradation of emergent contaminants by UV, UV/H2O2 and neutral photo-Fenton at pilot scale in a domestic wastewater treatment plant. Water Research 47 (15), 5836–5845.

De Laat, J., Maouala-Makata, P., Dore, M., 1996. Rate constants for reactions of ozone and hydroxyl radicals with several phenyl-ureas and acetamides. Environmental Technology (United Kingdom).

Deborde, M., von Gunten, U., 2008. Reactions of chlorine with inorganic and organic compounds during water treatment-Kinetics and mechanisms: A critical review. Water Research 42 (1-2), 13–51.

DellaGreca, M., Iesce, M.R., Pistillo, P., Previtera, L., Temussi, F., 2009. Unusual products of the aqueous chlorination of atenolol. Chemosphere 74 (5), 730–734.

Dickenson, E.R.V., Drewes, J.E., Sedlak, D.L., Wert, E.C., Snyder, S.A., 2009. Applying Surrogates and Indicators to Assess Removal Efficiency of Trace Organic Chemicals during Chemical Oxidation of Wastewaters. Environmental Science & Technology 43 (16), 6242–6247.

DIN 38 409, 1987. German standard methods for the examination of water, waste water and sludge; general measures of effects and substances (group H); determination of hydrogen peroxide and its adducts (H 15): DIN standard 38 409, part 15, DEV-18. DIN (German Industry Norms) e.V., Berlin. https://www.beuth.de/de/norm/din-38409-15/1348997.

Dodd, M.C., 2012. Potential impacts of disinfection processes on elimination and deactivation of antibiotic resistance genes during water and wastewater treatment. Journal of environmental monitoring : JEM 14 (7), 1754–1771.

Dodd, M.C., Buffle, M.-O., von Gunten, U., 2006. Oxidation of Antibacterial Molecules by Aqueous Ozone: Moiety-Specific Reaction Kinetics and Application to Ozone-Based Wastewater Treatment. Environmental Science & Technology 40 (6), 1969–1977.

Dogliotti, L., Hayon, E., 1967. Flash photolysis of persulfate ions in aqueous solutions. The sulfate and ozonide radical anions. The Journal of Physical Chemistry 71 (8), 2511–2516.

Dong, B., Kahl, A., Cheng, L., Vo, H., Ruehl, S., Zhang, T., Snyder, S.A., Sáez, A.E., Quanrud, D., Arnold, R.G., 2015a. Fate of trace organics in a wastewater effluent dependent stream. The Science of the total environment 518-519, 479–490.

Dong, M.M., Rosario-Ortiz, F.L., 2012. Photochemical formation of hydroxyl radical from effluent organic matter. Environmental Science & Technology 46 (7), 3788–3794.

Dong, S., Feng, J., Fan, M., Pi, Y., Hu, L., Han, X., Liu, M., Sun, J., Sun, J., 2015b. Recent developments in heterogeneous photocatalytic water treatment using visible light-responsive photocatalysts: A review. RSC Advances 5 (19), 14610–14630.

Drewes, J.E., Hoppe, C., Jennings, T., 2006. Fate and Transport of *N*-Nitrosamines Under Conditions Simulating Full-Scale Groundwater Recharge Operations. Water Environment Research 78 (13), 2466–2473.

Drewes, J.E., Khan, S., 2011. Water reuse for drinking water augmentation. Water Quality and Treatment Handbook, Sixth ed. McGraw-Hill.

Drewes, J.E., Khan, S.J., 2015. Contemporary design, operation, and monitoring of potable reuse systems. Journal of Water Reuse and Desalination 5 (1), 1.

Du, Y., Chen, H., Zhang, Y., Chang, Y., 2014. Photodegradation of gallic acid under UV irradiation: Insights regarding the pH effect on direct photolysis and the ROS oxidation-sensitized process of DOM. Chemosphere 99, 254–260.

Dürrenmatt, D.J., 2011. Data Mining and Data-Driven Modeling Approaches to Support Wastewater Treatment Plant Operation. Dissertation, ETH Zürich, Switzerland.

DVGW, 2006. UV disinfection devices for drinking water supply - requirements and testing. German Gas and Water Management Union (DVGW), Bonn, Germany.

Elovitz, M.S., von Gunten, U., 1999. Hydroxyl Radical/Ozone Ratios During Ozonation Processes. I. The R ct Concept. Ozone: Science & Engineering 21 (3), 239–260.

EPA, 1993. perox-pure™ Chemical Oxidation Technology Peroxidation Systems Inc., Applications Analysis Report. EPA 540/AR-93/501., Cincinnati, Ohio.

EPA, 1994. CAV-OX Cavitation Oxidation Process Magnum Water Technology Inc.,Application Analysis Report. EPA 540/AR-93/520.

EPA, 2003. Ultraviolet Disinfection Guidance Manual. EPA-815-D-03-007.

EPA, 2006. National Primary Drinking Water Regulations: Long Term 2 Enhanced Surface Water Treatment Rule; Final Rule. Environmental Protection Agency, Federal Register 40 CFR Parts 9, 141, and 142.

Escobar, I.C., Randall, A.A., Taylor, J.S., 2001. Bacterial Growth in Distribution Systems: Effect of Assimilable Organic Carbon and Biodegradable Dissolved Organic Carbon. Environmental Science & Technology 35 (17), 3442–3447.

Escudero, C.J., Iglesias, O., Dominguez, S., Rivero, M.J., Ortiz, I., 2016. Performance of electrochemical oxidation and photocatalysis in terms of kinetics and energy consumption. New insights into the p-cresol degradation. Journal of Environmental Management.

Even-Ezra, I., Mizrahi, A., Gerrity, D., Snyder, S., Salveson, A., Lahav, O., 2009. Application of a novel plasma-based advanced oxidation process for efficient and cost-effective destruction of refractory organics in tertiary effluents and contaminated groundwater. Desalination and Water Treatment 11 (1-3), 236–244.

Fang, C., Lou, X., Huang, Y., Feng, M., Wang, Z., Liu, J., 2017. Monochlorophenols degradation by UV/persulfate is immune to the presence of chloride: Illusion or reality? Chemical Engineering Journal 323, 124–133.

Fang, J., Fu, Y., Shang, C., 2014. The roles of reactive species in micropollutant degradation in the UV/free chlorine system. Environmental Science & Technology 48 (3), 1859–1868.

References

Fang, J.-Y., Shang, C., 2012. Bromate formation from bromide oxidation by the UV/persulfate process. Environmental Science & Technology 46 (16), 8976–8983.

Fast, S.A., Gude, V.G., Truax, D.D., Martin, J., Magbanua, B.S., 2017. A Critical Evaluation of Advanced Oxidation Processes for Emerging Contaminants Removal. Environmental Processes 4 (1), 283–302.

Feng, Y., Smith, D.W., Bolton, J.R., 2007. Photolysis of aqueous free chlorine species (HOCl and OCl⁻) with 254 nm ultraviolet light. Journal of Environmental Engineering and Science 6 (3), 277–284.

Fernandes, A., Santos, D., Pacheco, M.J., Ciríaco, L., Lopes, A., 2014. Nitrogen and organic load removal from sanitary landfill leachates by anodic oxidation at Ti/Pt/PbO2, Ti/Pt/SnO2-Sb2O4 and Si/BDD. Applied Catalysis B: Environmental 148-149, 288–294.

Fernandez de Canete, J., Del Saz-Orozco, P., Baratti, R., Mulas, M., Ruano, A., Garcia-Cerezo, A., 2016. Soft-sensing estimation of plant effluent concentrations in a biological wastewater treatment plant using an optimal neural network. Expert Systems with Applications 63, 8–19.

Festger, A., Royce, A., Stefan, M., Wetterau, G. A Full-Scale Demonstration Study Comparing UV/Cl2 and UV/H2O2 for the Treatment of 1,4-Dioxane in Potable Reuse. Conference Presentation at the Arizona Water Reuse 2015 Symposium. https://goo.gl/4cwzd4 (accessed 14.02.2018).

Gabet-Giraud, V., Miège, C., Jacquet, R., Coquery, M., 2014. Impact of wastewater treatment plants on receiving surface waters and a tentative risk evaluation: The case of estrogens and beta blockers. Environmental science and pollution research international 21 (3), 1708–1722.

Gagnon, C., Lajeunesse, A., Cejka, P., Gagné, F., Hausler, R., 2008. Degradation of Selected Acidic and Neutral Pharmaceutical Products in a Primary-Treated Wastewater by Disinfection Processes. Ozone: Science & Engineering 30 (5), 387–392.

Galus, M., Jeyaranjaan, J., Smith, E., Li, H., Metcalfe, C., Wilson, J.Y., 2013. Chronic effects of exposure to a pharmaceutical mixture and municipal wastewater in zebrafish. Aquatic toxicology 132-133, 212–222.

Gao, Y.-q., Gao, N.-Y., Deng, Y., Yin, D.-q., Zhang, Y.-s., 2015. Degradation of florfenicol in water by UV/Na2S2O8 process. Environmental science and pollution research 22 (11), 8693–8701.

Garcia-Ivars, J., Martella, L., Massella, M., Carbonell-Alcaina, C., Alcaina-Miranda, M.-I., Iborra-Clar, M.-I., 2017. Nanofiltration as tertiary treatment method for removing trace pharmaceutically active compounds in wastewater from wastewater treatment plants. Water Research 125, 360–373.

Gerrity, D., Gamage, S., Holady, J.C., Mawhinney, D.B., Quiñones, O., Trenholm, R.A., Snyder, S.A., 2011. Pilot-scale evaluation of ozone and biological activated carbon for trace organic contaminant mitigation and disinfection. Water Research 45 (5), 2155–2165.

Gerrity, D., Gamage, S., Jones, D., Korshin, G.V., Lee, Y., Pisarenko, A., Trenholm, R.A., von Gunten, U., Wert, E.C., Snyder, S.A., 2012. Development of surrogate

correlation models to predict trace organic contaminant oxidation and microbial inactivation during ozonation. Water Research 46 (19), 6257–6272.

Gerrity, D., Lee, Y., Gamage, S., Lee, M., Pisarenko, A.N., Trenholm, R.A., Gunten, U. von, Snyder, S.A., 2016. Emerging investigators series: Prediction of trace organic contaminant abatement with UV/H2O2: development and validation of semi-empirical models for municipal wastewater effluents. Environmental Science: Water Research & Technology 2 (3), 460–473.

Gerrity, D., Pecson, B., Trussell, R.S., Trussell, R.R., 2013. Potable reuse treatment trains throughout the world. Journal of Water Supply: Research and Technology—AQUA 62 (6), 321.

Gerrity, D., Stanford, B.D., Trenholm, R.A., Snyder, S.A., 2010. An evaluation of a pilot-scale nonthermal plasma advanced oxidation process for trace organic compound degradation. Water Research 44 (2), 493–504.

Getoff, N., 1991. Radiation- and photoinduced degradation of pollutants in water. A comparative study. International Journal of Radiation Applications and Instrumentation. Part C. Radiation Physics and Chemistry 37 (5-6), 673–680.

Ghazi, N.M., Lastra, A.A., Watts, M.J., 2014. Hydroxyl radical (OH) scavenging in young and mature landfill leachates. Water Research 56, 148–155.

Giannakis, S., Gamarra Vives, F.A., Grandjean, D., Magnet, A., Alencastro, L.F. de, Pulgarin, C., 2015. Effect of advanced oxidation processes on the micropollutants and the effluent organic matter contained in municipal wastewater previously treated by three different secondary methods. Water Research 84, 295–306.

Gibson, J., Drake, J., Karney, B., 2017. UV Disinfection of Wastewater and Combined Sewer Overflows, in: Ultraviolet Light in Human Health, Diseases and Environment. Springer International Publishing, Cham, 267–275.

Giggy, C., Winkler, H. (Ed.), 1993. Das perox-pure™ Verfahren zur Entfernung organischer Schadstoffe aus Wasser (The perox-pure™ process for the elimination of organic water pollutants).

Glaze, W.H., Lay, Y., Kang, J.-W., 1995. Advanced Oxidation Processes. A Kinetic Model for the Oxidation of 1,2-Dibromo-3-chloropropane in Water by the Combination of Hydrogen Peroxide and UV Radiation. Industrial & Engineering Chemistry Research 34 (7), 2314–2323.

Goel, M., Hongqiang, H., Mujumdar, A.S., Ray, M.B., 2004. Sonochemical decomposition of volatile and non-volatile organic compounds--a comparative study. Water Research 38 (19), 4247–4261.

Gonce, N., Voudrias, E.A., 1994. Removal of chlorite and chlorate ions from water using granular activated carbon. Water Research 28 (5), 1059–1069.

González, O., Justo, A., Bacardit, J., Ferrero, E., Malfeito, J.J., Sans, C., 2013. Characterization and fate of effluent organic matter treated with UV/H2O2 and ozonation. Chemical Engineering Journal 226, 402–408.

Grandclément, C., Seyssiecq, I., Piram, A., Wong-Wah-Chung, P., Vanot, G., Tiliacos, N., Roche, N., Doumenq, P., 2017. From the conventional biological wastewater treatment to hybrid processes, the evaluation of organic micropollutant removal: A review. Water Research 111, 297–317.

References

Grebel, J.E., Pignatello, J.J., Mitch, W.A., 2010. Effect of halide ions and carbonates on organic contaminant degradation by hydroxyl radical-based advanced oxidation processes in saline waters. Environmental Science & Technology 44 (17), 6822–6828.

Gros, M., Petrović, M., Ginebreda, A., Barceló, D., 2010. Removal of pharmaceuticals during wastewater treatment and environmental risk assessment using hazard indexes. Environment International 36 (1), 15–26.

Gryglik, D., Olak, M., Miller, J.S., 2010. Photodegradation kinetics of androgenic steroids boldenone and trenbolone in aqueous solutions. Journal of Photochemistry and Photobiology A: Chemistry 212 (1), 14–19.

Guan, Y.-H., Ma, J., Li, X.-C., Fang, J.-Y., Chen, L.-W., 2011. Influence of pH on the formation of sulfate and hydroxyl radicals in the UV/peroxymonosulfate system. Environmental Science & Technology 45 (21), 9308–9314.

Gül, Ş., Özcan-Yıldırım, Ö., 2009. Degradation of Reactive Red 194 and Reactive Yellow 145 azo dyes by O3 and H2O2/UV-C processes. Chemical Engineering Journal 155 (3), 684–690.

Gullian, M., Espinosa-Faller, F.J., Núñez, A., López-Barahona, N., 2012. Effect of turbidity on the ultraviolet disinfection performance in recirculating aquaculture systems with low water exchange. Aquaculture Research 43 (4), 595–606.

Günthert, F.-W., 2013. Evaluation of existing technologies for the elimination of anthropogenic trace organic compounds in municipal wastewater treatment plants (Bewertung vorhandener Technologien für die Elimination anthropogener Spurenstoffe auf kommunalen Kläranlagen): Final report on behalf of the Bavarian Environment Agency. Universität der Bundeswehr München, Institut für Wasserwesen, München.

Guo, K., Wu, Z., Shang, C., Yao, B., Hou, S., Yang, X., Song, W., Fang, J., 2017. Radical Chemistry and Structural Relationships of PPCP Degradation by UV/Chlorine Treatment in Simulated Drinking Water. Environmental Science & Technology 51 (18), 10431–10439.

Haag, W.R., Yao, C.C.D., 1992. Rate constants for reaction of hydroxyl radicals with several drinking water contaminants. Environmental Science & Technology 26 (5), 1005–1013.

Haenni, W., Baumann, H., Comninellis, C., Gandini, D., Niedermann, P., Perret, A., Skinner, N., 1998. Diamond-sensing microdevices for environmental control and analytical applications. Diamond and Related Materials 7 (2-5), 569–574.

Han, D.-H., Cha, S.-Y., Yang, H.-Y., 2004. Improvement of oxidative decomposition of aqueous phenol by microwave irradiation in UV/H2O2 process and kinetic study. Water Research 38 (11), 2782–2790.

Hansen, K.M.S., Andersen, H.R., 2012. Energy Effectiveness of Direct UV and UV/H2O2 Treatment of Estrogenic Chemicals in Biologically Treated Sewage. International Journal of Photoenergy 2012 (10), 1–9.

Hassen, A., Mahrouk, M., Ouzari, H., Cherif, M., Boudabous, A., Damelincourt, J.J., 2000. UV disinfection of treated wastewater in a large-scale pilot plant and inactivation of selected bacteria in a laboratory UV device. Bioresource Technology 74 (2), 141–150.

He, X., La Cruz, A.A. de, Dionysiou, D.D., 2013. Destruction of cyanobacterial toxin cylindrospermopsin by hydroxyl radicals and sulfate radicals using UV-254nm activation of hydrogen peroxide, persulfate and peroxymonosulfate. Journal of Photochemistry and Photobiology A: Chemistry 251, 160–166.

He, X., La Cruz, A.A. de, O'Shea, K.E., Dionysiou, D.D., 2014. Kinetics and mechanisms of cylindrospermopsin destruction by sulfate radical-based advanced oxidation processes. Water Research 63, 168–178.

Hellauer, K., Mergel, D., Ruhl, A., Filter, J., Hübner, U., Jekel, M., Drewes, J., 2017. Advancing Sequential Managed Aquifer Recharge Technology (SMART) Using Different Intermediate Oxidation Processes. Water 9 (3), 221.

Henderson, R.K., Baker, A., Murphy, K.R., Hambly, A., Stuetz, R.M., Khan, S.J., 2009. Fluorescence as a potential monitoring tool for recycled water systems: A review. Water Research 43 (4), 863–881.

Hijosa-Valsero, M., Molina, R., Bayona, J.M., 2014. Assessment of a dielectric barrier discharge plasma reactor at atmospheric pressure for the removal of bisphenol A and tributyltin. Environmental Technology 35 (9-12), 1418–1426.

Hirayama, H., Maeda, N., Fujikawa, S., Toyoda, S., Kamata, N., 2014. Recent progress and future prospects of AlGaN-based high-efficiency deep-ultraviolet light-emitting diodes. Japanese Journal of Applied Physics 53 (10), 100209.

Hislop, K.A., Bolton, J.R., 1999. The Photochemical Generation of Hydroxyl Radicals in the UV?: Vis/Ferrioxalate/H2O2 System. Environmental Science & Technology 33 (18), 3119–3126.

Hofman-Caris, C.H.M., Siegers, W.G., van de Merlen, K., Man, A.W.A. de, Hofman, J.A.M.H., 2017. Removal of pharmaceuticals from WWTP effluent: Removal of EfOM followed by advanced oxidation. Chemical Engineering Journal 327, 514–521.

Hofman-Caris, R.C.H.M., Harmsen, D.J.H., Puijker, L., Baken, K.A., Wols, B.A., Beerendonk, E.F., Keltjens, L.L.M., 2015. Influence of process conditions and water quality on the formation of mutagenic byproducts in UV/H2O2 processes. Water Research 74, 191–202.

Hofman-Caris, C.H.M., Beerendonk, E.F., 2011. New concepts of UV/H2O2 oxidation. Final Report. KWR - Water Research Institute, Nieuwegein, Netherlands. http://www.waterrf.org/publicreportlibrary/4040.pdf (accessed 14.02.2018).

Hoigné, J., 1998. Chemistry of Aqueous Ozone and Transformation of Pollutants by Ozonation and Advanced Oxidation Processes, in: Quality and Treatment of Drinking Water II. Springer Berlin Heidelberg, Berlin, Heidelberg, 83–141.

Holloway, R.W., Miller-Robbie, L., Patel, M., Stokes, J.R., Munakata-Marr, J., Dadakis, J., Cath, T.Y., 2016. Life-cycle assessment of two potable water reuse technologies: MF/RO/UV–AOP treatment and hybrid osmotic membrane bioreactors. Journal of Membrane Science 507, 165–178.

Holt, M.S., 2000. Sources of chemical contaminants and routes into the freshwater environment. Food and Chemical Toxicology 38, S21-S27.

Hori, H., Yamamoto, A., Hayakawa, E., Taniyasu, S., Yamashita, N., Kutsuna, S., Kiatagawa, H., Arakawa, R., 2005. Efficient Decomposition of Environmentally Persistent Perfluorocarboxylic Acids by Use of Persulfate as a Photochemical Oxidant. Environmental Science & Technology 39 (7), 2383–2388.

References

Hou, S., Ling, L., Dionysiou, D.D., Wang, Y., Huang, J., Guo, K., Li, X., Fang, J., 2018. Chlorate Formation Mechanism in the Presence of Sulfate Radical, Chloride, Bromide and Natural Organic Matter. Environmental Science & Technology 52 (11), 6317–6325.

Huang, W.-J., Fang, G.-C., Wang, C.-C., 2005. The determination and fate of disinfection by-products from ozonation of polluted raw water. Science of The Total Environment 345 (1-3), 261–272.

Huber, M.M., Canonica, S., Park, G.-Y., von Gunten, U., 2003. Oxidation of Pharmaceuticals during Ozonation and Advanced Oxidation Processes. Environmental Science & Technology 37 (5), 1016–1024.

Huber, M.M., Ternes, T.A., von Gunten, U., 2004. Removal of Estrogenic Activity and Formation of Oxidation Products during Ozonation of 17α-Ethinylestradiol. Environmental Science & Technology 38 (19), 5177–5186.

Huber, S., Popp, W., 2005. Examination of the killing or inactivation of selected pathogens in wastewater by UV radiation in comparison to the reduction of faecal indicator bacteria and studies on recontamination (Überprüfung der Abtötung bzw. Inaktivierung ausgewählter Krankheitserreger in Abwasser durch UV-Strahlung im Vergleich zur Reduktion von Fäkalindikatorbakterien und Untersuchungen zur Wiederverkeimung): Final report (Schlussbericht), Augsburg.

Hübner, U., von Gunten, U., Jekel, M., 2015a. Evaluation of the persistence of transformation products from ozonation of trace organic compounds - a critical review. Water Research 68, 150–170.

Hübner, U., Zucker, I., Jekel, M., 2015b. Options and limitations of hydrogen peroxide addition to enhance radical formation during ozonation of secondary effluents. Journal of Water Reuse and Desalination 5 (1), 8.

Huerta-Fontela, M., Galceran, M.T., Ventura, F., 2010. Fast liquid chromatography-quadrupole-linear ion trap mass spectrometry for the analysis of pharmaceuticals and hormones in water resources. Journal of Chromatography. A 1217 (25), 4212–4222.

Huie, R.E., Clifton, C.L., 1990. Temperature dependence of the rate constants for reactions of the sulfate radical, SO4-, with anions. Journal of Physical Chemistry 94 (23), 8561–8567.

Ibrahim, M.A.S., 2012. Commercial evaluation of UV-LED in Water Treatment Applications.

Ignat, A., Manzocco, L., Bartolomeoli, I., Maifreni, M., Nicoli, M.C., 2015. Minimization of water consumption in fresh-cut salad washing by UV-C light. Food Control 50, 491–496.

Ike, I.A., Linden, K.G., Orbell, J.D., Duke, M., 2018. Critical review of the science and sustainability of persulphate advanced oxidation processes. Chemical Engineering Journal.

ISO 21348, 2007. Definitions of Solar Irradiance Spectral Categories. http://www.spacewx.com/pdf/SET_21348_2004.pdf (accessed 17.05.2018).

Jacobsen, H.S., Lynggaard Jensen, A., 1998. On-line measurement in waste water treatment plants, in: Monitoring of Water Quality. Elsevier, 89–102.

Jayson, G.G., Parsons, B.J., Swallow, A.J., 1973. Some simple, highly reactive, inorganic chlorine derivatives in aqueous solution. Their formation using pulses of radiation and their role in the mechanism of the Fricke dosimeter. Journal of the Chemical Society, Faraday Transactions 1: Physical Chemistry in Condensed Phases 69 (0), 1597.

Ji, Y., Wang, L., Jiang, M., Lu, J., Ferronato, C., Chovelon, J.-M., 2017. The role of nitrite in sulfate radical-based degradation of phenolic compounds: An unexpected nitration process relevant to groundwater remediation by in-situ chemical oxidation (ISCO). Water Research 123, 249–257.

Jia, A., Escher, B.I., Leusch, F.D.L., Tang, J.Y.M., Prochazka, E., Dong, B., Snyder, E.M., Snyder, S.A., 2015. In vitro bioassays to evaluate complex chemical mixtures in recycled water. Water Research 80, 1–11.

Jiang, B., Zheng, J., Qiu, S., Wu, M., Zhang, Q., Yan, Z., Xue, Q., 2014. Review on electrical discharge plasma technology for wastewater remediation. Chemical Engineering Journal 236, 348–368.

Jiang, C., Pang, S., Ouyang, F., Ma, J., Jiang, J., 2010. A new insight into Fenton and Fenton-like processes for water treatment. Journal of Hazardous Materials 174 (1-3), 813–817.

Jin, J., El-Din, M.G., Bolton, J.R., 2011. Assessment of the UV/chlorine process as an advanced oxidation process. Water Research 45 (4), 1890–1896.

Jin, X., Peldszus, S., Huck, P.M., 2012. Reaction kinetics of selected micropollutants in ozonation and advanced oxidation processes. Water Research 46 (19), 6519–6530.

Joo, S.H., Mitch, W.A., 2007. Nitrile, Aldehyde, and Halonitroalkane Formation during Chlorination/Chloramination of Primary Amines. Environ. Sci. Technol. 41 (4), 1288–1296.

Kaiser, H.-P., Köster, O., Gresch, M., Périsset, P.M.J., Jäggi, P., Salhi, E., von Gunten, U., 2013. Process Control For Ozonation Systems: A Novel Real-Time Approach. Ozone: Science & Engineering 35 (3), 168–185.

Kalumuck, K.M., Chahine, G.L., 2000. The Use of Cavitating Jets to Oxidize Organic Compounds in Water. J. Fluids Eng. 122 (3), 465.

Kapałka, A., Fóti, G., Comninellis, C., 2009. The importance of electrode material in environmental electrochemistry. Electrochimica Acta 54 (7), 2018–2023.

Kaptijn, J.P., 1997. The Ecoclear® Process. Results from Full-Scale Installations. Ozone: Science & Engineering 19 (4), 297–305.

Karpel Vel Leitner, N., Laat, J. de, Dore, M., 1992. Photodecomposition du bioxyde de chlore et des ions chlorite par irradiation U.V. en milieu aqueux—partie I. Sous-produits de reaction. Water Research 26 (12), 1655–1664.

Karthikeyan, S., Gopalakrishnan, A.N., 2011. Degradation of phenol and m-cresol in aqueous solutions using indigenously developed microwave-ultraviolet reactor. Journal of Scientific and Industrial Research 70 (1), 71–76.

Katsoyiannis, I.A., Canonica, S., von Gunten, U., 2011. Efficiency and energy requirements for the transformation of organic micropollutants by ozone, O3/H2O2 and UV/H2O2. Water Research 45 (13), 3811–3822.

References

Keen, O.S., Linden, K.G., 2013a. Degradation of antibiotic activity during UV/H2O2 advanced oxidation and photolysis in wastewater effluent. Environmental Science & Technology 47 (22), 13020–13030.

Keen, O.S., Linden, K.G., 2013b. Re-engineering an artificial sweetener: Transforming sucralose residuals in water via advanced oxidation. Environmental Science & Technology 47 (13), 6799–6805.

Keen, O.S., Love, N.G., Aga, D.S., Linden, K.G., 2016. Biodegradability of iopromide products after UV/H2O2 advanced oxidation. Chemosphere 144, 989–994.

Keen, O.S., Love, N.G., Linden, K.G., 2012. The role of effluent nitrate in trace organic chemical oxidation during UV disinfection. Water Research 46 (16), 5224–5234.

Keen, O.S., McKay, G., Mezyk, S.P., Linden, K.G., Rosario-Ortiz, F.L., 2014. Identifying the factors that influence the reactivity of effluent organic matter with hydroxyl radicals. Water Research 50, 408–419.

Kesselman, J.M., Weres, O., Lewis, N.S., Hoffmann, M.R., 1997. Electrochemical Production of Hydroxyl Radical at Polycrystalline Nb-Doped TiO2 Electrodes and Estimation of the Partitioning between Hydroxyl Radical and Direct Hole Oxidation Pathways. The Journal of Physical Chemistry B 101 (14), 2637–2643.

Khan, J.A., He, X., Shah, N.S., Khan, H.M., Hapeshi, E., Fatta-Kassinos, D., Dionysiou, D.D., 2014. Kinetic and mechanism investigation on the photochemical degradation of atrazine with activated H2O2, S2O82– and HSO5–. Chemical Engineering Journal 252, 393–403.

Kim, T.-H., Kim, S.D., Kim, H.Y., Lim, S.J., Lee, M., Yu, S., 2012. Degradation and toxicity assessment of sulfamethoxazole and chlortetracycline using electron beam, ozone and UV. Journal of Hazardous Materials 227-228, 237–242.

Kimura, A., Osawa, M., Taguchi, M., 2012. Decomposition of persistent pharmaceuticals in wastewater by ionizing radiation. Radiation Physics and Chemistry 81 (9), 1508–1512.

Klasmeier, J., Kehrein, N., Berlekamp, J., Matthies, M., 2011. Micropollutants in surface waters: Determination of the need for action in municipal wastewater treatment plants (Mikroverunreinigungen in oberirdischen Gewässern: Ermittlung des Handlungsbedarfs bei kommunalen Kläranlagen): Final report on behalf of the Bavarian Environment Agency. Institute of Environmental Systems Research University Osnabrück, Osnabrück.

Klausen, M.M., Grønborg, O., 2010. Pilot scale testing of advanced oxidation processes for degradation of geosmin and MIB in recirculated aquaculture. Water Science and Technology: Water Supply 10 (2), 217.

Klavarioti, M., Mantzavinos, D., Kassinos, D., 2009. Removal of residual pharmaceuticals from aqueous systems by advanced oxidation processes. Environment International 35 (2), 402–417.

Köhler, C., Venditti, S., Igos, E., Klepiszewski, K., Benetto, E., Cornelissen, A., 2012. Elimination of pharmaceutical residues in biologically pre-treated hospital wastewater using advanced UV irradiation technology: a comparative assessment. Journal of Hazardous Materials 239-240, 70–77.

Kolkman, A., Martijn, B.J., Vughs, D., Baken, K.A., van Wezel, A.P., 2015. Tracing nitrogenous disinfection byproducts after medium pressure UV water treatment by

stable isotope labeling and high resolution mass spectrometry. Environmental Science & Technology 49 (7), 4458–4465.

Korshin, G.V., Sgroi, M., Ratnaweera, H., 2018. Spectroscopic surrogates for real time monitoring of water quality in wastewater treatment and water reuse. Current Opinion in Environmental Science & Health 2, 12–19.

Korshin, G.V., Wu, W.W., Benjamin, M.M., Hemingway, O., 2002. Correlations between differential absorbance and the formation of individual DBPs. Water Research 36 (13), 3273–3282.

Kruithof, J.C., Kamp, P.C., Belosevic, M., 2002. UV/H2O2-treatment: the ultimate solution for pesticide control and disinfection. Water Science and Technology: Water Supply 2 (1), 113–122.

Kruithof, J.C., Kamp, P.C., Martijn, B.J., 2007. UV/H2O2 Treatment: A Practical Solution for Organic Contaminant Control and Primary Disinfection. Ozone: Science & Engineering 29 (4), 273–280.

Kruithof, J.C., KAMP, P., Belosevic, M., Stefan, M., 2005. UV/H2O2 retrofit of PWN's water treatment plant Andijk for primary disinfection and organic contaminant control. 2nd IWA Leading-Edge on Water and Wastewater Treatment Technologies. IWA Publishing 4 (4), 53–65.

Kusic, H., Koprivanac, N., Bozic, A.L., 2006. Minimization of organic pollutant content in aqueous solution by means of AOPs: UV- and ozone-based technologies. Chemical Engineering Journal 123 (3), 127–137.

Kwon, J.-W., Armbrust, K.L., 2005. Degradation of citalopram by simulated sunlight. Environmental Toxicology and Chemistry 24 (7), 1618–1623.

Laat, J. de, Chramosta, N., Doré, M., Suty, H., Pouillot, M., 1994. Kinetic reaction constants of hydroxyl radicals on some oxidation by-products of atrazine per O 3 or per O3/H2O2 (Constantes cinétiques de réaction des radicaux hydroxyles sur quelques sous- produits d'oxydation de l'atrazine par O3 ou par O3/H2O2). Environmental Technology 15 (5), 419–428.

Lakowicz, J.R., 2010. Principles of fluorescence spectroscopy, Third edition ed. Springer, New York, NY.

Ledakowicz, S., Miller, J.S., Olejnik, D., 1999. Oxidation of PAHs in water solutions by ultraviolet radiation combined with hydrogen peroxide. International Journal of Photoenergy 1 (1), 55–60.

Lee, C., Yoon, J., von Gunten, U., 2007. Oxidative degradation of N-nitrosodimethylamine by conventional ozonation and the advanced oxidation process ozone/hydrogen peroxide. Water Research 41 (3), 581–590.

Lee, Y., Gerrity, D., Lee, M., Bogeat, A.E., Salhi, E., Gamage, S., Trenholm, R.A., Wert, E.C., Snyder, S.A., von Gunten, U., 2013. Prediction of micropollutant elimination during ozonation of municipal wastewater effluents: Use of kinetic and water specific information. Environmental Science & Technology 47 (11), 5872–5881.

Lee, Y., Gerrity, D., Lee, M., Gamage, S., Pisarenko, A., Trenholm, R.A., Canonica, S., Snyder, S.A., von Gunten, U., 2016. Organic Contaminant Abatement in Reclaimed Water by UV/H2O2 and a Combined Process Consisting of O3/H2O2 Followed by UV/H2O2: Prediction of Abatement Efficiency, Energy Consumption, and Byproduct Formation. Environmental Science & Technology 50 (7), 3809–3819.

Lee, Y., Kovalova, L., McArdell, C.S., von Gunten, U., 2014. Prediction of micropollutant elimination during ozonation of a hospital wastewater effluent. Water Research 64, 134–148.

Lee, Y., von Gunten, U., 2010a. Oxidative transformation of micropollutants during municipal wastewater treatment: Comparison of kinetic aspects of selective (chlorine, chlorine dioxide, ferrateVI, and ozone) and non-selective oxidants (hydroxyl radical). Water Research 44 (2), 555–566.

Lee, Y., von Gunten, U., 2010b. Oxidative transformation of micropollutants during municipal wastewater treatment: comparison of kinetic aspects of selective (chlorine, chlorine dioxide, ferrate VI, and ozone) and non-selective oxidants (hydroxyl radical). Water Research 44 (2), 555–566.

Legrini, O., Oliveros, E., Braun, A.M., 1993. Photochemical processes for water treatment. Chemical reviews 93 (2), 671–698.

Legube, B., Karpel Vel Leitner, N., 1999. Catalytic ozonation: a promising advanced oxidation technology for water treatment. Catalysis Today 53 (1), 61–72.

Lehto, K.-M., Vuorimaa, E., Lemmetyinen, H., 2000. Photolysis of polycyclic aromatic hydrocarbons (PAHs) in dilute aqueous solutions detected by fluorescence. Journal of Photochemistry and Photobiology A: Chemistry 136 (1-2), 53–60.

Leitzke, O., 1992. Eliminierung von Schadstoffen im Wasser (CSB, Elimination of pollutants in water (COD, AOX, CHC and PAH) by combining ozone and UV light (AOX, CKW und PAK) durch die Kombination von Ozon und UV-Licht). Brauwelt 132, 2516.

Lester, Y., Avisar, D., Gozlan, I., Mamane, H., 2011. Removal of pharmaceuticals using combination of UV/H2O2/O3 advanced oxidation process. Water Science and Technology: A Journal of the International Association on Water Pollution Research 64 (11), 2230–2238.

Lester, Y., Ferrer, I., Thurman, E.M., Linden, K.G., 2014. Demonstrating sucralose as a monitor of full-scale UV/AOP treatment of trace organic compounds. Journal of Hazardous Materials 280, 104–110.

Lester, Y., Sharpless, C.M., Mamane, H., Linden, K.G., 2013. Production of photo-oxidants by dissolved organic matter during UV water treatment. Environmental Science & Technology 47 (20), 11726–11733.

Letzel, M., Metzner, G., Letzel, T., 2009. Exposure assessment of the pharmaceutical diclofenac based on long-term measurements of the aquatic input. Environment International 35 (2), 363–368.

Li, K., Stefan, M.I., Crittenden, J.C., 2004. UV Photolysis of Trichloroethylene: Product Study and Kinetic Modeling. Environmental Science & Technology 38 (24), 6685–6693.

Li, W., Jain, T., Ishida, K., Liu, H., 2017. A mechanistic understanding of the degradation of trace organic contaminants by UV/hydrogen peroxide, UV/persulfate and UV/free chlorine for water reuse. Environmental Science: Water Research & Technology 3 (1), 128–138.

Li, W.-T., Majewsky, M., Abbt-Braun, G., Horn, H., Jin, J., Li, Q., Zhou, Q., Li, A.-M., 2016. Application of portable online LED UV fluorescence sensor to predict the

degradation of dissolved organic matter and trace organic contaminants during ozonation. Water Research 101, 262–271.

Li Puma, G., Puddu, V., Tsang, H.K., Gora, A., Toepfer, B., 2010. Photocatalytic oxidation of multicomponent mixtures of estrogens (estrone (E1), 17β-estradiol (E2), 17α-ethynylestradiol (EE2) and estriol (E3)) under UVA and UVC radiation: Photon absorption, quantum yields and rate constants independent of photon absorption. Applied Catalysis B: Environmental 99 (3-4), 388–397.

Lian, J., Qiang, Z., Li, M., Bolton, J.R., Qu, J., 2015. UV photolysis kinetics of sulfonamides in aqueous solution based on optimized fluence quantification. Water Research 75, 43–50.

Lian, L., Yao, B., Hou, S., Fang, J., Yan, S., Song, W., 2017. Kinetic Study of Hydroxyl and Sulfate Radical-mediated Oxidation of Pharmaceuticals in Wastewater Effluents. Environmental Science & Technology.

Liang, C., Huang, C.-F., Mohanty, N., Kurakalva, R.M., 2008. A rapid spectrophotometric determination of persulfate anion in ISCO. Chemosphere 73 (9), 1540–1543.

Liao, C.H., Gurol, M.D., 1995. Chemical oxidation by photolytic decomposition of hydrogen peroxide. Environmental Science & Technology 29 (12), 3007–3014.

Liao, C.-H., Kang, S.-F., Wu, F.-A., 2001. Hydroxyl radical scavenging role of chloride and bicarbonate ions in the H2O2/UV process. Chemosphere 44 (5), 1193–1200.

Lim, M.H., 2008. Fate of Wastewater-derived Contaminants in Surface Waters: Dissertation. University of California, Berkeley.

Lin, C.-C., Wu, M.-S., 2014. Degradation of ciprofloxacin by UV/S2O82− process in a large photoreactor. Journal of Photochemistry and Photobiology A: Chemistry 285, 1–6.

Lin, H., Niu, J., Xu, J., Huang, H., Li, D., Yue, Z., Feng, C., 2013. Highly efficient and mild electrochemical mineralization of long-chain perfluorocarboxylic acids (C9−C10) by Ti/SnO2−Sb−Ce, Ti/SnO2−Sb/Ce−PbO2, and Ti/BDD electrodes. Environmental Science & Technology 47 (22), 13039–13046.

Linden, K.G., Sharpless, C.M., Andrews, S., Atasi, K., Korategere, V., Stefan, M., Suffet, I.M., 2005. Innovative UV technologies to oxidize organic and organoleptic chemicals. Water Environment Research Foundation.

Liu, C., Qiang, Z., Tian, F., Zhang, T., 2009. Photodegradation of etridiazole by UV radiation during drinking water treatment. Chemosphere 76 (5), 609–615.

Liu, K., Roddick, F.A., Fan, L., 2012. Impact of salinity and pH on the UVC/H2O2 treatment of reverse osmosis concentrate produced from municipal wastewater reclamation. Water Research 46 (10), 3229–3239.

Liu, W., Andrews, S.A., Stefan, M.I., Bolton, J.R., 2003. Optimal methods for quenching H2O2 residuals prior to UFC testing. Water Research 37 (15), 3697–3703.

Liu, W.-R., Ying, G.-G., Zhao, J.-L., Liu, Y.-S., Hu, L.-X., Yao, L., Liang, Y.-Q., Tian, F., 2016a. Photodegradation of the azole fungicide climbazole by ultraviolet irradiation under different conditions: Kinetics, mechanism and toxicity evaluation. Journal of Hazardous Materials 318, 794–801.

Liu, Y., He, X., Duan, X., Fu, Y., Fatta-Kassinos, D., Dionysiou, D.D., 2016b. Significant role of UV and carbonate radical on the degradation of oxytetracycline in UV-AOPs: Kinetics and mechanism. Water Research 95, 195–204.

Locke, B.R., Sato, M., Sunka, P., Hoffmann, M.R., Chang, J.-S., 2006. Electrohydraulic Discharge and Nonthermal Plasma for Water Treatment. Industrial & Engineering Chemistry Research 45 (3), 882–905.

Lonappan, L., Brar, S.K., Das, R.K., Verma, M., Surampalli, R.Y., 2016. Diclofenac and its transformation products: Environmental occurrence and toxicity - A review. Environment International 96, 127–138.

Loos, R., Gawlik, B.M., Locoro, G., Rimaviciute, E., Contini, S., Bidoglio, G., 2009. EU-wide survey of polar organic persistent pollutants in European river waters. Environmental Pollution 157 (2), 561–568.

Lu, X., Shao, Y., Gao, N., Chen, J., Deng, H., Chu, W., An, N., Peng, F., 2018. Investigation of clofibric acid removal by UV/persulfate and UV/chlorine processes: Kinetics and formation of disinfection byproducts during subsequent chlor(am)ination. Chemical Engineering Journal 331, 364–371.

Lu, X., Shao, Y., Gao, N., Chen, J., Zhang, Y., Xiang, H., Guo, Y., 2017. Degradation of diclofenac by UV-activated persulfate process: Kinetic studies, degradation pathways and toxicity assessments. Ecotoxicology and Environmental Safety 141, 139–147.

Luo, Y., Guo, W., Ngo, H.H., Nghiem, L.D., Hai, F.I., Zhang, J., Liang, S., Wang, X.C., 2014. A review on the occurrence of micropollutants in the aquatic environment and their fate and removal during wastewater treatment. Science of The Total Environment 473-474, 619–641.

Lutterbeck, C.A., Machado, Ê.L., Kümmerer, K., 2015. Photodegradation of the antineoplastic cyclophosphamide: a comparative study of the efficiencies of UV/H2O2, UV/Fe2+/H2O2 and UV/TiO2 processes. Chemosphere 120, 538–546.

Lutze, H., 2005. Ozonation of Benzotriazoles (Ozonung von Benzotriazolen). Bachelor Thesis, University Duisburg - Essen.

Lutze, H., 2013. Sulfate radical based oxidation in water treatment. Dissertation, University of Duisburg-Essen, Germany.

Lutze, H.V., Bakkour, R., Kerlin, N., von Sonntag, C., Schmidt, T.C., 2014. Formation of bromate in sulfate radical based oxidation: mechanistic aspects and suppression by dissolved organic matter. Water Research 53, 370–377.

Lutze, H.V., Bircher, S., Rapp, I., Kerlin, N., Bakkour, R., Geisler, M., von Sonntag, C., Schmidt, T.C., 2015a. Degradation of chlorotriazine pesticides by sulfate radicals and the influence of organic matter. Environmental Science & Technology 49 (3), 1673–1680.

Lutze, H.V., Kerlin, N., Schmidt, T.C., 2015b. Sulfate radical-based water treatment in presence of chloride: formation of chlorate, inter-conversion of sulfate radicals into hydroxyl radicals and influence of bicarbonate. Water Research 72, 349–360.

Mack, J., Bolton, J.R., 1999. Photochemistry of nitrite and nitrate in aqueous solution: A review. Journal of Photochemistry and Photobiology A: Chemistry 128 (1-3), 1–13.

Magdeburg, A., Stalter, D., Schlüsener, M., Ternes, T., Oehlmann, J., 2014. Evaluating the efficiency of advanced wastewater treatment: Target analysis of organic

contaminants and (geno-)toxicity assessment tell a different story. Water Research 50, 35–47.

Mahamuni, N.N., Adewuyi, Y.G., 2010. Advanced oxidation processes (AOPs) involving ultrasound for waste water treatment: a review with emphasis on cost estimation. Ultrasonics Sonochemistry 17 (6), 990–1003.

Mahdi Ahmed, M., Barbati, S., Doumenq, P., Chiron, S., 2012. Sulfate radical anion oxidation of diclofenac and sulfamethoxazole for water decontamination. Chemical Engineering Journal 197, 440–447.

Mahdi-Ahmed, M., Chiron, S., 2014. Ciprofloxacin oxidation by UV-C activated peroxymonosulfate in wastewater. Journal of Hazardous Materials 265, 41–46.

Malpass, G.R.P., Miwa, D.W., Machado, S.A.S., Motheo, A.J., 2008. Decolourisation of real textile waste using electrochemical techniques: Effect of electrode composition. Journal of Hazardous Materials 156 (1-3), 170–177.

Martijn, A.J., Boersma, M.G., Vervoort, J.M., Rietjens, I.M.C.M., Kruithof, J.C., 2014. Formation of genotoxic compounds by medium pressure ultraviolet treatment of nitrate-rich water. Desalination and Water Treatment 52 (34-36), 6275–6281.

Martínez, C., Vilariño, S., Fernández, M.I., Faria, J., L., M.C., Santaballa, J.A., 2013. Mechanism of degradation of ketoprofen by heterogeneous photocatalysis in aqueous solution. Applied Catalysis B: Environmental 142-143, 633–646.

Martins, A., Guimarães, L., Guilhermino, L., 2013. Chronic toxicity of the veterinary antibiotic florfenicol to Daphnia magna assessed at two temperatures. Environmental toxicology and pharmacology 36 (3), 1022–1032.

Mason, T., Pétrier, C., 2004. Ultrasound processes. In: Advanced Oxidation Processes for Water and Wastewater Treatment. IWA Publishing, London, 185-208.

Masschelein, W., 2002. Ultraviolet light in water and wastewater sanitation: Edited by Rip G.Rice. CRC revivals. CRC Press, Boca Raton, FL.

Matta, R., Tlili, S., Chiron, S., Barbati, S., 2011. Removal of carbamazepine from urban wastewater by sulfate radical oxidation. Environmental Chemistry Letters 9 (3), 347–353.

Matthew, B.M., Anastasio, C., 2006. A chemical probe technique for the determination of reactive halogen species in aqueous solution: Part 1 - bromide solutions. Atmospheric Chemistry and Physics 6 (9), 2423–2437.

Mazellier, P., Leroy, É., De Laat, J., Legube, B., 2002a. Transformation of carbendazim induced by the H2O2/UV system in the presence of hydrogenocarbonate ions: Involvement of the carbonate radical. New Journal of Chemistry 26 (12), 1784–1790.

Mazellier, P., Leroy, É., Legube, B., 2002b. Photochemical behavior of the fungicide carbendazim in dilute aqueous solution. Journal of Photochemistry and Photobiology A: Chemistry 153 (1-3), 221–227.

McKay, G., Dong, M.M., Kleinman, J.L., Mezyk, S.P., Rosario-Ortiz, F.L., 2011. Temperature dependence of the reaction between the hydroxyl radical and organic matter. Environmental Science & Technology 45 (16), 6932–6937.

Meite, L., Szabo, R., Mazellier, P., Laat, J. de, 2010. Cinétique de phototransformation de polluants organiques émergents en solution aqueuse diluée. Revue des Sciences de l'eau 23 (1), 31.

Merel, S., Anumol, T., Park, M., Snyder, S.A., 2015. Application of surrogates, indicators, and high-resolution mass spectrometry to evaluate the efficacy of UV processes for attenuation of emerging contaminants in water. Journal of Hazardous Materials 282, 75–85.

Merényi, G., Lind, J., Naumov, S., von Sonntag, C., 2010a. Reaction of ozone with hydrogen peroxide (peroxone process): a revision of current mechanistic concepts based on thermokinetic and quantum-chemical considerations. Environmental Science & Technology 44 (9), 3505–3507.

Merényi, G., Lind, J., Naumov, S., von Sonntag, C., 2010b. The reaction of ozone with the hydroxide ion: Mechanistic considerations based on thermokinetic and quantum chemical calculations and the role of HO4- in superoxide dismutation. Chemistry 16 (4), 1372–1377.

Mertens, R., von Sonntag, C., 1995. Photolysis (λ = 354 nm of tetrachloroethene in aqueous solutions. Journal of Photochemistry and Photobiology A: Chemistry 85 (1-2), 1–9.

Miehe, U., Stapf, M., 2015. Pilotuntersuchungen verschiedener Nachbehandlungsstufen bei der Ozonung: Abschlussveranstaltung der Verbundprojekte ASKURIS und IST4R 14. September 2015. Kompetenzzentrum Wasser Berlin, Berlin.

Miklos, D.B., Hartl, R., Michel, P., Linden, K.G., Drewes, J.E., Hübner, U., 2018a. UV/H2O2 process stability and pilot-scale validation for trace organic chemical removal from wastewater treatment plant effluents. Water Research 136, 169–179.

Miklos, D.B., Remy, C., Jekel, M., Linden, K.G., Drewes, J.E., Hübner, U., 2018b. Evaluation of advanced oxidation processes for water and wastewater treatment – A critical review. Water Research 139, 118–131.

Miller, J.S., Olejnik, D., 2001. Photolysis of polycyclic aromatic hydrocarbons in water. Water Research 35 (1), 233–243.

Mills, A., Lee, S., 2004. Semiconductor photocatalysis. In: Advanced Oxidation Processes for Water and Wastewater Treatment. IWA Publishing, London, 137-166.

Miralles-Cuevas, S., Darowna, D., Wanag, A., Mozia, S., Malato, S., Oller, I., 2016. Comparison of UV/H2O2, UV/S2O82−, solar/Fe(II)/H2O2 and solar/Fe(II)/S2O82− at pilot plant scale for the elimination of micro-contaminants in natural water: An economic assessment. Chemical Engineering Journal 310 (2), 514–524.

Mitch, W.A., Sharp, J.O., Trussell, R.R., Valentine, R.L., Alvarez-Cohen, L., Sedlak, D.L., 2003. N -Nitrosodimethylamine (NDMA) as a Drinking Water Contaminant: A Review. Environmental Engineering Science 20 (5), 389–404.

Mohagheghian, A., Karimi, S.-A., Yang, J.-K, Shirzad-Siboni, M., 2015. Photocatalytic Degradation of a Textile Dye by Illuminated Tungsten Oxide Nanopowder. Journal of Advanced Oxidation Technologies 18 (1).

Mok, C.Y., Marriott, P., Ong, K.L., Yeo, G.N., 1987. Photodegradation of parathion. Bulletin of Environmental Contamination and Toxicology 38 (5), 820–826.

Mompelat, S., Le Bot, B., Thomas, O., 2009. Occurrence and fate of pharmaceutical products and by-products, from resource to drinking water. Environment International 35 (5), 803–814.

Montes-Grajales, D., Fennix-Agudelo, M., Miranda-Castro, W., 2017. Occurrence of personal care products as emerging chemicals of concern in water resources: A review. The Science of the total environment 595, 601–614.

Moreno-Andrés, J., Romero-Martínez, L., Acevedo-Merino, A., Nebot, E., 2016. Determining disinfection efficiency on E. faecalis in saltwater by photolysis of H2O2: Implications for ballast water treatment. Chemical Engineering Journal 283, 1339–1348.

Müller, J., 1998. Comparison of combined oxidation processes in a lab-scale continuous-flow plant: Dissertation. TU Berlin, Berlin.

Müller, J., Drewes, J.E., Hübner, U., 2017. Sequential biofiltration - A novel approach for enhanced biological removal of trace organic chemicals from wastewater treatment plant effluent. Water Research 127, 127–138.

Müller, J.P., Gottschalk, C., Jekel, M., 2001. Comparison of advanced oxidation processes in flow-through pilot plants (part II). Water Science and Technology: A Journal of the International Association on Water Pollution Research 44 (5), 311–315.

Müller, J.P., Jekel, M., 2001. Comparison of advanced oxidation processes in flow-through pilot plants (part I). Water Science and Technology: A Journal of the International Association on Water Pollution Research 44 (5), 303–309.

Murphy, K.R., Stedmon, C.A., Graeber, D., Bro, R., 2013. Fluorescence spectroscopy and multi-way techniques. PARAFAC. Anal. Methods 5 (23), 6557.

Murray, K.E., Thomas, S.M., Bodour, A.A., 2010. Prioritizing research for trace pollutants and emerging contaminants in the freshwater environment. Environmental Pollution 158 (12), 3462–3471.

Muschket, M., Di Paolo, C., Tindall, A.J., Touak, G., Phan, A., Krauss, M., Kirchner, K., Seiler, T.-B., Hollert, H., Brack, W., 2018. Identification of Unknown Antiandrogenic Compounds in Surface Waters by Effect-Directed Analysis (EDA) Using a Parallel Fractionation Approach. Environmental Science & Technology 52 (1), 288–297.

Nagarnaik, P.M., Boulanger, B., 2011. Advanced oxidation of alkylphenol ethoxylates in aqueous systems. Chemosphere 85 (5), 854–860.

Nawrocki, J., Kasprzyk-Hordern, B., 2010. The efficiency and mechanisms of catalytic ozonation. Applied Catalysis B: Environmental 99 (1-2), 27–42.

Neta, P., Huie, R.E., Ross, A.B., 1988. Rate Constants for Reactions of Inorganic Radicals in Aqueous Solution. Journal of Physical and Chemical Reference Data 17 (3), 1027.

Neta, P., Madhavan, V., Zemel, H., Fessenden, R.W., 1977. Rate constants and mechanism of reaction of sulfate radical anion with aromatic compounds. Journal of the American Chemical Society 99 (1), 163–164.

Nick, K., Schöler, H.F., Mark, G., Söylemez, T., Akhlaq, M.S., Schuchmann, H.P., von Sonntag, C., 1992. Degradation of some triazine herbicides by UV radiation such as used in the UV disinfection of drinking water. Aqua- Journal of Water Supply: Research and Technology (41(2)), 82–87.

Nickelsen, M., 1994. High energy electron beam generation of oxidants for the treatment of benzene and toluene in the presence of radical scavengers. Water Research 28 (5), 1227–1237.

Nihemaiti, M., Miklos, D.B., Hübner, U., Linden, K.G., Drewes, J.E., Croué, J.-P., 2018. Removal of trace organic chemicals in wastewater effluent by UV/H2O2 and UV/PDS. Water Research 145, 487–497.

Niu, J., Li, Y., Shang, E., Xu, Z., Liu, J., 2016. Electrochemical oxidation of perfluorinated compounds in water. Chemosphere 146, 526–538.

Niu, J., Lin, H., Xu, J., Wu, H., Li, Y., 2012. Electrochemical mineralization of perfluorocarboxylic acids (PFCAs) by ce-doped modified porous nanocrystalline PbO2 film electrode. Environmental Science & Technology 46 (18), 10191–10198.

Noguera-Oviedo, K., Aga, D.S., 2016. Lessons learned from more than two decades of research on emerging contaminants in the environment. Journal of Hazardous Materials 316, 242–251.

Nöthe, T., Fahlenkamp, H., von Sonntag, C., 2009. Ozonation of Wastewater: Rate of Ozone Consumption and Hydroxyl Radical Yield. Environmental Science & Technology 43 (15), 5990–5995.

Oliveira, H.G., Ferreira, L.H., Bertazzoli, R., Longo, C., 2015. Remediation of 17-α-ethinylestradiol aqueous solution by photocatalysis and electrochemically-assisted photocatalysis using TiO2 and TiO2/WO3 electrodes irradiated by a solar simulator. Water Research 72, 305–314.

Olmez-Hanci, T., Arslan-Alaton, I., 2013. Comparison of sulfate and hydroxyl radical based advanced oxidation of phenol. Chemical Engineering Journal 224, 10–16.

Olmez-Hanci, T., Imren, C., Arslan-Alaton, I., Kabdaşli, I., Tünay, O., 2009. H2O2/UV-C oxidation of potential endocrine disrupting compounds: a case study with dimethyl phthalate. Photochemical & Photobiological Sciences : Official Journal of the European Photochemistry Association and the European Society for Photobiology 8 (5), 620–627.

Olsen, R.O., Hoffmann, F., Hess-Erga, O.-K., Larsen, A., Thuestad, G., Hoell, I.A., 2016. Ultraviolet radiation as a ballast water treatment strategy: Inactivation of phytoplankton measured with flow cytometry. Marine pollution bulletin 103 (1-2), 270–275.

Oppenländer, T., 2003. Photochemical purification of water and air: Advanced Oxidation Processes (AOPs): principles, reaction mechanisms, reactor concepts. Wiley-VCH, Weinheim.

Padmaja, S., Neta, P., Huie, R.E., 1993. Rate constants for some reactions of inorganic radicals with inorganic ions. Temperature and solvent dependence. International Journal of Chemical Kinetics 25 (6), 445–455.

Palm, W.-U., Kopetzky, R., Ruck, W., 2003. OH-radical reactivity and direct photolysis of triphenyltin hydroxide in aqueous solution. Journal of Photochemistry and Photobiology A: Chemistry 156 (1-3), 105–114.

Pan, M., Wu, Z., Tang, C., Guo, K., Cao, Y., Fang, J., 2018. Comparative study of naproxen degradation by the UV/chlorine and the UV/ H2O2 advanced oxidation processes. Environmental Science: Water Research & Technology.

Pang, Y.L., Abdullah, A.Z., Bhatia, S., 2011. Review on sonochemical methods in the presence of catalysts and chemical additives for treatment of organic pollutants in wastewater. Desalination 277 (1-3), 1–14.

Pari, S., Wang, I.A., Liu, H., Wong, B.M., 2017. Sulfate radical oxidation of aromatic contaminants: A detailed assessment of density functional theory and high-level quantum chemical methods. Environmental Science. Processes & Impacts 19 (3), 395–404.

Park, H., 2010. Photolysis of aqueous perfluorooctanoate and perfluorooctane sulfonate. Revue Roumaine de Chimie 55 (10), 611–619.

Park, M., Anumol, T., Daniels, K.D., Wu, S., Ziska, A.D., Snyder, S.A., 2017. Predicting trace organic compound attenuation by ozone oxidation: Development of indicator and surrogate models. Water Research 119, 21–32.

Parsons, S. (Ed.), 2004. Advanced oxidation processes for water and wastewater treatment, reprinted. ed. IWA Publishing, London.

Pati, S.G., Arnold, W., 2018. Reaction rates and product formation during advanced oxidation of ionic liquid cations by UV/peroxide, UV/persulfate, and UV/chlorine. Environmental Science: Water Research & Technology.

Peng, F.-J., Pan, C.-G., Zhang, M., Zhang, N.-S., Windfeld, R., Salvito, D., Selck, H., van den Brink, P.J., Ying, G.-G., 2017. Occurrence and ecological risk assessment of emerging organic chemicals in urban rivers: Guangzhou as a case study in China. Science of The Total Environment 589, 46–55.

Pereira, V.J., Linden, K.G., Weinberg, H.S., 2007a. Evaluation of UV irradiation for photolytic and oxidative degradation of pharmaceutical compounds in water. Water Research 41 (19), 4413–4423.

Pereira, V.J., Weinberg, H.S., Linden, K.G., Singer, P.C., 2007b. UV Degradation Kinetics and Modeling of Pharmaceutical Compounds in Laboratory Grade and Surface Water via Direct and Indirect Photolysis at 254 nm. Environmental Science & Technology 41 (5), 1682–1688.

Petrie, B., Barden, R., Kasprzyk-Hordern, B., 2015. A review on emerging contaminants in wastewaters and the environment: Current knowledge, understudied areas and recommendations for future monitoring. Water Research 72, 3–27.

Pines, D.S., Reckhow, D.A., 2002. Effect of Dissolved Cobalt(II) on the Ozonation of Oxalic Acid. Environmental Science & Technology 36 (19), 4046–4051.

Pinkston, K.E., Sedlak, D.L., 2004. Transformation of Aromatic Ether- and Amine-Containing Pharmaceuticals during Chlorine Disinfection. Environmental Science & Technology 38 (14), 4019–4025.

Pinnekamp, J., Schulze-Hennings, U., Heurer, N., Montag, D., Möller, M., Dott, W., Stepkes, H., Niesen, M., Herr, J., Yüce, S., Jardin, N., 2014. Upgrading of municipal wastewater treatment plants through the use of processes with UV treatment (Mikrolight) - Phase 1 (Ertüchtigung kommunaler Kläranlagen durch den Einsatz von Verfahren mit UV-Behandlung (Mikrolight) - Phase 1): Final report, Bochum.

Pisarenko, A.N., Stanford, B.D., Yan, D., Gerrity, D., Snyder, S.A., 2012. Effects of ozone and ozone/peroxide on trace organic contaminants and NDMA in drinking water and water reuse applications. Water Research 46 (2), 316–326.

Piscitelli, D., Zingaretti, D., Verginelli, I., Gavasci, R., Baciocchi, R., 2015. The fate of MtBE during Fenton-like treatments through laboratory scale column tests. Journal of contaminant hydrology 183, 99–108.

Postigo, C., Richardson, S.D., 2014. Transformation of pharmaceuticals during oxidation/disinfection processes in drinking water treatment. Journal of Hazardous Materials 279, 461–475.

Prados-Joya, G., Sánchez-Polo, M., Rivera-Utrilla, J., Ferro-García, M., 2011. Photodegradation of the antibiotics nitroimidazoles in aqueous solution by ultraviolet radiation. Water Research 45 (1), 393–403.

Qian, F., He, M., Wu, J., Yu, H., Duan, L., 2018. Insight into removal of dissolved organic matter in post pharmaceutical wastewater by coagulation-UV/H2O2. Journal of Environmental Sciences.

Qu, X., Alvarez, P.J.J., Li, Q., 2013. Applications of nanotechnology in water and wastewater treatment. Water Research 47 (12), 3931–3946.

Quan, X., Cheng, Z., Chen, B., Zhu, X., 2013. Electrochemical oxidation of recalcitrant organic compounds in biologically treated municipal solid waste leachate in a flow reactor. Journal of Environmental Sciences 25 (10), 2023–2030.

Rahim Pouran, S., Abdul Aziz, A.R., Wan Daud, W.M.A., 2015. Review on the main advances in photo-Fenton oxidation system for recalcitrant wastewaters. Journal of Industrial and Engineering Chemistry 21, 53–69.

Rahim Pouran, S., Abdul Raman, A.A., Wan Daud, W.M.A., 2014. Review on the application of modified iron oxides as heterogeneous catalysts in Fenton reactions. Journal of Cleaner Production 64, 24–35.

Rajab, M., Heim, C., Greco, G., Helmreich, B., Letzel, T., 2013. Removal of Sulfamethoxazole from Wastewater Treatment Plant Effluents by a Boron-doped Diamond Electrode. International Journal of Environmental Pollution and Solutions.

Rajab, M., Heim, C., Letzel, T., Drewes, J.E., Helmreich, B., 2015. Electrochemical disinfection using boron-doped diamond electrode – The synergetic effects of in situ ozone and free chlorine generation. Chemosphere 121, 47–53.

Real, F.J., Acero, J.L., Benitez, F.J., Roldán, G., Fernández, L.C., 2010. Oxidation of hydrochlorothiazide by UV radiation, hydroxyl radicals and ozone: Kinetics and elimination from water systems. Chemical Engineering Journal 160 (1), 72–78.

Real, F.J., Benitez, F.J., Acero, J.L., Sagasti, J.J.P., Casas, F., 2009. Kinetics of the Chemical Oxidation of the Pharmaceuticals Primidone, Ketoprofen, and Diatrizoate in Ultrapure and Natural Waters. Industrial & Engineering Chemistry Research 48 (7), 3380–3388.

Real, F.J., Benitez, F.J., Rodríguez, C., 2007. Elimination of Benzene and Chlorobenzenes by Photodegradation and Ozonation Processes. Chemical Engineering Communications 194 (6), 811–827.

Reckhow, D.A., Linden, K.G., Kim, J., Shemer, H., Makdissy, G., 2010. Effect of UV treatment on DBP formation. American Water Works Association. Journal 102 (6), 100.

Redpath, J.L., Willson, R.L., 1975. Chain reactions and radiosensitization: Model enzyme studies. International Journal of Radiation Biology and Related Studies in Physics, Chemistry and Medicine 27 (4), 389–398.

Reemtsma, T., Berger, U., Arp, H.P.H., Gallard, H., Knepper, T.P., Neumann, M., Quintana, J.B., Voogt, P.d., 2016. Mind the Gap: Persistent and Mobile Organic Compounds-Water Contaminants That Slip Through. Environmental Science & Technology 50 (19), 10308–10315.

Reemtsma, T., Weiss, S., Mueller, J., Petrovic, M., González, S., Barcelo, D., Ventura, F., Knepper, T.P., 2006. Polar Pollutants Entry into the Water Cycle by Municipal Wastewater: A European Perspective. Environmental Science & Technology 40 (17), 5451–5458.

Regnery, J., Wing, A.D., Kautz, J., Drewes, J.E., 2016. Introducing sequential managed aquifer recharge technology (SMART) - From laboratory to full-scale application. Chemosphere 154, 8–16.

Reisz, E., Schmidt, W., Schuchmann, H.-P., von Sonntag, C., 2003. Photolysis of Ozone in Aqueous Solutions in the Presence of Tertiary Butanol. Environmental Science & Technology 37 (9), 1941–1948.

Richardson, M.L., Bowron, J.M., 1985. The fate of pharmaceutical chemicals in the aquatic environment. Journal of Pharmacy and Pharmacology 37 (1), 1–12.

Richardson, S.D., Plewa, M.J., Wagner, E.D., Schoeny, R., Demarini, D.M., 2007. Occurrence, genotoxicity, and carcinogenicity of regulated and emerging disinfection by-products in drinking water: A review and roadmap for research. Mutation research 636 (1-3), 178–242.

Rivas, J., Encinas, A., Beltrán, F., Graham, N., 2011a. Application of advanced oxidation processes to doxycycline and norfloxacin removal from water. Journal of environmental science and health. Part A, Toxic/hazardous substances & environmental engineering 46 (9), 944–951.

Rivas, J., Gimeno, O., Borralho, T., Carbajo, M., 2010. UV-C photolysis of endocrine disruptors. The influence of inorganic peroxides. Journal of Hazardous Materials 174 (1-3), 393–397.

Rivas, J., Gimeno, O., Borralho, T., Sagasti, J., 2011b. UV-C and UV-C/peroxide elimination of selected pharmaceuticals in secondary effluents. Desalination 279 (1-3), 115–120.

Roccaro, P., Chang, H.-S., Vagliasindi, F.G.A., Korshin, G.V., 2008. Differential absorbance study of effects of temperature on chlorine consumption and formation of disinfection by-products in chlorinated water. Water Research 42 (8-9), 1879–1888.

Roccaro, P., Vagliasindi, F.G.A., 2009. Differential vs. absolute UV absorbance approaches in studying NOM reactivity in DBPs formation: Comparison and applicability. Water Research 43 (3), 744–750.

Rodríguez, R., Espada, J.J., Pariente, M.I., Melero, J.A., Martínez, F., Molina, R., 2016. Comparative life cycle assessment (LCA) study of heterogeneous and homogenous Fenton processes for the treatment of pharmaceutical wastewater. Journal of Cleaner Production 124, 21–29.

Rosario-Ortiz, F.L., Mezyk, S.P., Doud, D.F.R., Snyder, S.A., 2008. Quantitative Correlation of Absolute Hydroxyl Radical Rate Constants with Non-Isolated Effluent Organic Matter Bulk Properties in Water. Environmental Science & Technology 42 (16), 5924–5930.

Rosario-Ortiz, F.L., Wert, E.C., Snyder, S.A., 2010. Evaluation of UV/H2O2 treatment for the oxidation of pharmaceuticals in wastewater. Water Research 44 (5), 1440–1448.

Rosenfeldt, E.J., Linden, K.G., 2004. Degradation of Endocrine Disrupting Chemicals Bisphenol A, Ethinyl Estradiol, and Estradiol during UV Photolysis and Advanced Oxidation Processes. Environmental Science & Technology 38 (20), 5476–5483.

Rosenfeldt, E.J., Linden, K.G., 2007. The ROH,UV Concept to Characterize and the Model UV/H2O2 Process in Natural Waters. Environmental Science & Technology 41 (7), 2548–2553.

Rosenfeldt, E.J., Linden, K.G., Canonica, S., von Gunten, U., 2006. Comparison of the efficiency of OH radical formation during ozonation and the advanced oxidation processes O3/H2O2 and UV/H2O2. Water Research 40 (20), 3695–3704.

Rosenfeldt, E.J., Melcher, B., Linden, K.G., 2005. UV and UV/H2O2 treatment of methylisoborneol (MIB) and geosmin in water. Journal of Water Supply: Research and Technology-AQUA 54 (7), 423–434.

Rott, E., Kuch, B., Lange, C., Richter, P., Minke, R., 2018. Influence of Ammonium Ions, Organic Load and Flow Rate on the UV/Chlorine AOP Applied to Effluent of a Wastewater Treatment Plant at Pilot Scale. International journal of environmental research and public health 15 (6).

Rubio, D., Casanueva, J.F., Nebot, E., 2015. Assessment of the antifouling effect of five different treatment strategies on a seawater cooling system. Applied Thermal Engineering 85, 124–134.

Safarzadeh-Amiri, A., 2001. O 3/H 2 O 2 treatment of methyl-tert-butyl ether (MTBE) in contaminated waters. Water Research 35 (15), 3706–3714.

Safarzadeh-Amiri, A., Bolton, JR, Cater, SR, 1996. The use of iron in advanced oxidation processes. Journal of Advanced Oxidation Technologies 1, 18–26.

Sanches, S., Barreto Crespo, M.T., Pereira, V.J., 2010. Drinking water treatment of priority pesticides using low pressure UV photolysis and advanced oxidation processes. Water Research 44 (6), 1809–1818.

Sanches, S., Leitão, C., Penetra, A., Cardoso, V.V., Ferreira, E., Benoliel, M.J., Crespo, M.T.B., Pereira, V.J., 2011. Direct photolysis of polycyclic aromatic hydrocarbons in drinking water sources. Journal of Hazardous Materials 192 (3), 1458–1465.

Sánchez Pérez, J.A., Román Sánchez, I.M., Carra, I., Cabrera Reina, A., Casas López, J.L., Malato, S., 2013. Economic evaluation of a combined photo-Fenton/MBR process using pesticides as model pollutant. Factors affecting costs. Journal of Hazardous Materials 244-245, 195–203.

Sánchez-Polo, M., Rivera-Utrilla, J., Prados-Joya, G., Ferro-García, M.A., Bautista-Toledo, I., 2008. Removal of pharmaceutical compounds, nitroimidazoles, from waters by using the ozone/carbon system. Water Research 42 (15), 4163–4171.

Sánchez-Polo, M., von Gunten, U., Rivera-Utrilla, J., 2005. Efficiency of activated carbon to transform ozone into *OH radicals: influence of operational parameters. Water Research 39 (14), 3189–3198.

Sarathy, S.R., Mohseni, M., 2007. The Impact of UV/H2O2 Advanced Oxidation on Molecular Size Distribution of Chromophoric Natural Organic Matter. Environmental Science & Technology 41 (24), 8315–8320.

Sarathy, S.R., Stefan, M.I., Royce, A., Mohseni, M., 2012. Pilot-scale UV/H2O2 advanced oxidation process for surface water treatment and downstream biological treatment: Effects on natural organic matter characteristics and DBP formation potential. Environmental Technology 32 (15), 1709–1718.

Sarkar, S., Ali, S., Rehmann, L., Nakhla, G., Ray, M.B., 2014. Degradation of estrone in water and wastewater by various advanced oxidation processes. Journal of Hazardous Materials 278, 16–24.

Schäfer, R.B., Ohe, P.C. von der, Kühne, R., Schuüuürmann, G., Liess, M., 2011. Occurrence and toxicity of 331 organic pollutants in large rivers of north Germany over a decade (1994 to 2004). Environmental Science & Technology 45 (14), 6167–6174.

Scheurer, M., Schmutz, B., Happel, O., Brauch, H.-J., Wulser, R., Storck, F.R., 2014. Transformation of the artificial sweetener acesulfame by UV light. The Science of the total environment 481, 425–432.

Scheurer, M., Storck, F.R., Brauch, H.-J., Lange, F.T., 2010. Performance of conventional multi-barrier drinking water treatment plants for the removal of four artificial sweeteners. Water Research 44 (12), 3573–3584.

Schriks, M., Heringa, M.B., van der Kooi, M.M.E., Voogt, P.d., van Wezel, A.P., 2010. Toxicological relevance of emerging contaminants for drinking water quality. Water Research 44 (2), 461–476.

Schwarzenbach, R.P., Escher, B.I., Fenner, K., Hofstetter, T.B., 2006. The Challenge of Micropollutants in Aquatic Systems. Science 313 (5790), 1072–1077.

Sengupta, A., Lyons, J.M., Smith, D.J., Drewes, J.E., Snyder, S.A., Heil, A., Maruya, K.A., 2014. The occurrence and fate of chemicals of emerging concern in coastal urban rivers receiving discharge of treated municipal wastewater effluent. Environmental Toxicology and Chemistry 33 (2), 350–358.

Sgroi, M., Roccaro, P., Korshin, G.V., Greco, V., Sciuto, S., Anumol, T., Snyder, S.A., Vagliasindi, F.G.A., 2017. Use of fluorescence EEM to monitor the removal of emerging contaminants in full scale wastewater treatment plants. Journal of Hazardous Materials 323 (Pt A), 367–376.

Shah, A.D., Dotson, A.D., Linden, K.G., Mitch, W.A., 2011. Impact of UV disinfection combined with chlorination/chloramination on the formation of halonitromethanes and haloacetonitriles in drinking water. Environmental Science & Technology 45 (8), 3657–3664.

Sharpless, C.M., 2012. Lifetimes of triplet dissolved natural organic matter (DOM) and the effect of $NaBH_4$ reduction on singlet oxygen quantum yields: Implications for DOM photophysics. Environmental Science & Technology 46 (8), 4466–4473.

Sharpless, C.M., Blough, N.V., 2014. The importance of charge-transfer interactions in determining chromophoric dissolved organic matter (CDOM) optical and

photochemical properties. Environmental Science. Processes & Impacts 16 (4), 654–671.

Sharpless, C.M., Linden, K.G., 2001. UV Photolysis of Nitrate: Effects of Natural Organic Matter and Dissolved Inorganic Carbon and Implications for UV Water Disinfection. Environmental Science & Technology 35 (14), 2949–2955.

Sharpless, C.M., Linden, K.G., 2003. Experimental and Model Comparisons of Low- and Medium-Pressure Hg Lamps for the Direct and H 2 O 2 Assisted UV Photodegradation of N -Nitrosodimethylamine in Simulated Drinking Water. Environmental Science & Technology 37 (9), 1933–1940.

Shirzad-Siboni, M., Farrokhi, M., Darvishi Cheshmeh Soltani, R., Khataee, A., Tajassosi, S., 2014. Photocatalytic Reduction of Hexavalent Chromium over ZnO Nanorods Immobilized on Kaolin. Industrial & Engineering Chemistry Research 53 (3), 1079–1087.

Shu, Z., Bolton, J.R., Belosevic, M., Gamal El Din, M., 2013. Photodegradation of emerging micropollutants using the medium-pressure UV/H2O2 Advanced Oxidation Process. Water Research 47 (8), 2881–2889.

Sichel, C., Garcia, C., Andre, K., 2011. Feasibility studies: UV/chlorine advanced oxidation treatment for the removal of emerging contaminants. Water Research 45 (19), 6371–6380.

Simonsen, M.E., Muff, J., Bennedsen, L.R., Kowalski, K.P., Søgaard, E.G., 2010. Photocatalytic bleaching of p-nitrosodimethylaniline and a comparison to the performance of other AOP technologies. Journal of Photochemistry and Photobiology A: Chemistry 216 (2-3), 244–249.

Solar, S., Getoff, N., Surdhar, P.S., Armstrong, D.A., Singh, A., 1991. Oxidation of tryptophan and N-methylindole by N3.cntdot., Br2.-, and (SCN)2.- radicals in light- and heavy-water solutions: A pulse radiolysis study. J. Phys. Chem. 95 (9), 3639–3643.

Sona, M., Baus, C., Brauch, H.-J., 2006. UV irradiation versus combined UV/hydrogen peroxide and UV/ozone treatment for the removal of persistent organic pollutants from water, 69–76.

Song, K., Mohseni, M., Taghipour, F., 2016. Application of ultraviolet light-emitting diodes (UV-LEDs) for water disinfection: A review. Water Research 94, 341–349.

Song, W., Cooper, W.J., Peake, B.M., Mezyk, S.P., Nickelsen, M.G., O'Shea, K.E., 2009. Free-radical-induced oxidative and reductive degradation of N,N'-diethyl-m-toluamide (DEET): Kinetic studies and degradation pathway. Water Research 43 (3), 635–642.

Stalter, D., O'Malley, E., von Gunten, U., Escher, B.I., 2016. Fingerprinting the reactive toxicity pathways of 50 drinking water disinfection by-products. Water Research 91, 19–30.

Stapf, M., Miehe, U., Jekel, M., 2016. Application of online UV absorption measurements for ozone process control in secondary effluent with variable nitrite concentration. Water Research 104, 111–118.

Stefan, M.I. (Ed.), 2018. Advanced oxidation processes for water treatment: Fundamentals and applications. IWA Publishing, London.

Stefan, M.I., Bolton, J.R., 2002. UV Direct Photolysis of N-Nitrosodimethylamine (NDMA): Kinetic and Product Study. Helvetica Chimica Acta 85 (5), 1416.

Sun, L., Bolton, J.R., 1996. Determination of the Quantum Yield for the Photochemical Generation of Hydroxyl Radicals in TiO 2 Suspensions. The Journal of Physical Chemistry 100 (10), 4127–4134.

Sutherland, J., Adams, C., Kekobad, J., 2004. Treatment of MTBE by air stripping, carbon adsorption, and advanced oxidation: technical and economic comparison for five groundwaters. Water Research 38 (1), 193–205.

Swietlik, J., Sikorska, E., 2004. Application of fluorescence spectroscopy in the studies of natural organic matter fractions reactivity with chlorine dioxide and ozone. Water Research 38 (17), 3791–3799.

Taheran, M., Brar, S.K., Verma, M., Surampalli, R.Y., Zhang, T.C., Valero, J.R., 2016. Membrane processes for removal of pharmaceutically active compounds (PhACs) from water and wastewaters. The Science of the total environment 547, 60–77.

Tan, C., Fu, D., Gao, N., Qin, Q., Xu, Y., Xiang, H., 2017. Kinetic degradation of chloramphenicol in water by UV/persulfate system. Journal of Photochemistry and Photobiology A: Chemistry 332, 406–412.

Tang, H.L., Xie, Y.F., 2016. Biologically active carbon filtration for haloacetic acid removal from swimming pool water. The Science of the total environment 541, 58–64.

Thomson, J., Parkinson, A., Roddick, F.A., 2004. Depolymerization of Chromophoric Natural Organic Matter. Environ. Sci. Technol. 38 (12), 3360–3369.

Toor, R., Mohseni, M., 2007. UV-H2O2 based AOP and its integration with biological activated carbon treatment for DBP reduction in drinking water. Chemosphere 66 (11), 2087–2095.

Traves, W.H., Gardner, E.A., Dennien, B., Spiller, D., 2008. Towards indirect potable reuse in South East Queensland. Water Science and Technology: A Journal of the International Association on Water Pollution Research 58 (1), 153–161.

Tröster, I., Schäfer, L., Fryda, M., Matthee, T., 2004. Electrochemical advanced oxidation process using DiaChem electrodes. Water Science and Technology 49 (4), 207–212.

Tuhkanen, T., 2004. UV/H2O2 processes. In: Advanced Oxidation Processes for Water and Wastewater Treatment. IWA Publishing, London, 86-110.

UBA, 2014. Environmental Quality Standard - Diclofenac, Dessau-Roßlau. https://bit.ly/2u1z0W5 (accessed 3.07.2018).

Ulliman, S.L., McKay, G., Rosario-Ortiz, F.L., Linden, K.G., 2018a. Low levels of iron enhance UV/H2O2 efficiency at neutral pH. Water Research 130, 234–242.

Ulliman, S.L., Miklos, D.B., Hübner, U., Drewes, J.E., Linden, K.G., 2018b. Improving UV/H2O2 performance following tertiary treatment of municipal wastewater. Environmental Science: Water Research & Technology 4 (9), 1321–1330.

Ureña de Vivanco, M., Rajab, M., Heim, C., Letzel, T., Helmreich, B., 2013. Setup and Energetic Considerations for Three Advanced Oxidation Reactors Treating Organic Compounds. Chemical Engineering & Technology 36 (2), 355–361.

References

Vahid, B., Khataee, A., 2013. Photoassisted electrochemical recirculation system with boron-doped diamond anode and carbon nanotubes containing cathode for degradation of a model azo dye. Electrochimica Acta 88, 614–620.

Vallejo, M., Fresnedo San Román, M., Ortiz, I., Irabien, A., 2015. Overview of the PCDD/Fs degradation potential and formation risk in the application of advanced oxidation processes (AOPs) to wastewater treatment. Chemosphere 118, 44–56.

van Arnam, F.D., 2008. A Practical Guide to REACH - The EU Chemical al Classification System. International Law News 37 (2), 1–3.

Varanasi, L., Coscarelli, E., Khaksari, M., Mazzoleni, L.R., Minakata, D., 2018. Transformations of dissolved organic matter induced by UV photolysis, Hydroxyl radicals, chlorine radicals, and sulfate radicals in aqueous-phase UV-Based advanced oxidation processes. Water Research 135, 22–30.

Vel Leitner, N.K., Roshani, B., 2010. Kinetic of benzotriazole oxidation by ozone and hydroxyl radical. Water Research 44 (6), 2058–2066.

Verhoeven, J.W., 1996. Glossary of terms used in photochemistry (IUPAC Recommendations 1996). Pure and Applied Chemistry 68 (12), 2223–2286.

Vieno, N., Sillanpää, M., 2014. Fate of diclofenac in municipal wastewater treatment plant - a review. Environment International 69, 28–39.

Vishnuganth, M.A., Remya, N., Kumar, M., Selvaraju, N., 2016. Photocatalytic degradation of carbofuran by TiO2-coated activated carbon: Model for kinetic, electrical energy per order and economic analysis. Journal of Environmental Management 181, 201–207.

Vohra, M., Davis, A.P., 2000. TiO2-Assisted photocatalysis of lead–EDTA. Water Research 34 (3), 952–964.

von Gunten, U., 2003a. Ozonation of drinking water: Part I. Oxidation kinetics and product formation. Water Research 37 (7), 1443–1467.

von Gunten, U., 2003b. Ozonation of drinking water: Part II. Disinfection and by-product formation in presence of bromide, iodide or chlorine. Water Research 37 (7), 1469–1487.

von Gunten, U., Oliveras, Y., 1998. Advanced Oxidation of Bromide-Containing Waters: Bromate Formation Mechanisms. Environmental Science & Technology 32 (1), 63–70.

von Sonntag, C., 2008. Advanced oxidation processes: Mechanistic aspects. Water Science and Technology 58 (5), 1015–1021.

Wacławek, S., Lutze, H.V., Grübel, K., Padil, V.V.T., Černík, M., Dionysiou, D.D., 2017. Chemistry of persulfates in water and wastewater treatment: A review. Chemical Engineering Journal 330, 44–62.

Wadley, S., Waite, T.D.I., 2004. Fenton process. In: Advanced Oxidation Processes for Water and Wastewater Treatment. IWA Publishing, London, 111–136.

Wan, H.B., Wong, M.K., Mok, C.Y., 1994. Comparative study on the quantum yields of direct photolysis of organophosphorus pesticides in aqueous solution. Journal of Agricultural and Food Chemistry 42 (11), 2625–2630.

Wang, D., 2015. Application of the UV/Chlorine Advanced Oxidation Process for Drinking Water Treatment. Dissertation, University of Toronto, Canada.

Wang, D., Bolton, J.R., Andrews, S.A., Hofmann, R., 2015. UV/chlorine control of drinking water taste and odor at pilot and full-scale. Chemosphere 136, 239–244.

Wang, W.-L., Wu, Q.-Y., Huang, N., Wang, T., Hu, H.-Y., 2016. Synergistic effect between UV and chlorine (UV/chlorine) on the degradation of carbamazepine: Influence factors and radical species. Water Research 98, 190–198.

Wang, W.-L., Wu, Q.-Y., Huang, N., Xu, Z.-B., Lee, M.-Y., Hu, H.-Y., 2018. Potential risks from UV/H2O2 oxidation and UV photocatalysis: A review of toxic, assimilable, and sensory-unpleasant transformation products. Water Research 141, 109–125.

Wang, W.-L., Wu, Q.-Y., Li, Z.-M., Lu, Y., Du, Y., Wang, T., Huang, N., Hu, H.-Y., 2017a. Light-emitting diodes as an emerging UV source for UV/chlorine oxidation: Carbamazepine degradation and toxicity changes. Chemical Engineering Journal 310, 148–156.

Wang, W.-L., Zhang, X., Wu, Q.-Y., Du, Y., Hu, H.-Y., 2017b. Degradation of natural organic matter by UV/chlorine oxidation: Molecular decomposition, formation of oxidation byproducts and cytotoxicity. Water Research 124, 251–258.

Wardman, P., 1989. Reduction Potentials of One-Electron Couples Involving Free Radicals in Aqueous Solution. Journal of Physical and Chemical Reference Data 18 (4), 1637–1755.

Watts, M.J., Linden, K.G., 2007. Chlorine photolysis and subsequent OH radical production during UV treatment of chlorinated water. Water Research 41 (13), 2871–2878.

Watts, M.J., Linden, K.G., 2009. Advanced Oxidation Kinetics of Aqueous Trialkyl Phosphate Flame Retardants and Plasticizers. Environmental Science & Technology 43 (8), 2937–2942.

Watts, M.J., Rosenfeldt, E.J., Linden, K.G., 2007. Comparative OH radical oxidation using UV-Cl and UV-HO processes. Journal of Water Supply: Research and Technology—AQUA 56 (8), 469.

Welshans, G., Topudurti, K., Sootkoos, B., Weinberg, S., 1990. Ultrox international ultraviolet radiation/oxidation technology: Applications analysis report. PRC Environmental Management, Inc., Chicago, IL (USA).

Wenk, J., Aeschbacher, M., Salhi, E., Canonica, S., Gunten, U. von, Sander, M., 2013. Chemical oxidation of dissolved organic matter by chlorine dioxide, chlorine, and ozone: Effects on its optical and antioxidant properties. Environmental Science & Technology 47 (19), 11147–11156.

Wert, E.C., Rosario-Ortiz, F.L., Snyder, S.A., 2009. Using Ultraviolet Absorbance and Color To Assess Pharmaceutical Oxidation during Ozonation of Wastewater. Environmental Science & Technology 43 (13), 4858–4863.

Westerhoff, P., Mezyk, S.P., Cooper, W.J., Minakata, D., 2007. Electron Pulse Radiolysis Determination of Hydroxyl Radical Rate Constants with Suwannee River Fulvic Acid and Other Dissolved Organic Matter Isolates. Environmental Science & Technology 41 (13), 4640–4646.

Westerhoff, P., Moon, H., Minakata, D., Crittenden, J., 2009. Oxidation of organics in retentates from reverse osmosis wastewater reuse facilities. Water Research 43 (16), 3992–3998.

References

Woisetschläger, D., Humpl, B., Koncar, M., Glasl, W., Siebenhofer, M. (Eds.), 2015. Electrochemical wastewater treatment: Oxidation of persistent wastewater constituents. Presentation at the 15th AIChE Annual Meeting.

Wols, B.A., Harmsen, D.J.H., Beerendonk, E.F., Hofman-Caris, C.H.M., 2014. Predicting pharmaceutical degradation by UV (LP)/H2O2 processes: A kinetic model. Chemical Engineering Journal 255, 334–343.

Wols, B.A., Harmsen, D.J.H., Wanders-Dijk, J., Beerendonk, E.F., Hofman-Caris, C.H.M., 2015. Degradation of pharmaceuticals in UV (LP)/H2O2 reactors simulated by means of kinetic modeling and computational fluid dynamics (CFD). Water Research 75, 11–24.

Wols, B.A., Hofman-Caris, C.H.M., 2012. Review of photochemical reaction constants of organic micropollutants required for UV advanced oxidation processes in water. Water Research 46 (9), 2815–2827.

Wols, B.A., Hofman-Caris, C.H.M., Harmsen, D.J.H., Beerendonk, E.F., 2013. Degradation of 40 selected pharmaceuticals by UV/H2O2. Water Research 47 (15), 5876–5888.

Wright, H., 2017. Implementing UV AOP for Potable Reuse Using State-of-the Art Models: Presentation at the IUVA 2017 World Congress and Exhibition in Dubrovnik, Croatia.

Wu, C., Linden, K.G., 2010. Phototransformation of selected organophosphorus pesticides: roles of hydroxyl and carbonate radicals. Water Research 44 (12), 3585–3594.

Wu, D., Liu, Y., He, H., Zhang, Y., 2016a. Magnetic pyrite cinder as an efficient heterogeneous ozonation catalyst and synergetic effect of deposited Ce. Chemosphere 155, 127–134.

Wu, J., Ma, L., Chen, Y., Cheng, Y., Liu, Y., Zha, X., 2016b. Catalytic ozonation of organic pollutants from bio-treated dyeing and finishing wastewater using recycled waste iron shavings as a catalyst: Removal and pathways. Water Research 92, 140–148.

Wu, Z., Guo, K., Fang, J., Yang, X., Xiao, H., Hou, S., Kong, X., Shang, C., Yang, X., Meng, F., Chen, L., 2017. Factors affecting the roles of reactive species in the degradation of micropollutants by the UV/chlorine process. Water Research 126, 351–360.

Xiang, Y., Fang, J., Shang, C., 2016. Kinetics and pathways of ibuprofen degradation by the UV/chlorine advanced oxidation process. Water Research 90, 301–308.

Xiao, R., Ye, T., Wei, Z., Luo, S., Yang, Z., Spinney, R., 2015. Quantitative Structure--Activity Relationship (QSAR) for the Oxidation of Trace Organic Contaminants by Sulfate Radical. Environmental Science & Technology 49 (22), 13394–13402.

Xiao, Y., Zhang, L., Zhang, W., Lim, K.-Y., Webster, R.D., Lim, T.-T., 2016. Comparative evaluation of iodoacids removal by UV/persulfate and UV/H2O2 processes. Water Research 102, 629–639.

Xing, S., Lu, X., Liu, J., Zhu, L., Ma, Z., Wu, Y., 2016. Catalytic ozonation of sulfosalicylic acid over manganese oxide supported on mesoporous ceria. Chemosphere 144, 7–12.

Xylem, 2015. City of Los Angeles Terminal Island Water Reclamation Plant selects innovative water reuse solution to address need for water security. Press release from June 3, 2015. https://goo.gl/92A5B9 accessed on February 14, 2018.

Yan, S., Yao, B., Lian, L., Lu, X., Snyder, S.A., Li, R., Song, W., 2017. Development of Fluorescence Surrogates to Predict the Photochemical Transformation of Pharmaceuticals in Wastewater Effluents. Environmental Science & Technology.

Yang, L., Chen, Z., Shen, J., Xu, Z., Liang, H., Tian, J., Ben, Y., Zhai, X., Shi, W., Li, G., 2009. Reinvestigation of the Nitrosamine-Formation Mechanism during Ozonation. Environmental Science & Technology 43 (14), 5481–5487.

Yang, X., Sun, J., Fu, W., Shang, C., Li, Y., Chen, Y., Gan, W., Fang, J., 2016a. PPCP degradation by UV/chlorine treatment and its impact on DBP formation potential in real waters. Water Research 98, 309–318.

Yang, Y., Lu, X., Jiang, J., Ma, J., Liu, G., Cao, Y., Liu, W., Li, J., Pang, S., Kong, X., Luo, C., 2017a. Degradation of sulfamethoxazole by UV, UV/H 2 O 2 and UV/persulfate (PDS): Formation of oxidation products and effect of bicarbonate. Water Research.

Yang, Y., Pignatello, J.J., Ma, J., Mitch, W.A., 2014. Comparison of halide impacts on the efficiency of contaminant degradation by sulfate and hydroxyl radical-based advanced oxidation processes (AOPs). Environmental Science & Technology 48 (4), 2344–2351.

Yang, Y., Pignatello, J.J., Ma, J., Mitch, W.A., 2016b. Effect of matrix components on UV/H2O2 and UV/S2O8(2-) advanced oxidation processes for trace organic degradation in reverse osmosis brines from municipal wastewater reuse facilities. Water Research 89, 192–200.

Yang, Y.-Y., Toor, G.S., Wilson, P.C., Williams, C.F., 2017b. Micropollutants in groundwater from septic systems: Transformations, transport mechanisms, and human health risk assessment. Water Research 123, 258–267.

Yao, D.C.C., Haag, W.R., 1991. Rate constants for direct reactions of ozone with several drinking water contaminants. Water Research 25 (7), 761–773.

Yao, H., Sun, P., Minakata, D., Crittenden, J.C., Huang, C.-H., 2013. Kinetics and modeling of degradation of ionophore antibiotics by UV and UV/H2O2. Environmental Science & Technology 47 (9), 4581–4589.

Yasar, A., Tabinda, A.B., 2010. Anaerobic treatment of industrial wastewater by UASB reactor integrated with chemical oxidation processes; an overview. Polish Journal of Environmental Studies 19, 1051–1061.

Ye, T., Wei, Z., Spinney, R., Tang, C.-J., Luo, S., Xiao, R., Dionysiou, D.D., 2017. Chemical structure-based predictive model for the oxidation of trace organic contaminants by sulfate radical. Water Research 116, 106–115.

Yoon, Y., Chung, H.J., Wen Di, D.Y., Dodd, M.C., Hur, H.-G., Lee, Y., 2017. Inactivation efficiency of plasmid-encoded antibiotic resistance genes during water treatment with chlorine, UV, and UV/H2O2. Water Research 123, 783–793.

Yoon, Y., Dodd, M.C., Lee, Y., 2018. Elimination of transforming activity and gene degradation during UV and UV/H 2 O 2 treatment of plasmid-encoded antibiotic resistance genes. Environmental Science: Water Research & Technology 8 (4), 251.

References

Yu, H.-W., Anumol, T., Park, M., Pepper, I., Scheideler, J., Snyder, S.A., 2015. On-line sensor monitoring for chemical contaminant attenuation during UV/H2O2 advanced oxidation process. Water Research 81, 250–260.

Yu, X.-Y., Barker, J.R., 2003. Hydrogen Peroxide Photolysis in Acidic Aqueous Solutions Containing Chloride Ions. I. Chemical Mechanism. The journal of physical chemistry. A 107 (9), 1313–1324.

Yuan, F., Hu, C., Hu, X., Qu, J., Yang, M., 2009. Degradation of selected pharmaceuticals in aqueous solution with UV and UV/H2O2. Water Research 43 (6), 1766–1774.

Yuan, F., Hu, C., Hu, X., Wei, D., Chen, Y., Qu, J., 2011a. Photodegradation and toxicity changes of antibiotics in UV and UV/H2O2 process. Journal of Hazardous Materials 185 (2-3), 1256–1263.

Yuan, R., Ramjaun, S.N., Wang, Z., Liu, J., 2011b. Effects of chloride ion on degradation of Acid Orange 7 by sulfate radical-based advanced oxidation process: Implications for formation of chlorinated aromatic compounds. Journal of Hazardous Materials 196, 173–179.

Yuan, R., Wang, Z., Hu, Y., Wang, B., Gao, S., 2014. Probing the radical chemistry in UV/persulfate-based saline wastewater treatment: Kinetics modeling and byproducts identification. Chemosphere 109, 106–112.

Zamy, C., Mazellier, P., Legube, B., 2004. Phototransformation of selected organophosphorus pesticides in dilute aqueous solutions. Water Research 38 (9), 2304–2313.

Zeegers, F., Tilquin, B., Hickel, B., 1992. Pulse radiolysis study of the reactivity of chloramphenicol, diazepam and clonazepam with the electron and the hydroxyl radical. Journal de pharmacie de Belgique 48 (6), 457–462.

Zhang, J.P., Chitnis, A., Adivarahan, V., Wu, S., Mandavilli, V., Pachipulusu, R., Shatalov, M., Simin, G., Yang, J.W., Khan, M.A., 2002. Milliwatt power deep ultraviolet light-emitting diodes over sapphire with emission at 278 nm. Applied Physics Letters 81 (26), 4910–4912.

Zhang, R., Sun, P., Boyer, T.H., Zhao, L., Huang, C.-H., 2015a. Degradation of pharmaceuticals and metabolite in synthetic human urine by UV, UV/H2O2, and UV/PDS. Environmental Science & Technology 49 (5), 3056–3066.

Zhang, R., Yang, Y., Huang, C.-H., Zhao, L., Sun, P., 2016. Kinetics and modeling of sulfonamide antibiotic degradation in wastewater and human urine by UV/H2O2 and UV/PDS. Water Research 103, 283–292.

Zhang, T., Zhu, H., Croué, J.-P., 2013. Production of sulfate radical from peroxymonosulfate induced by a magnetically separable CuFe2O4 spinel in water: Efficiency, stability, and mechanism. Environmental Science & Technology 47 (6), 2784–2791.

Zhang, Y., Geissen, S.-U., Gal, C., 2008. Carbamazepine and diclofenac: removal in wastewater treatment plants and occurrence in water bodies. Chemosphere 73 (8), 1151–1161.

Zhang, Y., Zhuang, Y., Geng, J., Ren, H., Zhang, Y., Ding, L., Xu, K., 2015b. Inactivation of antibiotic resistance genes in municipal wastewater effluent by chlorination and

sequential UV/chlorination disinfection. The Science of the total environment 512-513, 125–132.

Zhihui, A., Peng, Y., Xiaohua, L., 2005. Degradation of 4-chlorophenol by microwave irradiation enhanced advanced oxidation processes. Chemosphere 60 (6), 824–827.

Zhou, D., Huang, W., Wu, F., Han, C., Chen, Y., 2010. Photodegradation of chloromycetin in aqueous solutions: kinetics and influencing factors: Reaction Kinetics, Mechanisms and Catalysis. Water Environment Research 100 (1), 45–53.

Zhuang, Y., Ren, H., Geng, J., Zhang, Y., Zhang, Y., Ding, L., Xu, K., 2015. Inactivation of antibiotic resistance genes in municipal wastewater by chlorination, ultraviolet, and ozonation disinfection. Environmental science and pollution research international 22 (9), 7037–7044.

Zhuo, Q., Deng, S., Yang, B., Huang, J., Yu, G., 2011. Efficient electrochemical oxidation of perfluorooctanoate using a Ti/SnO2-Sb-Bi anode. Environmental Science & Technology 45 (7), 2973–2979.

Zimmermann, S.G., Schmukat, A., Schulz, M., Benner, J., von Gunten, U., Ternes, T.A., 2012. Kinetic and mechanistic investigations of the oxidation of tramadol by ferrate and ozone. Environmental Science & Technology 46 (2), 876–884.

Zoschke, K., Dietrich, N., Bornick, H., Worch, E., 2012. UV-based advanced oxidation processes for the treatment of odour compounds: efficiency and by-product formation. Water Research 46 (16), 5365–5373.

Zuo, Z., Cai, Z., Katsumura, Y., Chitose, N., Muroya, Y., 1999. Reinvestigation of the acid–base equilibrium of the (bi)carbonate radical and pH dependence of its reactivity with inorganic reactants. Radiation Physics and Chemistry 55 (1), 15–23.

Zwiener, C., Frimmel, F.H., 2000. Oxidative treatment of pharmaceuticals in water. Water Research 34 (6), 1881–1885.